

**DOCTORAL THESIS**

Changing Subsurface Oxygen  
Conditions in the Baltic Sea  
Basins – Analyzing the Drivers  
at Different Temporal Scales

Stella-Theresa Stoicescu

TALLINN UNIVERSITY OF TECHNOLOGY  
DOCTORAL THESIS  
48/2023

# **Changing Subsurface Oxygen Conditions in the Baltic Sea Basins – Analyzing the Drivers at Different Temporal Scales**

STELLA-THERESA STOICESCU



TALLINN UNIVERSITY OF TECHNOLOGY

School of Science

Department of Marine Systems

This dissertation was accepted for the defence of the degree of Doctor of Philosophy in Earth Sciences on 12/07/2023

**Supervisor:**

Prof. Urmas Lips  
Department of Marine Systems  
School of Science  
Tallinn University of Technology  
Tallinn, Estonia

**Opponents:**

Prof. Niels Jacob Carstensen  
Department of Ecoscience  
Faculty of Technical Sciences  
Aarhus University  
Aarhus, Denmark

Prof. Kalle Olli  
Chair of Hydrobiology and Fisheries  
Institute of Agricultural and Environmental Sciences  
Estonian University of Life Sciences  
Tartu, Estonia

**Defence of the thesis:** 27/10/2023, Tallinn

**Declaration:** Hereby I declare that this doctoral thesis, my original investigation and achievement, submitted for the doctoral degree at Tallinn University of Technology has not been submitted for doctoral or equivalent academic degree.

Stella-Theresa Stoicescu

-----  
signature



European Union  
European Regional  
Development Fund



Investing  
in your future

Copyright: Stella-Theresa Stoicescu, 2023

ISSN 2585-6898 (publication)

ISBN 978-9916-80-047-8 (publication)

ISSN 2585-6901 (PDF)

ISBN 978-9916-80-048-5 (PDF)

Printed by Koopia Niini & Rauam

TALLINNA TEHNIKAÜLIKOOL  
DOKTORITÖÖ  
48/2023

**Pinnaaluste hapnikutingimuste muutused  
Läänemere alambasseinides – erinevatel  
ajaskaaladel mõju avaldavate tegurite  
analüüs**

STELLA-THERESA STOICESCU







# Contents

List of publications .....	6
Author's contribution to the publications.....	7
Abbreviations .....	8
1 INTRODUCTION .....	9
1.1 Aim of the study .....	10
2 MATERIAL AND METHODS .....	11
2.1 Basins .....	11
2.2 Nutrients .....	12
2.3 Using oxygen to describe eutrophication levels .....	13
2.4 Data used in the study .....	14
3 RESULTS AND DISCUSSION .....	15
3.1 Long-term changes in deep-layer oxygen conditions .....	15
3.2 Interpreting the oxygen variability and trends on different time-scales.....	17
3.2.1 Processes contributing to oxygen dynamics .....	17
3.2.2 The drivers of long-term changes in the Eastern Gulf of Finland .....	18
3.2.3 Physical processes influencing hypoxia occurrence in the Gulf of Riga .....	20
3.2.4 High-resolution oxygen variability .....	22
3.3 Oxygen-based indicators for assessing eutrophication status .....	23
3.3.1 Oxygen debt .....	23
3.3.2 Oxygen consumption .....	24
3.3.3 The extent of low oxygen water.....	24
3.4 Considering future projections .....	25
4 CONCLUSIONS .....	26
REFERENCES .....	28
Acknowledgements.....	34
Abstract.....	35
Lühikokkuvõte.....	37
Appendix .....	39
Paper I.....	39
Paper II.....	57
Paper III.....	77
Paper IV .....	101
Curriculum vitae.....	111
Elulookirjeldus.....	113

## List of publications

- I Stoicescu, S-T., Lips, U. and Liblik, T., 2019. **Assessment of Eutrophication Status Based on Sub-Surface Oxygen Conditions in the Gulf of Finland (Baltic Sea)**. Front. Mar. Sci. 6:54. <https://doi.org/10.3389/fmars.2019.00054>
- II Stoicescu, S-T., Laanemets, J., Liblik, T., Skudra, M., Samlas, O., Lips, I., and Lips, U. 2022. **Causes of the extensive hypoxia in the Gulf of Riga in 2018**. Biogeosciences, 19, pp. 2903–2920. <https://doi.org/10.5194/bg-19-2903-2022>
- III Stoicescu, S-T., Hoikkala, L., Fleming, V., Lips, U, 2023. **Continuing long-term expansion of low-oxygen conditions in the Eastern Gulf of Finland**. Oceanologia, volume, pp. X:X. doi ...
- IV Liblik, T., Stoicescu, S-T., Buschmann, F., Lilovert, M-J., and Lips, U., 2023. **High-resolution characterization of the development and decay of seasonal hypoxia in the Gulf of Riga, Baltic Sea**. Front. Mar. Sci. 10:1119515. <https://doi.org/10.3389/fmars.2023.1119515>

## **Author's contribution to the publications**

Contribution to the papers in this thesis are:

- I The author played a major role in gathering and compiling the data, researching and developing the methods used in the analysis, and the interpretation of the results. The author wrote the manuscript with contributions from the co-authors and compiled the supporting information.
- II The author played a major role in gathering and compiling the data and the interpretation of the results. The author collaborated in writing the manuscript together with the other co-authors and compiled the supporting information.
- III The author played a major role in gathering and compiling the data, developing the methods, and the interpretation of the results. The author wrote the manuscript with contributions from the co-authors and compiled the supporting information.
- IV The author contributed to analyzing the data and writing of the manuscript.

## Abbreviations

CTD	Conductivity, temperature, pressure (depth) sensors
DNRA	Dissimilatory nitrate reductase to ammonium
DO	Dissolved oxygen
EGB	Eastern Gotland Basin
EGOF	Eastern Gulf of Finland
GOF	Gulf of Finland
GOR	Gulf of Riga
HELCOM	Helsinki Commission
MSFD	Marine Strategy Framework Directive
N	Nitrogen
N <sub>2</sub>	Nitrogen gas
NBP	Northern Baltic Proper
ODEBT	Oxygen debt
P	Phosphorus
S	Salinity
T	Temperature
WFD	Water Framework Directive

# 1 INTRODUCTION

With the continual growth of population and industrialization from the beginning of the 20<sup>th</sup> century, the environment has been under a lot of pressure. For instance, the use of nutrients in agriculture was not managed until the second half of the 20<sup>th</sup> century considering the effect on nature due to a lack of knowledge or timely regulations. The same goes for husbandry and the nutrient loads originating from farms.

The wide use of fertilizers and husbandry developments have resulted in excess inputs of nutrients into the marine environment. Negative anthropogenic effects of eutrophication, e.g. increased cyanobacterial blooms and oxygen-deficient areas and a decrease in bottom fauna distribution, have been observed worldwide (e.g. Diaz & Rosenberg, 2008). The Baltic Sea is a good case study for the overall problem, because of a long history of stressors, the consequent spread of oxygen deficient areas, practices in data gathering, and early application of environmental management (Hansson & Viktorsson, 2021; Reusch et al., 2018).

A way to keep track of the advancements in managing human influence on marine areas is to assess the status of the sea by using quantifiable metrics describing the pressures and state of the environment. The Baltic Sea is surrounded in majority by European Union member states and managed on the highest level by MSFD (entire sea area, 2008/56/EC) and the WFD (coastal waters, 2000/60/EC) regarding eutrophication. The Helsinki Commission (HELCOM) has been and is the key harmonizer/guide of the MSFD-derived commitments, among other things. HELCOM contracting parties have agreed to assess the status of the open sea areas, focusing on nutrients, chlorophyll-a levels, cyanobacterial blooms, water transparency, and near-bottom oxygen conditions and/or bottom fauna. The WFD regulates the assessment of coastal areas and focuses mainly on the biological quality elements (phytoplankton, bottom flora and fauna), viewing the physical and chemical parameters which are in the center of the MSFD assessments, e.g. nutrient concentrations, as supplementary information.

Quantifying human pressures through the nutrient concentrations in the surface layer is quite straightforward, knowing the input from rivers and having defined the natural background loads. Levels of chlorophyll-a, water transparency, and the extent of cyanobacterial blooms are also directly or indirectly related to nutrient loads. The distribution, species composition, and abundance of zoobenthos depend highly on oxygen availability. Oxygen content is influenced by the air-sea exchange rate, productivity in the euphotic layer, respiration, and the amount of organic matter degraded in the bottom areas. In the deep layer, oxygen concentrations are also influenced by hydrographic conditions. For instance, oxygen levels in the central Baltic Sea below the halocline exhibit a declining trend during periods of low or no inflows from the North Sea (e.g. Carstensen et al., 2014a; Mohrholz, 2018). Considering climate change, especially the increase in temperature, a declining trend in oxygen saturation concentrations is observed (e.g. Carstensen et al., 2014a; Stramma & Schmidtko, 2019), which means, that the water's ability to hold oxygen is decreasing. Increasing air temperature and runoff also strengthen stratification and weaken vertical mixing (Meier et al., 2022).

Since oxygen conditions in the sea are affected by many factors, it is essential to discriminate between human-induced and natural variability in order to devise appropriate measures. Keeping this in mind, HELCOM has developed and tested oxygen-based indicators, e.g., 'oxygen debt', which assesses the amount of 'missing oxygen' below the halocline (HELCOM, 2013). Whatever approach is chosen, it has to be focused on the anthropogenic influences.

## 1.1 Aim of the study

The motivation of this study was to better describe the variability of oxygen conditions at timescales from hours to decades, link it to natural processes and human-induced impacts, and predict potential future changes in two basins of the Baltic Sea with different hydrographic background. The Gulf of Finland represents a sea area with a free connection to the open sea, and the Gulf of Riga is a basin separated by sills from the open sea. The importance of using high-resolution data was emphasized to make environmental status assessments more confident.

The main objective was to describe the variability of oxygen concentrations in the subsurface and near-bottom layers at different time scales and explain the reasons behind the observed changes. The analysis focused on the following cases:

- A relatively deep sea area with a quasi-permanent halocline influenced by the freshwater discharge from rivers and unrestricted connection to the open sea (Paper I)
  - Central Gulf of Finland, where three layers separated by the seasonal thermocline and quasi-permanent halocline exist in summer; the assessment of seasonal oxygen consumption demands high-resolution measurements since the conditions are highly variable, influenced, e.g. by prevailing winds.
- A shallower area of the same basin where the halocline is mostly missing, but subsurface low-oxygen conditions can occur seasonally (Paper III)
  - Eastern Gulf of Finland, the aim was to reveal long-term patterns of changing oxygen conditions and link these to changes in hydrographic conditions, climate and nutrient loads.
- A shallow bay separated with sills from the adjacent open sea areas with a fully mixed water column in winter, but where the excess amount of nutrients and the limited water exchange promote the development of seasonal hypoxia (Papers II and IV)
  - Gulf of Riga, the aim was to find the reasons for an exceptional hypoxic event in 2018, predict whether such events could occur more often in the future considering projected climate change, and analyze how short-term variability influences assessment results.

Additional objectives included:

- Testing and developing oxygen indicators to describe better the human-induced impact on the status of the marine environment (Papers I, II and III);
- Highlighting the advantages of collecting high-resolution data for the assessment of the environmental status of marine areas (Papers I and IV).

## 2 MATERIAL AND METHODS

### 2.1 Basins

The Gulf of Finland (GOF) is an estuary-type sea area influenced by large freshwater discharge, nutrient inputs and unrestricted connection to the adjacent open sea areas. The environmental status of the gulf regarding eutrophication is not good (HELCOM, 2018), although the nutrient load to the gulf has significantly decreased since the 1980s (Gustafsson et al., 2012). In the GOF, the deep-layer oxygen conditions are highly dependent on the large runoff from river Neva in the east and the lateral east-west movement of more saline and deoxygenated water originating from the Northern Baltic Proper (NBP) (Fig. 1). On average, the outflow is dominating in the surface layer and the inflow in the subsurface layers. Under N-NE wind influence, the NPB deep-water can spread further towards the east as a compensation flow to the outflowing surface layer (Elken et al., 2003; Lips et al., 2008), enlarging the hypoxic/anoxic bottom area (Liblik et al., 2013, Paper I). Under prevailing SW winds, the hypoxic area is smaller and with stronger westerlies, the salt wedge recedes even more towards the NBP (Liblik et al., 2013; Lips et al., 2017). The sometimes-rapid changes in deep-layer DO concentrations can be well observed with high-frequency continuous measurements (Paper I), while regular monitoring cannot describe the temporal development of such hypoxic/anoxic events in detail.

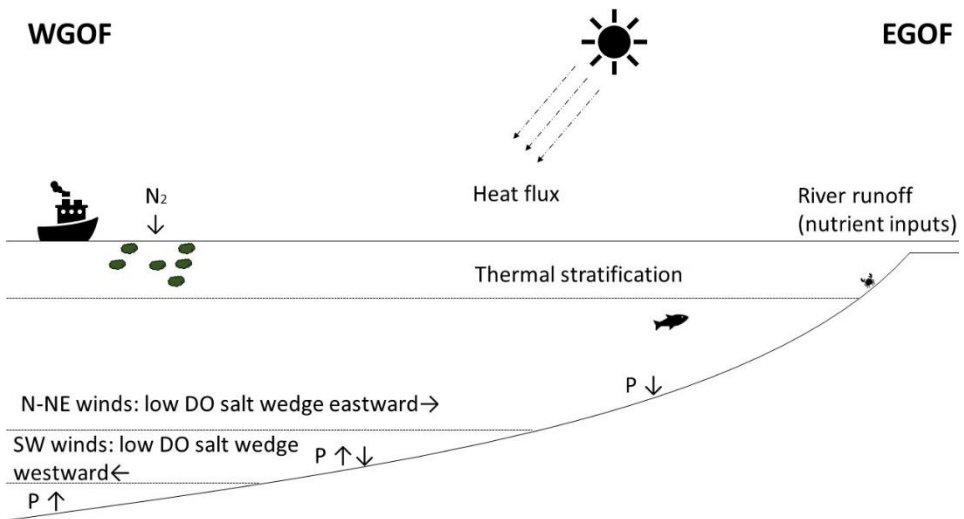


**Figure 1.** Simplified representation of an open-boundary basin on the Gulf of Finland example. P – phosphorus. N<sub>2</sub> – nitrogen gas.

The GOR can be generalized as a shallow basin with restricted water exchange with other sea areas. Nutrient inputs are high (HELCOM, 2022), and the gulf is influenced by eutrophication. Water exchange with the adjacent deeper Eastern Gotland Basin (EGB) occurs through the Irbe Strait (Astok et al., 1999; Petrov, 1979). The GOR is also connected to the shallow Moonsund area in the north, but inflows from there are in stratified conditions mostly arrested in the surface layer (Lips et al., 1995).



Although the GOR is not very deep, a high oxygen consumption rate in the near-bottom layer can lead to the development of hypoxia during the stratified season. Additional DO flux by advection or vertical mixing is needed to hinder hypoxia development in the central parts of the gulf. Advective DO flux appears when N-NE winds prevail, and upwelling occurs along the eastern coast of the EGB, and the inflow through the Irbe Strait is more saline than the GOR deep water and can spread along the bottom (Fig. 2) (Raudsepp & Elken, 1995). Besides bringing more DO to the central parts of the gulf, such inflows strengthen stratification and separate the bottom layer from the water column above. Stronger winds from the SW direction can cause downwelling near the western side of the Irbe Strait, which can promote the spread of buoyant sub-surface inflows when the inflowing water is less saline than the GOR near-bottom water (Liblik et al., 2017). Such buoyant inflows do not ventilate the gulf's bottom areas.

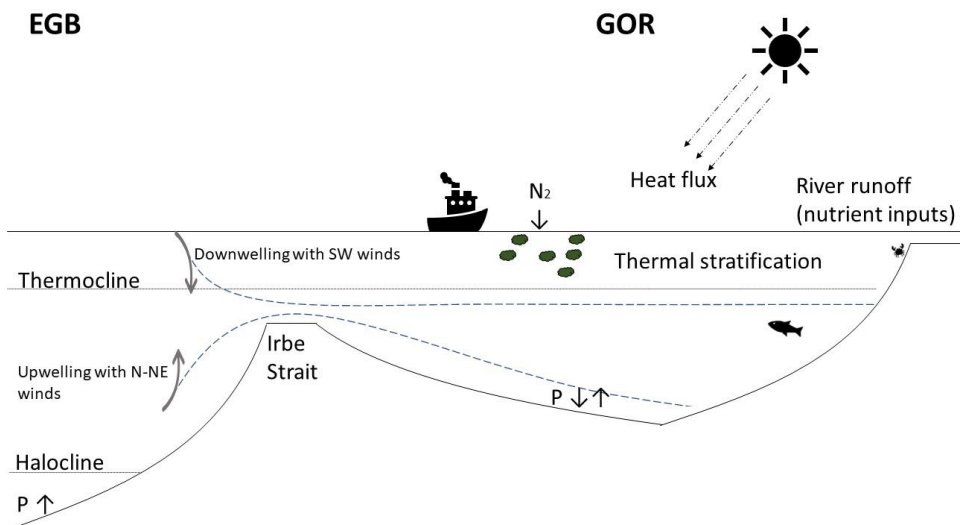


**Figure 2.** Simplified representation of a semi-enclosed basin separated from the open sea by a sill on the Gulf of Riga example. P – phosphorus. N<sub>2</sub> – nitrogen gas.

## 2.2 Nutrients

Elevated nutrient inputs to the Baltic Sea, although significantly reduced since the 1980-s, continue to affect the marine environment (Gustafsson et al., 2012; Murray et al., 2019). Nitrogen (N) loads originate mostly from land-based sources and reach the marine environment via rivers, direct inputs and the atmosphere. Primary producers use N in inorganic forms originating from land or remineralized in the marine environment. Cyanobacteria also fix nitrogen in the gaseous form (N<sub>2</sub>). Organic nitrogen is remineralized through the process of nitrification in oxic conditions. A nitrification-coupled process, denitrification, is a natural N-removal process, taking place in the anoxic layer of the sediments (Carstensen et al., 2014b; Jäntti & Hietanen, 2012). In the Baltic Sea, most of the nitrogen is removed through denitrification (Carstensen et al., 2014b). When the entire sediment profile and bottom layer are hypoxic, dissimilatory nitrate reduction to ammonium (DNRA) will reduce nitrate to

ammonium. Hence, generally, hypoxic conditions support the switch from N-removal (coupled nitrification-denitrification) to N-storage (DNRA) (Carstensen et al., 2014b). In the GOF, the switch to N-storage happens when DO concentrations are around 3.4 mg L<sup>-1</sup> (Jäntti & Hietanen, 2012).

Similarly to nitrogen, the phosphorus (P) cycle is also altered when hypoxic/anoxic conditions prevail. In well oxygenated bottom areas, P is bound to sediments in the organic form, iron oxide bound P, and in authigenic minerals (e.g., Kuliński et al., 2022). When low oxygen conditions prevail, these highly volatile iron-bound P forms release phosphorus back into the water column, where it is again available for primary producers (Pitkänen et al., 2001; van Helmond et al., 2020). Conley et al. (2002) showed that the dissolved inorganic phosphorus (DIP) pools were correlated with the extent of hypoxic areas in the Baltic Sea (including the GOF and GOR). Thus, considering the peculiarities of the studied basins, the P release and availability in the GOF are probably significantly influenced by the spread of low-oxygen waters from the NBP. In the GOR, the release of P from sediments could be more influenced by the supply of organic matter from the surface layer, local oxygen consumption and consequent near-bottom hypoxia.

## 2.3 Using oxygen to describe eutrophication levels

In HELCOM, an oxygen debt indicator (ODEBT) has been developed and applied in deeper open sea areas where a permanent halocline exists (HELCOM, 2013). The idea is to estimate the volume-specific amount of oxygen missing below the halocline. 'Missing' oxygen is found by subtracting the measured oxygen concentration (also taking into account hydrogen sulfide as negative oxygen, if present) from the saturated oxygen concentration, which is found using simultaneously measured temperature and salinity. Since the oxygen debt is significantly influenced by sub-halocline advection, the Major Baltic Inflows (MBI) have to be considered to assess the human-induced impacts. A modified oxygen debt indicator was applied in Paper I – the oxygen debt was estimated just below the halocline in the central GOF.

Besides estimating the 'missing' oxygen, another option is to estimate the amount of DO consumed in the subsurface layer during the period of seasonal thermal stratification. In Papers I and II, DO consumption was calculated based on collected vertical oxygen profiles and estimated oxygen fluxes due to advection and vertical diffusion. The diffusive flux was estimated based on vertical gradients of DO and density and the advective flux, using the relationship between DO concentration and salinity and the estimated change in salinity due to advection. While the hydrographic conditions least influence this indicator, it requires availability of vertical CTD and oxygen profiles with high enough resolution in time. High-resolution profiler data and a suggestion that the seasonal oxygen depletion in the intermediate layer between the thermocline and halocline is mostly related to the local consumption (respiration) and less influenced by hydrographic conditions have motivated to develop an oxygen consumption indicator for the assessment of eutrophication status.

The most easily understandable way to describe DO conditions in a sea area is to estimate the extent of waters or bottoms with low oxygen concentrations, as recently analyzed by e.g. Kõuts et al. (2021). For this, the depth where oxygen concentration falls below the hypoxia threshold (DO = 2.0 mL L<sup>-1</sup> or 2.9 mg L<sup>-1</sup>, Vaquer-Sunyer & Duarte, 2008) can be found and the area and volume of the low oxygen waters estimated (Paper I and II). Similarly, other DO concentrations can be used to describe the extent of low DO conditions. For the Eastern Gulf of Finland (EGOF, Paper III), DO = 6.0 mg L<sup>-1</sup> was selected

because this concentration is shown to be a limit below what about 75% of fish will experience stress due to low DO concentrations (Vaquer-Sunyer & Duarte, 2008). Since the deep-layer oxygen conditions in the EGOF area are affected by the spread of saline water from the west (Alenius et al., 1998), a method was developed (Paper III) to minimize the influence of hydrography on indicator results in order to obtain estimates mostly related to anthropogenic pressures (i.e. elevated nutrient inputs).

## 2.4 Data used in the study

The basis of the current study (and papers) is the oxygen data (with accompanying salinity and temperature data). To describe more recent changes, CTD and water sample data gathered on monitoring cruises were used (Table 2.1.). Historical data were gathered from local (e.g. KESE) and international (e.g. ICES/HELCOM) databases to characterize long-term variability and possible trends in selected parameters. To highlight the advantages of high-resolution data, profiles from an autonomous profiler and time series from a near-bottom sensor were used. To explain the reasons behind the changing oxygen conditions, meteorological, river runoff, and nutrient load data were analyzed. For describing the impact of hypoxia, data from water sample analysis of nutrient concentrations were used.

**Table 2.1.** *Data used in the study*

<b>Data type</b>	<b>Source</b>	<b>Parameters</b>
Autonomous profiler and point measurement data (Papers I and IV)	MSI	T, S, DO
CTD and water samples from r/v cruises (Papers I, II, and IV)	MSI	T, S, DO
Historical and environmental monitoring data (Papers I, II and III)	KESE, Latvian Environmental monitoring databases, ICES/HELCOM database, SeaDataNet, Finnish Environment Institute's national database Hertta, Gulf of Finland Year database, Finnish Meteorological Institute	T, S, DO, nutrients
Meteorology data (Papers I, II, and IV)	Finnish Meteorological Institute, ERA5 dataset via Copernicus Services	net solar radiation, air T, wind speed, wind direction
River runoff data (Paper II)	Latvian Environment, Geology and Meteorology Center and Estonian Environment Agency	runoff

## 3 RESULTS AND DISCUSSION

### 3.1 Long-term changes in deep-layer oxygen conditions

Changes in oxygen conditions in the aphotic water layer are influenced by oxygen consumption (respiration, degradation of organic matter) and oxygen fluxes controlled by physical processes (horizontal advection and vertical mixing) (e.g., Carstensen et al., 2014a; Lips et al., 2017). Consumption rates depend on the availability/amount of degradable organic matter (e.g., Conley et al., 2009; Conley & Johnstone, 1995). Thus, respiration depends on primary production that is limited by other factors, e.g. the availability of nutrients (Rabalais et al., 2009). Respiration and consumption rates increase with rising temperature (Boesch et al., 2007). Also, a decrease in DO can be caused by the increase in zooplankton biomass, as Meier et al. (2018) described in the GOF. Horizontal advection depends on the openness of the basin and the forcing regulating the water exchange, while diffusive fluxes are defined by vertical stratification and the forcing driving turbulent mixing. The increase (decrease) in temperature decreases (increases) oxygen solubility, meaning that water is able to hold less (more) oxygen (Carstensen et al., 2014a).

Fonselius & Valderrama (2003) showed that, in general, during the 20<sup>th</sup> century, deep and bottom water oxygen conditions have deteriorated in the central and northern basins of the Baltic Sea. According to Carstensen et al. (2014a), hypoxic areas have increased 10-fold from the beginning of the 20<sup>th</sup> century to 2012. Conley et al. (2011) identified that the frequency of hypoxia ( $DO < 2 \text{ mg L}^{-1}$ ) has increased in the coastal areas from roughly 2% of the profiles exhibiting hypoxia in the 1960s to ~5% in 2009. The present study has analyzed historical and monitoring data to reveal whether similar trends are characteristic of the EGOF (Paper III) and the GOR (Paper II) and what are the reasons for the observed changes in deep-layer oxygen conditions.

The long-term data from EGOF show that in 100+ years, oxygen conditions in the deep layer have deteriorated with a DO decrease rate of  $-0.22 \text{ mg L}^{-1}$  per decade (Paper III). The long-term trend for bottom water in the central Baltic Sea (station BY15, at 200m) has a similar decrease rate of DO concentrations, approximately  $-0.36 \text{ mg L}^{-1} \text{ decade}^{-1}$  (Fonselius & Valderrama, 2003). While the deep layer of the central Baltic Sea is oxygenated with MBIs, areas further north, including the GOF, see worsened oxygen conditions approximately nine months after an MBI event, because the deoxygenated water from the central Baltic Sea is pushed to more northerly positions (Liblik et al., 2018). During periods of no MBIs, the central Baltic area can suffer from increased hypoxic areas, as was observed in 1983-1993 (Lehmann et al. 2022). In the EGOF, this period of stagnation manifested itself as a period of higher DO concentrations and lower salinity in the subsurface layers (mid-1980s to mid-1990s, Fig. 3, Paper III). Such stagnation occurred mostly due to larger than average freshwater inputs and stronger than normal westerly winds (Lehmann et al., 2022; Meier & Kauker, 2003). Thus, although the GOF suffered from large nutrient inputs, the weak stratification conditions allowed for oxygen conditions to improve significantly (Laine et al., 2007).

Based on model data, Stockmayer & Lehmann (2023) found a  $-0.29 \text{ mg L}^{-1} \text{ decade}^{-1}$  decrease in DO concentrations in the GOF deeper area (~60m) for 1977-2018. Results from the last three decades (1990-2021) show that the oxygen decline has been steeper with a rate of  $-1.49 \text{ mg L}^{-1} \text{ decade}^{-1}$  (Fig. 3, Paper III). This very high rate of the decrease in DO concentrations is related to temporarily high DO concentrations in the EGOF deep

layer in the late 1980s and early 1990s and the return of characteristic stratification conditions in the late 1990s. In that sense, this result and the estimate by Stockmayer & Lehmann (2023) agree, because the period covered in the latter study included a period of increasing and then decreasing DO concentrations (Fig. 3). Thus, when a long-term DO trend is reported, the period for which it is estimated has to be stressed to relate the trend to the changes in driving forces or inputs.

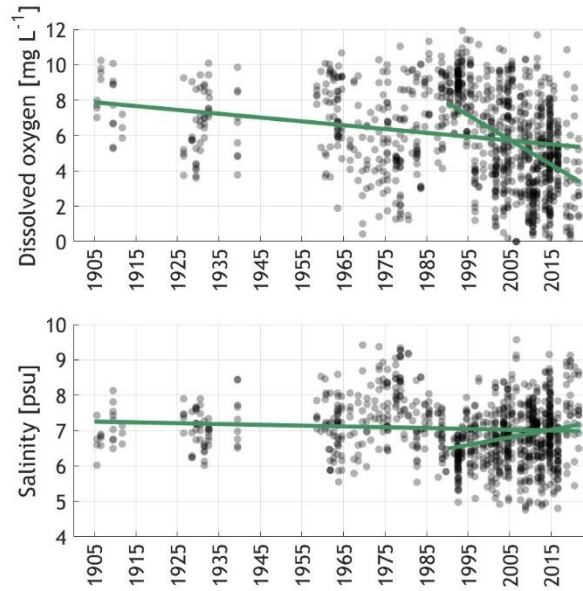


**Figure 3.** Oxygen (top) and salinity (bottom) values from 40-70m layer in the Eastern Gulf of Finland in July-October of 1905-2021 and regression lines based on yearly mean values from 1905-2021 and 1990-2021 (Paper III).

In the Gulf of Riga, such large decadal-scale changes in salinity, which could influence vertical stratification, are not observed because the shallow sill prevents sub-halocline waters from entering the gulf, and the water column is fully mixed in winter. However, a significant decreasing trend in DO concentrations in August was found for the 20-50m layer from 1963 to 1990 (Berzinsh, 1995). Based on more recent data (2005-2018), the trend in DO concentrations in the deep layer in August was insignificant, but a significant decrease of  $-0.45 \text{ mg L}^{-1}$  per year was found based on October-November data (Paper II). This very steep DO decline (about four times bigger than the rate from the second half of the 20<sup>th</sup> century) could have a different explanation than simply the deterioration of oxygen conditions due to eutrophication. The increasing surface water temperatures and related prolonged stratified period (Wasmund et al., 2019) could be a reason that more measurements in October-November recent years have captured the near-bottom hypoxia because the autumn stratification collapse is delayed.

## 3.2 Interpreting the oxygen variability and trends on different time-scales

### 3.2.1 Processes contributing to oxygen dynamics

It has been suggested that the decline in DO concentrations is largely influenced by eutrophication (Carstensen et al., 2014a; Meier et al., 2019), but also by the strengthening of the stratification (Lehtoranta et al., 2017; Liblik & Lips, 2019; Ma et al., 2023; Väli et al., 2013) and temperature increase (e.g., Carstensen et al., 2014a). Water temperature also defines the DO saturation concentration. During the stratified season, the oxygen content in the deep layer is determined by oxygen consumption, the flux of oxygen due to physical processes, and the length of the stratified period (e.g., Conley et al., 2009; Lennartz et al., 2014). Thus, oxygen depletion compared to an initial state (e.g. saturation concentration) in a sub-surface water mass of a basin is defined by the amount of DO consumed by organic matter degradation and respiration, oxygen advected to the area, and oxygen vertically diffused to the layer in question (Eq. 1; units are mg L<sup>-1</sup> per day, month or another period).

$$DO_{depletion} = DO_{consumption} - DO_{advection} - DO_{diffusion} \quad (1)$$

If DO consumption is not measured directly, Eq. 1 can be used for its estimation, where DO depletion is calculated based on consecutive oxygen measurements and DO advection and diffusion are estimated based on registered vertical and horizontal distributions of DO concentrations and other parameters. In the case of autumn-winter convection, DO diffusion overrules all other terms on the right side of Eq. 1, but during a stratified period, turbulent diffusive flux can be estimated using a simple gradient formula, as

$$F_{diff} = -k \frac{\partial DO}{\partial z}, \text{ where } k = \frac{\alpha}{N}, \quad (2)$$

the empirical intensity factor of turbulence ( $\alpha$ ) is a constant (1.5 10<sup>-7</sup> m<sup>2</sup> s<sup>-2</sup>) and Väisälä frequency ( $N$ ) is a measure of the vertical stratification strength

$$N^2 = -\frac{g}{\rho_0} \frac{\partial \rho}{\partial z} \quad (3)$$

To find the change in DO concentration due to diffusion ( $DO_{diffusion}$ ), diffusive flux ( $F_{diff}$ ) has to be multiplied by the surface area and divided by the volume of the water layer. Thus, in the case of a near-bottom layer, the change depends on its thickness, while in an intermediate layer, the difference in fluxes through the upper and lower borders and the thickness are considered.

Characteristic values of  $DO_{diffusion}$  for the intermediate layer 50-60 m in the GOF were -0.16 mg L<sup>-1</sup> month<sup>-1</sup> (mean value in May-September 2016, Paper I) and for the 9.5-12.0 m thick bottom layer in the GOR 0.50-1.05 mg L<sup>-1</sup> month<sup>-1</sup> (estimates for April-August 2018, Paper II). A negative value in the GOF example indicates that DO was transported out of the layer – the downward flux out of the layer was larger than the flux into the layer from above.

To find the amount of DO advected to the area in question, the change in salinity due to advection is estimated and a relationship between subsurface salinity and oxygen concentrations is applied. In the subsurface layer in the GOF, the salinity advection

( $S_{advection}$ ) was estimated based on the temporal change of salinity ( $S_{change}$ ) minus the salinity diffusion ( $S_{diffusion}$ ) (Eq. 4). This salinity advection was then multiplied by the coefficient of the linear regression between salinity and oxygen ( $a$ ) to get the oxygen advection estimate ( $DO_{advection}$ ).

$$S_{advection} = S_{change} - S_{diffusion}; DO_{advection} = S_{advection} * a \quad (4)$$

The oxygen advection in the near-bottom layer in the GOR was estimated, assuming that the water exchange mostly occurs via the Irbe Strait and it takes 1-1.5 months for inflowing waters to reach the central gulf (Paper II). Measured salinities in the inflowing waters and near-bottom waters of the central GOR and the estimated change in salinity due to diffusion allowed estimating the proportion ( $p$ ) of inflowing waters in the near-bottom water at the next time step. This proportion was used to estimate DO change due to advection as

$$DO_{advection} = (DO_{114}^{t_1} - DO_{G1}^{t_1}) * p; \text{ where } p = \frac{(S_{G1}^{t_2} - S_{diffusion}) - S_{G1}^{t_1}}{S_{114}^{t_1} - S_{G1}^{t_1}} \quad (5)$$

and where  $t_1$  and  $t_2$  are the consecutive time steps of monitoring and 114 and G1 denote monitoring stations in the Irbe Strait and the central GOR, respectively (see Fig. 1, Paper II).

The average DO advection was estimated at 0.28 mg L<sup>-1</sup> month<sup>-1</sup> to the intermediate layer 50-60 m in the GOF (May-September 2016, Paper I) and 0.80 mg L<sup>-1</sup> month<sup>-1</sup> to the near-bottom layer in the GOR (April-August 2018, Paper II).

Considering the measured oxygen depletion of 0.70 mg L<sup>-1</sup> month<sup>-1</sup> and the estimated advection and diffusion, DO in the intermediate layer of 50-60 m in the central GOF was consumed on average by 0.82 mg L<sup>-1</sup> month<sup>-1</sup> in the summer of 2016 (Paper I). In the ~10 m thick near-bottom layer of the GOR, the mean consumption value of 3.79 mg L<sup>-1</sup> month<sup>-1</sup> was found in April-August 2018 (Paper II).

The proportions of advection and diffusion are quite similar in both basins compared to the consumption rates. However, in the intermediate layer of the GOF, diffusion lowers the DO concentrations since oxygen is being diffused out of the layer to deeper areas faster than brought into this layer from above. In the GOR near-bottom layer, the diffusion process brings more DO to the near-bottom layer and, therefore, counteracts the consumption. Based on some previous studies, the consumption rates in the Baltic Sea are estimated at 0.25 mg L<sup>-1</sup> month<sup>-1</sup> (> 62m in the Baltic Proper in 1957-1982; Rahm 1987), 1.29 mg L<sup>-1</sup> month<sup>-1</sup> (in Öresund in 1965-1989; Mattsson and Stigebrandt 1993), and 0.51 mg L<sup>-1</sup> month<sup>-1</sup> (> 65m in the Bornholm Basin 1957-2011; Stigebrandt and Kalén 2013). Thus, the GOF intermediate layer estimates from the present study are comparable with the earlier studies, while the near-bottom layer GOR estimates are significantly larger. The latter could be related to the higher consumption rates at the sediment surface than in the water column.

### 3.2.2 The drivers of long-term changes in the Eastern Gulf of Finland

The temporal aspect should always be considered when interpreting the observed long-term changes in oxygen conditions. In the Baltic Sea, hydrographic conditions change on the scale of a few decades (Lehmann et al., 2022). The cooccurring trends or oscillations of salinity and oxygen have been observed in the central Baltic (Fonselius & Valderrama, 2003) and in the GOF (Stockmayer & Lehmann, 2023). Similar patterns were

shown in the eastern GOF, using long-term data since the early 1900s (Paper III). The significant negative correlation of oxygen and salinity in the 40-70m layer (Fig. 4) expressed in the opposite oscillatory long-term variability in oxygen and salinity (Fig. 3) supports the idea that low oxygen conditions in the EGOF sub-surface layer are strongly affected by changes in hydrography (Paper III). Considering the changes of stratification in the GOF area during the last 30-35 years (Paper III, Liblik & Lips, 2019) and the missing correlation between nutrient inputs and oxygen conditions for this period (Paper III), it can be suggested that the decreasing DO concentrations in the time-frame of a few recent decades have been more influenced by the changes in hydrographic conditions than eutrophication.

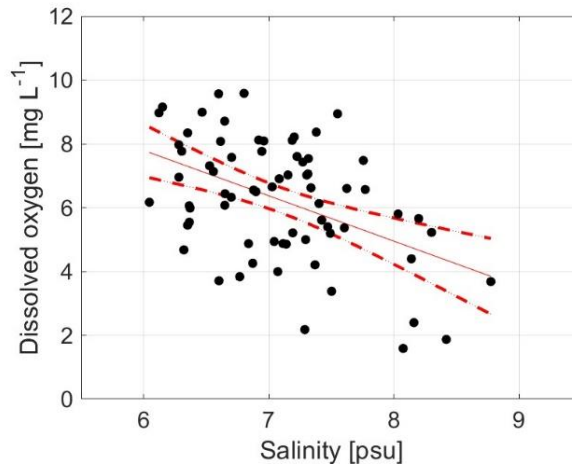


**Figure 4.** Scatter plot and linear regression ( $y = 1.42x + 16.33$ ,  $R^2 = 0.21$ ,  $p$ -value  $< 0.01$ ,  $N = 70$ ) line between salinity and oxygen in July-October in the 40-70m layer of the Eastern Gulf of Finland in 1905-2021. Regression line is shown by the red solid line; red dashed lines indicate the ranges of the 95% confidence level (Paper III).

In the Western Gulf of Finland, the deep layer DO conditions are more controlled by the lateral movements of the salt wedge compared to the EGOF since further east, the halocline is not strong and winter mixing could improve oxygen conditions. But there are occasions, when strong westerlies can cause the wintertime collapse of stratification also in the west (Liblik et al., 2013; Lips et al., 2017).

In the long term (1905-2021), salinity has no visible trend in the EGOF, and thus the deteriorating oxygen conditions cannot be explained by the influence of the changes in hydrographic conditions (Paper III). Considering the estimated proportion of the DO solubility decrease of 26% in the total DO decline since the early 1900s, the other factors (e.g. nutrient inputs, intensification of oxygen consumption due to the temperature increase) should have caused the rest of the decrease in DO concentrations. It is suggested that with the temperature increase of 0.78 °C in the deep water, respiration could increase by 29% (Bothnian Sea, 1992-2012, Ahlgren et al., 2017). Studies in the Chesapeake Bay have suggested that the observed increase in the hypoxic area due to climate warming can be assigned to the changes in DO solubility (55%), biological rates (33%) and stratification (11%) (Tian et al., 2022). More recently (in the last 30 years), when a clear salinity increase is evident in the sub-surface layer, the changes in



hydrographic conditions account for 22% (12-32%) of the DO decline (Paper III). Assuming a 17% DO solubility decrease, the proportion of other effects contributing to the DO decrease is almost the same in the last 30 years as in the long-term (Paper III).

### **3.2.3 Physical processes influencing hypoxia occurrence in the Gulf of Riga**

In the sill separated relatively shallow GOR, the water column gets mixed to the bottom in winter, similarly to the EGOF. However, during the productive (stratified) season, inflows from the Eastern Gotland Basin via the Irbe Strait (Lilover et al., 1998; Skudra & Lips, 2017) can bring additional oxygen into the GOR deep layer. It has been shown that northerly winds can induce upwelling near the Irbe Strait, forcing the inflows (Raudsepp & Kõuts, 2001). The wind influenced spreading of oxygenated and more saline water through the Irbe Strait is well demonstrated using May to July section data from 2018 (Paper II). In Fig. 5, a decrease in the cumulative wind stress and negative values in the wind stress denote the N-NE winds and in Fig 6, an inflow over the sill is well seen. These inflows bring more oxygen to the central GOR, but also strengthen the haline stratification of the deep layer. Thus, the inflows can decrease vertical mixing and promote the decline of DO concentrations (Paper II). Also, a proportion of the inflowed oxygen gets consumed and mixed already on the way to the central area, which decreases the ventilation effects notably (Paper IV). If a relatively thin-layered stratification develops, oxygen is depleted faster (Paper II), since most of the consumption takes place on the sediment surface (Boynton et al., 2018).

Also, when the stratified season is longer than usual, low oxygen conditions can prevail, even when there is no distinct stratification in the deep layer (Paper II). For example, the lack of a strong deep layer stratification was observed in 2015 in the GOR that could be a result of no inflows in the summer. Estimating the diffusive flux and considering a similar consumption rate as in 2018, it was shown that hypoxia could have developed in the central gulf by late October, 2015, which was also proved by observations. On the other hand, when wind forcing and temperature follow the long-term averages, the deep layer oxygen conditions remain above hypoxic levels (Fig. 7, Paper II). For example, in 2017, when no hypoxia was detected, the air temperatures were close to long-term means and the thermal stratification was not enhanced. Also, no strong N-NE wind events were observed early in the productive season, which could have separated the NBL from the water column above as in 2018. It is suggested that in the co-occurrence of certain forcing factors/conditions the probability of hypoxia occurrences in the gulf increases.

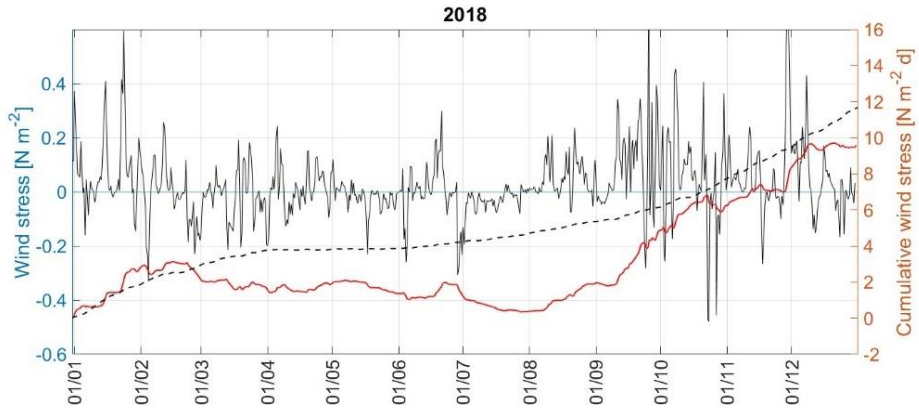


**Figure 5.** Time series of along-coast (NNE–SSW) component of wind stress  $\tau_{NNE}$  (solid black line) and cumulative wind stress in 2018 (solid red line, 6 h moving average is shown). Average cumulative wind stress curve for 1979–2018 is shown in black dashed line. Data were extracted from the ERA5 grid point outside the gulf of Riga (see Fig. 1, Paper II).

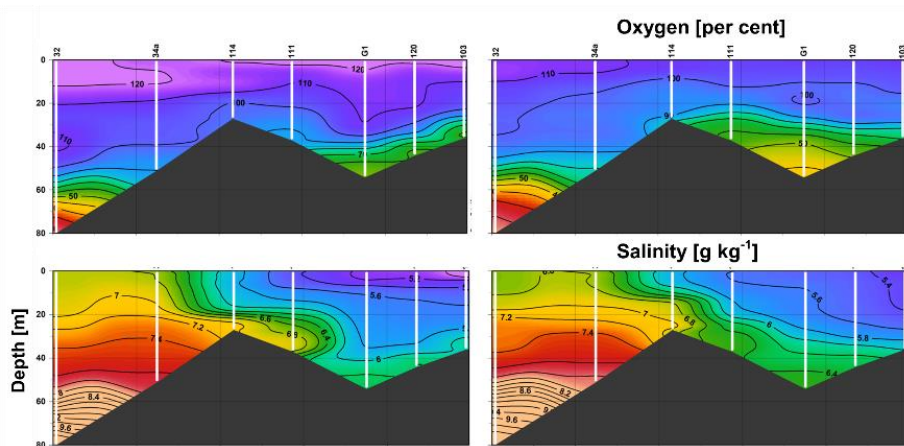


**Figure 6.** Vertical sections of oxygen saturation (top) and salinity (bottom) on 30 May (left) and 11 July (right) (Paper II).

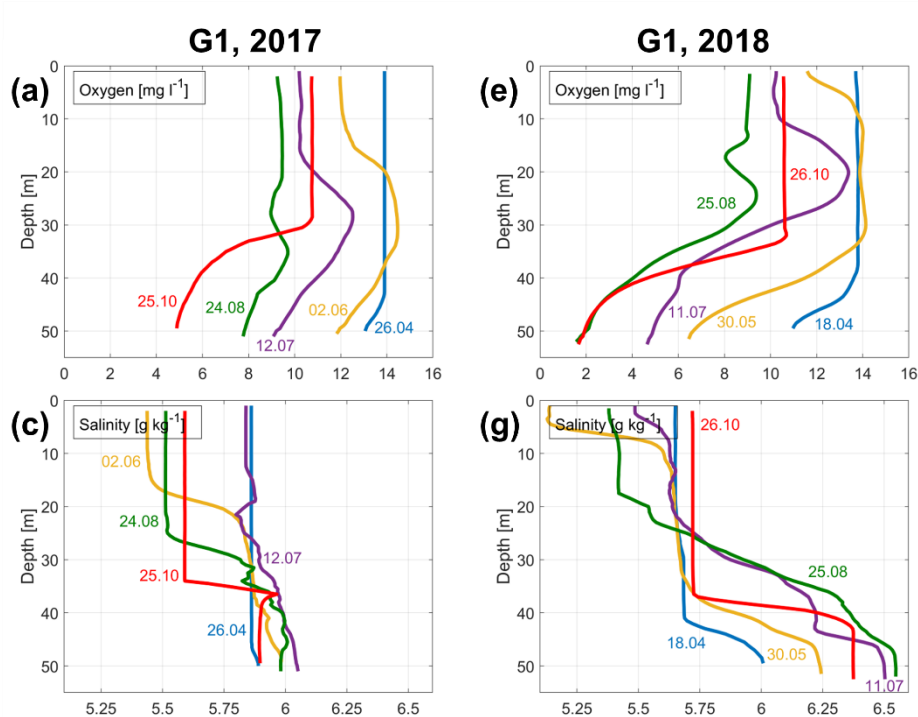


**Figure 7.** Vertical profiles of dissolved oxygen concentration (top) and salinity (bottom) measured in the Ruhnu Deep (station G1) in 2017 (left) and 2018 (right) (Paper II).

### 3.2.4 High-resolution oxygen variability

Although the seasonal decline in oxygen conditions can be determined using sparse regular monitoring data, the short-term variability in DO concentrations is only revealed when using high-frequency monitoring data (Fig. 8, Paper I and IV). Short-term variability can be divided into changes on a synoptic scale (ranging from a day to a week) and occurring in a few hours to days (Paper IV). An example of a synoptic scale variability was observed in the GOR starting from 29 August 2021 and lasting a few days, where a strong SW wind event enhanced vertical mixing and caused the simultaneous salinity decrease and oxygen increase in the deep layer (Paper IV). Changes happening from hours to days were described as being influenced by e.g., inertial oscillations and pycnocline movements (Paper IV).

Since DO concentrations are shown to change rapidly (Paper I, IV), it is important to keep it in mind when estimating the status, based on oxygen. Based on the high-resolution measurements, the monthly standard deviations of DO concentrations ranged from 0.67 to 2.82  $\text{mg L}^{-1}$ , and the estimated consumption rates between 1.20 to 3.33  $\text{mg L}^{-1} \text{ month}^{-1}$ . It is concluded that when estimating DO consumption rates based on single measurements apart a month, the error could be > 50% (Paper IV).

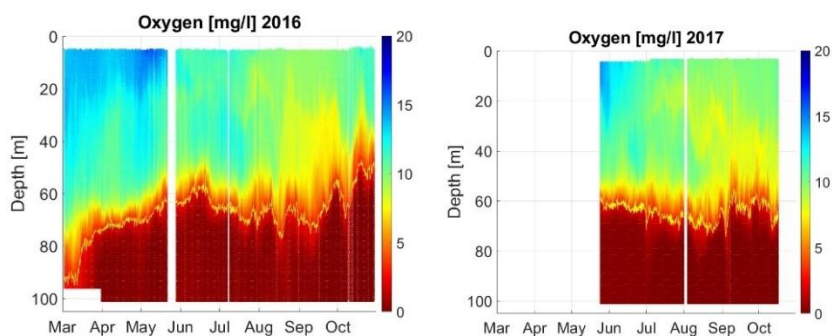


**Figure 8.** Temporal variability of vertical distributions of dissolved oxygen concentrations at the Keri bottom-mounted station in the GOF in 2016 and 2017. The yellow line shows the hypoxic ( $DO = 2.9 \text{ mg L}^{-1}$ ) boundary (Paper I).

### 3.3 Oxygen-based indicators for assessing eutrophication status

Baltic Sea countries have agreed a harmonized system to assess the status of the marine environment in order to devise measures to tackle eutrophication related negative anthropogenic effects. This MSFD (2008/56/EC) derived assessment system, focuses on nutrients, chlorophyll-a levels, cyanobacterial blooms, water transparency, and near-bottom oxygen conditions and/or bottom fauna.

In the HELCOM holistic assessments before HOLAS III, oxygen conditions were only assessed in deeper open sea basins, where a permanent halocline exists. But the work to develop additional indicators that could be also applied in shallower areas was ongoing and for the third holistic assessment, some pre-core oxygen indicators were proposed (e.g., Paper III).

#### 3.3.1 Oxygen debt

In Paper I, the oxygen debt indicator was tested with modified methods to better suit the GOF area. Originally, the oxygen debt indicator was calculated as the volume-based average of missing oxygen relative to the fully saturated water column below the halocline, using data from the entire year in EGB, NBP and GOF (HELCOM, 2013). Since the halocline could be weak or even absent in winter in the GOF (Liblik et al., 2013; Lips et al., 2017), it was suggested to assess the GOF separately and use data only from the stratified season (Paper I). For instance, in the beginning of March 2016, halocline was very deep in the central GOF, and the oxygen debt values were quite low, indicating strong vertical mixing and a westward movement of the salt wedge during the preceding winter (Paper I). This also suggests to reconsider the uniform threshold value of the indicator in all central basins of the Baltic Sea and GOF.

Another option is to assess oxygen debt just below the halocline, making the use of a single threshold more reasonable (Paper I). The May-October average oxygen debt value in the central GOF immediately below the halocline was  $11.3 \text{ mg L}^{-1}$  in 2016 and  $11.6 \text{ mg L}^{-1}$  in 2017 (Paper I). Despite the shallower position of the halocline and larger area with low-oxygen waters in 2016 than in 2017, the proposed method of calculating oxygen debt gave similar results for both years. In the last HELCOM assessment, the Baltic Proper assessment unit (which includes the GOF) results for 2016 and 2017 were  $12.95 \text{ mg L}^{-1}$  and  $12.49 \text{ mg L}^{-1}$ , respectively (HELCOM, 2023c). Thus, the proposed approach of considering the oxygen debt just below the halocline minimizes the impact of changes in hydrographic conditions.

### 3.3.2 Oxygen consumption

The decrease in DO concentrations due to eutrophication can be assessed by estimating the amount of oxygen consumed in the water column during a given period – a month or a season. DO consumption was estimated in the water layer between the seasonal thermocline and halocline in the GOF (Paper I) and in the near-bottom layer of the GOR (Paper II). The confidence of the estimated amounts of consumed DO depends on the availability of oxygen data and adequacy of the methods of calculating advection and diffusion fluxes.

The consumption estimates in the intermediate layer of the GOF in May-September were  $0.82 \text{ mg L}^{-1} \text{ month}^{-1}$  and  $0.31 \text{ mg L}^{-1} \text{ month}^{-1}$  for 2016 and 2017, respectively (Paper I). Based on the 2016 estimates, about 35% of DO consumed was advected into the area. Vertical diffusion contributed to oxygen depletion – amounting to about 20% of DO consumption. In 2017, these proportions of advection and diffusion were equal for the same period in 2016. However, when calculating the advection impact using the relationship between oxygen and salinity, consumption estimates could be biased when a unidirectional flow prevails in the selected sub-surface layer (Paper I).

For the GOR near-bottom layer, an average consumption rate of  $3.79 \text{ mg L}^{-1} \text{ month}^{-1}$  was found in 2018. Diffusion and advection did have a similar impact, both bringing, on average, ~20% of the DO consumed (Paper II). This result is higher than the estimates for the Baltic Proper (Koop et al., 1990) and the Gulf of Finland (Conley et al., 1997). It is found, that consumption rates have accelerated recently in the Baltic Proper area due to the increase in organic matter in the ventilating water originating from the surface (Meier et al., 2018). However, the main reason of the estimated high consumption rate in the near-bottom layer of the GOR could be related to the intense consumption at the sediment surface (Boynton et al., 2018).

### 3.3.3 The extent of low oxygen water

Considering the strong correlation between salinity and oxygen in the GOF (Papers I and III), a method was proposed to reduce the impact of changes in hydrographic conditions on the oxygen-based status assessments. For this, the measured oxygen values were adjusted, considering the salinity differences in the reference and the assessment periods. The developed indicator results showed a decrease in area/volume estimates in the EGOF, when measured salinities were higher than in the reference period (Paper III). For example, in 2016-2021, the volume of water with  $\text{DO} \leq 6 \text{ mg L}^{-1}$  was 16.0% of the total EGOF volume, but using the salinity correction method, the estimate was 13.4%.

The suggested method assumed a linear relationship between salinity and oxygen, although this would not be the case when considerable weakening or even a collapse of the stratification occurs. Therefore the proposed method does not remove the potential hydrographic effects completely, which is well observed (Paper III) in a weakly stratified period from the mid-1980s to the mid-1990s (Liblik & Lips, 2011). During this period, the vertical mixing was intense enough to mask the eutrophication effects in the near-bottom layer. Thus, the applied approach is applicable within certain limits of characteristic stratification conditions in this estuary (and other similar sub-basins).

The extent of low-oxygen waters, e.g., the area influenced by hypoxic conditions, can be estimated using high-resolution autonomous measurements. It was tested whether the autonomous profiling station Keri, which has the central position in the GoF (see Fig. 1, Paper I), can be used to represent the entire gulf (Paper I). An along-gulf inclination of the hypoxic border of 1.9 m per 100 km was found based on the ship-borne vertical

profiles of DO covering almost the entire deep part of the gulf. It was shown that the area and volume estimates of hypoxic waters using Keri data differed only by < 2 % and < 0.5 %, respectively, if the estimates were made assuming an inclined or a levelled hypoxia border (Paper I). Although these hypoxic area and volume estimates are not directly applicable as a eutrophication indicator, since other factors also influence oxygen conditions, they are very valuable and offer the opportunity to assess the temporal extent of hypoxia/anoxia influencing bottom fauna and the phosphorus fluxes.

### 3.4 Considering future projections

Future projections see increased air temperatures in the Baltic Sea area, especially in the northern part (Meier et al., 2022). Increasing temperatures affect the precipitation/river runoff regime, strengthen stratification and decrease DO solubility, and thus, can influence the extent of hypoxia (Almroth-Rosell et al., 2021; Meier et al., 2011). Precipitation is expected to increase in the whole Baltic Sea catchment area in winter and spring and also in summer in the northern areas (Christensen et al., 2022). The expected increase in wintertime runoff, due to intermittent melting (Stonevičius et al., 2017), would bring more nutrients and organic matter to the sea (Yurkovskis, 2004). It was suggested that the exceptionally large runoff values influence the development of hypoxia in the GOR, by bringing more nutrients to the gulf (Paper II). Although the decrease in riverine nutrient inputs could lead to reduced nutrient conditions in the marine environment (Friedland et al., 2021), the increase in water temperature can counteract the nutrient load reduction measures (Meier et al., 2012).

The projected strengthening of vertical stratification is influenced by the increase in sea surface temperatures (Gröger et al., 2019; Meier & Saraiva, 2020; Saraiva et al., 2019). In Paper II, the occurrence of a strong thermal stratification was suggested to be one of the factors favoring the development of hypoxia in the GOR.

Wind projections in the Baltic Sea area are uncertain (Christensen et al., 2015), but a slight decrease in wind speed is expected (Ruosteenoja et al., 2019), which would reduce vertical mixing and enhance stratification even more (Paper II).

Considering all the projected changes, mostly related to temperature (and runoff) increase, the increase and severity of low oxygen conditions in the deeper areas of stratified estuaries could be expected until the effect of nutrient decreases becomes evident. The latter is a delayed process, especially when considering the internal input of phosphorus. Du et al. (2018) suggested that the climate change affected worsened physical conditions in the Chesapeake Bay will amplify the eutrophication related human-induced adverse effects, and thus further reduction of nutrient inputs is needed to improve water quality. According to the latest HELCOM assessments, the nutrient inputs have decreased in most of the sub-basins (with the exception of total nitrogen in the GOR) (HELCOM, 2023b). Although the inputs have mostly decreased, the surface layer concentrations of nutrients do not always exhibit a correlating response. The majority of central and northern basins of the Baltic Sea, including the GOF and GOR, show a statistically significant increase in surface layer phosphates (HELCOM, 2023a). In the central GOR, the increase in phosphate concentrations with the development of hypoxia was observed in the near-bottom layer in 2018 from spring to late summer (Paper II). The sediment release of phosphates, estimated at up to  $13.5 \mu\text{mol m}^{-2} \text{h}^{-1}$ , was large enough to maintain the observed increase in concentrations, despite the physical processes (advection and diffusion) counteracting this flux. The obtained estimate of the sediment release of phosphates is similar to earlier studies done in the GOR (Aigars et al., 2015; Eglite et al., 2014) and the GOF (Pitkänen et al., 2001).

## 4 CONCLUSIONS

The historical excess amounts of nutrient inputs, although decreased nowadays, still influence the eutrophication status of marine areas due to accumulation in the environment and the changing nutrient cycles in the sea, e.g. the internal load of phosphates. Climate change, together with eutrophication, can have even more deteriorating effects on the marine environment.

A good indication of the level of marine eutrophication is the oxygen content below the euphotic layer. With more nutrient inputs and increased primary production, the oxygen content in the deeper layer decreases due to enhanced respiration and degradation processes, which can be referred to as consumption. Increasing temperature affects the oxygen content by decreasing the water's ability to hold oxygen and strengthening thermal stratification that restricts vertical mixing. Also, the increasing temperature enhances the respiration rates, thus contributing even more to the decreasing oxygen concentrations.

Physical processes, such as lateral advection and vertical diffusion, also influence oxygen content in the aphotic layer. In the case of strong stratification, the deep layer is separated from the water column above, and less oxygen can be brought to deeper areas. In certain wind conditions, oxygen conditions can be improved or deteriorated. For instance, in the Gulf of Finland, SW winds support the westward movement of the deoxygenated salt wedge, thus locally improving near-bottom (deep-layer) oxygen conditions. N-NE winds, however, support the up-estuary movement of the salt wedge in the Gulf of Finland. In the Gulf of Riga, northerly winds cause the inflow of saltier water from the Northern Baltic Proper, bringing oxygenated waters to the gulf's deep layer, but also strengthening the stratification, decreasing the vertical oxygen flux and increasing the probability of hypoxia occurrences.

Long-term data from this study show that oxygen concentrations have decreased in the Eastern Gulf of Finland since the early 1900s. Oxygen decline has been even more steep in recent decades. In the Eastern Gulf of Finland, the observed oxygen decline on a ~100-year scale cannot be explained by the changes in hydrographic conditions. Temperature increase effects, including the decrease in oxygen saturation concentration and the increase in respiration rate, contributed roughly 50% to this long-term oxygen decline. In the last ~30 years, the changes in hydrographic conditions, seen as the increased deep-layer salinity, and the temperature effects could together contribute roughly the same proportion to the oxygen decline as in the long term. Thus, the effect of other factors (including eutrophication) contributing to the oxygen decline has recently been almost the same as well.

In the Gulf of Riga, a decline in oxygen conditions was shown in earlier works, and a further decrease in near-bottom oxygen in autumn was revealed in this study. The latter could be related to the prolonged season with the stratified water column in recent years. It was suggested that the co-occurrence of certain conditions increases the probability of hypoxia occurrences in the gulf. Increased temperature in the surface layer in summer enhances thermal stratification, near-bottom inflows separate the bottom layer from the layers above, and large river runoff before the productive season brings more nutrients – all these factors contribute to the oxygen decline. The aforementioned factors influence oxygen conditions on a longer time scale, but oxygen variability also depends on short-term processes, e.g., inertial oscillations, (sub)mesoscale processes, deep layer currents, and pycnocline movements, which can change the conditions for a few hours or even days.

To assess the eutrophication status of the marine environment, oxygen-based indicators are developed. These indicators should concentrate on the proportion of anthropogenic impacts on the oxygen decline. For instance, oxygen consumption (rate) in the sub-surface layers can be used as a eutrophication proxy. It can be assessed by monitoring oxygen depletion and estimating the contribution of physical processes (diffusion and advection) to the changes in oxygen content. The effect of diffusion and advection on the changes in oxygen concentrations during the productive season in the Gulf of Finland and the Gulf of Riga had a similar contribution, which was roughly 20% of the change due to consumption.

Advection estimates in the Gulf of Riga rely on the assumption that throughout the assessment period, some degree of lateral inflow to the gulf's central area occurs via the Irbe Strait. Based on the Gulf of Riga consumption rate estimates, it is concluded that in conditions of weaker stratification but longer stratified season, near-bottom hypoxia can still develop. The observed inflow events through the Irbe Strait only slightly ventilated the low-oxygen conditions in the central Gulf of Riga, because mixing with the oxygen-depleted water of Gulf of Riga and local consumption decreased the nearly saturated inflow water to only slightly higher levels than observed in the central gulf.

Another option is to use the oxygen debt indicator, which can be applied in an area with a permanent halocline. In the shallower Eastern Gulf of Finland, an approach was developed to remove the influence of changing hydrographic conditions on the status assessment results. The analysis showed that in periods of relatively strong vertical stratification, the method reduces the hydrography effect on the assessment result. However, in periods of very weak stratification, deep-layer oxygen conditions are not the best indication of eutrophication status.

Whatever approach is used to assess the eutrophication status, an effort has to be made to remove the natural variations from the assessment results. Also, there is a strong need for high-frequency measurements due to the high temporal variability of oxygen conditions. It was suggested that regular monitoring conducted on a monthly or bi-monthly basis could have an assessment error of 50%.

Considering the future climate change projections, it is anticipated that the frequency and extent of hypoxia will likely increase. Also, since the internal load of phosphorus is linked to near-bottom oxygen conditions, this scenario does not predict a fast decrease in nutrient concentrations.



## REFERENCES

- Ahlgren, J., Grimvall, A., Omstedt, A., Rolff, C., & Wikner, J. (2017). Temperature, DOC level and basin interactions explain the declining oxygen concentrations in the Bothnian Sea. *Journal of Marine Systems*, 170, 22–30. <http://dx.doi.org/10.1016/j.jmarsys.2016.12.010>
- Aigars, J., Poikāne, R., Dalsgaard, T., Eglīte, E., & Jansons, M. (2015). Biogeochemistry of N, P and SI in the Gulf of Riga surface sediments: Implications of seasonally changing factors. *Continental Shelf Research*, 105, 112–120.
- Alenius, P., Myrberg, K., & Nekrasov, A. (1998). The physical oceanography of the Gulf of Finland: a review. *Boreal Environment Research*, 3(January), 97–125.
- Almroth-Rosell, E., Wählström, I., Hansson, M., Väli, G., Eilola, K., Andersson, P., Viktorsson, L., Hieronymus, M., & Arneborg, L. (2021). A Regime Shift Toward a More Anoxic Environment in a Eutrophic Sea in Northern Europe. *Frontiers in Marine Science*, 8. <https://doi.org/10.3389/fmars.2021.799936>
- Astok, V., Otsmann, M., & Suursaar, Ü. (1999). Water exchange as the main physical process in semi-enclosed marine systems: the Gulf of Riga case. *Hydrobiologia*, 393. <https://doi.org/10.1023/A:1003517110726>
- Berzinsh, V. (1995). Hydrology. In E. Ojaveer (Ed.), *Ecosystem of the Gulf of Riga between 1920-1990* (pp. 7–31). Estonian Academy Publishers.
- Boesch, D. F., Coles, V. J., Kimmel, D. G., & Miller, W. D. (2007). Ramifications of climate change for Chesapeake Bay hypoxia. In K. Ebi, G. Meehl, M. Blanchet, R. Twilley, & D. Boesch (Eds.), *Regional Impacts of Climate Change: Four Case Studies in the United States* (pp. 57–70). Pew Center on Global Climate Change. <https://www.c2es.org/site/assets/uploads/2007/12/regional-impacts-climate-change-four-case-studies-united-states.pdf>
- Boynton, W. R., Ceballos, M. A. C., Bailey, E. M., Hodgkins, C. L. S., Humphrey, J. L., & Testa, J. M. (2018). Oxygen and Nutrient Exchanges at the Sediment-Water Interface: a Global Synthesis and Critique of Estuarine and Coastal Data. *Estuaries and Coasts*, 41(2), 301–333. <https://doi.org/10.1007/s12237-017-0275-5>
- Carstensen, J., Andersen, J. H., Gustafsson, B. G., & Conley, D. J. (2014a). Deoxygenation of the Baltic Sea during the last century. *P Natl Acad Sci USA*, 111(15), 5628–5633. <http://www.pubmedcentral.nih.gov/articlerender.fcgi?artid=3992700&tool=pmc-entrez&rendertype=abstract>
- Carstensen, J., Conley, D. J., Bonsdorff, E., Gustafsson, B. G., Hietanen, S., Janas, U., Jilbert, T., Maximov, A., Norkko, A., Norkko, J., Reed, D. C., Slomp, C. P., Timmermann, K., & Voss, M. (2014b). Hypoxia in the Baltic Sea: Biogeochemical cycles, benthic fauna, and management. *Ambio*, 43(1), 26–36. <http://link.springer.com/article/10.1007%2Fs13280-013-0474-7>
- Christensen, O. B., Kjellström, E., Dieterich, C., Gröger, M., & Meier, H. E. M. (2022). Atmospheric regional climate projections for the Baltic Sea region until 2100. *Earth System Dynamics*, 13(1), 133–157. <https://doi.org/10.5194/esd-13-133-2022>
- Christensen, O. B., Kjellström, E., & Zorita, E. (2015). in Second Assessment of Climate Change for the Baltic Sea Basin. In BACC II Author Team (Ed.), *Second Assessment of Climate Change for the Baltic Sea Basin* (pp. 217–233). Springer International Publishing.

- Conley, D. J., Björck, S., Bonsdorff, E., Carstensen, J., Destouni, G., Gustafsson, B. G., Hietanen, S., Kortekaas, M., Kuosa, H., Meier, H. E. M., Müller-Karulis, B., Nordberg, K., Norkko, A., Nürnberg, G., Pitkänen, H., Rabalais, N. N., Rosenberg, R., Savchuk, O. P., Slomp, C. P., ... Zillén, L. (2009). Hypoxia-Related Processes in the Baltic Sea. *Environ. Sci. Technol.*, 43(10), 3412–3420. <http://pubs.acs.org/doi/abs/10.1021/es802762a>
- Conley, D. J., Carstensen, J., Aigars, J., Axe, P., Bonsdorff, E., Eremina, T., Haahti, B.-M., Humborg, C., Jonsson, P., Kotta, J., Lännegren, C., Larsson, U., Maximov, A., Medina, M. R., Lysiak-Pastuszek, E., Remeikaitė-Nikienė, N., Walve, J., Wilhelms, S., & Zillén, L. (2011). Hypoxia Is Increasing in the Coastal Zone of the Baltic Sea. *Environmental Science & Technology*, 45(16), 6777–6783. <https://doi.org/10.1021/es201212r>
- Conley, D. J., Humborg, C., Rahm, L., Savchuk, O. P., & Wulff, F. (2002). Hypoxia in the Baltic Sea and Basin-Scale Changes in Phosphorus Biogeochemistry. *Environ. Sci. Technol.*, 36, 5315–5320. <http://pubs.acs.org/doi/pdf/10.1021/es025763w>
- Conley, D. J., & Johnstone, R. W. (1995). Biogeochemistry of N, P and Si in Baltic Sea sediments: response to a simulated deposition of a spring diatom bloom. *Marine Ecology Progress Series*, 122, 265–276.
- Conley, D. J., Stockenberg, A., Carman, R., Johnstone, R. W., Rahm, L., & Wulff, F. (1997). Sediment-water Nutrient Fluxes in the Gulf of Finland, Baltic Sea. *Estuarine, Coastal and Shelf Science*, 45(5), 591–598.
- Diaz, R. J., & Rosenberg, R. (2008). Spreading Dead Zones and Consequences for Marine Ecosystems. *Science*, 321(5891), 926–929. <https://doi.org/10.1126/science.1156401>
- Du, J., Shen, J., Park, K., Wang, Y. P., & Yu, X. (2018). Worsened physical condition due to climate change contributes to the increasing hypoxia in Chesapeake Bay. *Science of The Total Environment*, 630, 707–717. <https://doi.org/https://doi.org/10.1016/j.scitotenv.2018.02.265>
- Eglīte, E., Lavrinovičs, A., Müller-Karulis, B., Aigars, J., & Poikāne, R. (2014). Nutrient turnover at the hypoxic boundary: flux measurements and model representation for the bottom water environment of the Gulf of Riga, Baltic Sea. *Oceanologia*, 56(4), 711–735.
- Elken, J., Raudsepp, U., & Lips, U. (2003). On the estuarine transport reversal in deep layers of the Gulf of Finland. *Journal of Sea Research*, 49, 267–274.
- Directive 2000/60/EC of the European Parliament and of the Council of 23 October 2000 establishing a framework for Community action in the field of water policy, (2000) (testimony of European Parliament and Council). <http://data.europa.eu/eli/dir/2000/60/2014-11-20>
- Directive 2008/56/EC of the European Parliament and of the Council of 17 June 2008 establishing a framework for community action in the field of marine environmental policy (Marine Strategy Framework Directive). *Off. J. Eur. Union L164*, 19–40, (2008) (testimony of European Parliament and Council). <http://data.europa.eu/eli/dir/2008/56/2017-06-07>
- Fonselius, S., & Valderrama, J. (2003). One hundred years of hydrographic measurements in the Baltic Sea. *Journal of Sea Research*, 49(4), 229–241. [https://doi.org/https://doi.org/10.1016/S1385-1101\(03\)00035-2](https://doi.org/https://doi.org/10.1016/S1385-1101(03)00035-2)

- Friedland, R., Macias, D., Cossarini, G., Daewel, U., Estournel, C., Garcia-Gorriz, E., Grizzetti, B., Grégoire, M., Gustafson, B., Kalaroni, S., Kerimoglu, O., Lazzari, P., Lenhart, H., Lessin, G., Maljutenko, I., Miladinova, S., Müller-Karulis, B., Neumann, T., Parn, O., ... Vandenbulcke, L. (2021). Effects of Nutrient Management Scenarios on Marine Eutrophication Indicators: A Pan-European, Multi-Model Assessment in Support of the Marine Strategy Framework Directive. *Frontiers in Marine Science*, 8. <https://doi.org/10.3389/fmars.2021.596126>
- Gröger, M., Arneborg, L., Dieterich, C., Höglund, A., & Meier, H. E. M. (2019). Summer hydrographic changes in the Baltic Sea, Kattegat and Skagerrak projected in an ensemble of climate scenarios downscaled with a coupled regional ocean–sea ice–atmosphere model. *Climate Dynamics*, 53(9), 5945–5966. <https://doi.org/10.1007/s00382-019-04908-9>
- Gustafsson, B. G., Schenk, F., Blenckner, T., Eilola, K., Meier, H. E. M., Müller-Karulis, B., Neumann, T., Ruoho-Airola, T., Savchuk, O. P., & Zorita, E. (2012). Reconstructing the Development of Baltic Sea Eutrophication 1850–2006. *Ambio*, 41, 534–548.
- Hansson, M., & Viktorsson, L. (2021). *REPORT OCEANOGRAPHY No. 72, 2021. Oxygen Survey in the Baltic Sea 2021 - Extent of Anoxia and Hypoxia, 1960-2021*. <https://doi.org/ISSN: 0283-1112>
- HELCOM. (2013). Approaches and methods for eutrophication target setting in the Baltic Sea region. *Balt. Sea Environ. Proc. No. 133*.
- HELCOM. (2018). *State of the Baltic Sea - Second HELCOM holistic assessment 2011-2016*. <http://www.helcom.fi/baltic-sea-trends/holistic-assessments/state-of-the-baltic-sea-2018/reports-and-materials/>
- HELCOM. (2022). *Inputs of nutrients to the sub-basins (2019). HELCOM core indicator report. Online*. <https://doi.org/ISSN 2343-2543>
- HELCOM. (2023a). *Dissolved inorganic phosphorus (DIP). HELCOM core indicator report. Online*. <https://doi.org/ISSN 2343-2543>.
- HELCOM. (2023b). *Inputs of nutrients to the sub-basins (2020). HELCOM core indicator report. Online*. <https://doi.org/ISSN 2343-2543>
- HELCOM. (2023c). *Oxygen debt. HELCOM core indicator report. Online*. <https://doi.org/ISSN 2343-2543>
- Jäntti, H., & Hietanen, S. (2012). The Effects of Hypoxia on Sediment Nitrogen Cycling in the Baltic Sea. *AMBIO*, 41(2), 161–169. <https://doi.org/10.1007/s13280-011-0233-6>
- Koop, K., Boynton, W. R., Wulff, F., & Carman, R. (1990). Sediment-water oxygen and nutrient exchanges along a depth gradient in the Baltic Sea. *Marine Ecology Progress Series*, 63, 65–77.
- Köuts, M., Maljutenko, I., Elken, J., Liu, Y., Hansson, M., Viktorsson, L., & Raudsepp, U. (2021). Recent regime of persistent hypoxia in the Baltic Sea. *Environmental Research Communications*, 3(7), 75004. <https://doi.org/10.1088/2515-7620/ac0cc4>
- Kuliński, K., Rehder, G., Asmala, E., Bartosova, A., Carstensen, J., Gustafsson, B., Hall, P. O. J., Humborg, C., Jilbert, T., Jürgens, K., Meier, H. E. M., Müller-Karulis, B., Naumann, M., Olesen, J. E., Savchuk, O., Schramm, A., Slomp, C. P., Sofiev, M., Sobek, A., ... Undeman, E. (2022). Biogeochemical functioning of the Baltic Sea. *Earth System Dynamics*, 13(1), 633–685. <https://doi.org/10.5194/esd-13-633-2022>
- Laine, A. O., Andersin, A.-B., Leiniö, S., & Zuur, A. F. (2007). Stratification-induced hypoxia as a structuring factor of macrozoobenthos in the open Gulf of Finland (Baltic Sea). *Journal of Sea Research*, 57(1), 65–77. <https://doi.org/10.1016/j.seares.2006.08.003>

- Lehmann, A., Myrberg, K., Post, P., Chubarenko, I., Dailidienė, I., Hinrichsen, H.-H., Hüseyin, K., Liblik, T., Meier, H. E. M., Lips, U., & Bukanova, T. (2022). Salinity dynamics of the Baltic Sea. *Earth System Dynamics*, 13(1), 373–392. <https://doi.org/10.5194/esd-13-373-2022>
- Lehtoranta, J., Savchuk, O. P., Elken, J., Kim, D., Kuosa, H., Raateoja, M., Kauppila, P., Räike, A., & Pitkänen, H. (2017). Atmospheric forcing controlling inter-annual nutrient dynamics in the open Gulf of Finland. *Journal of Marine Systems*, 171, 4–20.
- Lennartz, S. T., Lehmann, A., Herrford, J., Malien, F., Hansen, H.-P., Biester, H., & Bange, H. W. (2014). Long-term trends at the Boknis Eck time series station (Baltic Sea), 1957–2013: does climate change counteract the decline in eutrophication? *Biogeosciences*, 11(22), 6323–6339. <https://doi.org/10.5194/bg-11-6323-2014>
- Liblik, T., Laanemets, J., Raudsepp, U., Elken, J., & Suhhova, I. (2013). Estuarine circulation reversals and related rapid changes in winter near-bottom oxygen conditions in the Gulf of Finland, Baltic Sea. *Ocean Science*, 9, 917–930.
- Liblik, T., & Lips, U. (2011). Characteristics and variability of the vertical thermohaline structure in the Gulf of Finland in summer. *Boreal Environ. Res.*, 16A, 73–83.
- Liblik, T., & Lips, U. (2019). Stratification Has Strengthened in the Baltic Sea – An Analysis of 35 Years of Observational Data. *Front. Earth Sci.*, 7:174. <https://doi.org/10.3389/feart.2019.00174>
- Liblik, T., Naumann, M., Alenius, P., Hansson, M., Lips, U., Nausch, G., Tuomi, L., Wesslander, K., Laanemets, J., & Viktorsson, L. (2018). Propagation of Impact of the Recent Major Baltic Inflows From the Eastern Gotland Basin to the Gulf of Finland. *Frontiers in Marine Science*, 5, 1–23. <https://doi.org/10.3389/fmars.2018.00222>
- Liblik, T., Skudra, M., & Lips, U. (2017). On the buoyant sub-surface salinity maxima in the Gulf of Riga. *Oceanologia*, 59, 113–128.
- Lilover, M.-J., Lips, U., Laanearu, J., & Liljebladh, B. (1998). Flow regime in the Irbé Strait. *Aquatic Sciences*, 60, 253–265.
- Lips, U., Laanemets, J., Lips, I., Liblik, T., Suhhova, I., & Suursaar, Ü. (2017). Wind-driven residual circulation and related oxygen and nutrient dynamics in the Gulf of Finland (Baltic Sea) in winter. *Estuar Coast Shelf S*, 195, 4–15. <https://doi.org/10.1016/j.ecss.2016.10.006>
- Lips, U., Lilover, M.-J., Raudsepp, U., & Talpsepp, L. (1995). Water renewal processes and related hydrographic structures in the Gulf of Riga. In A. Toompuu & J. Elken (Eds.), *Est. Mar. Inst. Rep. Ser.* (pp. 1–34).
- Lips, U., Lips, I., Liblik, T., & Elken, J. (2008). Estuarine transport versus vertical movement and mixing of water masses in the Gulf of Finland (Baltic Sea). 2008 IEEE/OES US/EU-Baltic International Symposium, 1–8. <https://doi.org/10.1109/BALTIC.2008.4625535>
- Ma, J., Li, X., Song, J., Wen, L., Wang, Q., Xu, K., Dai, J., & Zhong, G. (2023). The effects of seawater thermodynamic parameters on the oxygen minimum zone (OMZ) in the tropical western Pacific Ocean. *Marine Pollution Bulletin*, 187, 114579. <https://doi.org/https://doi.org/10.1016/j.marpolbul.2023.114579>
- Mattsson, J., & Stigebrandt, A. (1993). The vertical flux of organic matter in the Öresund estimated by two different methods using oxygen measurements. *Estuarine, Coastal and Shelf Science*, 37, 329–342.

- Meier, H E M, Andersson, H. C., Eilola, K., Gustafsson, B. G., Kuznetsov, I., Müller-Karulis, B., Neumann, T., & Savchuk, O. P. (2011). Hypoxia in future climates: A model ensemble study for the Baltic Sea. *Geophysical Research Letters*, 38(24). <https://doi.org/https://doi.org/10.1029/2011GL049929>
- Meier, H E M, Eilola, K., Almroth-Rosell, E., Schimanke, S., Kniebusch, M., Höglund, A., Pemberton, P., Liu, Y., Väli, G., & Saraiva, S. (2019). Disentangling the impact of nutrient load and climate changes on Baltic Sea hypoxia and eutrophication since 1850. *Clim Dynam*, 53(1), 1145–1166. <https://doi.org/10.1007/s00382-018-4296-y>
- Meier, H E M, Kniebusch, M., Dieterich, C., Gröger, M., Zorita, E., Elmgren, R., Myrberg, K., Ahola, M. P., Bartosova, A., Bonsdorff, E., Börgel, F., Capell, R., Carlén, I., Carlund, T., Carstensen, J., Christensen, O. B., Dierschke, V., Frauen, C., Frederiksen, M., ... Zhang, W. (2022). Climate change in the Baltic Sea region: a summary. *Earth Syst Dynam*, 13(1), 457–593. <https://doi.org/10.5194/esd-13-457-2022>
- Meier, H E Markus, & Kauker, F. (2003). Modeling decadal variability of the Baltic Sea: 2. Role of freshwater inflow and large-scale atmospheric circulation for salinity. *Journal of Geophysical Research: Oceans*, 108(C11). <https://doi.org/https://doi.org/10.1029/2003JC001799>
- Meier, H E Markus, & Saraiva, S. (2020). *Projected Oceanographical Changes in the Baltic Sea until 2100*. Oxford University Press. <https://doi.org/10.1093/acrefore/9780190228620.013.699>
- Meier, H E Markus, Väli, G., Naumann, M., Eilola, K., & Frauen, C. (2018). Recently Accelerated Oxygen Consumption Rates Amplify Deoxygenation in the Baltic Sea. *J Geophys Res-Oceans*, 123(5), 3227–3240. <https://doi.org/https://doi.org/10.1029/2017JC013686>
- Meier, M., Eilola, K., Gustavsson, B. G., Kuznetsov, I., Neumann, T., & Savchuk, O. P. (2012). *Uncertainty assessment of projected ecological quality indicators in future climate* (Oceanografi, Issue 112). SMHI.
- Mohrholz, V. (2018). Major Baltic Inflow Statistics – Revised. *Frontiers in Marine Science*, 5. <https://doi.org/10.3389/fmars.2018.00384>
- Murray, C. J., Müller-Karulis, B., Carstensen, J., Conley, D. J., Gustafsson, B. G., & Andersen, J. H. (2019). Past, Present and Future Eutrophication Status of the Baltic Sea. *Frontiers in Marine Science*, 6. <https://doi.org/10.3389/fmars.2019.00002>
- Petrov, V. (1979). Water balance and water exchange between the Gulf of Riga and the Baltic Proper. *Sbornik Rabot Rizhskoj GO*, 18, 20–40.
- Pitkänen, H., Lehtoranta, J., & Räike, A. (2001). Internal Nutrient Fluxes Counteract Decreases in External Load: The Case of the Estuarial Eastern Gulf of Finland, Baltic Sea. *AMBIO: A Journal of the Human Environment*, 30(4), 195–201. <https://doi.org/10.1579/0044-7447-30.4.195>
- Rabalais, N. N., Turner, R. E., Diaz, R. J., & Justić, D. (2009). Global change and eutrophication of coastal waters. *ICES Journal of Marine Science*, 66(7).
- Rahm, L. (1987). Oxygen consumption in the Baltic Proper. *Limnol. Oceanogr.*, 32(4), 978–978.
- Raudsepp, U., & Elken, J. (1995). Application of the GFDL circulation model for the Gulf of Riga. In: Toompuu, A., Elken, J. (Eds.). *Estonian Marine Institute Report Series*, 1, 143–176.
- Raudsepp, U., & Kõuts, T. (2001). Observations of near-bottom currents in the Gulf of Riga, Baltic Sea. *Aquatic Sciences*, 63, 385–405.

- Reusch, T. B. H., Dierking, J., Andersson, H. C., Bonsdorff, E., Carstensen, J., Casini, M., Czajkowski, M., Hasler, B., Hinsby, K., Hyytiäinen, K., Johannesson, K., Jomaa, S., Jormalainen, V., Kuosa, H., Kurland, S., Laikre, L., MacKenzie, B. R., Margonski, P., Melzner, F., ... Zandersen, M. (2018). The Baltic Sea as a time machine for the future coastal ocean. *Science Advances*, 4(5), eaar8195. <https://doi.org/10.1126/sciadv.aar8195>
- Ruosteenoja, K., Vihma, T., & Venäläinen, A. (2019). Projected Changes in European and North Atlantic Seasonal Wind Climate Derived from CMIP5 Simulations. *Journal of Climate*, 32(19), 6467–6490. <https://doi.org/10.1175/JCLI-D-19-0023.1>
- Saraiva, S., Meier, H. E. M., Andersson, H., Höglund, A., Dieterich, C., Gröger, M., Hordoir, R., & Eilola, K. (2019). Uncertainties in Projections of the Baltic Sea Ecosystem Driven by an Ensemble of Global Climate Models. *Frontiers in Earth Science*, 6, 244. <https://doi.org/10.3389/feart.2018.00244>
- Skudra, M., & Lips, U. (2017). Characteristics and inter-annual changes in temperature, salinity and density distribution in the Gulf of Riga. *Oceanologia*, 59, 37–48.
- Stigebrandt, A., & Kalén, O. (2013). Improving Oxygen Conditions in the Deeper Parts of Bornholm Sea by Pumped Injection of Winter Water. *Ambio*, 42, 587–595.
- Stockmayer, V., & Lehmann, A. (2023). Variations of temperature, salinity and oxygen of the Baltic Sea for the period 1950 to 2020. *Oceanologia*. <https://doi.org/https://doi.org/10.1016/j.oceano.2023.02.002>
- Stonevičius, E., Rimkus, E., Štaras, A., Kažys, J., & Valiuškevičius, G. (2017). Climate change impact on the Nemunas River basin hydrology in the 21st century. *Boreal Environ. Res.*, 22, 49–65.
- Stramma, L., & Schmidtko, S. (2019). Global evidence of ocean deoxygenation. In D. Laffoley & J. M. Baxter (Eds.), *Ocean deoxygenation: everyone's problem. Causes, impacts, consequences and solutions* (pp. 25–36). IUCN, Gland, Switzerland. <https://doi.org/http://dx.doi.org/10.2305/IUCN.CH.2019.13.en>
- Tian, R., Cerco, C. F., Bhatt, G., Linker, L. C., & Shenk, G. W. (2022). Mechanisms Controlling Climate Warming Impact on the Occurrence of Hypoxia in Chesapeake Bay. *JAWRA Journal of the American Water Resources Association*, 58(6), 855–875. <https://doi.org/https://doi.org/10.1111/1752-1688.12907>
- Väli, G., Meier, H. E. M., & Elken, J. (2013). Simulated halocline variability in the baltic sea and its impact on hypoxia during 1961–2007. *Journal of Geophysical Research: Oceans*, 118(12). <https://doi.org/10.1002/2013JC009192>
- van Helmond, N. A. G. M., Robertson, E. K., Conley, D. J., Hermans, M., Humborg, C., Kubeneck, L. J., Lenstra, W. K., & Slomp, C. P. (2020). Removal of phosphorus and nitrogen in sediments of the eutrophic Stockholm archipelago, Baltic Sea. *Biogeosciences*, 17(10), 2745–2766. <https://doi.org/10.5194/bg-17-2745-2020>
- Vaquier-Sunyer, R., & Duarte, C. M. (2008). Thresholds of hypoxia for marine biodiversity. *P Natl Acad Sci USA*, 105(40), 15452–15457. <https://doi.org/10.1073/pnas.0803833105>
- Wasmund, N., Nausch, G., Gerth, M., Busch, S., Burmeister, C., Hansen, R., & Sadkowiak, B. (2019). Extension of the growing season of phytoplankton in the western Baltic Sea in response to climate change. *Marine Ecology Progress Series*, 622, 1–16. <https://doi.org/https://doi.org/10.3354/meps12994>
- Yurkovskis, A. (2004). Long-term land-based and internal forcing of the nutrient state of the Gulf of Riga (Baltic Sea). *Journal of Marine Systems*, 50, 181–197. <https://doi.org/10.1016/j.jmarsys.2004.01.004>

## Acknowledgements

First and foremost, I'd like to thank my supervisor, professor Urmas Lips, for his guidance and patience throughout my master's and doctoral studies. I am grateful for my colleagues in the Department of Marine Systems at TUT, who have supported me with providing scientific advice and who at times have had to endure my venting. A special thanks goes for the people engaged in collecting in-situ data, and Taavi Liblik and Germo Väli, who gave advice and suggestions on how to improve the current thesis.

A separate section is needed for professor emeritus Sirje Keevallik, who is in every way special and has contributed to my journey probably even more than I realize.

Lastly, I want to express gratitude to my family, especially Ain, Orm, Luki, and my mom for all their support and patience.

In its different phases, this work was supported by the Institutional Research Funding of the Estonian Ministry of Education and Research (grant no. IUT19-6), the Estonian Research Council (grant no. PRG602), the joint Baltic Sea research and development program (Art 185) through grant no. 03F0773A (BONUS INTEGRAL), and Environmental Investment Center environmental program project KIK17144.

## **Abstract**

### **Changing subsurface oxygen conditions in the Baltic Sea basins – analysing the drivers at different temporal scales**

The wide use of fertilizers and husbandry developments have resulted in excess inputs of nutrients to the sea, which have a detrimental effect on the marine environment through increased eutrophication. A way to keep track of the advancements in managing human influence on marine environment is to assess the status of the sea by describing the pressures and state of the environment. Eutrophication manifests itself through increased nutrient concentrations and primary production, enhanced respiration and degradation processes, decreased water transparency and bottom fauna abundance/distribution, and declining oxygen levels. The eutrophication related harmful effects on the environment can be further exacerbated through climate change.

The main objective of this study was to describe the variability of oxygen concentrations in the subsurface and near-bottom layers of the Gulf of Finland and the Gulf of Riga at different time scales and explain the reasons behind the observed changes. For this, historical data, and more recent CTD data of oxygen, salinity, and temperature were used. Additional objectives included testing and developing oxygen indicators to describe the anthropogenic impact on the status of the marine environment. Also, the advantages of collecting high-resolution data for the assessment of the environmental status of marine areas were highlighted using autonomously gathered data.

Since there is no primary production below the euphotic layer, the oxygen content in the aphotic layer is influenced by the amount of oxygen consumed and physical processes, such as lateral advection and vertical diffusion. For instance, the oxygen conditions in the deep layer of the Gulf of Finland are influenced by the east-west movement of the deoxygenated salt-wedge, forced by prevailing wind. The data from 100+ years, show that in long-term, hydrographic conditions and related contribution to the oxygen decrease in the Eastern Gulf of Finland have not changed, although patterns of decadal change are visible. The long-term decline in oxygen is fueled by climate change and eutrophication. More recent data, from the last 30+ years, suggest the increase of hydrography influence in the deep layer oxygen decrease. Considering the climate change effects related to the temperature increase, the effects of other factors, e.g. eutrophication, have decreased recently.

Deep layer advection affects also the stratification strength, which has an influence on the vertical transport of oxygen. Stratification is enhanced with increased temperature in the surface layer and river runoff. In the Gulf of Riga, exceptional hypoxic conditions were observed with the co-occurrence of several forcing factors – an inflow of saltier waters in spring that created deep layer stratification, enhanced thermal stratification, and increased river runoff in previous autumn/winter. The found consumption rate suggests that even with a weaker but longer stratified period hypoxia can also develop. But when forcing factors follow the long-term average values, low oxygen conditions are not observed. Future projections, mainly temperature increase, favor the increase in hypoxia occurrences. The increasing low-oxygen events affect the nutrient cycles, e.g. promote the phosphate release from sediments, which in turn counteracts the nutrient reduction efforts.

To get the measure of eutrophication, oxygen-based indicators are developed. A HELCOM oxygen debt indicator is applied in basins with a permanent halocline.



The assessments based on the latter indicator could benefit from some suggested changes, including the separation of the assessment area to smaller basins, and the use of oxygen debt values at the halocline base (versus the volume-averaged oxygen debt below the halocline). Another option is to estimate the amount of oxygen consumed in a sub-surface or near-bottom layer, which is directly related to organic matter production in a sea area. The changes in oxygen concentrations are also affected by the amount of oxygen brought to the area or moved away from the area. These processes can be quantified by estimating oxygen advection and diffusion. In the Gulf of Finland and the Gulf of Riga, both, advection and diffusion had approximately the same proportion in comparison to the consumption estimates. In the intermediate layer of the Gulf of Finland, more oxygen was leaving the layer in question through the lower boundary compared to the amount brought into the layer from the water column above. In the Gulf of Riga, oxygen was brought to the deep layer from the water above due to diffusion. This approach requires high-resolution temporal and spatial data. Some reservations in the advection and diffusion estimates have to be kept in mind when estimating the consumption rates.

In a shallower open sea area, where the oxygen debt indicator cannot be applied, another approach is needed. The results from the Eastern Gulf of Finland showed that compared to the beginning of 1900s, the low-oxygen area has increased significantly. The observed fluctuations in oxygen conditions were partly smoothed out when the developed approach to minimize the hydrography influence was applied. But still, this approach has a limitation in weakly stratified periods.

Whatever approach is used for estimating the human-induced influence on the marine environment, the natural variability has to be excluded from the assessments. Also, considering the sparse monitoring practices, it has to be kept in mind, that the error in status assessments could be over 50%. To improve the confidence of status assessments, the deployment of autonomous high-frequency measurement systems is crucial.

## Lühikokkuvõte

### **Pinna-aluste hapnikutingimuste muutused Läänemere alambasseinides – erinevatel ajaskaaladel mõju avaldavate tegurite analüüs**

Liigest toitainete koormusest tingitud eutrofeerumine kahjustab merekeskkonna seisundit. Majandamaks merekeskkonnale avalduvat inimõju hinnatakse merele mõjuvaid surveid ja mere seisundit. Eutrofeerumine kui selline, avaldub eelkõige läbi suurenenud toitainete koormuste/sisalduste. Eutrofeerumise tulemusena suureneb primaarproduktioon ja erinevad hapniku tarbimisega seotud protsessid (nagu näiteks hingamine ja orgaanilise materjali lagundamine) muutuvad intensiivsemaks. Rohkema orgaanilise materjali tõttu väheneb vee läbipaistvus ja orgaanika settimisel veekogu põhja tarbitakse sealset hapnikku, mille tulemusena võib tekkida hapniku vaegus (hüpoksia) või puudus (anoksia). Kliimamuutustest tingitud mõjud, eelkõige temperatuuri tõus, võivad veelgi süvendada eutrofeerumise tagajärjel tekkinud kahjulikke mõjusid.

Käesoleva töö eesmärk oli kirjeldada hapnikutingimuste varieeruvust pinna-aluses (Soome lahe näitel) ja põhja-lähedases (Soome lahe ja Liivi lahe näitel) kihis erinevatel ajaskaaladel ja analüüsida täheldatud muutuste põhjuseid. Selle jaoks kasutati ajaloolisi ja viimasel ajal CTD sondide abil kogutud andmeid hapniku, soolsuse ja temperatuuri jaotuse kohta. Üheks täiendavaks eesmärgiks oli välja töötada madalale merele rakendatav hapniku indikaator, mis hindaks peamiselt antropogeense survega seotud mõjusid. Lisaks, kirjeldati autonoomsete profileerijate poolt kogutud kõrge resolutsiooniga andmete eeliseid ja nende rakendamise vajadust keskkonnaseisundi hindamisel.

Hapnikutingimused afootses kihis, kus ei esine produktsiooni, sõltuvad tarbimise määra ja füüsikalistest protsessidest, nagu näiteks advektioon ja difusioon. Soome lahe sügavama kihi hapniku tingimused on suuresti mõjutatud Ava-Läänemere põhjabasseinist pärineva hapnikuvaese ja soolasema veekihi ida-lääne suunalisest liikumisest, mis omakorda sõltub valitsevatest tuultest. Pikaajased andmed, enam kui 100 aastast, näitavad, et pikal ajaskaalal ei ole hüdrograafilised tingimused ja seotud hapnikutingimused Soome lahe idaosas olulised muutunud, kuid muutused skaalal paar aastakümnet on märgatavad. Ajalooline hapnikulangus põhjakihi on suures osas mõjutatud kliimamuutustega seotud temperatuuri tõusust ja eutrofeerumisest. Viimase 30 aasta jooksul on aga põhjalähedase kihi soolsuse kasv (st. et hapnikuvaesem soolakeel ulatub järjest kaugemale idapoole ja stratifikatsioon on tugevnenud) mõjutanud hapniku sisalduse vähenemist ~25-47% kogu selle muutustest. Arvestades ~40% kliimamuutuste mõjuga võib väita, et eutrofeerumise ja muude faktorite osakaal hapniku vähenemises on praegusel ajal väiksem kui pikal ajaskaalal (100 aastat).

Lisaks otseselt hapniku transpordile, mõjutab põhjakihi advektioon ka stratifikatsiooni, mis omakorda mõjub hapniku vertikaalset voogu. Pinnakihi stratifikatsioon on mõjutatud temperatuurist ja mageda vee sissevoolust. Liivi lahes registreeriti erakordsed hüpoksilised tingimused, mis olid tingitud mitme mõjufaktori kokkulangemisest. Hüpoksia areng oli tingitud varasemast ja tugevamast põhjakihi stratifikatsioonist (sh õhemast põhjakihist), kõrgemast temperatuurist ja suuremast jõe sissevoolust produktsiooniperioodile eelnenud sügistalvel. Hinnatud hapnikutarbimise määra põhjal leiti, et ka nõrgema stratifikatsiooniga, aga pikema stratifitseeritud

perioodiga võib tekkida lahe keskosas hapnikuvaegus. Kui aga mõjutavad faktorid, nagu temperatuur, stratifikatsioon ja mageda vee sissevool, järgivad pikaajalist keskmist sesoonset käiku, siis hüpoksiat suure tõenäosusega ei teki. Arvestades kliimamuutuste prognoosi, sh prognoositud temperatuuri tõusu, võib oodata sarnaste hüpoksiliste tingimuste kordumise sagenemist tulevikus. Hüpoksiliste sündmuste kordumine mõjutab ka toitainete ringlust, sh võib viia setetest fosfaatide vabanemise suurenemisele, mis omakorda pärsib rakendatud toitainete koormuse vähendamise meetmete tulemuslikkust.

Hindamaks mere keskkonnaseisundit eutrofeerumise vallas on välja töötatud erinevaid hapniku indikaatoreid. HELCOMis rakendatav hapnikuvõla indikaator on kasutatav ainult püsiva halokliiniga merealadel. Nimetatud indikaatori hinnanguid saaks potentsiaalselt parandada kui rakendada seda eraldi nt Soome lahele ja kasutades ainult halokliini aluse punkti väärtusi. Teine võimalus seisundi kirjeldamiseks on hinnata tarbimise määra pinnaaluses või põhjalähedases kihis. Hapniku tarbimine sõltub mh ka juurde toodud või ära viidud hapniku hulgast, mida saab kvantifitseerida läbi adveksiooni ja difusiooni hinnangute. Soome lahe ja Liivi lahe näitel on difusiooni ja adveksiooni hinnangud võrreldes tarbimise hinnangutega samades proportsioonides. Tarbimise hinnangu usaldusväärsus ja kvaliteet sõltuvad adveksiooni ja difusiooni hinnangutest, mistõttu vajab nimetatud lähenemine kõrglahutuslikke andmeid.

Madalama mere jaoks, kus ei saa kasutada hapnikuvõla indikaatorit, on vaja teistsugust lähenemist. Soome lahe idaosa andmeanalüüs näitas, et viimase 100+ aasta jooksul on madala hapnikuga ala oluliselt suurenenud. Arvestades hapnikutingimuste sõltuvust hüdrograafiast, töötati välja mitte-antropogeenseid mõjutusi minimeeriv indikaator. Antud indikaator parandas seisundihinnangu tulemusi (võrreldes reaalseste hapnikutingimustega) juhul kui hinnanguperioodil oli sügavama kihi soolsus suurem kui referentsperioodil. Antud indikaatorit ei saa kasutada nõrga stratifikatsiooni korral, kuna siis ei täheldata kontsentratsioone, mis on valitud madalate hapnikutingimuste iseloomustamiseks.

Mis iganes indikaator valida eutrofeerumise seisundi hinnanguteks, peab see peegeldama ainult antropogeenset mõju merekeskkonnale. Lisaks, lähtuvalt vähese sagedusega seirest, tuleb arvestada, et seisundihinnangute viga võib olla üle 50%, mistõttu on väga oluline merekeskkonna seires rakendada kõrglahutuslikke autonoomseid profileerijaid ja/või punktmõõtmisi.

## Appendix

### Paper I

Stoicescu, S-T., Lips, U. and Liblik, T., 2019. Assessment of Eutrophication Status Based on Sub-Surface Oxygen Conditions in the Gulf of Finland (Baltic Sea). Front. Mar. Sci. 6:54. <https://doi.org/10.3389/fmars.2019.00054>





# Assessment of Eutrophication Status Based on Sub-Surface Oxygen Conditions in the Gulf of Finland (Baltic Sea)

Stella-Theresa Stoicescu\*, Urmaz Lips and Taavi Liblik

Department of Marine Systems, Tallinn University of Technology, Tallinn, Estonia

## OPEN ACCESS

### Edited by:

Jacob Carstensen,  
Aarhus University, Denmark

### Reviewed by:

Qian Zhang,  
University of Maryland Center  
for Environmental Science (UMCES),  
United States  
Kari Juhani Eilola,  
Swedish Meteorological  
and Hydrological Institute, Sweden

### \*Correspondence:

Stella-Theresa Stoicescu  
Stella.Stoicescu@taltech.ee

### Specialty section:

This article was submitted to  
Marine Ecosystem Ecology,  
a section of the journal  
Frontiers in Marine Science

**Received:** 01 October 2018

**Accepted:** 31 January 2019

**Published:** 19 February 2019

### Citation:

Stoicescu S-T, Lips U and Liblik T  
(2019) Assessment of Eutrophication  
Status Based on Sub-Surface Oxygen  
Conditions in the Gulf of Finland  
(Baltic Sea). *Front. Mar. Sci.* 6:54.  
doi: 10.3389/fmars.2019.00054

Sub-halocline oxygen conditions in the deep Baltic Sea basins depend on natural forcing and anthropogenic impact. HELCOM has a long tradition of characterizing the status of the seabed and deep waters by estimating the extent of anoxic and hypoxic bottoms. A eutrophication-related indicator “oxygen debt” has been used in the recent HELCOM assessments and a more sophisticated “oxygen consumption” indicator has been introduced. We describe the oxygen conditions in the Gulf of Finland (GoF) in 2016–2017 based on observations at the Keri profiling station where vertical profiles of temperature, salinity and oxygen were acquired up to 8 times a day. The main aim of the study is to test the applicability of high-frequency data from this fixed automated station and the three adapted oxygen indicators for the eutrophication-related status assessments. The results show that the GoF bottom area affected by hypoxia varied in large ranges from 900 to 7800 km<sup>2</sup> with a seasonal maximum in autumn (>25% of bottoms were hypoxic in autumn 2016). Oxygen debt is the simplest indicator, and the assessment results are less influenced by the wind-induced changes in hydrographic conditions. We suggest that oxygen debt should be assessed just below the halocline and based on data from the stratified season only since, in the GoF, the halocline could be destroyed in winter. For the “oxygen consumption” indicator, a rough oxygen budget, where the contributions of advection and mixing are included, was formulated. Average seasonal consumption values of 0.82 and 0.31 mg·l<sup>-1</sup>·month<sup>-1</sup> were estimated in the 50–60 m water layer of the GoF in 2016 and 2017, respectively. The found large difference in consumption values between 2016 and 2017 could partly be related to the uncertainties of advection estimates. We concluded that all three indicators have their advantages and methodological challenges. To increase the confidence of eutrophication assessments both high-frequency profiling should be implemented in the monitoring programs and more accurate estimates of changes due to physical processes are required.

**Keywords:** eutrophication, assessment, hypoxia, Baltic Sea, Gulf of Finland, bottom waters, oxygen

## INTRODUCTION

The Baltic Sea is an area where oxygen conditions are influenced by climate change (Kabel et al., 2012) and increased eutrophication (Conley et al., 2009; Gustafsson et al., 2012). Eutrophication is driven by excessive inputs of nutrients from rivers and atmosphere (mostly land-based sources) which lead to increased sedimentation of organic material and oxygen depletion in the bottom

layer and the internal loading of phosphorus (Vahtera et al., 2007). The oxygen conditions in the near-bottom layer of the central deep basins of the Baltic Sea are occasionally improved by the Major Baltic Inflows (MBI) (Matthäus and Franck, 1992; Schinke and Matthäus, 1998). The MBIs also strengthen stratification and therefore potentially increase areas with oxygen depletion by inhibiting ventilation of deep layers (Gerlach, 1994; Conley et al., 2002).

The Gulf of Finland (GoF) is an elongated estuarine basin with the largest single freshwater input and the highest nutrient loading to the Baltic Sea from the Neva River (Alenius et al., 1998). Beside the eutrophication effects, the sub-surface distribution and variability of dissolved oxygen (DO) in the GoF are related to multi-scale physical processes. These processes range from short-term oscillations and mixing events to wind-driven alterations of estuarine circulation, seasonal development and decay of stratification and sub-halocline transport of hypoxic/anoxic waters from the Northern Baltic Proper, for instance, associated with the MBIs (Elken et al., 2003; Liblik et al., 2013, 2018; Lips et al., 2017). The lack of MBIs during stagnation periods affects the GoF in a way that stratification and hypoxia are decreased (Conley et al., 2009; Laine et al., 2007). Oxygen in the near-bottom layer is dependent on wind conditions as north-easterly and northerly winds support the estuarine circulation and strong south-westerly wind forcing causes the reversal of estuarine circulation (Lehtoranta et al., 2017). The estuarine circulation is characterized by the up-estuary (eastward) flow in the deep layer and the down-estuary (westward) in the upper layer. The reversed circulation bears opposite results – the up-estuary flow in the surface layer and the down-estuary (westward) flow in the deeper layer (Elken et al., 2003). Prevailing of the estuarine circulation leads to strengthening of the halocline while reversals cause weakening of stratification. The wintertime deep-water oxygen conditions are strongly dependent on the spatiotemporal variability of the salt wedge originating from the Northern Baltic Proper (Liblik et al., 2013), which moves eastward and westward at the gulf's bottom depending on wind conditions.

According to the Marine Strategy Framework Directive's (MSFD; Directive 2008/56/EC of the European Parliament and of the Council, 2008) Article 11, all member states have to establish and implement monitoring programs to assess the status of their marine environment. The monitoring programs have to provide data that enable the application of different indicators in order to assess the status of marine waters, including in regard to eutrophication effects. HELCOM (Baltic Marine Environment Protection Commission – Helsinki Commission) has set out a number of core indicators (according to MSFD) for describing the eutrophication status where nutrient levels are based on dissolved inorganic nitrogen and phosphorus as well as total nitrogen and phosphorus. Direct effects of eutrophication are assessed based on chlorophyll *a* levels and water transparency (Secchi depth). Oxygen conditions are used to describe the indirect effects. The overall assessment is given using a tool called HEAT (HELCOM Eutrophication Assessment Tool) which determines the distance between the measured value of an indicator and good environmental status (GES, a predefined

threshold value), aggregates the indicator evaluations and gives the confidence of the assessment (HELCOM, 2014).

While indicators based on nutrient levels and direct effects for assessing eutrophication status are applicable in all Baltic Sea sub-basins, the use of oxygen indicators, describing the indirect effects, is restricted to the deep basins, including the GoF. The approved core indicator evaluates the oxygen debt (the “missing” oxygen relative to a fully saturated water column) below the halocline found based on salinity profiles and discrete oxygen concentrations measured at standard depths (HELCOM, 2013). The threshold values are uniform for most of the basins, including the GoF (8.66 mg/l). The latest results for oxygen debt assessments in the GoF are 10.54 mg/l for 2007–2011 and 10.67 mg/l for 2011–2016 (HELCOM, 2014, 2018a), both indicating that GES has not been achieved. Data used for oxygen debt indicator assessments originate from temporally sparse monitoring (in Estonia, national monitoring is carried out six times a year) which could miss the variability of deep-water oxygen conditions, and therefore, the assessment results could be biased. To get a more confident assessment of oxygen conditions in the deep water the data acquired with better temporal coverage could be used.

The development of a more uniform indicator was initiated in the frames of the HELCOM EUTRO-OPER project in 2015. The idea was to estimate the oxygen consumption during summer in the layer below the productive surface layer, it means in the so-called stagnant layer located between the thermocline and the halocline. Oxygen consumption is calculated based on oxygen depletion, diffusion and advection. Due to small temporal differences in salinity and temperature within the stagnant layer, advection was neglected in the first tests of this indicator (HELCOM, 2015b).

Oxygen conditions can also be described by the spatial extent of hypoxia which could be one of the possible indicators of indirect effects of eutrophication (Conley et al., 2009). Considering the hypoxic area as a eutrophication status indicator, the natural variability of oxygen, e.g., the changes due to hydrographical influences and the anthropogenic component have to be separated in order to seclude human-induced effects. The yearly extent of the hypoxic and anoxic bottom area in the Baltic Sea is assessed and presented on HELCOM Environment fact sheets (Naumann et al., 2018; Viktorsson, 2018). The results differ a bit between these latest two assessments due to the temporal and spatial coverage of data used. The first estimate, produced by the Swedish Meteorological and Hydrological Institute (SMHI), uses data from the autumn period, August to October for the whole Baltic Sea, and the second, produced by the Baltic Sea Research Institute, Warnemünde (IOW), uses data from May and excludes the Bothnian Sea, Danish straits, Gulf of Riga and the GoF.

In this study, we defined hypoxia by a threshold of  $2.9 \text{ mg} \cdot \text{l}^{-1}$ , which is one of the two most commonly used thresholds (the other being  $2.0 \text{ mg} \cdot \text{l}^{-1}$ ) in literature, based on an extensive review by Vaquer-Sunyer and Duarte (2008). They concluded that a single threshold could not adequately describe the influence of hypoxia to different benthic marine organisms and argue that the conventionally accepted threshold of  $2.0 \text{ mg/l}$  is well below

the oxygen thresholds for more sensitive taxa. It is important to define a proper hypoxia level for the Baltic Sea and GoF, but we do not discuss this issue here since the hypoxia area estimate methodology will still be the same and the hypoxia threshold could be addressed together with setting the border between the GES and sub-GES.

The hypoxic area assessments by SMHI show that the areal extent and the volume of anoxia and hypoxia have continuously been elevated since the regime shift in 1999 (Hansson et al., 2011). The latest results (for 2017, mean areal results) show that anoxic conditions affect around 18% and hypoxia around 28% of the bottom areas in the Baltic Sea, including the GoF and the Gulf of Riga (Hansson et al., 2017). In the IOW hypoxic area estimations, the GoF is unfortunately excluded, but it is seen that the anoxic conditions in the Northern Baltic Proper in 2016 have changed into hypoxic conditions in 2017 (Naumann et al., 2018).

All above-described assessments are based on data from spatially distributed monitoring stations with low temporal resolution. An alternative approach could be to apply data from automated profiling stations which also catch temporal variability due to prevailing hydrographic processes. In the present study, we analyze the high-resolution time series of vertical profiles of oxygen in the GoF in 2016–2017. The main aim is to demonstrate how these observations could be applied to assess the status of this stratified estuary in relation to the eutrophication effects using the adapted versions of the three possible indicators.

## MATERIALS AND METHODS

### Core Data Set

The core data set used in the present study originates from the autonomous bottom-mounted profiler, which is deployed at the

depth of 110 m near the Keri Island in the GoF since March 2016 (Figure 1). The data acquired in 2016 and 2017 were used. The system was developed by Flydog Solutions Ltd., (Estonia) and includes, as the main measurement device, an OS316plus CTD probe (Idronaut s.r.l., Italy) with Idronaut oxygen sensor and Trilux fluorescence sensor (Chelsea Technologies Group Ltd.). The profiler records temperature, salinity, DO content, chlorophyll-a, phycocyanin and turbidity at a rate of 8–9 Hz while moving up with an average speed of 8–10 cm·s<sup>-1</sup>. In May–June 2017, a Seabird Electronics SBE19plus probe with SBE43 oxygen sensor provided by the Finnish Meteorological Institute was used instead of the OS316plus probe. The accuracy of the used Idronaut oxygen sensors is 0.1 mg·l<sup>-1</sup>.

The data were pre-processed to exclude spikes and recordings when the probe movement was reversed (e.g., due to waves moving the buoyant probe up and down in the near-surface layer) and to compensate the time lag of sensors. While the Idronaut oxygen sensor has a time constant of about 8 s, the time constant of SBE43 sensor was set to 4 s. After the pre-processing of data, the vertical profiles were stored with a constant step of 0.5 m. The data were collected in the water column between 100 and 4 m.

All used CTD probes and oxygen sensors were calibrated at the factory before the deployment. In addition, the core data set was quality controlled against the quality-assured data from the research vessel based measurements conducted regularly (once a month) close to the profiling station using a CTD probe OS320plus (Idronaut s.r.l., Italy) and laboratory analyses of water samples. See the applied methods and onboard quality assurance procedures in the next sub-section. Since the oxygen sensor had a drift in time, the oxygen profiles were corrected using ship-borne measurement results. For each vessel visit, a linear regression line equation with the intercept set to zero was found

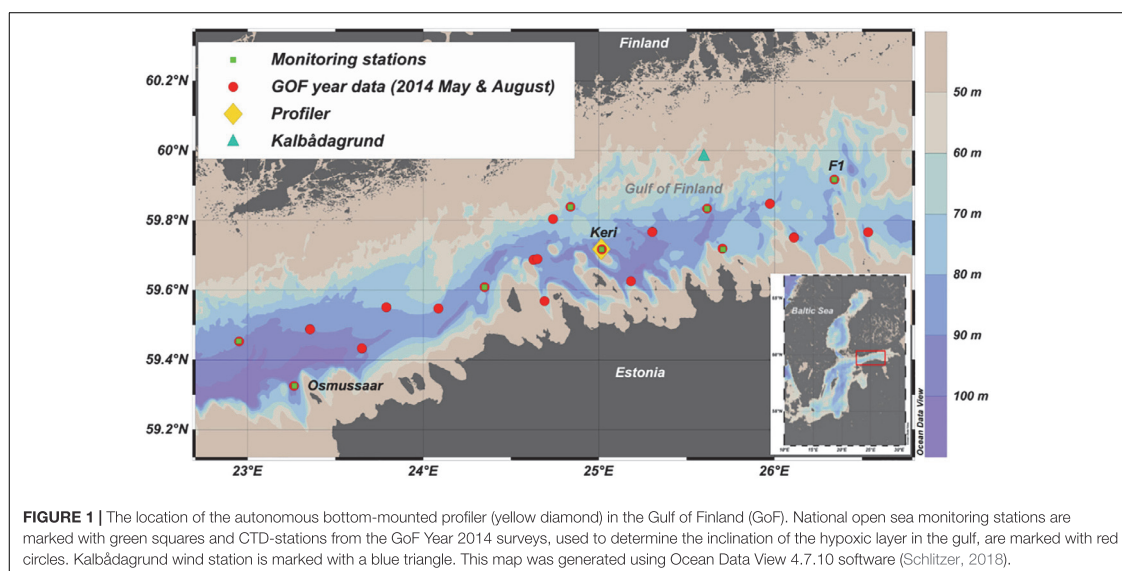


**FIGURE 1 |** The location of the autonomous bottom-mounted profiler (yellow diamond) in the Gulf of Finland (GoF). National open sea monitoring stations are marked with green squares and CTD-stations from the GoF Year 2014 surveys, used to determine the inclination of the hypoxic layer in the gulf, are marked with red circles. Kalbådagrund wind station is marked with a blue triangle. This map was generated using Ocean Data View 4.7.10 software (Schlitzer, 2018).



by comparison of the ship-borne oxygen profile and the closest oxygen profile from the bottom-mounted profiler. The oxygen profiles between the two consecutive vessel visits were corrected using the coefficient (the slope of the regression line) assuming its linear trend in time. If such ship-borne measurements were not available from a specific period, all data from that period were excluded from the further analysis.

The temporal continuity of the analyzed data can be described by the months covered and the number of quality controlled profiles available (Table 1). In both years, the majority of the productive season is covered. The exclusion of data due to quality problems and the stops in the operation of the bottom-mounted profiler (for instance, in January–April 2017) due to different reasons are seen in Table 1 as well as the next section as blank areas in the graphs. The higher number of profiles per month in summer 2017 was due to the setup of profiling frequency of 8 profiles per day while it was 4 profiles per day in 2016.

### Ship-Borne Data Collected in 2014–2017

Data from the research vessel cruises were used for the quality assurance of the measurements by the bottom-mounted profiler and determining the spatial variability in the vertical distribution of DO in the gulf. Also, the relationship between the oxygen and salinity in the sub-surface layers in the vicinity of the profiler was found using the ship-borne observations. The analyzed CTD data were gathered in the frames of national monitoring and GoF Year 2014 programs in 2014–2017 (Figure 1) as well as additional monthly visits to the Keri station in 2016–2017. The oxygen sensor attached to the OS320plus was calibrated before each cruise. Oxygen profiles used for the analysis were quality checked against the laboratory analysis of water samples using an OX 400 I DO (WWR International, LCC). The accuracy of the Idronaut oxygen sensor on board the research vessel is 0.1 mg·l<sup>-1</sup> while the accuracy of the laboratory DO analyzer is 0.5% of the

measured value. Altogether 336 ship-borne vertical profiles of DO were available for the present study.

Also the temperature and salinity data of both, the research vessel CTD and the profiler CTD, were quality checked against water samples analyses using a high-precision salinometer 8410A Portasal (Guildline). The average difference of the salinity values was less than 0.02 g·kg<sup>-1</sup> that indicated no need for the correction of the CTD data.

### Indicators

#### Extent of Hypoxic Area

Bathymetric data from Andrejev et al. (2010, 2011) with the horizontal resolution of 463 m were used to calculate the hypsographic curve of the GoF, and based on this dataset, the GoF area was set equal to ~27631 km<sup>2</sup> and volume to ~1042 km<sup>3</sup>. We selected the threshold for hypoxia of 2.9 mg·l<sup>-1</sup> (equal to 2.0 ml l<sup>-1</sup> and 89.3 μmol l<sup>-1</sup>) as also applied in HELCOM Baltic Environmental Fact Sheets (Naumann et al., 2018; Viktorsson, 2018) and many research papers (e.g., Diaz and Rosenberg, 2008; Conley et al., 2009). The upper border of the hypoxic layer was defined for each measured vertical profile as the minimum depth where DO content was below the defined threshold (see examples in Figure 2). In some cases (some profiles from March 2016) hypoxic depth was not possible to define from the profiles, and the hypoxic depth was assumed to be deeper than the deepest measured value. Here the depth of hypoxia was found based on the assumption that DO content decreases linearly when moving deeper. The change in DO content with depth was found comparing DO measured at the last depth and DO measured five meters above the last depth.

$$depth_{hypoxia} = depth_{max} + x, \tag{1}$$

where  $depth_{max}$  is the deepest measured depth value and  $x$  is the change of depth from last measured depth value to the depth value where DO = 2.9 mg·l<sup>-1</sup>;  $x$  was defined as:

$$x = \frac{5 \cdot (2.9 - DO_{depth(max)})}{DO_{depth(max)} - DO_{depth(max) - 5}}, \tag{2}$$

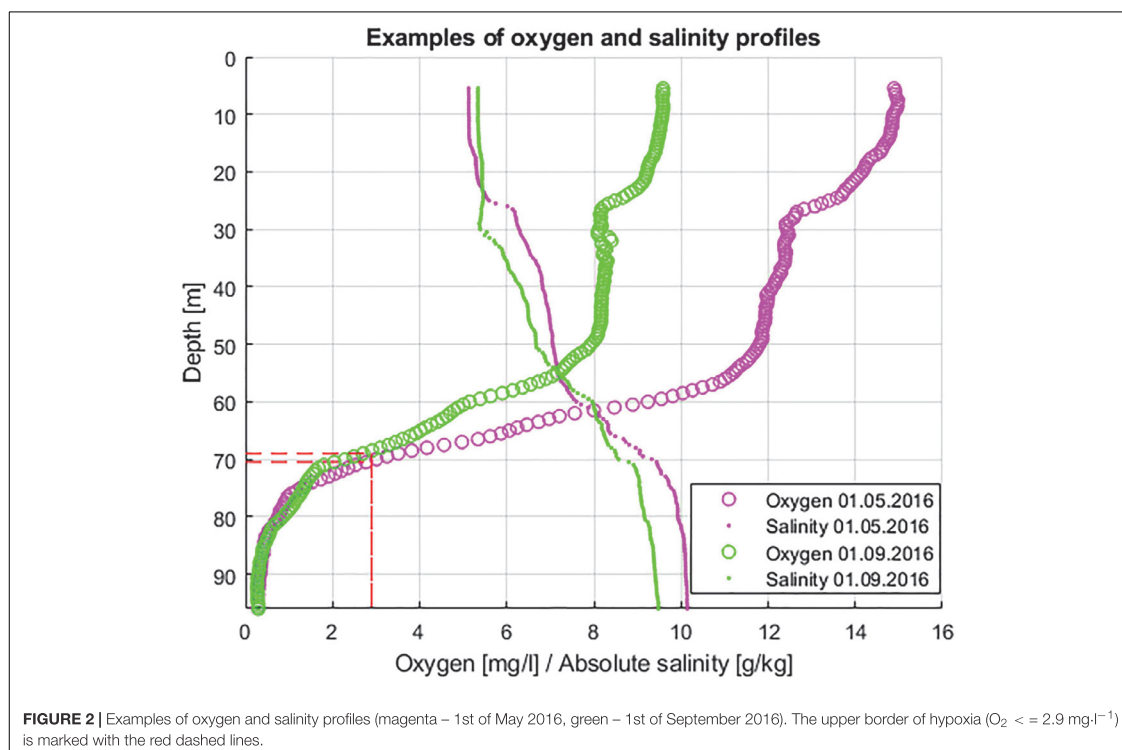
where 5 is depth interval (in meters) between the two DO measurements used to find the linear change in DO; 2.9 is the concentration of DO (in mg·l<sup>-1</sup>) which marks hypoxia;  $DO_{depth(max)}$  is the deepest measured DO value and  $DO_{depth(max)-5}$  is the DO value measured 5 m above the deepest value. If  $x < 0$  or  $DO_{hypoxia} > 115$  m, then the value  $DO_{hypoxia} = 115$  m was used, which is the maximum depth in the Keri area and it is deeper than the maximum depth in the used bathymetric data.

To determine the average spatial inclination of the upper border of the hypoxic layer along the GoF, data from two cruises in May and August 2014 with spatially well distributed station network (Figure 1) were analyzed. First, the start of hypoxia was found (same method as for the indicator) for every measured profile. Then these depths were plotted against station longitude, and the linear regression line, indicating the change of hypoxic depth in the east-west direction, was found.

**TABLE 1** | The number of available quality checked profiles from the Keri autonomous profiler.

Month\Year	2016	2017
January	–	–
February	–	–
March	124	–
April	119	–
May	96	57
June	117	236
July	112	237
August	119	219
September	117	228
October	95	120
November	10	–
December	28	–
ALL YEAR	<b>937</b>	<b>1097</b>
April to September	680	977

The values in bold represent the total number of profiles available in both years.



Based on the found hypoxic depth values and the hypsographic curve, corresponding area and volume of hypoxia in the GoF were calculated by applying a developed script (we used software package MATLAB R2016a). Two estimates of both parameters were found (1) assuming that the border of the hypoxic layer was a horizontal plane and (2) assuming that it had a constant inclination in the east-west direction. The monthly values of the estimates are presented since we suggest that it is a long enough period to filter out the impact of spatial variability at mesoscale (remember that we use observations for a single station).

To compare hypoxic area extent results with prevailing wind conditions we used wind data from the only real open sea automatic weather station (other stations are mainly located near the coast) at Kalbådagrund (59°58'N, 25°37'E) (Alenius et al., 1998). Wind data was corrected to represent wind speed at 10 m (measured wind speed was multiplied by 0.91) (Launiainen and Laurila, 1984). First, the monthly mean hypoxic area extent was related to the prevailing wind direction and speed calculated for the preceding 30 days. For example, the hypoxic area in June was compared with wind data from the 16th of May to the 15th of June. The number of days used for wind analysis was selected to be 30 because that is the time frame used for the calculation of average hypoxic extent. Secondly, the linear correlation between the 3-week average wind stress component

from N-NE ( $20\pi$ ) and the hypoxic depth was found. This choice of the wind direction and period was based on a study by Liblik and Lips (2011) where they showed that the 3-week average wind component correlated best with the changes in the vertical thermohaline structure in the GoF in summer. Drag coefficient used when finding wind stress was according to Large and Pond (1981).

### Oxygen Debt Indicator

In the latest HELCOM eutrophication assessments (HELCOM, 2014, 2018b), an oxygen debt indicator proposed during the HELCOM TARGREV project was used. Because the monitoring data are only available from the standard depths, a special procedure was applied to estimate the sub-halocline DO content. First, the salinity profiles were modeled to identify the halocline. Then, the linear segments of the oxygen profile in the halocline and below it were constructed. Oxygen debt was calculated by subtracting the monitored DO content from the concentration of saturation, taking into account the temperature and salinity values. Finally, the volume specific oxygen debt was found for the sub-halocline layer (see more about the method in HELCOM, 2013).

In the present work, the oxygen debt value just below the halocline and not the volume specific average was used as the oxygen debt indicator. The halocline was determined as the

depth range where the vertical salinity gradient was greater than  $0.07 \text{ g}\cdot\text{kg}^{-1}\cdot\text{m}^{-1}$  (Liblik and Lips, 2011), whereas the salinity gradient was found based on smoothed profiles (over 2.5 m). Temperature, salinity and DO content values just below the halocline were found for each measured profile, and the corresponding oxygen debt values were calculated. In order to assess the eutrophication status, monthly and seasonal averages of oxygen debt were estimated.

For the HELCOM oxygen debt indicator, a constant target value in the GoB, the Northern Baltic Proper and the Eastern Gotland Basin is defined at  $8.66 \text{ mg}\cdot\text{l}^{-1}$  as an annual average (HELCOM, 2013). We suggest that the uniform target value should not be applied since the basins have different depths and a linear oxygen change below the halocline was assumed. However, if the oxygen debt value just below the halocline is used, the targets could be similar, though still to be defined, for all mentioned basins. The other reason not to use the volume specific average oxygen debt is that we lack hydrogen sulfide observations at the profiling station and the oxygen debt estimate near the seabed could be biased.

### Oxygen Consumption Indicator

An alternative oxygen indicator is being developed by the experts working with eutrophication-related issues in the HELCOM community, although it is not fully ready nor applied yet (HELCOM, 2015b). The idea is to base the indicator on estimated oxygen consumption in the summer season (June to September) below the productive layer but above the halocline – in a so-called stagnant layer. In the HELCOM report, the sparse monitoring data were used and the advective processes were not taken into account when estimating oxygen consumption. We test this indicator based on vertical profiles of DO content acquired with a high temporal resolution at a fixed position.

According to HELCOM (2015a), oxygen consumption (CONS) in a water layer between its upper ( $u$ ) and deeper ( $d$ ) border is calculated as:

$$\text{CONS}_{(u,d)} = \text{DEPL}_{(u,d)} + \text{DIFF}_{(u,d)} + \text{ADV}_{(u,d)} \quad (1)$$

where *DEPL* is oxygen depletion (decrease in oxygen has a positive value) and *DIFF* and *ADV* are the change in oxygen content due to vertical diffusion and advection (both horizontal and vertical), respectively. The layer with the borders  $u$  and  $d$  is selected for a studied year based on vertical thermohaline structure (see section “Oxygen Consumption”).

Changes in DO content due to diffusion are estimated as:

$$\text{DIFF}_{(u,d)} = -A(u) \left( \kappa(u) \frac{\partial O_2(u)}{\partial z} - \frac{A(d)}{A(u)} \kappa(d) \frac{\partial O_2(d)}{\partial z} \right) \quad (2)$$

where  $A(u)$  and  $A(d)$  are the horizontal cross-sectional area of the studied layer,  $\frac{\partial O_2(u)}{\partial z}$  and  $\frac{\partial O_2(d)}{\partial z}$  the vertical gradient of oxygen and  $\kappa(u)$  and  $\kappa(d)$  the vertical diffusivity coefficient at its upper and deeper border, respectively. The latter is calculated as:

$$\kappa_{(u,d)} = \frac{\alpha_{(u,d)}}{N_{(u,d)}} \quad (3)$$

where  $\alpha$  is an empirical intensity factor of turbulence.  $N$  is the Brunt–Väisälä frequency, defined as:

$$N_{(u,d)}^2 = -\frac{g}{\rho_0} \frac{\partial \rho(u,d)}{\partial z} \quad (4)$$

where  $g$  is the acceleration due to gravity,  $\rho_0$  is density of the seawater and  $\frac{\partial \rho(u,d)}{\partial z}$  is the vertical gradient of density. In the present study, we assumed that the areas  $A(u)$  and  $A(d)$  are equal (it is correct for deep enough regions) as well as the empirical intensity factor of turbulence is a constant ( $\alpha = 1.5 \cdot 10^{-7} \text{ m}^2 \cdot \text{s}^{-2}$ ).

The increase in oxygen content due to advection was calculated based on the estimated salinity advection and an assumption that a linear correlation exists between the changes in salinity and oxygen. Since neither salinity sources nor sinks exist in the sub-surface layer, salinity advection could be found as:

$$\text{ADV}_{(u,d)\text{SA}} = \text{CHANGE}_{\text{SA}} - \text{DIFF}_{(u,d)\text{SA}} \quad (5)$$

where *CHANGE* is the salinity change between the two profiles in the selected layer and *DIFF* is the estimated change in salinity due to vertical diffusion (a similar formula was applied as for oxygen diffusion). Oxygen advection was thus calculated as:

$$\text{ADV}_{(u,d)\text{O}_2} = \text{ADV}_{(u,d)\text{SA}} * a \quad (6)$$

where  $a$  is the oxygen change corresponding to a unit change in salinity. This coefficient was found as the slope value of the linear regression line based on salinity and oxygen data from the monitoring cruise in April of the corresponding year, thus, before the analyzed period. For the regression analysis, a layer from 30 to 70 m was selected which is broader than the stagnant layer where oxygen consumption was estimated in the present study.

Oxygen depletion was calculated based on the monthly mean average oxygen concentrations in the selected layer. For example, to find oxygen depletion between June and May, the average concentration in June was subtracted from the average concentration in May. The total monthly change in DO content due to diffusion was found as the daily average diffusion during 30–31 days (e.g., from mid-May until mid-June) multiplied by the number of days. The monthly changes in both, salinity and oxygen, due to advection were also estimated over the similar monthly time step. Finally, monthly oxygen consumption values were obtained as expressed in Eq. (1). A month was chosen as a minimum time step since the consumption estimates for a shorter period are close to the accuracy of the DO measurements.

## RESULTS

### High-Resolution View on Temporal Variability of Dissolved Oxygen Content

The time series of vertical distributions of temperature, salinity and DO concentration from spring until autumn in 2016 and 2017 (Figure 3) show both the seasonal course and the short-term variations. The surface layer warming and development of the seasonal thermocline with its sharp down- and upward movements between 10 and 40 m depth were the

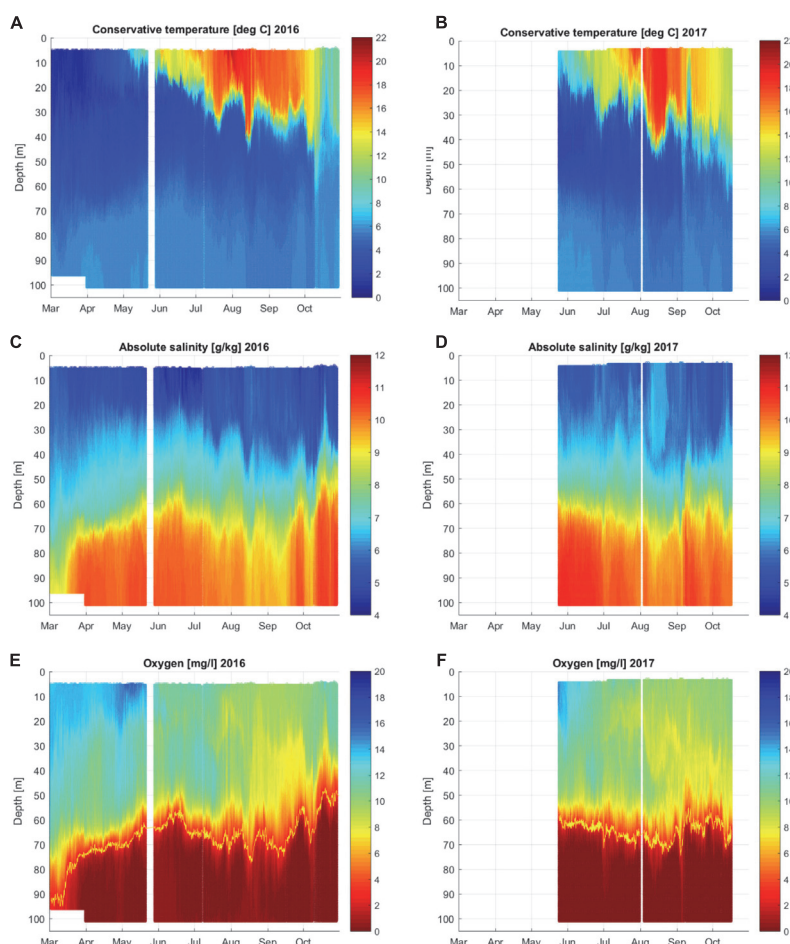


**FIGURE 3 |** Temporal variability of vertical distributions of temperature (A,B), salinity (C,D) and dissolved oxygen concentration (E,F) at the Keri bottom-mounted station in the GoF in 2016 and 2017. The yellow line in the lower panel shows the border of hypoxia ( $2.9 \text{ mg l}^{-1}$ ). White strips/areas indicate periods when no data was available.

characteristic features of the temperature distribution time-series. The halocline fluctuated between the depths of 60 to 80 m. If to consider a general temporal development of salinity distribution in the deep layer from May to October, then the halocline penetrated deeper from June to late August and got shallower in late September and October in both studied years.

The seasonal course of the vertical distribution of oxygen followed the mentioned development of the thermohaline structure. Oxygen concentrations decreased in the upper layer from spring to late summer mostly due to the decay of the vernal phytoplankton bloom and the temperature increase in the summer months, as it leads to the decrease in saturation concentration. The boundary of the near-bottom hypoxic layer, defined here as the oxygen concentration of  $2.9 \text{ mg l}^{-1}$  (the

yellow line in **Figure 3** lower panel), moved up- and downward together with the halocline. It is also seen that the oxygen concentrations decreased in the layer between the thermocline and halocline. At least partly this decrease in oxygen content could be related to the oxygen consumption that will be analyzed in more detail in the present study.

### Hypoxic Area

The depth, at which hypoxia starts in the water column, varied throughout the year and between the 2 years (**Figure 4**) with an average from May to October of 64.5 m in 2016 and 64.6 m in 2017. The upward movement of the border of the hypoxic layer from winter to spring occurred in 2016. In June–September of both years, the hypoxia border moved

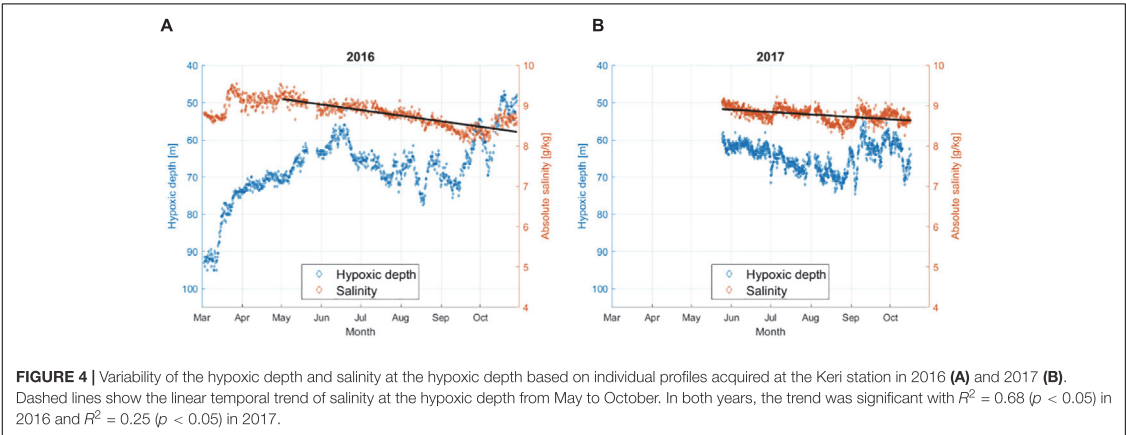


**TABLE 2 |** Monthly averages of the bottom area and volume (percent of total area/volume) for the leveled and the inclined border of the hypoxic layer in 2016 and 2017; “incl” stands for the inclined layer, “A” for area and “V” for volume.

	2016					2017				
	A%	A% incl	V%	V% incl	Prevailing wind 2016	A%	A% incl	V%	V% incl	Prevailing wind 2017
January	–	–	–	–	–	–	–	–	–	–
February	–	–	–	–	–	–	–	–	–	–
March	3.3	3.3	0.4	0.4	SW-S 6.2	–	–	–	–	SW 8.6
April	10.6	10.9	2.6	2.6	SW-W 5.9	–	–	–	–	SW-W 7.2
May	14.1	14.6	4.3	4.3	SW-W 5.9	18.2	19.3	6.4	6.5	W-SW 6.4
June	18.2	19.2	6.4	6.5	NW-N 5.7	17.4	18.3	6.0	6.1	W-SW 6.4
July	12.9	13.3	3.7	3.7	SW-W 6.6	14.0	14.5	4.2	4.3	W-SW 7.4
August	12.7	13.1	3.5	3.6	SW-W 5.7	12.4	12.8	3.4	3.5	SW-W 6.3
September	13.9	14.4	4.2	4.3	W-SW 6.6	17.2	18.1	5.9	6.0	SW-W 4.3
October	26.0	27.8	9.8	10.2	NE-N 7.9	15.8	16.6	5.2	5.3	SE-E 7.5
November	28.2	29.7	10.9	11.4	E-NE 8.5	–	–	–	–	SW-W 8.6
December	22.5	24.3	8.3	8.6	W-NW 8.7	–	–	–	–	S-SW 9.2

Also, the average wind speed ( $m \cdot s^{-1}$ ) and direction at Kalbådagrund during the preceding 30 days for each month is given; e.g., for June from the 16th of May to the 15th of June.

downward in the water column from about 60 to 70 m, and after that, it rose again to 60 m in both years and even shallower in late October 2016. At the same time, as the hypoxia border deepened, a significant salinity decrease at the minimum depth of the hypoxia was observed ( $p < 0.05$ ) in both years from May to October (Figure 4). This result suggests either the local consumption of oxygen, since it corresponds to a decrease in oxygen content at a fixed salinity value, or a change in water properties due to physical processes, such as advection of water masses with a different oxygen-salinity relationship.

Since the depth of the upper border of the hypoxic layer (hypoxic depth) revealed high short-term variability (Figure 4), the estimates of the hypoxic area and volume of hypoxic waters were analyzed based on the monthly averages. Both approaches, assuming the leveled and the inclined border of the hypoxic layer were applied (Table 2). The linear inclination of the

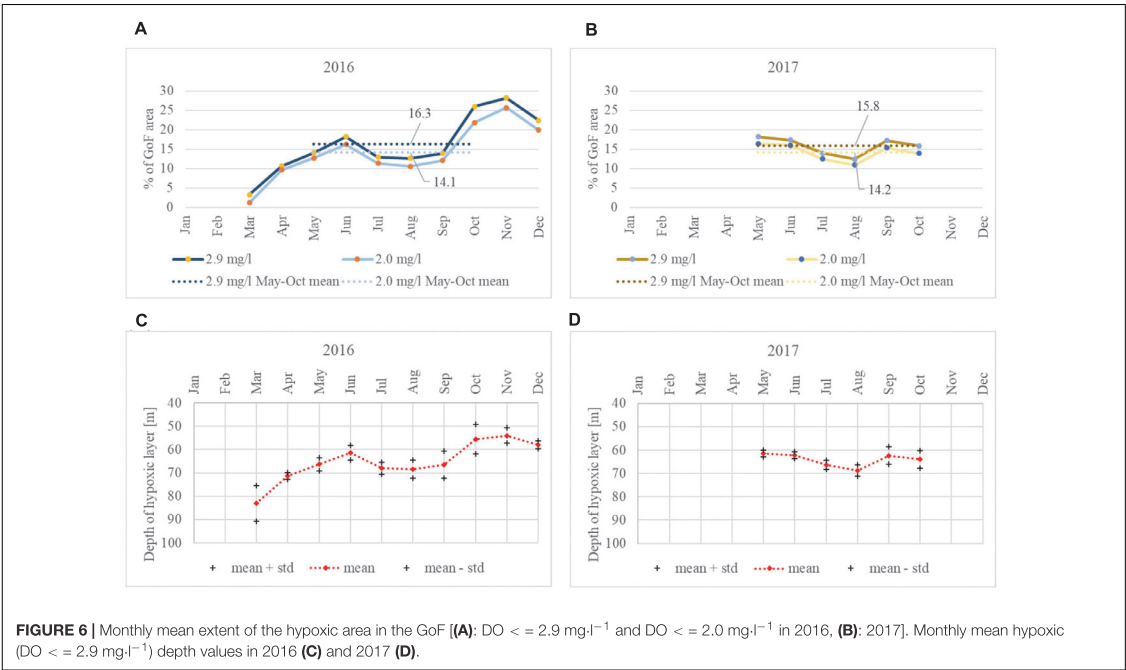
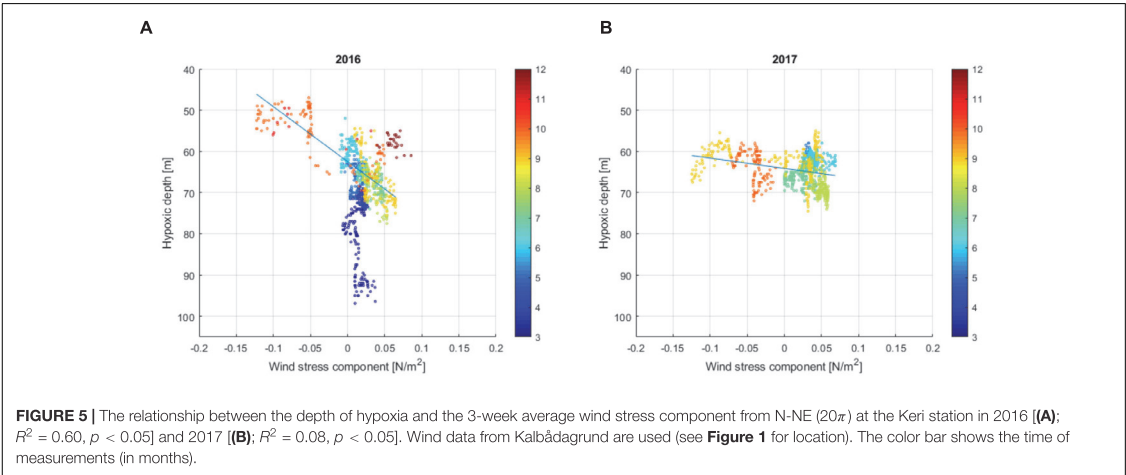
border of the hypoxic layer of 1.9 m per 100 km along the GoF from west to east, found based on the GoF Year 2014 data [see stations network in Figure 1; correlation between the start of hypoxia and longitude was significant ( $R^2 = 0.16$ ,  $p < 0.05$ )], was used. As seen in Table 2, the estimates of the area and volume of the hypoxic waters differed only by  $<2$  and  $<0.5\%$ , respectively, if the estimates based on the leveled and the inclined border of the hypoxic layer were compared. This good coincidence of the estimates, although an average inclination of the border of hypoxia exists, is most probably explained by a central location of the Keri station in the GoF.

We compared the monthly average extent of the hypoxic area with the average wind vector from the preceding 30 days (Table 2). It is seen that for 2016, when the N-NE winds prevailed, then the hypoxic area was enlarged, while with the W-SW winds, the area was somewhat smaller. However, in 2017, the



wind forcing could not explain the observed changes so well. The hypoxic area was biggest in May–June and in September but the corresponding winds for these months from the sector between east and north were almost absent. We also compared the 3-week average wind component from N-NE ( $20\pi$ ) with the hypoxic depth at the Keri station (Figure 5). If the early spring data were excluded, then the linear correlation was significant ( $p < 0.05$ ) for both years with a much stronger relationship for 2016 May–October than for 2017 May–October (Figure 5).

Almost identical seasonal course in the development of the hypoxic area was observed in both summers when the area affected by hypoxia decreased from the early summer until August and started to grow again in September–October (Figure 6). When comparing the hypoxic extent monthly results obtained using different hypoxia thresholds ( $\text{DO} \leq 2.9 \text{ mg}\cdot\text{l}^{-1}$  and  $\text{DO} \leq 2.0 \text{ mg}\cdot\text{l}^{-1}$ ), the dynamics are the same and the averages differ only slightly. In 2016, the May to October mean hypoxic area was 2.2% bigger with the hypoxic threshold



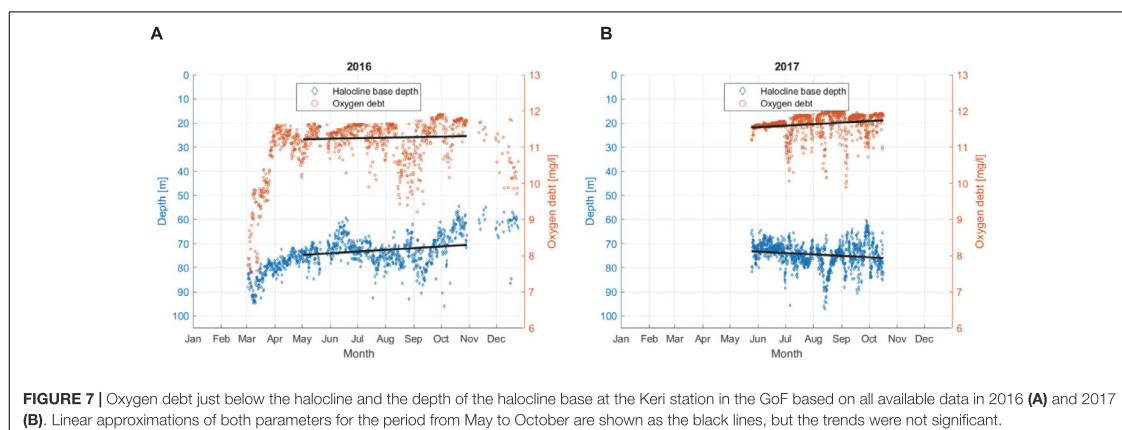


**FIGURE 7 |** Oxygen debt just below the halocline and the depth of the halocline base at the Keri station in the GoF based on all available data in 2016 (A) and 2017 (B). Linear approximations of both parameters for the period from May to October are shown as the black lines, but the trends were not significant.

$DO \leq 2.9 \text{ mg}\cdot\text{l}^{-1}$  compared to the area found using the threshold  $DO \leq 2.0 \text{ mg}\cdot\text{l}^{-1}$ , while in 2017, the area was 1.6% bigger.

## Oxygen Debt

Oxygen debt values just below the halocline were calculated for every vertical profile of DO (Figure 7). Halocline, defined using the vertical salinity gradient criterion of  $0.07 \text{ g}\cdot\text{kg}^{-1}\cdot\text{m}^{-1}$ , was detected for all profiles in both years. The mean depth of the point below the halocline, for which the oxygen debt was estimated, was 74.2 m in 2016 and 74.5 m in 2017. If for 2016 the period from May to October was considered (when the data were available in 2017), then the mean depth of this point was 72.4 m. The temporal variability (May to October) could be characterized as the maximum and minimum values of 96.0 and 54.5 m in 2016 and 97.0 and 60.5 m in 2017, respectively, and the 5th and 95th percentiles of 62.0 and 81.5 m for 2016 and 67.0 and 83.6 m for 2017.

For the period from May to October (when data were available for both years), the mean oxygen debt was  $11.3 \text{ mg}\cdot\text{l}^{-1}$  in 2016 and  $11.6 \text{ mg}\cdot\text{l}^{-1}$  in 2017. The minimum, maximum, 5th and 95th percentile values of oxygen debt were  $8.5 \text{ mg}\cdot\text{l}^{-1}$ ,  $11.9 \text{ mg}\cdot\text{l}^{-1}$ ,  $10.2 \text{ mg}\cdot\text{l}^{-1}$ , and  $11.8 \text{ mg}\cdot\text{l}^{-1}$  in 2016 and  $9.9 \text{ mg}\cdot\text{l}^{-1}$ ,  $12 \text{ mg}\cdot\text{l}^{-1}$ ,  $11 \text{ mg}\cdot\text{l}^{-1}$ , and  $12 \text{ mg}\cdot\text{l}^{-1}$  in 2017. If also early spring period for 2016 was taken into account, then the minimum oxygen debt was estimated as  $7.1 \text{ mg}\cdot\text{l}^{-1}$ .

In both years, we found no linear trend for the halocline base depth from May to October, and the oxygen debt showed no clear seasonal dynamics. However, there was a significant correlation between the halocline base depth and oxygen debt values in 2017 ( $R^2 = 0.23$ ,  $p < 0.05$ ).

If monthly mean values are considered, the halocline base depth and oxygen debt showed similar dynamics in both years. Considering the period from May to October, the mean halocline base depth ranged from 66.0 to 75.1 m in 2016 and from 72.2 to 77.2 m in 2017. A smaller variation in monthly mean oxygen debt values in 2017 is also evident, with the values ranging from 11.5 to

$11.8 \text{ mg}\cdot\text{l}^{-1}$ , compared to 2016 where the monthly oxygen debt values were between 10.9 and  $11.5 \text{ mg}\cdot\text{l}^{-1}$  (Figure 8).

## Oxygen Consumption

Oxygen consumption was calculated for the period from May to September for the stagnant layer which was defined based on the monthly average profiles of absolute salinity (SA) and conservative temperature (CT) (Figure 9). In both years, it was defined as the layer between 50 and 60 m, and the extended layer for the analysis (needed for the calculation of diffusion) was defined by adding data from additional 3 m to both sides of the stagnant layer; so, a depth range of 47–63 m was used. To estimate the sensitivity of the results to the choice of the stagnant layer, the estimates for diffusion, advection and consumption were also found for the layer 45–55 m.

Changes in the oxygen concentration due to advection were calculated based on estimated salinity advection and the correlation between salinity and oxygen. In both years, vertical profiles in the depth range of 30–70 m acquired in April at the national monitoring stations distributed along the GoF (see Figure 1) were used for the correlation analysis. The found relationships were statistically significant – in 2016,  $DO = -3.39 \cdot SA + 34.54$ ,  $R^2 = 0.84$ ,  $p < 0.05$  and, in 2017,  $DO = -3.57 \cdot SA + 36.43$ ,  $R^2 = 0.73$ ,  $p < 0.05$ .

Positive monthly average oxygen depletion values show that during the period in question, oxygen content in the stagnant layer decreased (Figure 10). Negative diffusion values indicate that more oxygen left the layer through the deeper boundary than was brought in through the upper boundary of the layer. Positive advection values show that more oxygenated water was brought into the study area (area of the profiling station).

The results show that the changes in oxygen on the monthly scale were mostly related to advection since the depletion and advection had the largest values and were moving in opposite directions (Figure 10; remember that a positive value of depletion means that oxygen is decreasing). Monthly depletion values were in the range of  $\pm 2.0 \text{ mg}\cdot\text{l}^{-1}\cdot\text{month}^{-1}$  while advection values ranged from  $-1.9 \text{ mg}\cdot\text{l}^{-1}\cdot\text{month}^{-1}$  to  $1.7 \text{ mg}\cdot\text{l}^{-1}\cdot\text{month}^{-1}$ . On

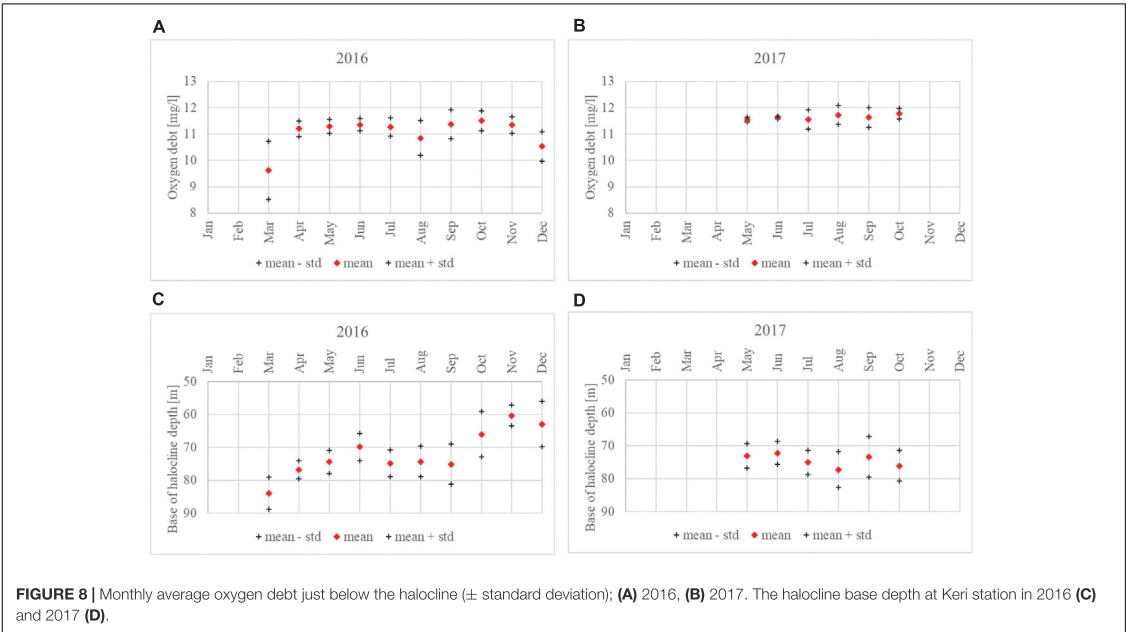


**FIGURE 8 |** Monthly average oxygen debt just below the halocline ( $\pm$  standard deviation); **(A)** 2016, **(B)** 2017. The halocline base depth at Keri station in 2016 **(C)** and 2017 **(D)**.

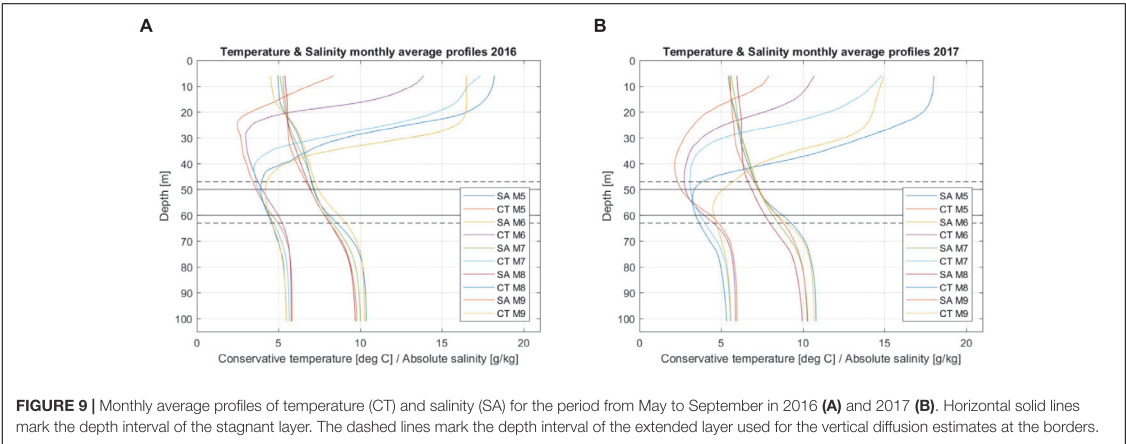


**FIGURE 9 |** Monthly average profiles of temperature (CT) and salinity (SA) for the period from May to September in 2016 **(A)** and 2017 **(B)**. Horizontal solid lines mark the depth interval of the stagnant layer. The dashed lines mark the depth interval of the extended layer used for the vertical diffusion estimates at the borders.

a monthly scale, the diffusion had the lowest contribution with the values varying in the range from 0 to  $-0.4 \text{ mg} \cdot \text{l}^{-1} \cdot \text{month}^{-1}$ . The resulting monthly average consumption estimates were in the range of  $-0.5$  and  $1.6 \text{ mg} \cdot \text{l}^{-1} \cdot \text{month}^{-1}$  with the lowest values in June–July and the maximum in July–August. This pattern was evident in both years. Note that the consumption values should be positive since no oxygen production should exist in the analyzed stagnant layer. However, the applied method gave small negative values of consumption for June–July in both years.

The total seasonal consumption from May to September as well as monthly average consumption rates were almost three times larger in 2016 than in 2017 – 0.82 and

$0.31 \text{ mg} \cdot \text{l}^{-1} \cdot \text{month}^{-1}$ , respectively (Table 3). It is interesting that the consumption rate estimates did not change much if, instead of the layer 50–60 m, the layer 45–55 m was analyzed although depletion was higher in the layer 45–55 m in both years. According to our estimates, consumption gave the highest contribution to the seasonal oxygen depletion. For the layer 50–60 m in 2017 and 45–55 m in 2016, diffusion and advection almost entirely compensated each other. Diffusion values did not vary between the 2 years much while advection was considerably higher in 2016 than in 2017, especially for the layer 45–55 m. This result is in agreement with the observed concurrent decrease of salinity in these depth ranges (see



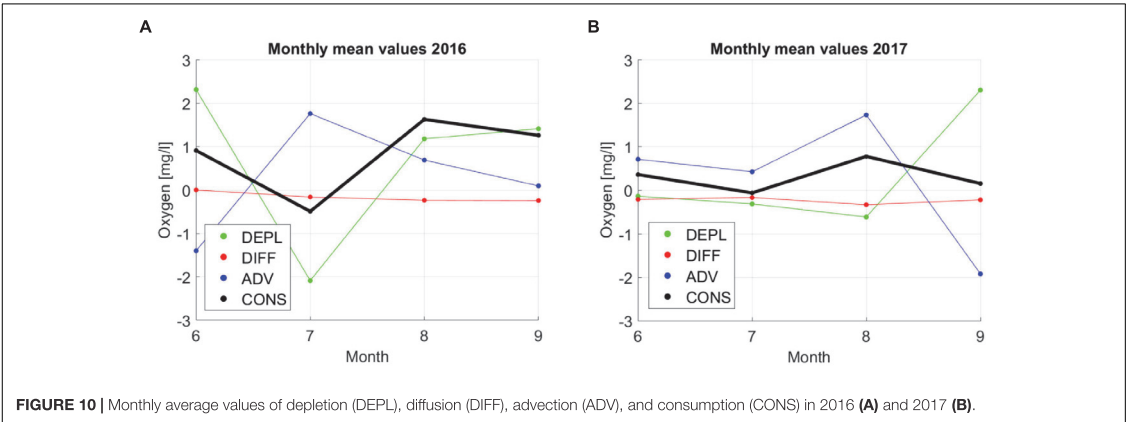


**FIGURE 10 |** Monthly average values of depletion (DEPL), diffusion (DIFF), advection (ADV), and consumption (CONS) in 2016 (A) and 2017 (B).

**TABLE 3 |** Average values of depletion (DEPL), diffusion (DIFF), advection (ADV), and consumption (CONS).

Year:	2016		2017	
Layer:	50–60 m	45–55 m	50–60 m	45–55 m
DEPL (mg·l <sup>-1</sup> in May–September)	2.81	3.43	1.23	2.17
DIFF (mg·l <sup>-1</sup> in May–September)	−0.65	−1.32	−0.94	−1.50
ADV (mg·l <sup>-1</sup> in May–September)	1.14	1.30	0.94	0.55
CONS (mg·l <sup>-1</sup> in May–September)	3.30	3.41	1.22	1.22
Average monthly CONS (mg·l <sup>-1</sup> ·month <sup>-1</sup> )	0.82	0.85	0.31	0.31

**Figure 3;** the decrease was larger in 2016 than in 2017) since the oxygen advection was estimated based on salinity advection and linear correlation between oxygen and salinity. Still, the much larger consumption in 2016 than in 2017 has to be analyzed further.

We also analyzed the sensitivity of the consumption estimates to the following assumptions: neglecting the changes in oxygen content due to changes in solubility; constant empirical intensity factor for turbulent flux estimates; linear regression between oxygen and salinity used to estimate oxygen advection.

We calculated monthly average temperature and salinity in the analyzed layer 50–60 m and found that due to their changes ranging, respectively, from 3.27 to 4.66°C and from 7.25 to 8.01 g·kg<sup>-1</sup>, the oxygen saturation concentration varied between 11.61 and 12.06 mg·l<sup>-1</sup>. Since the monthly average oxygen concentration in this layer ranged between 5.70 and 8.74 mg·l<sup>-1</sup>, the changes in solubility could cause less than about 15% of the observed variability.

For diffusion estimates, we used the value of the empirical intensity factor of  $\alpha = 1.5 \times 10^{-7} \text{ m}^2 \cdot \text{s}^{-2}$ . It is an average value based on earlier studies, where the values ranging from  $\alpha = 0.5 \times 10^{-7} \text{ m}^2 \cdot \text{s}^{-2}$  to  $\alpha = 2.5 \times 10^{-7} \text{ m}^2 \cdot \text{s}^{-2}$  have been applied (Gargett, 1984; Stigebrandt, 1987; Axell, 1998; Meier, 2001). Using these minimum and maximum values of the factor we found that for the 2016 data, the consumption estimates varied only from 0.80 to 0.85 mg·l<sup>-1</sup>·month<sup>-1</sup> while for the 2017 data, the ranges were larger – from 0.25 to 0.36 mg·l<sup>-1</sup>·month<sup>-1</sup>. Although for the latter case, the difference between the minimum and the maximum was about 30% of

the estimate, the choice of the factor changed the result only by 0.1 mg·l<sup>-1</sup>·month<sup>-1</sup>.

For the advection estimates we used the linear correlation between salinity and oxygen based on data from the monitoring stations in the GoF from the Osmussaar Island to the eastern GoF (station F1; see **Figure 1**) This assumption of the linear relationship between salinity and oxygen content is valid only in a limited area (see the correlation estimates above) but not for the entire Baltic Sea; thus, also in the GoF, along-isohaline gradients exist. For instance, based on the data from the monitoring cruises in May/June, July, August and October of both years, the average change in oxygen concentration in the GoF along an isohaline corresponding to the average salinity in the layer 50–60 m was 0.9 mg·l<sup>-1</sup> per a longitudinal degree. In the case of oscillating up- and down-estuary flow in the studied layer, the oxygen advection estimates are not biased, but a relatively large bias could occur if unidirectional flow prevails for a long period. Taking the estimated horizontal oxygen gradient and assuming a constant flow of 2 cm·s<sup>-1</sup> for a month could result in a change of oxygen content by 0.83 mg·l<sup>-1</sup>·month<sup>-1</sup>.

DISCUSSION

We analyzed high-resolution time series of vertical profiles of oxygen at a central, deep station in the GoF close to the Keri Island in 2016–2017. The main study question was whether these observations could be applied to assess the status of this stratified estuary in relation to the eutrophication effects using

three suggested indicators. The present monitoring programs contain observations of DO content at a few stations a few times a year (in Estonia, 6 times a year, and only the surface and near-bottom layer are sampled). Beside the eutrophication effects, the sub-surface distribution and variability of DO in the GoF are related to multi-scale physical processes. Thus, the differentiation between the natural variability and the effects of eutrophication could require high-resolution monitoring data. Since due to economic reasons it is not possible to arrange measurements with high temporal resolution at many stations, we analyzed the applicability of data from one profiling station to assess the oxygen conditions using the following indicators – the extent of hypoxia, oxygen debt, and oxygen consumption.

Although large-scale surveys of the vertical oxygen distribution revealed an along-gulf inclination of the border of the hypoxic layer of 1.9 m per 100 km, the estimates of the extent of hypoxia based on the hypoxic depth from Keri station with and without inclination were very close to each other. In addition, it was shown by Liblik and Lips (2017) that there exists almost no average cross-gulf inclination of the halocline in the GoF. Thus, we conclude that the Keri station is a representative station to assess the sub-halocline oxygen conditions in the entire GoF on seasonal timescales.

Since wind conditions play a major role defining the areal extent of the near-bottom hypoxia in the GoF, the effect of the prevailing wind has to be taken into account when using the hypoxic area extent as a eutrophication indicator. It is known that with prevailing south-westerly winds the estuarine circulation is reversed which moves the surface layer into the gulf and the deep layer out of the gulf (Elken et al., 2003). North-easterly winds have the opposite effect and the deep water – deoxygenated and phosphate-rich salt wedge moves into the gulf from the Northern Baltic Proper (Liblik and Lips, 2011; Lips et al., 2017).

When comparing the monthly average hypoxic area extent with the local wind conditions using wind data from Kalbådgrund we found that for 2016, when the N-NE winds prevailed, the hypoxic area was enlarged, while with the W-SW winds, the area was smaller (Table 2). This result is in accordance with a recent analysis of long-term monitoring data by Lehtoranta et al. (2017) and a study by Väli et al. (2013) where the authors concluded that the increase in bottom oxygen concentrations in the GoF in 1990–1995 could be explained by stronger ventilation of the bottom layers due to increased westerlies. Also, a comparison of the 3-week average wind stress component from N-NE ( $20\pi$ ) with the hypoxic depth at the Keri station (Figure 5) showed significant correlation between these parameters if early spring data from 2016 were excluded. The very deep hypoxic depth in March 2016 could be explained by weaker stratification and mixing of the water column (and a possible collapse of stratification) as it was observed earlier in winter by Liblik et al. (2013) and Lips et al. (2017). In 2017, the winds from the sector from east to north were almost absent, and thus, the intensification of estuarine circulation leading to the penetration of the near-bottom salt wedge into the GoF did not manifest itself in the same extent as in 2016. Secondly, we suggest that the high variability and large extent of hypoxia in late 2016 could be attributed to the influence of the 2014 MBI,

which impact reached the GoF in 2016 (Liblik et al., 2018). The MBI influence constituted itself as a deep-water inflow of former deoxygenated water from the NBP to the GoF, which pushed the existing bottom water in the GoF upward resulting in an increase in volume and areal extent of hypoxic waters.

In conclusion, although the extent of hypoxia is an easily understandable indicator of near-bottom oxygen conditions in the GoF, still some issues have to be solved. An analysis of long-term data should be conducted to differentiate between the eutrophication-related and the wind- or inflow-related impacts (a first attempt is made by Lehtoranta et al., 2017). Also, the reference and target values – what percentage corresponds to the good status, have to be defined. For this purpose, the links of the extent of hypoxia with the nutrient load, nutrient concentrations and productivity have to be shown. Also, it is important to consider the feedback that the extent of hypoxia has on nutrient concentrations via the internal nutrient fluxes from the sediments in poor oxygen conditions (Pitkänen et al., 2001).

Oxygen debt indicator is the other easily understandable characteristic of oxygen conditions which could be understood as the apparent oxygen utilization – the difference between the oxygen saturation concentration and measured concentration. As seen in Figure 7, the oxygen debt estimates based on a single profile had very high short-term variability. It could be mostly explained by the observed halocline dynamics in the GoF displayed in Figure 3 and shown by Liblik and Lips (2017). Internal waves cause up- and downward movement of the halocline and influence the depth range with the vertical salinity gradient larger than  $0.07 \text{ g}\cdot\text{kg}^{-1}\cdot\text{m}^{-1}$  within the halocline layer. Consequently, the estimates of the oxygen debt based on separate profiles could reveal a relatively high variability, but an average of these estimates over a large number of profiles characterizes the sub-halocline oxygen conditions quite well.

Since we did not have the time-series of oxygen profiles covering the winter months, we were not able to calculate the yearly average oxygen debt as required by the HELCOM oxygen debt indicator description (HELCOM, 2018a). However, we suggest that for the GoF, where the halocline could be weak or occasionally absent in winter (Liblik et al., 2013; Lips et al., 2017), the oxygen debt could be estimated on the basis of seasonal data from May to September (or October). It also means that a new threshold for good environmental status should be suggested since the value  $8.66 \text{ mg}\cdot\text{l}^{-1}$ , which is applied for most of the deep basins in the Baltic Sea, was defined as a volume specific average and for the yearly average (HELCOM, 2018a). We also suggest that the uniform threshold value for the volume specific average oxygen depth should be reconsidered since the basins have different depths while the DO content decreases with the depth. Instead, the oxygen debt just below the halocline could be used which might have similar threshold values for most of the Baltic Sea deep basins.

An advantage of the oxygen debt indicator compared to the extent of hypoxia is that it seems to be less dependent on the advection of the hypoxic salt wedge into and out from the inner GoF since an increase/decrease in the volume of hypoxic waters due to the horizontal advection results in upward/downward movement of the halocline and not in a decrease in DO

content just below the halocline. For instance, from September to October 2016, the extent of hypoxia almost doubled while the oxygen debt increased only from 11.4 mg·l<sup>-1</sup> in September to 11.5 mg·l<sup>-1</sup> in October.

Oxygen consumption results found in this study as averages for the whole period from spring to autumn (June–September) are in the range of other published results (Table 4). While in the earlier estimates, the monthly consumption rates varied between 0.25 and 1.29 mg l<sup>-1</sup> month<sup>-1</sup>, in the present study, the estimates in the Gulf of Finland were 0.82 mg l<sup>-1</sup> month<sup>-1</sup> for 2016 and 0.31 mg l<sup>-1</sup> month<sup>-1</sup> for 2017. This comparison is not entirely correct since the earlier estimates were mostly for longer (multi-year) periods and our study dealt only with the productive season, as well as we made our analysis for the intermediate layer (50–60 m) while in the earlier studies deeper (sub-halocline) layers were considered. However, this agreement between different results confirms that the method proposed in our study is applicable to rough consumption estimates. The other question is whether it is accurate enough to be used for eutrophication status assessment. For instance, the negative values of monthly consumption estimates in July of both years indicate that the approach may not be appropriate for shorter periods.

We analyzed the sensitivity of the results regarding different choices and assumptions in the suggested method of consumption estimates. We showed that a slight change of the depth limits for the analyzed stagnant layer would almost not alter the results. The changes in solubility, which were not included in the suggested approach, could cause a bias less than about 15% of the observed variability (see section “Oxygen Consumption”). The choice of the empirical intensity factor of turbulence could change the diffusion estimate and consequently the consumption estimate only by 0.1 mg·l<sup>-1</sup>·month<sup>-1</sup>.

For the advection estimates, we used the linear correlation between salinity and oxygen, which is significant based on the data from the GoF. At the same time, we showed that the average change in oxygen concentration in the GoF along an isohaline in the layer under consideration could be as large as 0.9 mg·l<sup>-1</sup> per a longitudinal degree. Thus, a relatively large bias in the consumption estimates up to 0.83 mg·l<sup>-1</sup>·month<sup>-1</sup> could occur if unidirectional flow prevails for a long period. Such on average unidirectional flow in the intermediate layer could exist in the GoF for a few months as shown by Liloer et al. (2017) although the characteristic current velocities there are usually smaller than in the surface and near-bottom layer (Suhhova et al., 2018). This

bias estimate has the value close to the consumption estimates, and thus, it has to be addressed in the further analysis. For instance, in 2016, the saline and oxygen-deficient sub-halocline waters of the northern Baltic Proper were pushed by the MBI north-eastward to the GoF near-bottom layer (Liblik et al., 2018). It could cause uplift of old near-bottom water in the central and eastern GoF and the westward flow in the intermediate layer which could lead to an oxygen decrease. The observed decrease in oxygen content from July to September 2016 by 2.59 mg·l<sup>-1</sup> was mostly assigned to consumption since the average salinity increase was only 0.18 g·kg<sup>-1</sup> and the corresponding oxygen decrease due to advection should not be as large according to the present calculation method based on a linear regression between salinity and oxygen content. This method, which has a bias in advection estimates when the flow is on average unidirectional in the analyzed layer, could also cause the large difference between the seasonal consumption estimates in 2016 and 2017. As a way forward, simultaneous observations of vertical structure of currents near the Keri station has been initiated in 2018.

The assumption of an equal surface area of the upper and lower border of the analyzed layer and no explicit water-sediment oxygen fluxes means that the downward oxygen flux through the lower boundary is entirely estimated as a turbulent flux in the water column. This approach is correct for an open sea area; however, one could expect that the oxygen flux from water to the sediments at the slopes of the basin (Holtermann et al., 2017) and a horizontal mixing toward the basin interior impact the consumption estimate results. As shown by Koop et al. (1990) the oxygen flux from the water to the sediments under oxic conditions could be as large as 777 μmol·O·m<sup>-2</sup> h<sup>-1</sup> corresponding to approximately 1.8 mg·l<sup>-1</sup>·month<sup>-1</sup> if a 10 m thick water layer above the seabed is considered. The maximum oxygen flux through the lower border of the analyzed layer found in the present study could cause a decrease in DO content of 0.7 mg·l<sup>-1</sup>·month<sup>-1</sup>. Thus, an additional export of oxygen from the stagnant layer due to the flux from water to the sediments and horizontal mixing should increase the consumption estimates. When interpreting our results, one has to consider that the consumption values include both the local consumption in the studied open-sea area and a part of consumption in the sediments at the surrounding slopes of the basin. This additional export of oxygen from the stagnant layer should increase the consumption estimates. Thus, it does not explain the negative values found in

TABLE 4 | Monthly average oxygen consumption results found in the literature.

Location	Period	Depth	mg l <sup>-1</sup> month <sup>-1</sup>	Source
Baltic proper	1957–1982	> 62 m	0.25	Rahm, 1987
Öresund	1965–1989	?	1.29	Mattsson and Stigebrandt, 1993
Bornholm Basin	1957–2011	> 65 m	0.51	Stigebrandt and Kalén, 2013
Baltic proper, deep water	1972–1980	?	0.26	Shaffer and Rönner, 1984
Gotland Basin	1968–1977	?	0.34	Rydberg, 1978
Bornholm Basin	1968–1977	?	0.43	Rydberg, 1978
Gulf of Finland	2016	50–60 m	0.82	This study
Gulf of Finland	2017	50–60 m	0.31	This study

our study for June–July 2016 and 2017 which most probably are related to the bias in advection estimates.

A comparison of the three indicators reveals that their average seasonal values almost did not vary between the two analyzed years for the hypoxic area extent and oxygen debt while about 2.7 times higher oxygen consumption was found in 2016 than in 2017. The average hypoxic depth in May–October was 64.5 m in 2016 and 64.6 m in 2017, which result in an almost equal hypoxic area extent for both years. The average oxygen debt in May–October was  $11.3 \text{ mg}\cdot\text{l}^{-1}$  in 2016 and  $11.6 \text{ mg}\cdot\text{l}^{-1}$  in 2017. These values differ only by  $0.3 \text{ mg}\cdot\text{l}^{-1}$ , which is  $<3\%$  of the indicator result. We suggest that the found large difference in oxygen consumption estimates between 2016 and 2017, which is inconsistent with the other indicator results, could be related to the applied methodology and/or the fact that the consumption estimates were found for the intermediate layer while hypoxic area and oxygen debt for the sub-halocline layer. What could be the main natural factors causing this large difference, e.g., influence of productivity or riverine water, since in 2016 the upper layer was fresher than in 2017, needs future studies. The largest uncertainty is caused by the too simplified estimate of the oxygen advection. Although oxygen consumption would be the best indicator, which should directly be dependent on the productivity of the sea area, it requires further development. Regarding the observational program, simultaneous measurements of current profiles could be beneficial to decrease the uncertainty of advection estimates.

## CONCLUSION

We have described the oxygen conditions in the GoF in 2016–2017 based on observations mostly at the Keri profiling station where vertical profiles of temperature, salinity and oxygen were acquired up to 8 times a day. The applicability of high-frequency data from this fixed automated station and the three adapted oxygen indicators for the eutrophication status assessments were tested. The main results of the analysis are:

- the GoF bottom area affected by hypoxia varied between 3.3 and 28.2% with a minimum in March 2016, maximum in November 2016 and an average extent of about 15% in May–September 2016–2017;
- since the halocline in the GoF could be destroyed in winter, the “oxygen debt” indicator should be based on data from the stratified season only, and we suggest that only oxygen debt just below the halocline should be used;

## REFERENCES

- Alenius, P., Myrberg, K., and Nekrasov, A. (1998). The physical oceanography of the Gulf of Finland: a review. *Boreal Environ. Res.* 3, 97–125.
- Andrejev, O., Sokolov, A., Soomere, T., Värvi, R., and Viikmäe, B. (2010). The use of high-resolution bathymetry for circulation modelling in the Gulf of Finland. *Est. J. Eng.* 16, 187–210. doi: 10.3176/eng.2010.3.01
- Andrejev, O., Soomere, T., Sokolov, A., and Myrberg, K. (2011). The role of spatial resolution of a three-dimensional hydrodynamic model for marine transport risk assessment. *Oceanologia* 53, 309–334. doi: 10.5697/oc.53-1-TI.309

- the formulated oxygen budget, where depletion, diffusion, advection and consumption are taken into account, gave an average seasonal oxygen consumption in the 50–60 m water layer of the GoF in 2016 and 2017 as high as  $0.82$  and  $0.31 \text{ mg}\cdot\text{l}^{-1}\cdot\text{month}^{-1}$ , respectively;
- this large difference in consumption values between 2016 and 2017 could partly be related to the uncertainties of advection estimates.

We concluded that all three tested indicators have methodological challenges to be solved if they are used for the eutrophication effects assessment. The main issue is related to the differentiation between natural changes and eutrophication-related impacts. To increase the confidence of eutrophication assessments both high-frequency profiling should be implemented in the monitoring programs and more accurate estimates of changes due to physical processes are required.

## DATA AVAILABILITY STATEMENT

Part of the data (temperature, salinity) can be found on EMODnet Physics <http://www.emodnet-physics.eu/Map/DefaultMap.aspx> when searching for “KeriCable” station. Oxygen datasets are available on request.

## AUTHOR CONTRIBUTIONS

S-TS was the main responsible person in developing methods, analyzing data, and writing the manuscript. UL contributed to developing methods and writing the manuscript. TL contributed to analyzing data regarding the influence of hydrography.

## FUNDING

The work was financially supported by the Institutional Research Funding IUT (IUT19-6) of the Estonian Ministry of Education and Research and Environmental Investment Center environmental program project KIK17144.

## ACKNOWLEDGMENTS

We would like to thank the Finnish Meteorological Centre, for providing wind data, the crew of r/v Salme and our colleagues.

- Axell, L. B. (1998). On the variability of Baltic Sea deepwater mixing. *J. Geophys. Res.* 103, 21667–21682. doi: 10.1029/98JC01714
- Conley, D. J., Björck, S., Bonsdorff, E., Carstensen, J., Destouni, G., Gustafsson, B. G., et al. (2009). Hypoxia-related processes in the Baltic Sea. *Environ. Sci. Technol.* 43, 3412–3420. doi: 10.1021/es802762a
- Conley, D. J., Humborg, C., Rahm, L., Savchuk, O. P., and Wulff, F. (2002). Hypoxia in the Baltic Sea and basin-scale changes in phosphorus biogeochemistry. *Environ. Sci. Technol.* 36, 5315–5320. doi: 10.1021/es025763w
- Diaz, R. J., and Rosenberg, R. (2008). Spreading dead zones and consequences for marine ecosystems. *Science* 321, 926–929. doi: 10.1126/science.1156401



- Directive 2008/56/EC of the European Parliament and of the Council (2008). *Establishing a Framework for Community Action in the Field of Marine Environmental Policy (Marine Strategy Framework Directive)*. Available at: <http://eur-lex.europa.eu/legal-content/EN/TXT/PDF/?uri=CELEX:32008L0056&from=EN>
- Elken, J., Raudsepp, U., and Lips, U. (2003). On the estuarine transport reversal in deep layers of the Gulf of Finland. *J. Sea Res.* 49, 267–274. doi: 10.1016/S1385-1101(03)00018-2
- Gargett, A. E. (1984). Vertical eddy diffusivity in the ocean interior. *J. Mar. Res.* 42, 359–393. doi: 10.1357/002224084788502756
- Gerlach, S. A. (1994). Oxygen conditions improve when the salinity in the Baltic Sea decreases. *Mar. Pollut. Bull.* 28, 413–416. doi: 10.1016/0025-326X(94)90126-0
- Gustafsson, B. G., Schenk, F., Blenckner, T., Eilola, K., Meier, H. E. M., Müller-Karulis, B., et al. (2012). Reconstructing the development of Baltic Sea eutrophication 1850–2006. *Ambio* 41, 534–548. doi: 10.1007/s13280-012-0318-x
- Hansson, M., Andersson, L., and Axe, P. (2011). *REPORT OCEANOGRAPHY No. 42. Areal Extent and Volume of Anoxia and Hypoxia in the Baltic Sea, 1960–2011*. Available at: [http://www.smhi.se/polopoly\\_fs/1.19219/Oxygen\\_timeseries\\_1960\\_2010\\_20111219.pdf](http://www.smhi.se/polopoly_fs/1.19219/Oxygen_timeseries_1960_2010_20111219.pdf)
- Hansson, M., Viktorsson, L., and Andersson, L. (2017). *REPORT OCEANOGRAPHY No. 63. Oxygen Survey in the Baltic Sea 2016 - Extent of Anoxia and Hypoxia, 1960–2017*. Available at: [https://www.smhi.se/polopoly\\_fs/1.132189/Oxygen\\_timeseries\\_1960\\_2017.pdf](https://www.smhi.se/polopoly_fs/1.132189/Oxygen_timeseries_1960_2017.pdf)
- HELCOM (2013). *Approaches and Methods for Eutrophication Target Setting in the Baltic Sea Region*. Helsinki: HELCOM.
- HELCOM (2014). *Eutrophication Status of the Baltic Sea 2007–2011. A Concise Thematic Assessment*. Helsinki: HELCOM.
- HELCOM (2015a). *EUTRO-OPER 4–2015. Development of Oxygen Consumption Indicator*. Available at: <https://portal.helcom.fi/meetings/EUTRO-OPER%204-2015-217/default.aspx>
- HELCOM (2015b). *Final Report of the Project, Making HELCOM Eutrophication Assessments Operational (HELCOM EUTRO-OPER)*. Available at: <http://www.helcom.fi/Documents/EUTRO-OPERprojectreport.pdf>
- HELCOM (2018a). *Oxygen Debt - HELCOM Core Indicator Report*. Available at: <http://www.helcom.fi/baltic-sea-trends/indicators/oxygen-debt/>
- HELCOM (2018b). *State of the Baltic Sea - Second HELCOM Holistic Assessment 2011–2016*. Available at: <http://www.helcom.fi/baltic-sea-trends/holistic-assessments/state-of-the-baltic-sea-2018/reports-and-materials/>
- Holtermann, P. L., Prien, R., Naumann, M., Mohrholz, V., and Umlauf, L. (2017). Deepwater dynamics and mixing processes during a major inflow event in the central Baltic Sea. *J. Geophys. Res.* 122, 6648–6667. doi: 10.1002/2017JC013050
- Kabel, K., Moros, M., Porsche, C., Neumann, T., Adolphi, F., Andersen, T. J., et al. (2012). Impact of climate change on the Baltic Sea ecosystem over the past 1,000 years. *Nat. Clim. Chang.* 2, 871–874. doi: 10.1038/nclimate1595
- Koop, K., Boynton, W. R., Wulff, F., and Carman, R. (1990). Sediment-water oxygen and nutrient exchanges along a depth gradient in the Baltic Sea. *Mar. Ecol. Prog. Ser.* 63, 65–77. doi: 10.3354/meps063065
- Laine, A. O., Andersin, A.-B., Leiniö, S., and Zuur, A. F. (2007). Stratification-induced hypoxia as a structuring factor of macrozoobenthos in the open Gulf of Finland (Baltic Sea). *J. Sea Res.* 57, 65–77. doi: 10.1016/j.seares.2006.08.003
- Large, W. G., and Pond, S. (1981). Open ocean momentum flux measurements in moderate to strong winds. *J. Phys. Oceanogr.* 11, 324–336. doi: 10.1175/1520-0485(1981)011<0324:OOMFMI>2.0.CO;2
- Launiainen, J., and Laurila, T. (1984). Wind characteristics at Finnish automatic marine weather stations in the Northern Baltic Sea. *Finn. Mar. Res.* 250, 52–86.
- Lehtoranta, J., Savchuk, O. P., Elken, J., Kim, D., Kuosa, H., Raateoja, M., et al. (2017). Atmospheric forcing controlling inter-annual nutrient dynamics in the open Gulf of Finland. *J. Mar. Syst.* 171, 4–20. doi: 10.1016/j.jmarsys.2017.02.001
- Liblik, T., Laanemets, J., Raudsepp, U., Elken, J., and Suhhova, I. (2013). Estuarine circulation reversals and related rapid changes in winter near-bottom oxygen conditions in the Gulf of Finland, Baltic Sea. *Ocean Sci.* 9, 917–930. doi: 10.5194/os-9-917-2013
- Liblik, T., and Lips, U. (2011). Characteristics and variability of the vertical thermohaline structure in the Gulf of Finland in summer. *Boreal Environ. Res.* 16A, 73–83.
- Liblik, T., and Lips, U. (2017). Variability of pycnoclines in a three-layer, large estuary: the Gulf of Finland. *Boreal Environ. Res.* 22, 27–47.
- Liblik, T., Naumann, M., Alenius, P., Hansson, M., Lips, U., Nausch, G., et al. (2018). Propagation of impact of the recent Major Baltic Inflows from the Eastern Gotland basin to the Gulf of Finland. *Front. Mar. Sci.* 5:222. doi: 10.3389/fmars.2018.00222
- Lilover, M.-J., Elken, J., Suhhova, I., and Liblik, T. (2017). Observed flow variability along the thalweg, and on the coastal slopes of the Gulf of Finland, Baltic Sea. *Estuar. Coast. Shelf Sci.* 195, 23–33. doi: 10.1016/j.ecss.2016.11.002
- Lips, U., Laanemets, J., Lips, I., Liblik, T., Suhhova, I., and Suursaar, Ü. (2017). Wind-driven residual circulation and related oxygen and nutrient dynamics in the Gulf of Finland (Baltic Sea) in winter. *Estuar. Coast. Shelf Sci.* 195, 4–15. doi: 10.1016/j.ecss.2016.10.006
- Matthäus, W., and Franck, H. (1992). Characteristics of major Baltic inflows—a statistical analysis. *Cont. Shelf Res.* 12, 1375–1400. doi: 10.1016/0278-4343(92)90060-W
- Mattsson, J., and Stigebrandt, A. (1993). The vertical flux of organic matter in the Öresund estimated by two different methods using oxygen measurements. *Estuar. Coast. Shelf Sci.* 37, 329–342. doi: 10.1006/ecss.1993.1060
- Meier, H. E. M. (2001). On the parameterization of mixing in three-dimensional Baltic Sea models. *J. Geophys. Res.* 106, 30997–31016. doi: 10.1029/2000JC000631
- Naumann, M., Mohrholz, V., and Waniek, J. J. (2018). *Water Exchange and Conditions in the Deep Basins*. Available at: <http://www.helcom.fi/baltic-sea-trends/environment-fact-sheets/>
- Pitkänen, H., Lehtoranta, J., and Räske, A. (2001). Internal nutrient fluxes counteract decreases in external load: the case of the estuarine eastern Gulf of Finland, Baltic Sea. *Ambio* 30, 195–201. doi: 10.1579/0044-7447-30.4.195
- Rahm, L. (1987). Oxygen consumption in the Baltic Proper. *Limnol. Oceanogr.* 32, 978–978. doi: 10.4319/lo.1987.32.4.0973
- Rydberg, L. (1978). *Deep Water Flow and Oxygen Consumption within the Baltic*. Report No. 27. Göteborg: Department of Physical Oceanography, Göteborg University.
- Schinke, H., and Matthäus, W. (1998). On the causes of major Baltic inflows — an analysis of long time series. *Cont. Shelf Res.* 18, 67–97. doi: 10.1016/S0278-4343(97)00071-X
- Schlitzer, R. (2018). *Ocean Data View*. Available at: <https://odv.awi.de>
- Shaffer, G., and Rönner, U. (1984). Denitrification in the Baltic proper deep water. *Deep Sea Res A* 31, 197–220. doi: 10.1016/0198-0149(84)90102-X
- Stigebrandt, A. (1987). A model for the vertical circulation of the Baltic deep water. *J. Phys. Oceanogr.* 17, 1772–1785. doi: 10.1007/s13280-017-0933-7
- Stigebrandt, A., and Kalén, O. (2013). Improving oxygen conditions in the deeper parts of bornholm sea by pumped injection of winter water. *Ambio* 42, 587–595. doi: 10.1007/s13280-012-0356-4
- Suhhova, I., Liblik, T., Lilover, M.-J., and Lips, U. (2018). A descriptive analysis of the linkage between the vertical stratification and current oscillations in the Gulf of Finland. *Boreal Environ. Res.* 23, 83–103.
- Vahtera, E., Conley, D. J., Gustafsson, B. G., Kuosa, H., Pitkänen, H., Savchuk, O. P., et al. (2007). Internal ecosystem feedbacks enhance nitrogen-fixing cyanobacteria blooms and complicate management in the Baltic Sea. *Ambio* 36, 186–194. doi: 10.1579/0044-7447(2007)36[186:IEFENC]2.0.CO;2
- Väli, G., Meier, H. E. M., and Elken, J. (2013). Simulated halocline variability in the Baltic sea and its impact on hypoxia during 1961–2007. *J. Geophys. Res.* 118, 6982–7000. doi: 10.1002/2013JC009192
- Vaquero-Sunyer, R., and Duarte, C. M. (2008). Thresholds of hypoxia for marine biodiversity. *Proc. Natl. Acad. Sci. U.S.A.* 105, 15452–15457. doi: 10.1073/pnas.0803833105
- Viktorsson, L. (2018). *Hydrography and Oxygen in the Deep Basins*. Helsinki: HELCOM Baltic Sea environment fact sheets.

**Conflict of Interest Statement:** The authors declare that the research was conducted in the absence of any commercial or financial relationships that could be construed as a potential conflict of interest.

Copyright © 2019 Stoicescu, Lips and Liblik. This is an open-access article distributed under the terms of the Creative Commons Attribution License (CC BY). The use, distribution or reproduction in other forums is permitted, provided the original author(s) and the copyright owner(s) are credited and that the original publication in this journal is cited, in accordance with accepted academic practice. No use, distribution or reproduction is permitted which does not comply with these terms.

## **Paper II**

Stoicescu, S-T., Laanemets, J., Liblik, T., Skudra, M., Samlas, O., Lips, I., and Lips, U. 2022. Causes of the extensive hypoxia in the Gulf of Riga in 2018. Biogeosciences, 19, pp. 2903–2920. <https://doi.org/10.5194/bg-19-2903-2022>





# Causes of the extensive hypoxia in the Gulf of Riga in 2018

Stella-Theresa Stoicescu<sup>1</sup>, Jaan Laanemets<sup>1</sup>, Taavi Liblik<sup>1</sup>, Māris Skudra<sup>2</sup>, Oliver Samlas<sup>1</sup>, Inga Lips<sup>1,3</sup>, and Urmas Lips<sup>1</sup>

<sup>1</sup>Department of Marine Systems, Tallinn University of Technology, Tallinn, 19086, Estonia

<sup>2</sup>Latvian Institute of Aquatic Ecology, Riga, 1007, Latvia

<sup>3</sup>EuroGOOS AISBL, Brussels, 1000, Belgium

**Correspondence:** Stella-Theresa Stoicescu (stella.stoicescu@taltech.ee)

Received: 18 June 2021 – Discussion started: 28 June 2021

Revised: 3 May 2022 – Accepted: 24 May 2022 – Published: 14 June 2022

**Abstract.** The Gulf of Riga is a relatively shallow bay connected to the deeper central Baltic Sea (Baltic Proper) via straits with sills. The decrease in the near-bottom oxygen levels from spring to autumn is a common feature in the gulf, but in 2018, extensive hypoxia was observed. We analyzed temperature, salinity, oxygen, and nutrient data collected in 2018, along with historical data available from environmental databases. Meteorological and hydrological data from the study year were compared with their long-term means and variability. We suggest that pronounced oxygen depletion occurred in 2018 due to a distinct development of vertical stratification. Seasonal stratification developed early and was stronger in spring–summer 2018 than on average due to high heat flux and weak winds. Dominating north-easterly winds in early spring and summer supported the inflow of saltier waters from the Baltic Proper that created an additional deep pycnocline restricting vertical transport between the near-bottom layer (NBL) and the water column above. The estimated oxygen consumption rate in the NBL in spring–summer 2018 was about  $1.7 \text{ mmol O}_2 \text{ m}^{-2} \text{ h}^{-1}$ , which exceeded the oxygen input to the NBL due to advection and vertical mixing. Such a consumption rate leads to near-bottom hypoxia in all years when vertical mixing in autumn reaches the seabed later than on average according to the long-term (1979–2018) meteorological conditions. The observed increase in phosphate concentrations in the NBL in summer 2018 suggests a significant sediment phosphorus release in hypoxic conditions counteracting the mitigation measures to combat eutrophication. Since climate change projections predict that meteorological conditions comparable to those in 2018 will occur more frequently, extensive hypoxia would be more common in the Gulf of Riga and other

coastal basins with similar morphology and human-induced elevated input of nutrients.

## 1 Introduction

Coastal dead zones have expanded in the oceans since the 1960s, a phenomenon which is mostly caused by increased primary production as a result of eutrophication (Diaz and Rosenberg, 2008). Geographic settings such as openness of the basin and hydrographic conditions such as the strength and onset of stratification affect the magnitude of near-bottom hypoxia (Codiga et al., 2009; Liblik et al., 2020; Murphy et al., 2011; Ukrainskii and Popov, 2009; Zhang et al., 2010). Current and projected climate changes continue to affect the marine environment; e.g., increased temperature and strengthening of stratification in estuaries cause decreases in oxygen solubility and vertical mixing, respectively, which could lead to enhanced oxygen depletion of bottom waters (Bindoff et al., 2019).

The Baltic Sea is strongly influenced by eutrophication and changing climate conditions (Conley et al., 2009; Gustafsson et al., 2012; Kabel et al., 2012). The primary drivers behind eutrophication are excessive amounts of nutrients that enter the marine environment through rivers and the atmosphere (HELCOM, 2018b; Reusch et al., 2018). Hypoxic conditions have been found throughout the Baltic Sea as quasi-permanent, seasonal, or exceptional infrequent phenomena (Carstensen and Conley, 2019; Conley et al., 2007, 2011; Karlson et al., 2002). Hypoxia and anoxia have occurred in open water areas of the Baltic Proper below the halocline ( $\sim 70\text{--}80 \text{ m}$ ) on an almost permanent basis since



the 1950s (HELCOM, 2018c; Karlson et al., 2002). Occasionally, oxygen conditions in this central basin are improved by Major Baltic Inflows (e.g., Matthäus and Franck, 1992; Schinke and Matthäus, 1998; Schmale et al., 2016; Liblik et al., 2018). However, these improved oxygen conditions are short-lived because, in the long-term, the inflows enhance stratification and thereby reduce vertical oxygen transport (Conley et al., 2002).

In the shallower regions, where the halocline is absent, but a seasonal thermocline restricts vertical mixing, oxygen consumption could lead to temporal near-bottom hypoxia and sediment phosphorus release in late summer–autumn (Lukkari et al., 2009; Puttonen et al., 2014, 2016; Walve et al., 2018). For instance, such seasonal hypoxic events have occurred in the northern Baltic coastal areas and Åland archipelago, influenced by large-scale eutrophication driven by nutrients from agriculture and local fish farms (Bonsdorff et al., 1996). Sedimentation of organic matter, stimulated by nutrient inputs, can cause severe oxygen deficiency under specific meteorological and hydrographic conditions, as observed in the southern Baltic in 1994 and 2002 (e.g., Conley et al., 2007; Powilleit and Kube, 1999).

One of the shallow areas where seasonal hypoxia can occur is the Gulf of Riga (GoR) in the eastern part of the Baltic Sea (e.g., Berzinsh, 1995, and references therein; Aigars and Carman, 2001; Eglite et al., 2014; Aigars et al., 2015). The Gulf of Riga is a semi-enclosed basin (Fig. 1) with a surface area of 16 330 km<sup>2</sup>, a volume of 424 km<sup>3</sup>, and a mean depth of 26 m (Ojaveer, 1995; HELCOM, 2002). Its deeper central area, situated east of the island of Ruhnu, has depths of up to 56 m (Stiebrins and Väling, 1996). The water and salt budgets of the gulf are governed by river discharge, precipitation–evaporation balance, and water exchange with the Baltic Proper through the connecting straits. The long-term (1950–2015) mean river runoff is about 36 km<sup>3</sup> yr<sup>−1</sup> (Johansson, 2016), and the average freshwater flux due to the difference between the surface precipitation and evaporation rates is about 2.5 km<sup>3</sup> yr<sup>−1</sup> (Omstedt et al., 1997). Five larger rivers (Daugava, Lielupe, Gauja, Pärnu, and Salaca) enter the southern and eastern parts of the gulf, with the Daugava River contributing about 70 % of the total riverine input (Yurkovskis et al., 1993). Considering the gulf's annual water volume and salt content balance, Lilover et al. (1998) estimated that its water renewal period would be about 3 years.

GoR water exchange with the Baltic Proper takes place via the Irbe Strait in the west (about 70 %–80 % of water exchange) and the Suur Strait in the north (Astok et al., 1999; Petrov, 1979). The Irbe Strait has a sill depth of 25 m and a cross-section area of 0.4 km<sup>2</sup>, while these hydrographical features are 5 m and 0.04 km<sup>2</sup>, respectively, for the Suur Strait. Lips et al. (1995) suggested that the gulf's deep waters could be renewed in summer by inflows of saltier water from the eastern Baltic Proper over the sill in the Irbe Strait – which is deeper and wider – while inflows through the shallow Suur Strait are arrested in the surface layer. The near-

bottom inflows through the Irbe Strait are intensified by the northerly and northeasterly winds, which cause upwelling events along the eastern coast of the Baltic Proper. Model simulations by Raudsepp and Elken (1995) also showed that strong northerly wind events could create substantial near-bottom inflows of saltier Baltic Proper waters. However, when downwelling occurs along the eastern coast of the Baltic Proper, the inflowing water is warmer than that of the near-bottom waters in the Gulf of Riga in summer and can spread buoyantly at the intermediate depths (Liblik et al., 2017).

Because of the shallowness of the basin, the entire water column is well mixed in winter. In summer, stratification is mainly maintained by the seasonal thermocline, which begins developing in April and is at its strongest in August, while the contribution of haline stratification is relatively moderate (Stipa et al., 1999; Liblik et al., 2017). Based on conductivity–temperature–depth (CTD) profiles from 1993–2012, Skudra and Lips (2017) revealed that the strongest stratification occurred in the years with the highest summer surface temperature and spring river discharge. A high correlation between the deep layer salinity in the Irbe Strait and the gulf was found by Skudra and Lips (2017), in accordance with the suggestion that the majority of water exchange between the Baltic Proper and the gulf occurs through the Irbe Strait.

Based on data from 1963 to 1990, a statistically significant decreasing trend of oxygen concentration in August was found for the entire 20–50 m layer in the gulf (Berzinsh, 1995). No trend was detected after that (HELCOM, 2009). The latest monitoring data are not analyzed for long-term trends and inter-annual variations in near-bottom oxygen concentrations; rather, model outcomes are used to describe the oxygen conditions (e.g., Jansson et al., 2020). It is well documented, however, that the anoxic and hypoxic areas have been expanding in the entire Baltic Sea in recent decades, due to both eutrophication and changes in climatic conditions (Hansson and Viktorsson, 2020; the analysis also included data from the Gulf of Riga).

Total annual nitrogen and phosphorus loads to the Gulf of Riga were estimated for 2017 at levels of 90 544 and 2 427 t yr<sup>−1</sup>, respectively, and are still higher than the maximum allowable inputs, according to the Baltic Sea Action Plan (HELCOM, 2022). Based on monitoring data since 1974, the phosphorus pool in the Gulf of Riga constantly increased until the mid-1990s (Yurkovskis, 2004) and was followed by stagnation (HELCOM, 2018a). Since riverine phosphorus input is < 15 % compared to the phosphorus pool in the water column (Yurkovskis, 2004), the changes in the latter are largely governed by internal processes. The phosphate flux from the sediments to the water column depends on the near-bottom oxygen conditions with maximum values at low DO concentrations. For instance, phosphorus release on the order of 100 µmol PO<sub>4</sub><sup>3−</sup> m<sup>−2</sup> d<sup>−1</sup> was simulated at oxygen concentrations of 1–2 mg L<sup>−1</sup> (Eglite et al., 2014).

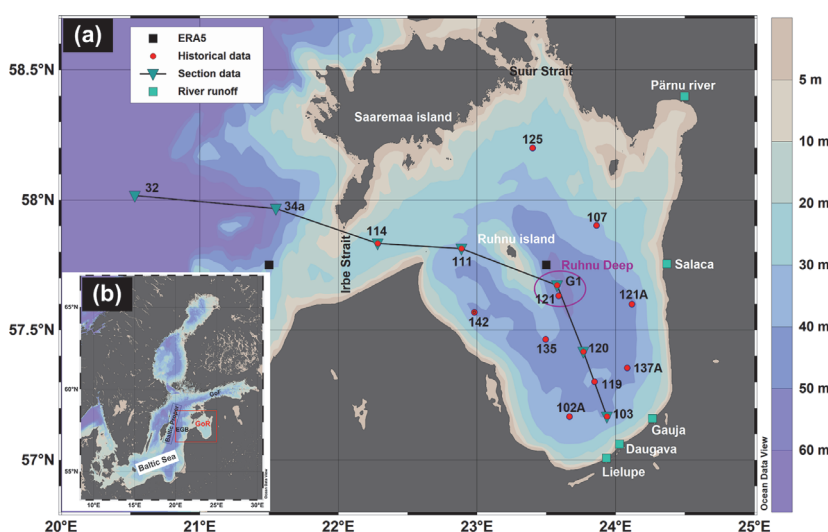


**Figure 1.** (a) – Map of the study area in the Gulf of Riga (GoR) with bottom topography. Red-filled circles represent the locations of monitoring stations. Inverted triangles represent the stations used for section figures. Black-filled squares represent the grid cell center points of ERA5 data (grid cell resolution  $0.25^\circ \times 0.25^\circ$ ). Green-filled squares denote rivers from which runoff data were used. EGB – Eastern Gotland Basin and GoF – Gulf of Finland. (b) Study area in the Baltic Sea. This map was generated using Ocean Data View 5.2.0 software (Schlitzer, 2019).

Thus, the reoccurrence of conditions of low near-bottom oxygen supports sediment phosphorus release, which counteracts potential decreases in the external phosphorus load to the gulf.

Data from regular monitoring cruises and targeted surveys revealed extensive near-bottom hypoxia in the Gulf of Riga in summer–autumn 2018. Additionally, the weather conditions were extreme in summer 2018, manifested by a new air temperature maximum in Europe for April–September (Hoy et al., 2020). We have formulated three main questions for this study. Was the observed near-bottom hypoxia in the GoR in 2018 an exceptional event? What were the reasons behind the observed hypoxia? Was it a feature that could occur in the GoR and similar basins regularly and/or even more often in the future? We hypothesize that the earlier onset, strength, and duration of stratification, together with the unusually high winter river runoff, were the main contributors to the extensive near-bottom hypoxia in 2018. If this hypothesis holds, then one may speculate that the future occurrences of such events will likely increase. To test our hypotheses, we analyzed oceanographic and meteorological conditions in 2018 and compared them with the preceding years (2012–2017) and long-term means and variability.

## 2 Material and methods

Historical data on the near-bottom temperature, salinity, dissolved oxygen, and nutrient concentrations were downloaded from the Estonian environmental monitoring information system (KESE), Latvian environmental monitoring databases, ICES/HELCOM database, and SeaDataNet Pan-European infrastructure for ocean and marine data management (<http://www.seadatanet.org>, last access: 9 April 2019). More consistent near-bottom oxygen data were available from 2005; therefore, we limited the analysis to 2005–2018. HELCOM guidelines (HELCOM, 2017) were followed for the sampling and analytical detection of oxygen and nutrient concentrations in the monitoring laboratories.

Vertical profiles of temperature, salinity, and dissolved oxygen with temporal resolution of at least six times a year are available since 2012. The profiles were recorded using an Ocean Seven 320plus CTD probe (Idronaut s.r.l.) on board R/V *Salme* during Estonian and Latvian monitoring cruises (stations are shown in Fig. 1). The salinity and density anomaly is shown in the present study as absolute salinity ( $\text{g kg}^{-1}$ ) and sigma-0 ( $\text{kg m}^{-3}$ ) and were calculated using the TEOS-10 formula (IOC et al., 2010). The oxygen sensor (Idronaut s.r.l.) attached to the OS320plus probe was calibrated prior to each cruise. Oxygen profiles used for the analysis were quality-checked against the laboratory analysis of water samples using an OX 400 L DO (VWR International, LCC) analyzer. The accuracy of the Idronaut oxygen sensor

is  $0.1 \text{ mg L}^{-1}$ , while the accuracy of the laboratory dissolved oxygen analyzer is 0.5 % of the measured value. The primary dataset used to characterize the water column structure and dissolved oxygen and phosphates concentrations in 2018 was collected on 9–10 January, 17–18 April, 30 May, 11 July, 25 August, and 26–27 October.

The depth of the upper mixed layer (UML) was defined according to Liblik and Lips (2012) as the minimum depth, where  $\rho_z - \rho_3 > 0.25 \text{ kg m}^{-3}$ , where  $\rho_z$  is the density anomaly at depth  $z$  and  $\rho_3$  at depth 3 m. The depth of the near-bottom mixed layer (NBL) was found similarly to UML, as the maximum depth, where  $|\rho_z - \rho_{\text{last}}| > 0.1 \text{ kg m}^{-3}$ , where  $\rho_{\text{last}}$  is the density anomaly at the maximum depth of a profile. An oxygen concentration of  $2.9 \text{ mg L}^{-1}$  ( $2 \text{ mL L}^{-1}$ ) was used as the threshold concentration for defining hypoxia, and the upper boundary of the hypoxic layer was found as the minimum depth at which oxygen concentration was below the threshold. The estimated depth of the upper boundary of the hypoxic layer at station G1 and the gridded topography (EMODnet Bathymetry Consortium, 2020) were used to find the lateral extent of the hypoxic area, assuming an even horizontal depth distribution for the occurrence of hypoxia. The sea depth at station G1 is 54 m (Fig. 1). The profiles covered – in most cases – the depth range from 2 to 52 m. The water column structure was characterized by temperature, salinity, and density in the UML and NBL, and potential energy anomaly (PEA; Simpson et al., 1990) was calculated as

$$\text{PEA} = \frac{1}{h} \int_{-h}^0 (\bar{\rho} - \rho) g z dz, \quad \text{where } \bar{\rho} = \frac{1}{h} \int_{-h}^0 \rho dz, \quad (1)$$

where  $h$  is the water column depth (50 m),  $\rho$  is water density,  $z$  is depth (vertical coordinate), and  $g = 9.81 \text{ m s}^{-2}$ .

Meteorological data for 1979–2018 were extracted from the ERA5 dataset (Hersbach et al., 2018) via Copernicus Services for characterizing local conditions in the gulf and upwelling-favorable conditions along the eastern coast of the Baltic Proper. Based on hourly data from a grid cell in the central gulf (see Fig. 1), the monthly mean net solar radiation, air temperature (2 m above surface), and wind speed (at the 10 m height) in 2018 were calculated and compared with monthly mean values and variability in 1979–2018. Runoff data of rivers Salaca, Gauja, Lielupe, and Daugava (Fig. 1) from 1993 to 2018 were received from the Latvian Environment, Geology and Meteorology Center as the estimated monthly runoff ( $\text{m}^3 \text{ s}^{-1}$ ). River Pärnu runoff data were obtained from the Estonian Weather Service.

For a more detailed analysis of the impact of meteorological and hydrological conditions on the development of stratification, changes in potential energy anomaly due to surface heating-cooling ( $S_b$ ), wind mixing ( $S_m$ ), and freshwater discharge from rivers ( $S_r$ ) were estimated for the years 2012–2018:

$$\frac{d\text{PEA}}{dt} = S_b + S_m + S_r. \quad (2)$$

The two former parameters were calculated as suggested by Simpson et al. (1990):

$$S_b = \frac{\alpha_v g Q_{\text{TOT}}}{2c_p} \quad \text{and} \quad S_m = -\delta C_D \rho_a \frac{W^3}{h}, \quad (3)$$

where  $Q_{\text{TOT}}$  is the surface heat flux and  $W$  is the wind speed.  $Q_{\text{TOT}}$  is the sum of the shortwave radiative heat flux, longwave radiative heat flux, sensible heat flux, and latent heat flux estimated using ERA5 data and surface salinity obtained from CTD casts interpolated between the measurements. Thermal expansion coefficient  $\alpha_v$  was calculated using the TEOS-10 formula (IOC et al., 2010), and specific heat of seawater  $c_p = 4000 \text{ J (kg K)}^{-1}$  was applied. In the formula for the shortwave radiative heat flux, an average albedo of 0.055 was used (Groeskamp and Iudicone, 2018; Séférian et al., 2017). Otherwise, we used the same methods of calculating surface heat flux components as Liblik and Lips (2012). For estimating  $S_m$ , constant values of efficiency of mixing  $\delta = 10^{-3}$  and air density  $\rho_a = 1.25 \text{ kg m}^{-3}$  were applied, and the effective drag coefficient  $C_D$  was calculated according to Wu (1982). The changes in stratification due to river discharge were estimated using monthly runoff from the previous month. The flow in  $\text{m}^3 \text{ s}^{-1}$  was multiplied by a constant, which was found assuming that the average yearly change in PEA in 2012–2018 was equal to the change caused by the average runoff of  $36 \text{ km yr}^{-3}$  evenly distributed over the entire surface area of the gulf.

Wind data from a grid cell outside the gulf, but close to the Irbe Strait (see Fig. 1), were extracted from ERA5 data to calculate the north-northeast (NNE) component of wind stress as  $\tau_{\text{NNE}} = C_D \rho_a |W| W_{\text{NNE}}$ , where  $W_{\text{NNE}}$  is the wind speed component directed towards NNE (south-southwest wind component). It is used to find the periods with upwelling-favorable conditions along the eastern coast of the Baltic Proper and for a more detailed analysis of inflows–outflows through the Irbe Strait in 2012–2018. Cumulative wind stress is calculated by summing up the hourly NNE components of wind stress multiplied by the time step of 1 h starting from 1 January each year.

We introduce a coarse method estimating oxygen consumption rates in the gulf NBL. The considered physical processes contributing to the measured changes in salinity and oxygen concentration in the NBL were (1) vertical diffusion and (2) lateral advection and mixing. Diffusive flux of salt and oxygen through the border between the NBL and the water column above was estimated using a similar approach as Stoicescu et al. (2019):

$$\text{DIFF}_S = -k \cdot \frac{\partial S}{\partial z} \quad \text{and} \quad \text{DIFF}_{\text{O}_2} = -k \cdot \frac{\partial \text{O}_2}{\partial z}, \quad (4)$$

where the vertical diffusivity coefficient is calculated as  $k = \frac{\alpha}{N}$ ,  $\alpha$  is the empirical intensity factor of turbulence (we applied a constant value  $\alpha = 1.5 \times 10^{-7} \text{ m}^2 \text{ s}^{-2}$ ), and  $N$  is the Brunt–Väisälä frequency defined by the vertical density gradient. The changes in salinity and oxygen concentration in

the NBL can be found by multiplying the value of diffusive fluxes by the time between two measurements ( $t_2 - t_1$ ) and dividing it by the thickness of the NBL ( $h_{\text{NBL}}$ ) as

$$\begin{aligned}\Delta S^{\text{DIFF}} &= \text{DIFF}_S \cdot \frac{t_2 - t_1}{h_{\text{NBL}}} \text{ and} \\ \Delta \text{O}_2^{\text{DIFF}} &= \text{DIFF}_{\text{O}_2} \cdot \frac{t_2 - t_1}{h_{\text{NBL}}}.\end{aligned}\quad (5)$$

Knowing salinities of inflowing waters and gulf NBL waters at time steps  $t_1$  and  $t_2$  and the changes due to vertical diffusion, we can estimate the proportion of inflowing waters in the near-bottom water mass at time step  $t_2$ . Using this proportion, we can also estimate the expected changes in the NBL oxygen concentration due to lateral transport and mixing as

$$\begin{aligned}\Delta \text{O}_2^{\text{ADV}} &= (\text{O}_2^{t_1}(114) - \text{O}_2^{t_1}(\text{G1})) \\ &\times \left[ \frac{\text{Sal}^{t_2}(\text{G1}) - \text{Sal}^{t_1}(\text{G1})}{\text{Sal}^{t_1}(114) - \text{Sal}^{t_1}(\text{G1})} \right],\end{aligned}\quad (6)$$

where  $\text{Sal}^{t_1}(\text{G1})$  and  $\text{O}_2^{t_1}(\text{G1})$  are salinity and oxygen concentration in the NBL at station G1 and  $\text{Sal}^{t_1}(114)$  and  $\text{O}_2^{t_1}(114)$  at station 114 in the Irbe Strait (see Fig. 1) at an initial time step  $t_1$ .  $\text{Sal}^{t_2}(\text{G1})$  is measured salinity in the NBL at station G1 at time step  $t_2$  corrected by the estimated salinity change due to vertical diffusion.

Due to oxygen consumption, measured oxygen concentration in the NBL at station G1 at time step  $t_2$  ( $\text{O}_2^{t_2\text{m}}(\text{G1})$ ) should be lower than that found when considering only changes due to physical processes since no production is expected in the near-bottom layer that is well below the euphotic depth. Oxygen depletion due to consumption can be found as the sum of the measured oxygen depletion and changes in concentration due to diffusion and lateral advection and mixing:

$$\begin{aligned}\Delta \text{O}_2^{\text{CONS}}(\text{G1}) &= -(\text{O}_2^{t_2\text{m}}(\text{G1}) - \text{O}_2^{t_1}(\text{G1})) \\ &+ \Delta \text{O}_2^{\text{DIFF}} + \Delta \text{O}_2^{\text{ADV}}.\end{aligned}\quad (7)$$

Oxygen consumption rate per unit bottom area is calculated as

$$\text{O}_2^{\text{CONS rate}} = \frac{\Delta \text{O}_2^{\text{CONS}}}{t_2 - t_1} \cdot h_{\text{NBL}}.\quad (8)$$

We have chosen the time step of 1 month or longer to estimate oxygen consumption rates based on the distance between the Irbe Strait and the Ruhnu Deep (120 km, measured along the deeper area of the gulf) and average (monthly) flow rates in the gulf of  $5 \text{ cm s}^{-1}$  (e.g., Soosaar et al., 2014; Lips et al., 2016).

The same methods were used to estimate phosphate fluxes due to physical processes and phosphorus release from the sediments. The measured concentrations in the near-bottom layer at station G1 were assigned to the gulf's water and at

station 114 to the inflowing water. In Eqs. (4)–(8), oxygen concentration was replaced by phosphate concentration, and the difference in measured and expected phosphate concentrations in the gulf near-bottom layer was associated with the phosphorus release from the sediments. Since the vertical resolution of nutrient sampling was scarce (step was 10 m), we used only the deepest measured phosphate concentration as the value characterizing the entire NBL, and the vertical gradient was estimated between the phosphate concentrations at the deepest sampling point and 10–12 m above it.

### 3 Results

#### 3.1 Inter-annual variability of dissolved oxygen in the near-bottom layer

We characterized the long-term development of oxygen conditions in the Gulf of Riga using near-bottom oxygen measurements at the deepest stations G1 and 121 (bottom depth 54 m) and yearly average late summer (August) and autumn (October–November) near-bottom oxygen concentrations at all stations with depth  $\geq 40 \text{ m}$  (see station locations in Fig. 1). Based on the data obtained from the deepest stations, late summer–autumn hypoxia occurred in about 50 % of years in 2005–2018 (Fig. 2). No hypoxia was observed in 2006–2011, except for one value close to  $2.9 \text{ mg L}^{-1}$  in 2009, but note the lower sampling frequency. Hypoxic conditions have been recorded every year since 2012, except for 2016 and 2017. Based on the data from all monitoring stations from 2005–2018, no trend in the deep layer oxygen concentrations was detected in summer, but a statistically significant ( $p < 0.05$ ) trend at a rate of  $0.45 \text{ mg L}^{-1} \text{ yr}^{-1}$  was found in autumn ( $R^2 = 0.50$ ,  $n = 13$ ). Thus, the monitoring data suggest that the hypoxic conditions observed in 2018 are – in general – in line with the long-term trend.

We studied the links between the long-term trend and variability of near-bottom oxygen and other environmental parameters, such as salinity and nutrient concentrations. No significant trend in near-bottom salinity was revealed in 2005–2018. Using simultaneously measured near-bottom salinity and oxygen values at station G1 from August to November in 2005–2018, we found a statistically significant ( $R^2 = 0.24$ ,  $n = 36$ ,  $p < 0.05$ ) negative relationship – low oxygen concentrations corresponded to high salinity values. However, there are examples where hypoxia occurred at salinities of  $5.8 \text{ g kg}^{-1}$  (in 2012 and 2015) and did not at  $6.5 \text{ g kg}^{-1}$  (in 2010).

The analysis of near-bottom phosphate concentrations at stations with depth  $\geq 40 \text{ m}$  revealed a statistically significant increase in concentrations in late summer ( $0.08 \text{ } \mu\text{M yr}^{-1}$ ,  $R^2 = 0.47$ ,  $n = 14$ ) and autumn ( $0.12 \text{ } \mu\text{M yr}^{-1}$ ,  $R^2 = 0.34$ ,  $n = 13$ ). A statistically significant negative correlation was obtained between the deep layer oxygen and phosphate con-

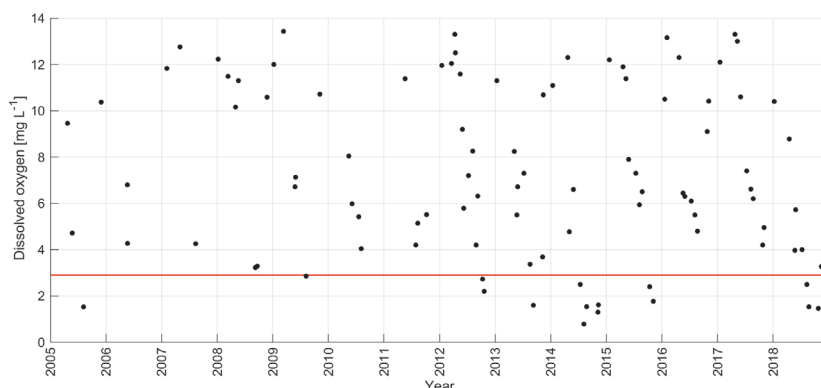


**Figure 2.** Inter-annual variability of near-bottom dissolved oxygen concentration at monitoring stations G1 and 121 in 2005–2018. The red line denotes the oxygen concentration  $2.9 \text{ mg L}^{-1}$  (threshold concentration for hypoxia).

centrations in autumn ( $R^2=0.79$ ,  $n=13$ ,  $p<0.05$ ). The near-bottom-layer oxygen in autumn also significantly correlated with the next year's winter (January) phosphate concentration in the entire water column ( $R^2=0.45$ ,  $n=9$ ,  $p<0.05$ ). Thus, the impact of the hypoxia deepening is also seen in the trends of phosphate concentrations.

### 3.2 Seasonal and inter-annual variability in the vertical distribution

Based on the vertical profiles of dissolved oxygen collected at least every 2 months in 2012–2018, a clear seasonal pattern was apparent at all depths, with the largest amplitude occurring in the near-bottom layer (Fig. 3a). The lowest oxygen concentrations were measured in late summer–autumn, but the oxygen levels did not always drop below the hypoxia threshold (as in 2016 and 2017). The lowest oxygen concentrations were observed in 2014 ( $0.8 \text{ mg L}^{-1}$ ) and 2018 ( $1.5 \text{ mg L}^{-1}$ ). As pointed out above, hypoxia was observed in 2012–2015 and 2018, but the duration and vertical extent of hypoxia differed between the years (Fig. 3a, Table 1). The first occurrence of the seasonal hypoxia was observed in July in 2014, August in 2018, September in 2013, and October 2012 and 2015. The upper boundary of the hypoxic layer was at its shallowest depth in 2018 (45.0 m). Accordingly, the estimated spatial extent of hypoxia was the largest in 2018, when the hypoxic waters covered 5.2 % ( $830 \text{ km}^2$ ) of the gulf's bottom area. In the other years with hypoxia (2012–2015), the estimates of the bottom area covered by hypoxic waters did not differ greatly, varying between 2.1 % and 2.7 % ( $340\text{--}430 \text{ km}^2$ ).

Seasonal patterns also dominated the variability of vertical distributions of temperature, salinity, and density anomaly (Fig. 3b–d), but certain inter-annual differences in water column parameters can be noticed (Table 1). The observed UML temperature maxima were higher in the summers of 2014 and

2018. Lower summer UML salinities ( $\leq 5.2 \text{ g kg}^{-1}$ ) were observed in 2012, 2013, and 2018, and increased NBL salinity values ( $\geq 6.5 \text{ g kg}^{-1}$ ) were registered in the summers of 2013 and 2018. The largest density differences between the bottom and surface layer,  $3.4$  and  $3.5 \text{ kg m}^{-3}$  – which were mostly associated with high UML temperatures – were found in 2014 and 2018. High NBL salinity and low UML salinity contributed to the observed relatively strong water column stratification in 2013 (the third strongest stratification in 2012–2018), although the summer UML temperature remained low in 2013 (Table 1). The weakest vertical stratification was observed in 2017, when the density difference between the NBL and UML was close to  $2.0 \text{ kg m}^{-3}$ .

Thus, the years with strong stratification (2013, 2014, and 2018; Table 1) were associated with high UML temperature, low UML salinity, and high NBL salinity and were among those with near-bottom hypoxia. In 2017, the stratification was the weakest, and hypoxia did not develop. Still, the density difference between the NBL and UML was weaker in 2012 and 2015 than in 2016 – but in 2012 and 2015, hypoxia was observed, whereas in 2016, it was not. A further, more detailed analysis of water column stratification is presented in Sect. 3.4 together with the description of meteorological and hydrological forcing data.

### 3.3 Temporal development of hypoxia in 2018

To demonstrate the development of hypoxia and vertical stratification in 2018 in more detail and to compare it with that of the previous year without hypoxia, we present vertical profiles of temperature, salinity, density, and dissolved oxygen concentration in the Ruhnu Deep in 2017 and 2018 (Fig. 4). A major difference between the years is evident in a much faster decrease in near-bottom oxygen concentrations in spring 2018 than in 2017. Also, the development of vertical stratification in spring–early summer differed be-

**Table 1.** Characteristics of seasonal hypoxia and stratification parameters in the Gulf of Riga in 2012–2018, based on CTD profiles from May to November at stations G1 and 121. Observed maxima of UML temperature, NBL salinity, and density difference between NBL and UML and minima of UML salinity are given.

Year	Earliest hypoxia detection month	Min. depth of hypoxia m	Max. hypoxic area % (km <sup>2</sup> )	UML max temperature °C	UML min salinity g kg <sup>-1</sup>	NBL max salinity g kg <sup>-1</sup>	NBL–UML density kg m <sup>-3</sup>
2012	October	48.5	2.7 (430)	18.97	5.16	5.77	2.20
2013	September	49.0	2.4 (380)	18.59	5.21	6.51	2.72
2014	July	49.0	2.4 (380)	23.46	5.28	6.08	3.38
2015	October	49.5	2.1 (340)	19.41	5.65	5.82	2.22
2016	–	–	–	19.37	5.38	6.21	2.35
2017	–	–	–	18.50	5.26	6.01	2.05
2018	August	45.0	5.2 (830)	22.36	5.17	6.51	3.46

tween these two years. In 2018, salinity stratification in the deep layer was established in the middle of April, and a very strong seasonal thermocline was formed by the end of May. In 2017, the seasonal thermocline was remarkably weaker in the beginning of June, compared to late May of 2018, and no secondary pycnocline developed in the deep layer in spring–summer.

The vertical sections of oxygen, salinity, and temperature (Fig. 5) demonstrate the spreading of waters from the eastern Baltic Proper to the Gulf of Riga over the Irbe Strait sill in late May and July 2018. However, at the end of August, the distribution patterns indicate that outflow from the gulf likely prevailed below the seasonal thermocline through the Irbe Strait (Fig. 5 lower panel). Oxygen concentrations in the near-bottom layer in the central gulf were at a level of 60 % saturation in late May, decreasing further to 40 % of saturation ( $< 5 \text{ mg L}^{-1}$ ) by mid-July, and hypoxic conditions with oxygen saturation below 20 % were established by late August. We also point to an increase in salinity in the water layer of 35–45 m, which is seen on the consecutive profiles measured in July and August at station G1 (Fig. 4).

### 3.4 Analysis of meteorological and hydrological conditions

Solar radiation in 2018 was higher than that of the long-term average for all months from spring to autumn (Fig. 6a). Seasonal variation in air temperature in 2018 differed from the average, as well, with a rapid increase in April–May and higher monthly mean values than the long-term averages until October (Fig. 6b). The monthly average wind speed from February to August was lower in 2018 than the long-term mean for the respective month, except in April (Fig. 6c). The lowest wind speed for May in 1979–2018 was found in 2018. All these anomalies in meteorological conditions supported the observed fast development and strength of seasonal stratification in the GoR. As opposed to 2018, the solar radiation, air temperature, and wind speed in 2017 were mostly close to the long-term averages (Fig. 6a–c).

A comparison of monthly river runoff values from 2018 with the long-term mean values (1993–2018) shows that the 2018 runoff was mostly lower than the long-term mean – although within standard deviation limits (Fig. 6d). An exception was found in January 2018, when runoff was the largest on the record, being more than twice as large ( $5.11 \text{ km}^3$  per month) as the long-term mean ( $2.44 \text{ km}^3$  per month). The maximum or close to the maximum value of monthly river runoff was also observed in September–December 2017.

The development of vertical stratification characterized by potential energy anomaly estimated using meteorological and river runoff data (Fig. 7) in general reflects the same differences between the years as the simple comparison of temperature, salinity, and density in the UML and NBL (Table 1). The fastest development of stratification and the strongest stratification at its peak were predicted for the summers of 2013 and 2018, and strong stratification was also characteristic for the summers of 2014 and 2016. The years 2012, 2015, and 2017 were among the years with the weakest stratification. A critical difference between the years can also be noticed during destratification in autumn. The longest stratified period was found for 2013, which was a remarkable year with the largest river runoff in spring (considering the period 2012–2018) and relatively high air temperatures in early summer and autumn. The earliest decay of vertical stratification is predicted for 2016 and 2017 – the water column was fully mixed by the end of October in both years. In comparison, the water column was fully mixed remarkably later in 2015 – in the second half of November.

The analysis of the time series of the along-coast component (NNE–SSW) of wind stress supports the described inflow–outflow suggestions for 2018 (see Sect. 3.3). Upwelling-favorable winds with negative wind stress  $\tau_{\text{NNE}}$  exceeding  $-0.2 \text{ Nm}^{-2}$  that could be related to the inflows of saltier waters into the Gulf of Riga were observed in February–March, May, early June, and late June 2018 (Fig. 8a). A major deviation from the long-term pattern is also evident in cumulative wind stress in 2018 – wind forcing from February to the end of July supported the near-



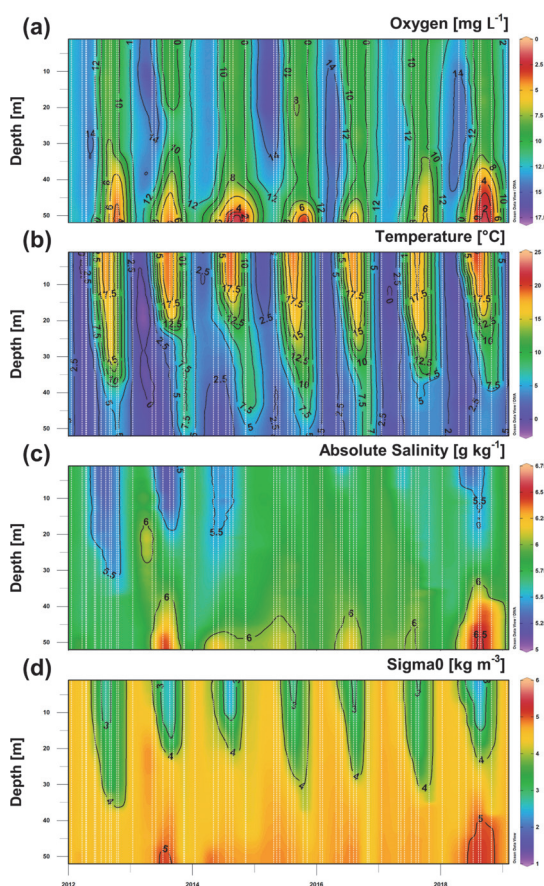


**Figure 3.** Time series of the vertical distribution of oxygen concentration (a), temperature (b), salinity (c), and density anomaly (d) at stations G1 and I21 in 2012–2018 (including January 2019). Vertical white dashed lines mark the time of measured profiles.

bottom inflows (seen as the decrease in the cumulative wind stress; Fig. 8a). The winds from the opposite direction prevailed from the beginning of August. Thus, the inflows of sub-thermocline waters into the Gulf of Riga could have been blocked in late summer 2018, as also seen in Fig. 5, demonstrating the outflow of gulf deep layer waters to the Irbe Strait at the end of August.

Similar to 2018, the cumulative wind stress in 2013 largely deviated from the long-term mean (Fig. 8b). The inflow-favorable winds dominated in spring–summer, supporting the development of vertical stratification in the gulf’s deep layer. A significant difference between these two years appeared in September – in 2013, the inflow-favorable winds persisted, while in 2018, the winds from opposite directions started to prevail. Inflow-supporting wind conditions were

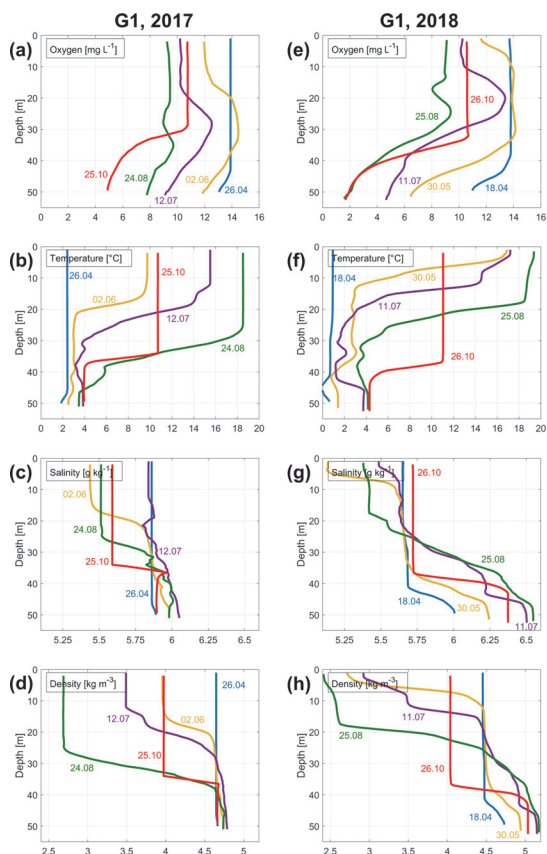


**Figure 4.** Vertical profiles of dissolved oxygen concentration (a, e), temperature (b, f), salinity (c, g), and density anomaly (d, h) measured in the Ruhnu Deep (station G1; see location in Fig. 1) in 2017 (a–d) and 2018 (e–h).

also observed in late spring–summer 2014, forming a relatively thin NBL (with its boundary at 46 m), and hypoxia appeared already in July 2014. Almost no inflow-supporting winds occurred in 2015. Although stratification was not strong and the NBL salinity was low this year (see Table 1), hypoxia developed in 2015, but later – in late October, while hypoxia in the other years was observed in July–September (Figs. 2 and 3). Cumulative wind stress graphs generally followed the long-term mean in 2016 and 2017 (Fig. 8b), and in these years, no hypoxia was observed.

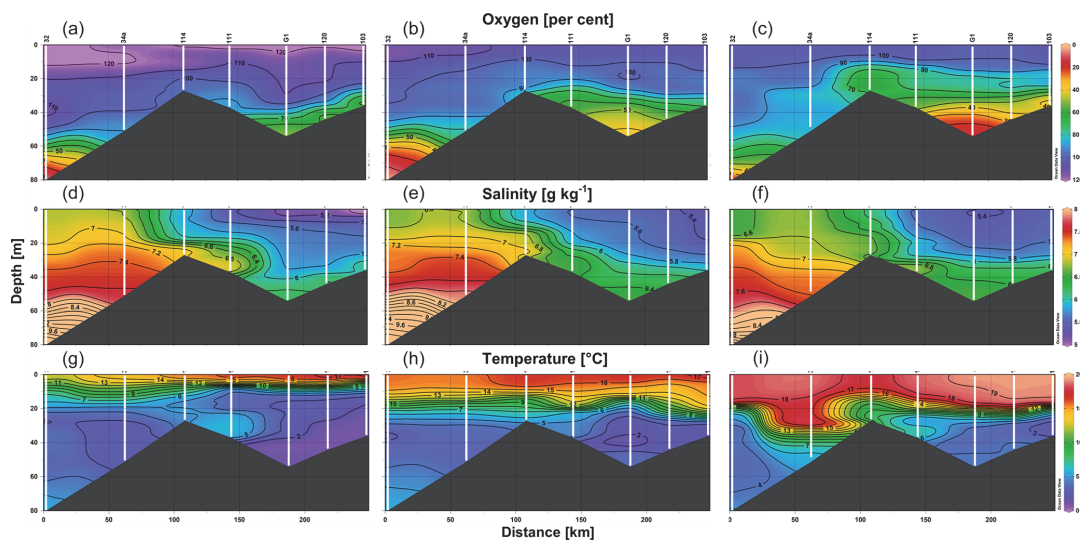


**Figure 5.** Vertical sections of oxygen saturation (a–c), salinity (d–f), and temperature (g–i) on 30 May (a, d, g), 11 July (b, e, h), and 25–26 August (c, f, i) 2018 along the route from station 32 in the Baltic Proper through the Irbe Strait to station 103 near the Daugava River mouth in the Gulf of Riga (see the locations in Fig. 1).

**Table 2.** Estimated changes in NBL salinity and oxygen concentration due to advection and diffusion (presented as the changes per month to ease the comparison between the periods) and estimated consumption rates from mid-April to late August 2018.

Period start ( $t_1$ ) and end ( $t_2$ )		18 Apr–30 May	30 May–11 Jul	11 Jul–25 Aug
$O_2^{t_1}$ (114)	$\text{mg L}^{-1}$	13.42	12.46	11.08
$O_2^{t_1}$ (G1)	$\text{mg L}^{-1}$	12.01	8.27	5.16
$O_2^{t_2\text{m}}$ (G1)	$\text{mg L}^{-1}$	8.27	5.16	2.52
Measured $O_2$ depletion at G1	$\text{mg L}^{-1}$ per month	2.67	2.22	1.76
$Sal^{t_1}$ (114)	$\text{g kg}^{-1}$	6.77	7.17	7.27
$Sal^{t_1}$ (G1)	$\text{g kg}^{-1}$	5.99	6.22	6.48
$Sal^{t_2}$ (G1)	$\text{g kg}^{-1}$	6.22	6.48	6.51
Average NBL thickness	m	9.5	9.5	12.0
Salinity change due to vertical diffusion	$\text{g kg}^{-1}$ per month	−0.10	−0.09	−0.08
Vertical diffusion of $O_2$	$\text{mmol O}_2 \text{ m}^{-2} \text{ h}^{-1}$	0.43	0.32	0.26
$O_2$ change due to diffusion	$\text{mg L}^{-1}$ per month	1.05	0.78	0.50
$O_2$ change due to advection	$\text{mg L}^{-1}$ per month	0.48	1.24	0.68
$O_2$ change due to consumption	$\text{mg L}^{-1}$ per month	4.20	4.24	2.94
$O_2$ consumption rate	$\text{mmol O}_2 \text{ m}^{-2} \text{ h}^{-1}$	1.72	1.75	1.53

3.5 Estimates of oxygen consumption and sediment release of phosphates

We estimated fluxes of dissolved oxygen to the NBL at station G1 in summer 2018 due to vertical diffusion and lateral advection and mixing. Based on the gradient method (Eqs. 4 and 5), the estimated vertical diffusive flux varied between 0.26 and 0.43  $\text{mmol O}_2 \text{ m}^{-2} \text{ h}^{-1}$ , corresponding to the changes in NBL oxygen concentration from 0.50 to 1.05  $\text{mg L}^{-1}$  per month (Table 2). The estimated changes in

oxygen concentration due to advection (Eq. 6) had comparable values, varying from 0.48 to 1.24  $\text{mg L}^{-1}$  per month. According to the measurements, the NBL oxygen concentration continuously decreased in summer 2018, showing that oxygen consumption had to be large enough to exhaust oxygen brought by diffusion and advection and cause further oxygen depletion in the NBL. We found that respiration could cause oxygen depletion in the NBL by 2.94–4.24  $\text{mg L}^{-1}$  per month or, in total, by 16.2  $\text{mg L}^{-1}$  from mid-April to late August 2018 (Eq. 7). The corresponding



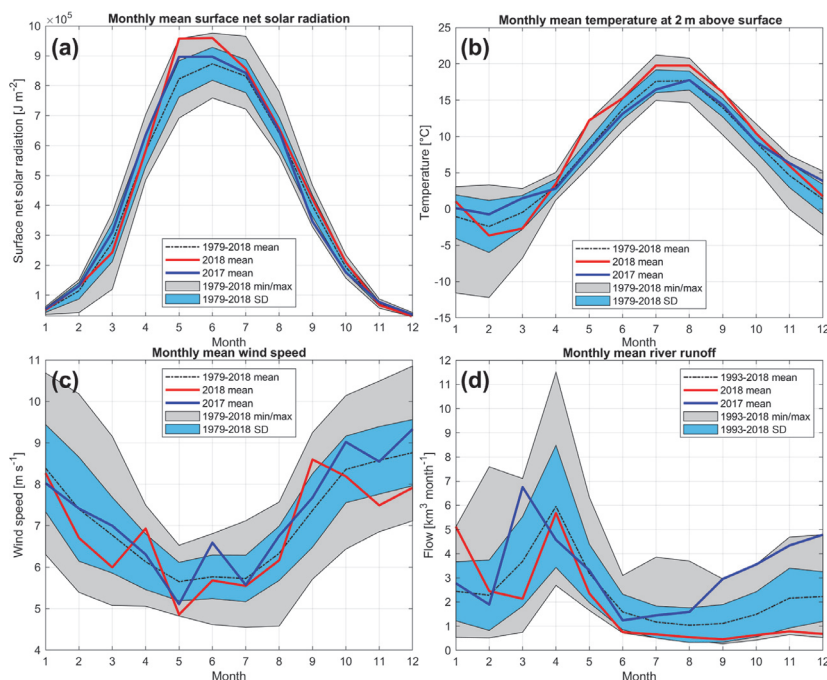


**Figure 6.** Courses of monthly mean, minimum and maximum, and standard deviation of (a) surface radiation, (b) air temperature, and (c) wind speed for the period of 1979–2018 and (d) river runoff for the period of 1993–2018. The monthly mean values of listed parameters for 2017 and 2018 are shown as blue and red lines, respectively. For meteorological parameters, ERA5 data are used from the central Gulf of Riga (see the location of the grid cell in Fig. 1).

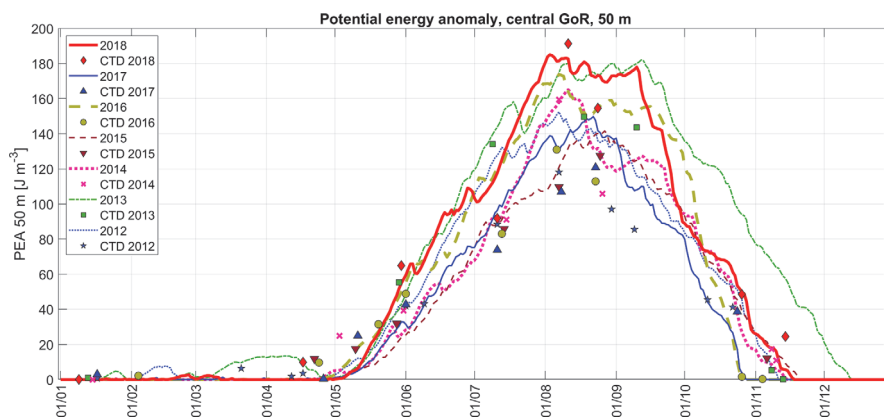


**Figure 7.** Changes in vertical stratification (potential energy anomaly, PEA, characterizing energy needed to mix the water column fully) in the central Gulf of Riga in 2012–2018 based on CTD profiles (markers) and estimated using meteorological (ERA5 data are from the central Gulf of Riga) and river runoff data (curves; the methods are presented in Sect. 2).

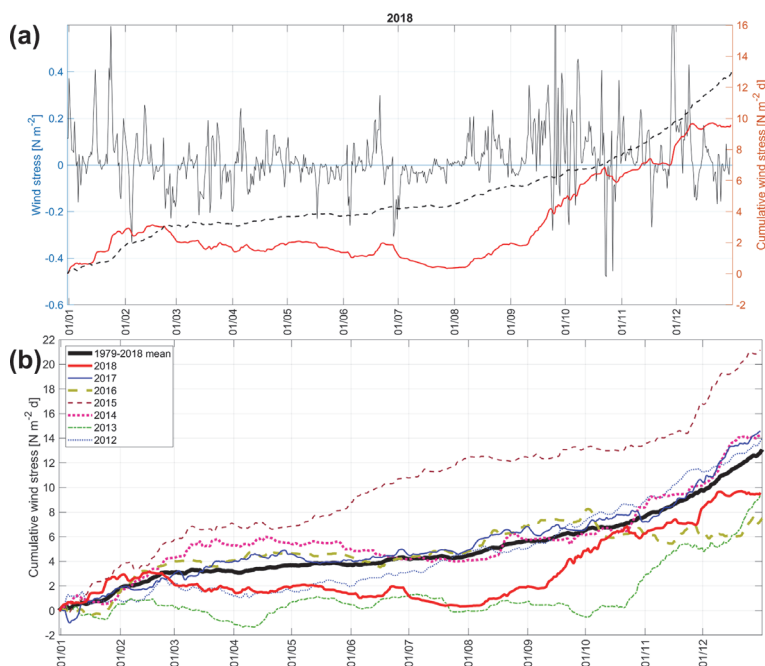


**Figure 8.** (a) Time series of along-coast (NNE–SSW) component of wind stress  $\tau_{NNE}$  and cumulative wind stress in 2018 (6 h moving average is shown). (b) Cumulative wind stress for each year in 2012–2018. Average cumulative wind stress curve for 1979–2018 is shown in both panels. Data were extracted from the ERA5 grid point outside the gulf (see location in Fig. 1).

consumption rate per unit bottom area (Eq. 8) varied from 1.53 to  $1.75 \text{ mmol O}_2 \text{ m}^{-2} \text{ h}^{-1}$  in 2018.

For the periods when inflows through the Irbe Strait are absent, the only physical process contributing to the changes in oxygen concentration in the gulf NBL is vertical diffusion/mixing. We suggested that such conditions of no inflows occurred in summer 2015, based on prevailing winds (Fig. 8b) and observed low salinity in the NBL at station G1 (Table 1). The vertical diffusive flux of oxygen was estimated at  $0.49 \text{ mmol m}^{-2} \text{ h}^{-1}$  in April–November 2015. If considering a similar oxygen consumption rate in 2015 as in 2018 ( $1.67 \text{ mmol O}_2 \text{ m}^{-2} \text{ h}^{-1}$ ), oxygen depletion in the NBL (with an average thickness of 16 m) could be  $1.70 \text{ mg L}^{-1}$  per month. Thus, this rate is enough to cause hypoxia in the near-bottom layer of the central gulf in late October 2015, as it was observed (see Figs. 2 and 3), but not earlier.

Simultaneously with the development of hypoxia, phosphate concentrations increased in the NBL at station G1 in summer 2018 (Fig. 9). The phosphate concentrations were already elevated in July when oxygen concentrations did not indicate hypoxic conditions at 2–3 m from the seabed. The estimated changes in phosphate concentrations due to lateral advection and mixing and vertical diffusion varied be-

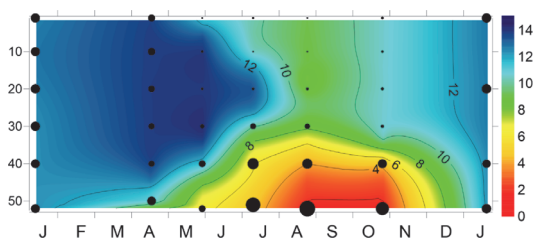


**Figure 9.** Time series of vertical distribution of oxygen and phosphate concentration at station G1 in the Gulf of Riga from January 2018 to January 2019. Phosphate concentrations are indicated as black dots. The size of the dots is proportional to the measured concentrations ranging from the lower detection range of 0.06 to  $2.25 \text{ } \mu\text{M}$ .

tween  $-0.18$  to  $-0.21$  and  $-0.04$  to  $-0.13 \text{ } \mu\text{M}$  per month, respectively (Table 3). Since phosphate concentrations in the NBL continuously increased from spring to late summer (August), the sediment release of phosphates had to be large enough to compensate for the flux by physical processes and maintain the observed accumulation. The largest estimated phosphate flux from the sediments was  $13.6 \text{ } \mu\text{mol m}^{-2} \text{ h}^{-1}$

**Table 3.** Estimated changes in NBL phosphate concentration due to advection and diffusion and estimated sediment release of phosphates in the Gulf of Riga between the monitoring campaigns in 2018.

Period start ( $t_1$ ) and end ( $t_2$ )		18 Apr–30 May	30 May–11 Jul	11 Jul–25 Aug
$\text{PO}_4^{f_1}$ (I14)	$\mu\text{M}$	0.49	0.21	0.33
$\text{PO}_4^{f_1}$ (G1)	$\mu\text{M}$	1.12	0.82	1.95
$\text{PO}_4^{f_{2m}}$ (G1) (measured)	$\mu\text{M}$	0.82	1.95	2.11
Average NBL thickness	m	9.5	9.5	12.0
$\text{PO}_4$ change due to diffusion	$\mu\text{M}$ per month	−0.04	−0.05	−0.13
$\text{PO}_4$ change due to advection and lateral mixing	$\mu\text{M}$ per month	−0.20	−0.18	−0.21
Estimated rate of the sediment $\text{PO}_4$ release	$(\mu\text{M m}^{-2} \text{ h}^{-1})$	0.4	13.6	7.4

for the period from the end of May to mid-July 2018. From late April to late May, the phosphate flux from the sediments was minimal, which might be explained by relatively high oxygen concentrations in the NBL. Although the oxygen concentrations decreased and fell below the hypoxia threshold from mid-July to late August, the estimated sediment release for this period was lower ( $7.4 \mu\text{mol m}^{-2} \text{ h}^{-1}$ ) than from late May to mid-July.

#### 4 Discussion

Declining oxygen levels and more frequent hypoxia have been reported in many coastal environments, including the Baltic Sea (Caballero-Alfonso et al., 2015; Carstensen et al., 2014; Conley et al., 2009). We found a similar tendency in the Gulf of Riga with more frequent hypoxia in recent years and a statistically significant decreasing trend of deep layer oxygen concentrations (based on data in autumn 2005–2018). Thus, in general, we can state that the observed extensive hypoxia in 2018 was in agreement with the long-term changes in the GoR oxygen dynamics (Berzinsh, 1995; HELCOM, 2009). However, the reasons behind the largest extent of hypoxia, as observed in 2018, need further explanation.

It is well documented that the main causes of near-bottom hypoxia are elevated nutrient inputs, leading to high oxygen demand for organic matter decomposition, and topographic–hydrographic characteristics of coastal areas, restricting oxygen supply by physical processes (Carstensen et al., 2014; Virtanen et al., 2019). If oxygen consumption exceeds oxygen supply by vertical mixing and advection for a long enough period, hypoxia or even anoxia could occur (Fennel and Testa, 2019). Seasonal stratification is a major factor restricting oxygen supply to the near-bottom layer depending on its strength (Kralj et al., 2019) and the duration between its onset and decay (Fennel and Testa, 2019).

In 2018, fast warming of the surface layer and weak wind-induced mixing in spring resulted in strong vertical stratification. The peak of the spring bloom, which generates most of the sedimented organic material, is observed in the Gulf of Riga in April–May (Olli and Heiskanen, 1999; Purina et al., 2018). When the spring bloom material reaches the

sediment surface, it triggers enhanced oxygen consumption, with the rate and delay depending on the bloom species composition, e.g., diatom-to-dinoflagellate ratio (Spilling et al., 2018). Aigars et al. (2015) found higher consumption rates in late spring–early summer than in late summer–autumn and related this result to the availability of degradable organic material, i.e., settling of spring bloom. Thus, the strength of stratification in spring–early summer is a crucial factor influencing the extent of seasonal hypoxia in the Gulf of Riga and similar coastal basins.

Since oxygen consumption at the sediment–water interface can have a large share in depth-integrated respiration (Boynton et al., 2018), separation of the near-bottom layer from the waters above may accelerate oxygen depletion in the NBL. For instance, Jokinen et al. (2018) suggested that a decrease in the water volume between the pycnocline and the seabed increased the probability of hypoxia occurrences in a shallow basin of the Archipelago Sea (Haverö). We suggest that besides the strong seasonal stratification and reduced vertical mixing, the haline stratification in the deep layer that already existed in spring was a crucial precondition for hypoxia development in 2018. A similar thin near-bottom layer with higher salinity was observed in early summer 2014, and in both years, summer deoxygenation was higher compared to other years. The year 2018 was specific since additional inflows of saltier waters in summer caused an uplift of the almost oxygen-depleted near-bottom waters. As a consequence, the boundary of hypoxic waters was at its shallowest depth, and the estimated extent of hypoxic bottoms was the largest in late summer–autumn 2018. Thus, although the development of hypoxia in 2018 was in accordance with the long-term trend, the co-occurrence of several factors made it an exceptional event.

Based on the introduced method, we estimated the oxygen consumption rate at  $1.67 \text{ mmol O}_2 \text{ m}^{-2} \text{ h}^{-1}$  for spring–summer 2018. This result is higher than the estimates of consumption rates obtained for the Baltic Proper and the Gulf of Finland –  $0.11$ – $0.39 \text{ mmol O}_2 \text{ m}^{-2} \text{ h}^{-1}$  (Koop et al., 1990) and  $0.46$ – $0.53 \text{ mmol O}_2 \text{ m}^{-2} \text{ h}^{-1}$  (Conley et al., 1997), respectively, and closer to but slightly lower than the estimates based on the direct measurements in the Gulf of Riga by

Aigars et al. (2015) – on average  $2.3 \text{ mmol O}_2 \text{ m}^{-2} \text{ h}^{-1}$ . On the other hand, our estimates are much higher than found for the deep areas of the Baltic Proper, although it is stated that the consumption rates there have accelerated recently (Meier et al., 2018). We used the estimated consumption rate to explain the occurrence of hypoxia in 2015 with relatively weak stratification and suggest that seasonal stratification lasted long enough to reach hypoxia levels in late October 2015. No hypoxia was observed in 2016, although seasonal stratification was strong at its peak, because the water column was fully mixed before the autumn monitoring cruise in late October. We suggest that a longer duration of the stratified season in recent years, as also revealed by other authors, e.g., Wasmund et al. (2019), has increased the probability of hypoxia occurrences in the near-bottom layer of seasonally stratified coastal basins in autumn.

We analyzed the seasonal dynamics of vertical stratification depending on the local meteorological conditions to reveal the potential development of near-bottom oxygen conditions due to predicted climate changes. Stratification has strengthened in the Baltic Sea mostly due to increased surface layer temperature (Kniefbusch et al., 2019; Liblik and Lips, 2019). In our assessment of the development of vertical stratification, according to Simpson et al. (1990), the surface heat flux and wind-induced mixing were the main contributors to its changes. River runoff had, in general, a lower contribution, although its influence was seen, e.g., in early spring 2013, which was the year with the highest river discharge (considering the period 2012–2018).

Earlier modeling studies have stated that possible future changes in climate, including warming that causes the strengthening of stratification and decreased oxygen solubility, and changes in precipitation/river runoff, influence the extent of hypoxia in the Baltic Sea (Meier et al., 2011). Strengthening of vertical stratification is predicted by the projected future increase in sea surface temperatures (Gröger et al., 2019; Meier and Saraiva, 2020; Saraiva et al., 2019b). Also, an increase in the total runoff to the Baltic Sea is predicted (Saraiva et al., 2019a,b), which could lead to a decrease in surface salinity, but these predictions are uncertain. Although climate projections for wind are uncertain in the Baltic Sea area (Christensen et al., 2015), a slight decrease in wind speed in spring is expected (Ruostenoja et al., 2019). Lower wind speed reduces vertical mixing and enhances stratification. Thus, in general, the future projections seem to favor a strengthened stratification regime. When also considering a predicted winter river runoff increase due to intermittent melting (Stonevičius et al., 2017) – which would potentially bring additional nutrients and organic matter to the sea (Yurkovskis, 2004) – hypoxic events in the future would probably occur more often and perhaps be even more severe.

Although phosphorus inputs into the Gulf of Riga have decreased (HELCOM, 2018b), they are still higher than the maximum allowable inputs by about  $1000 \text{ t yr}^{-1}$  (HELCOM,

2022). Our analysis of the long-term nutrient data revealed a statistically significant increasing trend in near-bottom phosphate and total phosphorus concentrations in the stratified season. A negative correlation between the near-bottom phosphate and oxygen concentrations points to the internal load – the release of phosphates from the bottom sediments under low oxygen concentrations (van Helmond et al., 2020; Pitkänen et al., 2001). This result agrees with other studies based on long-term monitoring and targeted research data stating that the phosphorus dynamics in the Baltic Sea basins is largely defined by the meteorological and hydrographic conditions (Lehtoranta et al., 2017; Lips et al., 2017). Such internal phosphorus load also supports cyanobacterial nitrogen fixation and, thus, counteracts not only external phosphorus load reduction but also external nitrogen load reduction (Savchuk, 2018).

Based on the indirect method suggested in this study, the estimated phosphate fluxes from sediments reached up to  $13.5 \mu\text{mol m}^{-2} \text{ h}^{-1}$  from the end of May to mid-July 2018. This estimate agrees with the earlier studies in the Gulf of Riga by Eglite et al. (2014) and Aigars et al. (2015) and in the Gulf of Finland, e.g., by Pitkänen et al. (2001), who obtained a flux estimate of  $13 \text{ kg km}^{-2} \text{ d}^{-1}$  or  $17 \mu\text{mol m}^{-2} \text{ h}^{-1}$ . The observed increase in phosphate concentrations in the NBL in summer 2018, already before hypoxia development, agrees with the results by Aigars et al. (2015), showing that the phosphate flux did increase substantially at oxygen concentration  $< 6 \text{ mg L}^{-1}$ . They also found that the average phosphate fluxes from sediments gradually increased from low values of  $2\text{--}5 \mu\text{mol m}^{-2} \text{ h}^{-1}$  in April–May to  $55 \mu\text{mol m}^{-2} \text{ h}^{-1}$  in October 2012. Our maximum flux estimates from late May to mid-July are close to the values obtained by Aigars et al. (2015) in June–August, but we did not observe a further substantial increase in NBL phosphate concentrations in late summer–autumn 2018. The latter could indicate that almost all mobile phosphorus is released from the surface sediments in low-oxygen conditions (e.g., Walve et al., 2018). It is difficult to suggest what has been the major factor causing the observed long-term (2005–2018) increasing trend in near-bottom phosphate concentrations – either the strengthening of stratification and prolongation of the stratified season, larger phosphorus flux associated with the near-bottom inflow of saltier waters, or accumulation of mobile phosphorus in the sediments. An indication of increased phosphorus flux from the Baltic Proper is the revealed positive trend in phosphate concentrations in the near-bottom layer of the Irbe Strait. On the other hand, a shorter mixed season in winter could hinder the formation of an Fe-oxide-bound P pool, as suggested by van Helmond et al. (2020) for similar sites in the Stockholm archipelago with relatively low mixing and low bottom water oxygen concentrations in summer.

In conclusion, we suggest that the sequence of certain processes triggered the observed extensive hypoxia in the Gulf of Riga in 2018. Enhanced seasonal stratification was cre-

ated by the rapid warming of the surface layer and calm wind conditions in spring, leading to restricted vertical mixing. Inflows of saltier waters through the Irbe Strait in spring–early summer maintained haline stratification in the deep layer that additionally constrained vertical mixing. Due to high respiration, hypoxia developed in the entire saltier near-bottom layer separated from the water layers above by the secondary pycnocline. Furthermore, the estimated oxygen consumption rate is large enough to lead to near-bottom hypoxia also in conditions of weaker stratification but a prolonged stratified season. The projections of meteorological and hydrological conditions anticipate that the frequency and extent of hypoxia will likely increase in the future. Since the internal load of phosphorus is linked to the near-bottom oxygen conditions, this scenario also predicts no fast reduction of nutrient concentrations in the Gulf of Riga and similar coastal basins.

**Data availability.** Historical and forcing data can be found in databases (see Sect. 2). CTD data can be downloaded or accessed via SeaDataNet (<https://www.seadatanet.org>, last access: 18 June 2021; organization: Department of Marine Systems at Tallinn University of Technology).

**Author contributions.** STS was the main responsible person for developing methods, analyzing data, and writing the manuscript. UL and JL contributed to developing methods and writing the manuscript. TL contributed by analyzing the data and reviewing the manuscript. MS provided river inflow and Latvian CTD data and contributed to reviewing the manuscript. OS contributed by collecting and analyzing CTD data. IL contributed by analyzing the nutrient data and reviewing the manuscript.

**Competing interests.** The contact author has declared that neither they nor their co-authors have any competing interests.

**Disclaimer.** Publisher's note: Copernicus Publications remains neutral with regard to jurisdictional claims in published maps and institutional affiliations.

**Acknowledgements.** We thank the agencies and institutes funding and implementing the marine environmental monitoring programs in Estonia and Latvia. Data were provided through the Estonian environmental monitoring information system (KESE), Latvian environmental monitoring database (Latvian Environmental, Geology and Meteorology Center), HELCOM/ICES database, SeaDataNet Pan-European infrastructure for ocean and marine data management, and Copernicus Climate Change Service information. We are thankful to the crew of RV *Salme* and colleagues who participated in the cruises and data exploration (Ilja Maljutenko for the help with ERA5 data).

**Financial support.** This work was supported by the Estonian Ministry of Education institutional research funding (grant no. IUT19-6), the Estonian Research Council (grant no. PRG602), and the joint Baltic Sea research and development program (Art 185) through grant no. 03F0773A (BONUS INTEGRAL).

**Review statement.** This paper was edited by Caroline P. Slomp and reviewed by Jacob Carstensen and two anonymous referees.

## References

- Aigars, J. and Carman, R.: Seasonal and spatial variations of carbon and nitrogen distribution in the surface sediments of the Gulf of Riga, Baltic Sea, *Chemosphere*, 43, 313–320, 2001.
- Aigars, J., Poikāne, R., Dalsgaard, T., Eglīte, E., and Jansons, M.: Biogeochemistry of N, P and SI in the Gulf of Riga surface sediments: Implications of seasonally changing factors, *Cont. Shelf Res.*, 105, 112–120, 2015.
- Astok, V., Ottsmann, M., and Suursaar, Ü.: Water exchange as the main physical process in semi-enclosed marine systems: the Gulf of Riga case, *Hydrobiologia*, 393, 11–18, <https://doi.org/10.1023/A:1003517110726>, 1999.
- Berzins, V.: Hydrology, in: *Ecosystem of the Gulf of Riga between 1920–1990*, edited by: Ojaveer, E., Estonian Academy Publishers, Tallinn, 7–31, ISBN 9985-50-065-2, 1995.
- Bindoff, N. L., Cheung, W. W. L., Kairo, J. G., Aristegui, J., Guinder, V. A., Hallberg, R., Hilmi, N., Jiao, N., Karim, M. S., Levin, L., O'Donoghue, S., Cuicapusa, S. R. P., Rinkevich, B., Suga, T., Tagliabue, A., and Williamson, P.: Changing Ocean, Marine Ecosystems, and Dependent Communities, in: *IPCC Special Report on the Ocean and Cryosphere in a Changing Climate*, edited by: Pörtner, H.-O., Roberts, D. C., Masson-Delmotte, V., Zhai, P., Tignor, M., Poloczanska, E., Mintenbeck, K., Alegria, A., Nicolai, M., Okem, A., Petzold, J., Rama, B., and Weyer, N. M., Cambridge University Press, Cambridge, UK and New York, NY, USA, 447–587, <https://doi.org/10.1017/9781009157964.007>, 2019.
- Bonsdorff, E., Diaz, R. J., Rosenberg, R., Norkko, A., and Cutter Jr, G. R.: Characterization of soft-bottom benthic habitats of the Åland Islands, norther Baltic Sea, *Mar. Ecol.-Prog. Ser.*, 142, 235–245, 1996.
- Boynton, W. R., Ceballos, M. A. C., Bailey, E. M., Hodgkins, C. L. S., Humphrey, J. L., and Testa, J. M.: Oxygen and Nutrient Exchanges at the Sediment-Water Interface: a Global Synthesis and Critique of Estuarine and Coastal Data, *Estuar. Coast.*, 41, 301–333, <https://doi.org/10.1007/s12237-017-0275-5>, 2018.
- Caballero-Alfonso, A. M., Carstensen, J., and Conley, D. J.: Biogeochemical and environmental drivers of coastal hypoxia, *J. Marine Syst.*, 141, 190–199, 2015.
- Carstensen, J. and Conley, D. J.: Baltic Sea Hypoxia Takes Many Shapes and Sizes, *Limnol. Oceanogr. Bull.*, 28, 125–129, <https://doi.org/10.1002/lob.10350>, 2019.
- Carstensen, J., Andersen, J. H., Gustafsson, B. G., and Conley, D. J.: Deoxygenation of the Baltic Sea during the last century, *P. Natl. Acad. Sci. USA*, 111, 5628–5633, 2014.
- Christensen, O. B., Kjellström, E., and Zorita, E.: in *Second Assessment of Climate Change for the Baltic Sea Basin*, in: *Second*

- Assessment of Climate Change for the Baltic Sea Basin, edited by: BACC II Author Team, Springer International Publishing, 217–233, [https://doi.org/10.1007/978-3-319-16006-1\\_11](https://doi.org/10.1007/978-3-319-16006-1_11), 2015.
- Codiga, D. L., Stoffel, H. E., Decautis, C. F., Kiernan, S., and Oviatt, C. A.: Narragansett Bay Hypoxic Event Characteristics Based on Fixed-Site Monitoring Network Time Series: Intermittency, Geographic Distribution, Spatial Synchronicity, and Interannual Variability, *Estuar. Coast.*, 32, 621–641, <https://doi.org/10.1007/s12237-009-9165-9>, 2009.
- Conley, D. J., Stockenberg, A., Carman, R., Johnstone, R. W., Rahm, L., and Wulff, F.: Sediment-water Nutrient Fluxes in the Gulf of Finland, Baltic Sea, *Estuar. Coast. Shelf S.*, 45, 591–598, 1997.
- Conley, D. J., Humborg, C., Rahm, L., Savchuk, O. P., and Wulff, F.: Hypoxia in the Baltic Sea and Basin-Scale Changes in Phosphorus Biogeochemistry, *Environ. Sci. Technol.*, 36, 5315–5320, <https://doi.org/10.1021/es025763w>, 2002.
- Conley, D. J., Carstensen, J., Ærtebjerg, G., Christensen, P. B., Dalsgaard, T., Hansen, J. L. S., and Josefson, A. B.: LONG-TERM CHANGES AND IMPACTS OF HYPOXIA IN DANISH COASTAL WATERS, *Ecol. Appl.*, 17, S165–S184, <https://doi.org/10.1890/05-0766.1>, 2007.
- Conley, D. J., Björck, S., Bonsdorff, E., Carstensen, J., Destouni, G., Gustafsson, B. G., Hietanen, S., Kortekaas, M., Kuosa, H., Meier, H. E. M., Müller-Karulis, B., Nordberg, K., Norkko, A., Nürnberg, G., Pitkänen, H., Rabalais, N. N., Rosenberg, R., Savchuk, O. P., Slomp, C. P., Voss, M., Wulff, F., and Zillén, L.: Hypoxia-Related Processes in the Baltic Sea, *Environ. Sci. Technol.*, 43, 3412–3420, <https://doi.org/10.1021/es802762a>, 2009.
- Conley, D. J., Carstensen, J., Aigars, J., Axe, P., Bonsdorff, E., Eremina, T., Haahti, B.-M., Humborg, C., Jonsson, P., Kotta, J., Lännegren, C., Larsson, U., Maximov, A., Medina, M. R., Lysiak-Pastuszak, E., Remeikaitė-Nikienė, N., Walve, J., Wilhelm, S., and Zillén, L.: Hypoxia Is Increasing in the Coastal Zone of the Baltic Sea, *Environ. Sci. Technol.*, 45, 6777–6783, <https://doi.org/10.1021/es201212r>, 2011.
- Diaz, R. J. and Rosenberg, R.: Spreading Dead Zones and Consequences for Marine Ecosystems, *Science* (80-), 321, 926–929, <https://doi.org/10.1126/science.1156401>, 2008.
- Eglite, E., Lavrinovičs, A., Müller-Karulis, B., Aigars, J., and Poikāne, R.: Nutrient turnover at the hypoxic boundary: flux measurements and model representation for the bottom water environment of the Gulf of Riga, *Baltic Sea, Oceanologia*, 56, 711–735, 2014.
- EMODnet Bathymetry Consortium: EMODnet Digital Bathymetry (DTM), <https://sextant.ifremer.fr/record/bb6a87dd-e579-4036-abe1-e649cea9881a/> (last access: 28 April 2021), 2020.
- Estonian Environment Agency: KESE [data set], <https://kese.envir.ee/kese/>, last access: 4 April 2019.
- Estonian Weather Service: Hydrological data [data set], <https://www.ilmateenistus.ee/siseveed/ajaloolised-vaatlusandmed/vooluhulgad/>, last access: 23 March 2022.
- Fennel, K. and Testa, J. M.: Biogeochemical Controls on Coastal Hypoxia, *Annu. Rev. Mar. Sci.*, 11, 105–130, <https://doi.org/10.1146/annurev-marine-010318-095138>, 2019.
- Groeskamp, S. and Iudicone, D.: The Effect of Air-Sea Flux Products, Shortwave Radiation Depth Penetration, and Albedo on the Upper Ocean Overturning Circulation, *Geophys. Res. Lett.*, 45, 9087–9097, <https://doi.org/10.1029/2018GL078442>, 2018.
- Gröger, M., Arneborg, L., Dieterich, C., Höglund, A., and Meier, H. E. M.: Summer hydrographic changes in the Baltic Sea, Kattegat and Skagerrak projected in an ensemble of climate scenarios downscaled with a coupled regional ocean–sea ice–atmosphere model, *Clim. Dynam.*, 53, 5945–5966, <https://doi.org/10.1007/s00382-019-04908-9>, 2019.
- Gustafsson, B. G., Schenk, F., Blenckner, T., Eilola, K., Meier, H. E. M., Müller-Karulis, B., Neumann, T., Ruoho-Airola, T., Savchuk, O. P., and Zorita, E.: Reconstructing the Development of Baltic Sea Eutrophication 1850–2006, *Ambio*, 41, 534–548, 2012.
- Hansson, M. and Viktorsson, L.: REPORT OCEANOGRAPHY No. 70, 2020. Oxygen Survey in the Baltic Sea 2020 – Extent of Anoxia and Hypoxia, SMHI, ISSN 0283-1112, 1960–2020, 2020.
- HELCOM: Environment of the Baltic Sea area 1994–1998, *Balt. Sea Environ. Proc.* No. 82B, Helsinki Commission, ISSN 0357-2994, 215, 2002.
- HELCOM: Eutrophication in the Baltic Sea – An Integrated thematic assessment of the effects of nutrient enrichment and eutrophication in the Baltic Sea region, *Balt. Sea Environ. Proc.* No. 115B, Helsinki Commission, ISSN 0357-2994, 148, 2009.
- HELCOM: Manual for the Marine Monitoring in the COMBINE Programme of HELCOM, <https://helcom.fi/action-areas/monitoring-and-assessment/monitoring-guidelines/combine-manual/> (last access: 21 June 2021), 2017.
- HELCOM: HELCOM Thematic assessment of eutrophication 2011–2016. Baltic Sea Environment Proceedings No. 156, Baltic Marine Environment Protection Commission, ISSN 0357-2994, 2018a.
- HELCOM: Sources and pathways of nutrients to the Baltic Sea. Baltic Sea Environment Proceedings No. 153, Baltic Marine Environment Protection Commission, ISSN 0357-2994, 2018b.
- HELCOM: State of the Baltic Sea – Second HELCOM holistic assessment 2011–2016. Baltic Sea Environment Proceedings 155, Baltic Marine Environment Protection Commission, ISSN 0357-2994, 2018c.
- HELCOM: Inputs of nutrients to the sub-basins (2019), HELCOM core indicator report, <https://helcom.fi/wp-content/uploads/2017/06/HELCOM-core-indicator-on-inputs-of-nutrients-for-period-1995-2019.pdf> (last access: 10 January 2022), 2022.
- Hersbach, H., Bell, B., Berrisford, P., Biavati, G., Horányi, A., Muñoz Sabater, J., Nicolas, J., Peubey, C., Radu, R., Rozum, I., Schepers, D., Simmons, A., Soci, C., Dee, D., and Thépaut, J.-N.: ERA5 hourly data on single levels from 1979 to present, *Copernicus Clim. Chang. Serv. Clim. Data Store* [data set], <https://doi.org/10.24381/cds.adbb2d47>, 2018.
- Hoy, A., Hänsel, S., and Maugeri, M.: An endless summer: 2018 heat episodes in Europe in the context of secular temperature variability and change, *Int. J. Climatol.*, 40, 6315–6336, <https://doi.org/10.1002/joc.6582>, 2020.
- ICES: Oceanographic database [data set], <https://www.ices.dk/data/dataset-collections/pages/default.aspx>, last access: 16 April 2019.
- IOC, SCOR and IAPSO: The International Thermodynamic Equation of Seawater – 2010: Calculation and Use of Thermodynamic Properties, Intergovernmental Oceanographic Commis-

- sion, Manuals and Guides No. 56, UNESCO (English), 196 pp., 2010.
- Jansson, A., Klais-Peets, R., Grininė, E., Rubene, G., Semenova, A., Lewandowska, A., and Engström-Öst, J.: Functional shifts in estuarine zooplankton in response to climate variability, *Ecol. Evol.*, 10, 11591–11606, <https://doi.org/10.1002/ece3.6793>, 2020.
- Johansson, J.: Total and regional runoff to the Baltic Sea, HELCOM Balt. Sea Environ. Fact Sheets, Online, Helsinki Commission, [https://helcom.fi/media/documents/BSEFS\\_Total-and-regional-runoff-to-the-Baltic-Sea-in-2015.pdf](https://helcom.fi/media/documents/BSEFS_Total-and-regional-runoff-to-the-Baltic-Sea-in-2015.pdf) (last access: 9 June 2022), 2016.
- Jokinen, S. A., Virtasalo, J. J., Jilbert, T., Kaiser, J., Dellwig, O., Arz, H. W., Hänninen, J., Arppe, L., Collander, M., and Saarinen, T.: A 1500-year multiproxy record of coastal hypoxia from the northern Baltic Sea indicates unprecedented deoxygenation over the 20th century, *Biogeosciences*, 15, 3975–4001, <https://doi.org/10.5194/bg-15-3975-2018>, 2018.
- Kabel, K., Moros, M., Porsche, C., Neumann, T., Adolphi, F., Andersen, T. J., Siegel, H., Gerth, M., Leipe, T., Jansen, E., and Damsté, J. S. S.: Impact of climate change on the Baltic Sea ecosystem over the past 1,000 years, *Nat. Clim. Change*, 2, 871–874, 2012.
- Karlson, K., Rosenberg, R., and Bonsdorff, E.: Temporal and spatial large-scale effects of eutrophication and oxygen deficiency on benthic fauna in Scandinavian and Baltic waters: a review, edited by: Gibson, R. N. et al. *Oceanogr. Mar. Biol. Ann. Rev.*, 40, 427–489, 2002.
- Kniesbusch, M., Meier, H. E. M., Neumann, T., and Börgel, F.: Temperature Variability of the Baltic Sea Since 1850 and Attribution to Atmospheric Forcing Variables, *J. Geophys. Res.-Oceans*, 124, 4168–4187, <https://doi.org/10.1029/2018JC013948>, 2019.
- Koop, K., Boynton, W. R., Wulff, F., and Carman, R.: Sediment-water oxygen and nutrient exchanges along a depth gradient in the Baltic Sea, *Mar. Ecol. Prog. Ser.*, 63, 65–77, 1990.
- Kralj, M., Lipizer, M., Čermelj, B., Celio, M., Fabbro, C., Brunetti, F., Francé, J., Mozetič, P., and Giani, M.: Hypoxia and dissolved oxygen trends in the northeastern Adriatic Sea (Gulf of Trieste), *Deep-Sea Res. Pt. II*, 164, 74–88, <https://doi.org/10.1016/j.dsr2.2019.06.002>, 2019.
- Latvian Environment: Geology and Meteorology Center [data set], <https://videscenrtr.lv/gmc.lv/>, 2019.
- Lehtoranta, J., Savchuk, O. P., Elken, J., Kim, D., Kuosa, H., Raateoja, M., Kauppila, P., Räsänen, A., and Pitkänen, H.: Atmospheric forcing controlling inter-annual nutrient dynamics in the open Gulf of Finland, *J. Marine Syst.*, 171, 4–20, 2017.
- Liblik, T. and Lips, U.: Variability of synoptic-scale quasi-stationary thermohaline stratification patterns in the Gulf of Finland in summer 2009, *Ocean Sci.*, 8, 603–614, <https://doi.org/10.5194/os-8-603-2012>, 2012.
- Liblik, T. and Lips, U.: Stratification Has Strengthened in the Baltic Sea – An Analysis of 35 Years of Observational Data, *Front. Earth. Sci.*, 7, 174, <https://doi.org/10.3389/feart.2019.00174>, 2019.
- Liblik, T., Skudra, M., and Lips, U.: On the buoyant sub-surface salinity maxima in the Gulf of Riga, *Oceanologia*, 59, 113–128, 2017.
- Liblik, T., Naumann, M., Alenius, P., Hansson, M., Lips, U., Nausch, G., Tuomi, L., Wesslander, K., Laanemets, J., and Viktorsson, L.: Propagation of Impact of the Recent Major Baltic Inflows From the Eastern Gotland Basin to the Gulf of Finland, *Front. Mar. Sci.*, 5, 222, <https://doi.org/10.3389/fmars.2018.00222>, 2018.
- Liblik, T., Wu, Y., Fan, D., and Shang, D.: Wind-driven stratification patterns and dissolved oxygen depletion off the Changjiang (Yangtze) Estuary, *Biogeosciences*, 17, 2875–2895, <https://doi.org/10.5194/bg-17-2875-2020>, 2020.
- Lilover, M.-J., Lips, U., Laanearu, J., and Liljebadh, B.: Flow regime in the Irbe Strait, *Aquat. Sci.*, 60, 253–265, 1998.
- Lips, U., Lilover, M.-J., Raudsepp, U., and Talpsepp, L.: Water renewal processes and related hydrographic structures in the Gulf of Riga, in: *Hydrographic studies within the Gulf of Riga Project, 1993–1994*, edited by: Toompuu, A. and Elken, J., Estonian Marine Institute Report Series No. 1, 1–34, ISBN 9985-9058-0-6, 1995.
- Lips, U., Zhurbas, V., Skudra, M., and Väli, G.: A numerical study of circulation in the Gulf of Riga, Baltic Sea. Part I: Whole-basin gyres and mean currents, *Cont. Shelf Res.*, 112, 1–13, 2016.
- Lips, U., Laanemets, J., Lips, I., Liblik, T., Suhhova, I., and Suurasaar, Ü.: Wind-driven residual circulation and related oxygen and nutrient dynamics in the Gulf of Finland (Baltic Sea) in winter, *Estuar. Coast. Shelf S.*, 195, 4–15, 2017.
- Lukkari, K., Leivuori, M., Vallius, H., and Kotilainen, A.: The chemical character and burial of phosphorus in shallow coastal sediments in the northeastern Baltic Sea, *Biogeochemistry*, 94, 141–162, <https://doi.org/10.1007/s10533-009-9315-y>, 2009.
- Matthäus, W. and Franck, H.: Characteristics of major Baltic inflows—a statistical analysis, *Cont. Shelf Res.*, 12, 1375–1400, [https://doi.org/doi:10.1016/0278-4343\(92\)90060-W](https://doi.org/doi:10.1016/0278-4343(92)90060-W), 1992.
- Meier, H. E. M. and Saraiva, S.: Projected Oceanographical Changes in the Baltic Sea until 2100, *Oxford Research Encyclopedia of Climate Science*, <https://doi.org/10.1093/acrefore/9780190228620.013.699>, 2020.
- Meier, H. E. M., Andersson, H. C., Eilola, K., Gustafsson, B. G., Kuznetsov, I., Müller-Karulis, B., Neumann, T., and Savchuk, O. P.: Hypoxia in future climates: A model ensemble study for the Baltic Sea, *Geophys. Res. Lett.*, 38, L24608, <https://doi.org/10.1029/2011GL049929>, 2011.
- Meier, H. E. M., Väli, G., Naumann, M., Eilola, K., and Frauen, C.: Recently Accelerated Oxygen Consumption Rates Amplify Deoxygenation in the Baltic Sea, *J. Geophys. Res.-Oceans*, 123, 3227–3240, <https://doi.org/10.1029/2017JC013686>, 2018.
- Murphy, R. R., Kemp, W. M., and Ball, W. P.: Long-Term Trends in Chesapeake Bay Seasonal Hypoxia, Stratification, and Nutrient Loading, *Estuar. Coast.*, 34, 1293–1309, <https://doi.org/10.1007/s12237-011-9413-7>, 2011.
- Ojaveer, E. (Ed.): *Ecosystem of the Gulf of Riga between 1920 and 1990*, Estonian Academy Publishers, Tallinn, 1995.
- Olli, K. and Heiskanen, A.-S.: Seasonal stages of phytoplankton community structure and sinking loss in the Gulf of Riga, *J. Marine Syst.*, 23, 165–184, [https://doi.org/10.1016/S0924-7963\(99\)00056-1](https://doi.org/10.1016/S0924-7963(99)00056-1), 1999.
- Omstedt, A., Mueller, L., and Nyberg, L.: Interannual, Seasonal and Regional Variations of Precipitation and Evaporation over the Baltic Sea, *Ambio*, 26, 484–492, 1997.

- Petrov, V.: Water balance and water exchange between the Gulf of Riga and the Baltic Proper, *Sb. Rab. Rzhskoj GO*, 18, 20–40, 1979.
- Pitkänen, H., Lehtoranta, J., and Rääke, A.: Internal Nutrient Fluxes Counteract Decreases in External Load: The Case of the Estuarial Eastern Gulf of Finland, *Baltic Sea, Ambio*, 30, 195–201, <https://doi.org/10.1579/0044-7447-30.4.195>, 2001.
- Powilleit, M. and Kube, J.: Effects of severe oxygen depletion on macrobenthos in the Pomeranian Bay (southern Baltic Sea): a case study in a shallow, sublittoral habitat characterised by low species richness, *J. Sea Res.*, 42, 221–234, 1999.
- Purina, I., Labucis, A., Barda, I., Jurgensone, I., and Aigars, J.: Primary productivity in the Gulf of Riga (Baltic Sea) in relation to phytoplankton species and nutrient variability, *Oceanologia*, 60, 544–552, <https://doi.org/10.1016/j.oceano.2018.04.005>, 2018.
- Puttonen, I., Mattila, J., Jonsson, P., Karlsson, O. M., Kohonen, T., Kotilainen, A., Lukkari, K., Malmäus, J. M., and Rydin, E.: Distribution and estimated release of sediment phosphorus in the northern Baltic Sea archipelagos, *Estuar. Coast. Shelf S.*, 145, 9–21, <https://doi.org/10.1016/j.ecss.2014.04.010>, 2014.
- Puttonen, I., Kohonen, T., and Mattila, J.: Factors controlling phosphorus release from sediments in coastal archipelago areas, *Mar. Pollut. Bull.*, 108, 77–86, <https://doi.org/10.1016/j.marpolbul.2016.04.059>, 2016.
- Raudsepp, U. and Elken, J.: Application of the GFDL circulation model for the Gulf of Riga, in: *Hydrographic studies within the Gulf of Riga Project, 1993–1994*, edited by: Toompuu, A. and Elken, J., Estonian Marine Institute Report Series No. 1, 143–176, ISBN 9985-9058-0-6, 1995.
- Reusch, T. B. H., Dierking, J., Andersson, H. C., Bonsdorff, E., Carstensen, J., Casini, M., Czajkowski, M., Hasler, B., Hinsby, K., Hytiäinen, K., Johannesson, K., Jomaa, S., Jormalainen, V., Kuosa, H., Kurland, S., Laikre, L., MacKenzie, B. R., Margonski, P., Melzner, F., Oesterwind, D., Ojaveer, H., Refsgaard, J. C., Sandström, A., Schwarz, G., Tonderski, K., Winder, M., and Zandersen, M.: The Baltic Sea as a time machine for the future coastal ocean, *Sci. Adv.*, 4, eaar8195, <https://doi.org/10.1126/sciadv.aar8195>, 2018.
- Ruosteenoja, K., Vihma, T., and Venäläinen, A.: Projected Changes in European and North Atlantic Seasonal Wind Climate Derived from CMIP5 Simulations, *J. Climate*, 32, 6467–6490, <https://doi.org/10.1175/JCLI-D-19-0023.1>, 2019.
- Saraiva, S., Markus Meier, H. E., Andersson, H., Höglund, A., Dieterich, C., Gröger, M., Hordoir, R., and Eilola, K.: Baltic Sea ecosystem response to various nutrient load scenarios in present and future climates, *Clim. Dynam.*, 52, 3369–3387, <https://doi.org/10.1007/s00382-018-4330-0>, 2019a.
- Saraiva, S., Meier, H. E. M., Andersson, H., Höglund, A., Dieterich, C., Gröger, M., Hordoir, R., and Eilola, K.: Uncertainties in Projections of the Baltic Sea Ecosystem Driven by an Ensemble of Global Climate Models, *Front. Earth Sci.*, 6, 244, <https://doi.org/10.3389/feart.2018.00244>, 2019b.
- Savchuk, O. P.: Large-Scale Nutrient Dynamics in the Baltic Sea, 1970–2016, *Front. Mar. Sci.*, 5, <https://doi.org/10.3389/fmars.2018.00095>, 2018.
- Schinke, H. and Matthäus, W.: On the causes of major Baltic inflows – an analysis of long time series, *Cont. Shelf Res.*, 18, 67–97, [https://doi.org/10.1016/S0278-4343\(97\)00071-X](https://doi.org/10.1016/S0278-4343(97)00071-X), 1998.
- Schlitzer, R.: Ocean Data View, [code] <https://odv.awi.de> (last access: 9 January 2020), 2019.
- Schmale, O., Krause, S., Holtermann, P., Power Guerra, N. C., and Umlauf, L.: Dense bottom gravity currents and their impact on pelagic methanotrophy at oxic/anoxic transition zones, *Geophys. Res. Lett.*, 43, 5225–5232, <https://doi.org/10.1002/2016GL069032>, 2016.
- SeaDataNet: SeaDataNet Pan-European infrastructure for ocean and marine data management [data set], <http://www.seadatanet.org>, last access: 9 April 2019.
- Séférian, R., Baek, S., Boucher, O., Dufresne, J.-L., Decharme, B., Saint-Martin, D., and Roehrig, R.: An interactive ocean surface albedo scheme (OSAv1.0): formulation and evaluation in ARPEGE-Climat (V6.1) and LMDZ (V5A), *Geosci. Model Dev.*, 11, 321–338, <https://doi.org/10.5194/gmd-11-321-2018>, 2018.
- Simpson, J. H., Brown, J., Matthews, J., and Allen, G.: Tidal Straining, Density Currents, and Stirring in the Control of Estuarine Stratification, *Estuaries*, 13, 125–132, <https://doi.org/10.2307/1351581>, 1990.
- Skudra, M. and Lips, U.: Characteristics and inter-annual changes in temperature, salinity and density distribution in the Gulf of Riga, *Oceanologia*, 59, 37–48, 2017.
- Soosaar, E., Maljutenko, I., Raudsepp, U., and Elken, J.: An investigation of anticyclonic circulation in the southern Gulf of Riga during the spring period, *Cont. Shelf Res.*, 78, 75–84, <https://doi.org/10.1016/j.csr.2014.02.009>, 2014.
- Spilling, K., Olli, K., Lehtoranta, J., Kremp, A., Tedesco, L., Tamelander, T., Klais, R., Peltonen, H., and Tamminen, T.: Shifting Diatom–Dinoflagellate Dominance During Spring Bloom in the Baltic Sea and its Potential Effects on Biogeochemical Cycling, *Front. Mar. Sci.*, 5, 92–108, <https://doi.org/10.3389/fmars.2018.00327>, 2018.
- Stiebrins, O. and Väiling, P.: Bottom sediments of the Gulf of Riga, *Geol. Surv. Latv. Riga*, 4, ISBN 9984-9130-0-7, 1996.
- Stipa, T., Tamminen, T., and Seppälä, J.: On the creation and maintenance of stratification in the Gulf of Riga, *J. Marine Syst.*, 23, 27–49, 1999.
- Stoicescu, S.-T., Lips, U., and Liblik, T.: Assessment of Eutrophication Status Based on Sub-Surface Oxygen Conditions in the Gulf of Finland (Baltic Sea), *Front. Mar. Sci.*, 6, 54, <https://doi.org/10.3389/fmars.2019.00054>, 2019.
- Stonevičius, E., Rimkus, E., Štaras, A., Kažys, J., and Valiūškevičius, G.: Climate change impact on the Nemunas River basin hydrology in the 21st century, *Boreal Environ. Res.*, 22, 49–65, 2017.
- Ukrainskii, V. V. and Popov, Y. I.: Climatic and hydrophysical conditions of the development of hypoxia in waters of the northwest shelf of the Black Sea, *Phys. Oceanogr.*, 19, 140, <https://doi.org/10.1007/s11110-009-9046-6>, 2009.
- van Helmond, N. A. G. M., Robertson, E. K., Conley, D. J., Hermans, M., Humborg, C., Kubeneck, L. J., Lenstra, W. K., and Slomp, C. P.: Removal of phosphorus and nitrogen in sediments of the eutrophic Stockholm archipelago, *Baltic Sea, Biogeosciences*, 17, 2745–2766, <https://doi.org/10.5194/bg-17-2745-2020>, 2020.
- Virtanen, E. A., Norkko, A., Nyström Sandman, A., and Vitasalo, M.: Identifying areas prone to coastal hypoxia –



- the role of topography, *Biogeosciences*, 16, 3183–3195, <https://doi.org/10.5194/bg-16-3183-2019>, 2019.
- Walve, J., Sandberg, M., Larsson, U., and Lännergren, C.: A Baltic Sea estuary as a phosphorus source and sink after drastic load reduction: seasonal and long-term mass balances for the Stockholm inner archipelago for 1968–2015, *Biogeosciences*, 15, 3003–3025, <https://doi.org/10.5194/bg-15-3003-2018>, 2018.
- Wasmund, N., Nausch, G., Gerth, M., Busch, S., Burmeister, C., Hansen, R., and Sadkowiak, B.: Extension of the growing season of phytoplankton in the western Baltic Sea in response to climate change, *Mar. Ecol.-Prog. Ser.*, 622, 1–16, 2019.
- Wu, J.: Wind-stress coefficients over sea surface from breeze to hurricane, *J. Geophys. Res.-Oceans*, 87, 9704–9706, <https://doi.org/10.1029/JC087iC12p09704>, 1982.
- Yurkovskis, A.: Long-term land-based and internal forcing of the nutrient state of the Gulf of Riga (Baltic Sea), *J. Marine Syst.*, 50, 181–197, <https://doi.org/10.1016/j.jmarsys.2004.01.004>, 2004.
- Yurkovskis, A., Wulff, F., Rahm, L., Andruzaitis, A., and Rodriguez-Medina, M.: A Nutrient Budget of the Gulf of Riga; Baltic Sea, *Estuar. Coast. Shelf S.*, 37, 113–127, <https://doi.org/10.1006/ecss.1993.1046>, 1993.
- Zhang, J., Gilbert, D., Gooday, A. J., Levin, L., Naqvi, S. W. A., Middelburg, J. J., Scranton, M., Ekau, W., Peña, A., Dewitte, B., Oguz, T., Monteiro, P. M. S., Urban, E., Rabalais, N. N., Ittekkot, V., Kemp, W. M., Ulloa, O., Elmgren, R., Escobar-Briones, E., and Van der Plas, A. K.: Natural and human-induced hypoxia and consequences for coastal areas: synthesis and future development, *Biogeosciences*, 7, 1443–1467, <https://doi.org/10.5194/bg-7-1443-2010>, 2010.

### **Paper III**

Stoicescu, S-T., Hoikkala, L., Fleming, V., Lips, U, 2023. Continuing long-term expansion of low-oxygen conditions in the Eastern Gulf of Finland. *Oceanologia*, volume, pp. X:X.



# Continuing long-term expansion of low-oxygen conditions in the Eastern Gulf of Finland

Stella-Theresa Stoicescu<sup>1</sup>, Laura Hoikkala<sup>2</sup>, Vivi Fleming<sup>2</sup>, Urmas Lips<sup>1</sup>

<sup>1</sup> Department of Marine Systems, Tallinn University of Technology, Tallinn, 19086, Estonia

<sup>2</sup> Finnish Environment Institute (SYKE), Latokartanonkaari 11, 00790 Helsinki, Finland

## Abstract

To develop an oxygen indicator for the eastern part of the Gulf of Finland (EGOF), a dataset was compiled covering 1900-2021. The analysis revealed a long-term declining trend in dissolved oxygen concentrations in the 40-70 m water layer of  $0.022 \text{ mg L}^{-1} \text{ a}^{-1}$  and multi-decadal variations associated with the observed changes in salinity. About 26% of the long-term decline in oxygen concentrations can be assigned to the decrease in oxygen solubility due to the observed temperature increase. The detected steep decline of oxygen concentrations of  $0.149 \text{ mg L}^{-1} \text{ a}^{-1}$  since 1990 can be explained only by 17% by the temperature-related decrease in oxygen solubility and 22% by the changes in hydrographic conditions. The water volume and bottom area under low oxygen conditions in 2016-2021, characterized by dissolved oxygen concentrations  $\leq 6 \text{ mg L}^{-1}$ , have increased, compared to the selected reference period with almost no human impact in the 1920s-1950s, from  $7.9 \text{ km}^3$  to  $59.4 \text{ km}^3$  (from 2.1% to 16.0% of the EGOF total volume) and from  $1030 \text{ km}^2$  to  $4320 \text{ km}^2$  (from 11.7% to 48.8% of the EGOF total area), respectively. The environmental status of the EGOF was assessed as not good based on the presented oxygen indicator. We conclude that the water volume and bottom area under low oxygen conditions have expanded mostly due to the worsening of the eutrophication status and climate change. Further studies are needed to discriminate between the impacts of the excess load and accumulation of nutrients in the system and temperature-related changes in biogeochemical processes and fluxes.

Keywords: dissolved oxygen, Baltic Sea, Eastern Gulf of Finland, eutrophication, climate change effects

## 1. Introduction

The Baltic Sea is influenced by eutrophication (Kabel et al., 2012) and the changing climate (Conley et al., 2009; Gustafsson et al., 2012). The driving force behind eutrophication is the excess amount of nutrients reaching the marine environment via rivers and the atmosphere (e.g. Reusch et al., 2018). Climate change has affected the seas and will continue to do so in the future, mainly through increased temperature, which decreases oxygen solubility and may accelerate respiration and strengthen stratification (e.g., Bindoff et al., 2019; Oschlies et al., 2018). Stronger stratification hinders vertical mixing, which, together with a prolonged stratified period, could lead to more frequent seasonal oxygen depletion in the near-bottom layer of coastal basins (Stoicescu et al., 2022).

In order to describe and manage the eutrophication related negative anthropogenic effects on the marine environment, Baltic Sea countries have agreed to assess the status of open sea areas, focusing on nutrients, chlorophyll-a levels, cyanobacterial blooms, water transparency, and near-bottom oxygen conditions and/or bottom fauna, according to the MSFD (European Parliament and Council, 2008). The environmental status of coastal waters is assessed under the WFD (European Parliament and Council, 2000), and the outcome relies mainly on the biological quality elements (phytoplankton, bottom flora and fauna). The physical and chemical parameters, e.g. nutrient concentrations, provide only supplementary information. In the frames of the Baltic Marine Environment Protection Commission (HELCOM), open sea and coastal areas are assessed similarly, grouping different indicators into nutrient levels and direct and indirect effects of eutrophication, and compiling an aggregated eutrophication status assessment (HELCOM, 2014, 2018d).

In the previous HELCOM assessment of the state of the Baltic Sea, HOLAS II, covering the years 2011-2016, oxygen conditions were assessed using an oxygen debt indicator applicable in deeper areas where a permanent halocline exists (HELCOM, 2018d). However, this indicator cannot be applied in the shallower eastern Gulf of Finland (EGOF; Fig. 1) due to the absence of the halocline in most of this sub-basin. Subsequently, a new oxygen indicator is needed since the criterion “oxygen conditions” is one of the primary criteria of MSFD descriptor 5 on eutrophication. Recently, different approaches have been suggested and tested (Piehl et al., 2022; Stoicescu et al., 2019), and “shallow-water oxygen indicators” are currently being developed in the frames of HELCOM.

One of the challenges in using oxygen as a status assessment indicator in the EGOF and similar estuarine regions (Codiga et al., 2022; Liblik et al., 2020) is the difficulty to pinpoint the reasons behind the changes in oxygen concentrations. Although the excess amount of nutrient inputs (past and present) is considered to be the main culprit causing oxygen decline in the Baltic Sea, climate change, more specifically, the increase in water temperature and physical circulation are important factors influencing oxygen conditions (Carstensen et al., 2014). The near-bottom oxygen concentrations in the EGOF are also strongly influenced by changes in hydrographic conditions (Alenius et al., 1998).

Due to the lack of major sills on the western border of the Gulf of Finland (GOF), its deep layer is influenced by the deep water from the Northern Baltic Proper (NBP), which among other factors is affected by the Major Baltic Inflows (e.g. Liblik et al., 2018). East-west spread of the more saline, low-oxygen deep water from the NBP depends on temporal variability in the wind pattern (e.g. Alenius et al., 2016; Lehtoranta et al., 2017). Although, there is no permanent halocline in the EGOF, the deep layer is influenced by the spread of saline water from the west, and the surface layer is affected by freshwater input from the river Neva in the east (Alenius et al., 1998). River Neva has the largest discharge to the Baltic Sea (Alenius et al.

al., 1998), and with the nutrient input levels exceeding the set maximum allowable inputs (HELCOM, 2023c), the river load still has strong implications on the health of the EGOF (HELCOM, 2014, 2018d).

The aim of the present study was to analyze the long-term changes in the sub-surface oxygen conditions and the reasons behind these changes in the Eastern Gulf of Finland and to suggest a potential indicator for the eutrophication status assessment. The data series are examined to reveal the long-term trends, interannual variations, and relationships between the changes in oxygen concentrations and hydrographic variables (temperature and salinity) and nutrient load. To address primarily the anthropogenic factors causing the decline in oxygen concentrations, we introduce a method to reduce the hydrography effects related to advection in the deep layer, which could be evaluated based on salinity measured simultaneously with oxygen. We also estimate the probable decrease in oxygen concentrations caused by the temperature increase and assess the extent of its influence.

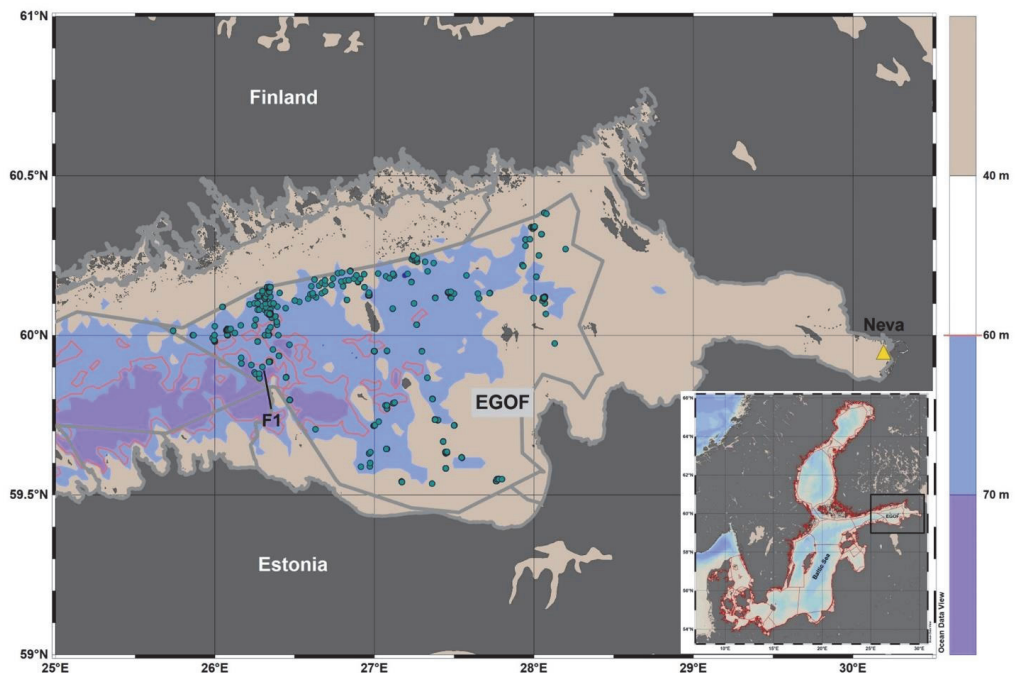


Figure 1. Study area – Eastern Gulf of Finland (EGOF). Location of monitoring stations used in analysis are indicated by blue dots, Neva river mouth by the yellow triangle, and HELCOM sub-basin division lines by the gray lines, including open sea and coastal area division. Light blue area defines the bottom depth range of 40-70 m. Orange line defines the 60 m depth contour.

## 2. Material and methods

### 2.1. Core data set

All available data on oxygen concentrations, temperature and salinity in the eastern part of the Gulf of Finland (the area is shown in Fig. 1) were pooled from ICES, Finnish Environment Institute's national database Hertta ([http://www.syke.fi/en-US/Open\\_information](http://www.syke.fi/en-US/Open_information), in Finnish), Gulf of Finland Year database, CTD oxygen data from stations in the national monitoring program from Finnish Meteorological Institute, and Estonian environmental database (KESE). After removing duplicates, a core dataset was compiled for further analysis. The data are available from 1900, resulting in almost 1500 profiles (station locations are shown in Fig. 1 and data availability in Fig. 2), but more consistent data with multiple profiles per season and at least three depths per profile are available since the late 1950s.

We used all available data regardless of the analysis method. Most of the earlier oxygen concentrations were determined by the Winkler method. Recent data are partly obtained using electrochemical sensors or analyzers, but the relevant HELCOM guidelines (HELCOM, 2018c) are followed. We did not incorporate data on hydrogen sulfide concentration since these were not available for the first half of the 20<sup>th</sup> century.

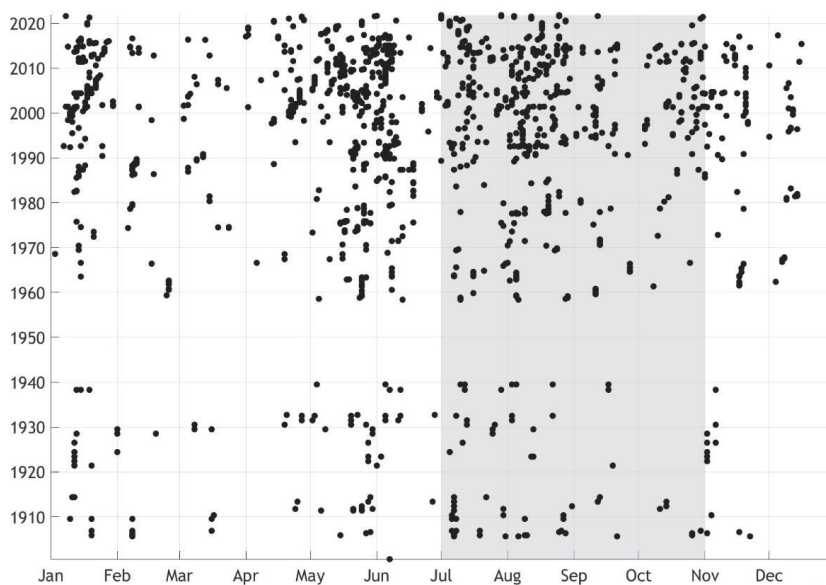


Figure 2. Availability of data used in the analysis in the EGOF area (x-axis: month, y-axis: year). Each dot represents one unique profile. The grey area indicates the months July–October, from where the data are used for the analysis and indicator calculation.

## 2.2. Long-term trends and oxygen-salinity and oxygen-temperature relationships

Long-term trends in oxygen concentrations, temperature and salinity are estimated for the entire period with available data since the early 1900s and for selected shorter periods with certain visible tendencies. As the minimum near-bottom dissolved oxygen (DO) concentrations in the Baltic Sea basins without the permanent halocline are observed in late summer–early autumn (Piehl et al., 2022; Stoicescu et al., 2022), we focused our analysis on July–October data (Fig. 2). The trends are analyzed for the depth groups with an interval of 5 m and three layers, representing the surface layer (0–20 m), the layer just below the summer thermocline (20–40 m) and the deep layer (40–70 m) where seasonal low-oxygen conditions occur.

Earlier studies (Lehtoranta et al., 2016, 2017; Lips et al., 2017; Stoicescu et al., 2019) have shown that deep-layer oxygen concentration and salinity are negatively correlated in the Gulf of Finland. This negative relationship holds because the vertical gradients of salinity and oxygen are opposite and oxygen concentrations in the saltier inflowing deep water are lower than those in the less saline inflowing water. Lips et al., (2017) have suggested that according to the estuarine parameter space introduced by Geyer and MacCready (2014), the Gulf of Finland is a stratified estuary but could correspond to a partially stratified estuary depending on the prevailing forcing. High river discharge, occurrence of Major Baltic Inflows and calm weather conditions (or prevailing north-easterly winds) strengthen vertical stratification. In contrast, low river discharge, low inflow activity and prevailing strong westerlies alter the hydrographic conditions towards a partially stratified estuary. Since corresponding changes in estuarine circulation alter the salinity distribution (Elken et al., 2003; Liblik and Lips, 2011; Lips et al., 2008), we suggest to use deep-layer salinity as a proxy of prevailing hydrographic conditions.

We found linear regressions between the annual average July–October oxygen concentration and salinity for the defined depths and layers to estimate the effects of changing hydrography on oxygen conditions. Uncertainties of using a linear relationship are evaluated.

To estimate the effect of climate change on dissolved oxygen concentrations, we analyzed the changes in oxygen solubility and will discuss other temperature-related processes influencing oxygen conditions. Oxygen saturation concentrations were estimated according to TEOS-10 (IOC et al., 2010). This analysis allows us to estimate how much the observed oxygen concentrations and their long-term trends were affected by the decrease in saturation concentration.

## 2.3. Defining the extent of low-oxygen waters

To estimate the basin bottom area and volume affected by low-oxygen conditions, we chose dissolved oxygen concentration of  $6.0 \text{ mg L}^{-1}$  as a limit. This concentration is considered to be a threshold value where approximately 75% of fish will experience stress caused by low oxygen conditions (Vaquer-Sunyer and Duarte, 2008). Baltic bottom fauna has been found sensitive to oxygen concentrations below  $4.6 \text{ mg L}^{-1}$  (Norkko et al., 2015). It has been suggested as a precautionary limit, which would maintain all but the most sensitive species (Vaquer-Sunyer and Duarte, 2008). However, since such low concentrations do not occur at all open sea stations in the EGOF area yearly, the former ( $6 \text{ mg L}^{-1}$ ) was selected as the threshold for the volume estimation.

A challenge for finding a characteristic depth of DO isoline  $6 \text{ mg L}^{-1}$  in the entire assessment area and period is the temporally and spatially sparse data. We used station data with at least 3 measured depths



and interpolated oxygen concentrations on 5-meter step profiles using a second-degree polynomial fit. As the next step, all profiles from July-October of the selected assessment period (e.g. 6 years) were used to compile the characteristic/average oxygen profile from the sea surface to the maximum depth of 106 m. The third-order polynomial fit was chosen for this since it best followed the common oxygen profile in the study area and period with the existing seasonal thermocline. The same method was used to construct average salinity profiles. If DO concentrations estimated by this method remained above 6 mg L<sup>-1</sup> in the entire water column, as it was found for the period of weak stratification from the mid-1980s to the mid-1990s, the maximum depth in the area and the volume and bottom area equal to zero were used as the respective estimates.

To calculate the area and volume of the low-oxygen bottom water, the hypsographic curve constructed for the EGOF based on EMODnet bathymetry data (<https://portal.emodnet-bathymetry.eu/>) and an assumption that isosurface 6 mg L<sup>-1</sup> is a horizontal plane were applied.

The earliest available data, prior to 1926, were obtained at a very few stations – 11 stations/sampling sites/events altogether. Because of the low number of available profiles in the beginning of the 1900s, we proposed a later period – 1926 to 1960, as a period with no or low human-induced impact (the reference period).

#### 2.4. Adjusting indicator results to the changes in hydrographic conditions

The changes in hydrographic conditions affecting oxygen conditions, as the movement of saltier and less oxygenated waters along the GOF axis and vertical stratification strength, are assessed based on salinity in the 40-70 m water layer. The suggested oxygen correction is applied in relation to the average salinity in the reference period. Salinity adjusted oxygen concentration profile was calculated by adding a correction to the measured oxygen value (Eq. 1). The correction was equal to the difference between the annual (July-October) average salinity at the depths of 40-70 m and this depth group specific reference period salinity multiplied by the slope of the linear model defined by the ordinary least squares (OLS) method, as

$$O_{2\text{ adjusted}} = O_{2\text{ measured}} + slope_g * (S_{ref} - S) \quad (1)$$

where  $O_{2\text{ measured}}$  is measured oxygen in mg L<sup>-1</sup>,  $slope_g$  is the slope of the linear model,  $S_{ref}$  is the average salinity in the reference period (1926-1960), and  $S$  is measured salinity. All salinity values in the present paper are given according to the Practical Salinity Scale 1978 as stored in the databases. Although dimensionless, we present salinity in the graphs and text in units [psu].

Correcting oxygen to salinity gives higher adjusted DO values (compared to measured DO) when the average measured salinity is higher than the depth group's average salinity in the reference period. Higher adjusted DO values, compared to measured DO, move the isoline DO = 6 mg L<sup>-1</sup> deeper in the water column, resulting in a smaller adjusted area and volume of low-oxygen waters. Thus, the applied method allows us to reduce the hydrographic (natural) impacts from the indicator results.

### 3. Results

#### 3.1. Long-term trends in near-bottom oxygen, salinity and temperature

The deep-layer (40-70 m) oxygen concentrations in the EGOF in July-October show a declining long-term trend of  $-0.22 \text{ mg L}^{-1}$  per decade ( $n = 71$ ,  $R^2 = 0.12$ ,  $p < 0.05$ ; Fig. 3 and Table 1), and the total decrease in oxygen concentrations by  $-2.53 \text{ mg L}^{-1}$  for 1905-2021. A steeper decline of  $-1.49 \text{ mg L}^{-1}$  per decade is revealed from 1990-2021 ( $n = 31$ ,  $R^2 = 0.44$ ,  $p < 0.05$ ). The analysis did not include the hydrogen sulfide data due to the lack of earlier measurements. However,  $\text{H}_2\text{S}$  can rarely occur at depths of 40-70 m. The average  $\text{H}_2\text{S}$  concentration at 77-80 m depth at station F1 in July-October 2014-2021 was  $0.1 \text{ mg L}^{-1}$ , and the maximum concentration observed was  $1.1 \text{ mg L}^{-1}$ .

A significant positive trend in temperature of  $0.18 \text{ }^\circ\text{C}$  per decade is detected based on July-October data from 40-70 m layer for 1905-2021 ( $n = 70$ ,  $R^2 = 0.29$ ,  $p < 0.05$ ), which is especially steep in the last three decades ( $0.73 \text{ }^\circ\text{C}$  per decade,  $n = 30$ ,  $R^2 = 0.44$ ,  $p < 0.05$ ; see Fig. 3). The long-term increase in temperature in the surface layer was larger ( $0.25 \text{ }^\circ\text{C}$  per decade) than in the deep layer, while the trend was insignificant in the surface layer in the last three decades. Note that the effect of the temperature increase on density (decrease) is much larger in the surface layer than in the deep layer. For instance, if the surface layer temperature increased from  $13$  to  $16 \text{ }^\circ\text{C}$  at salinities of about  $5 \text{ g kg}^{-1}$ , the density decrease would be  $0.43 \text{ kg m}^{-3}$ . If a similar increase in temperature ( $3 \text{ }^\circ\text{C}$ ) occurred in the deep layer, e.g. from  $2$  to  $5 \text{ }^\circ\text{C}$  (at characteristic salinities of  $7 \text{ g kg}^{-1}$ ), the density decrease would be as low as  $0.04 \text{ kg m}^{-3}$ .

The near-bottom salinity does not have a significant long-term trend; however, periods with decreasing (in the 1980s and early 1990s) and increasing (from the beginning of 1990s to nowadays) salinities can be observed (Fig. 3). These periods are associated with distinct changes in oxygen conditions – a decrease in salinity corresponds to an increase in oxygen values, and *vice versa* (Figs. 3-4). Since the observed lower salinities in the deep layer coincided with the slightly higher sea surface salinities in the 1980s – the early 1990s compared to the periods before and after, vertical stratification of the water column was significantly weaker during this period.

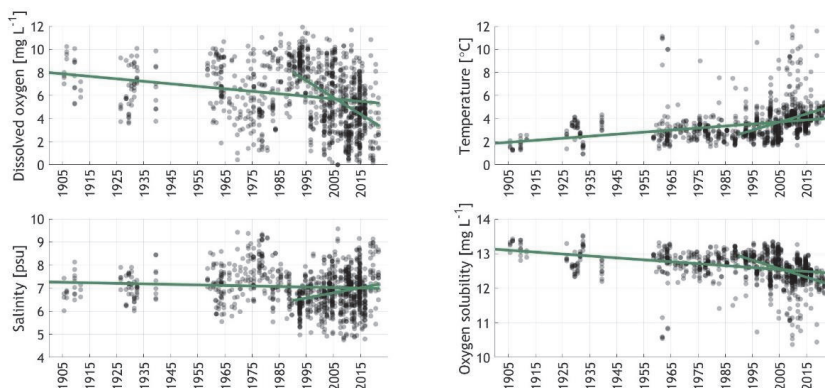


Figure 3. Annual average oxygen (top left), salinity (bottom left), temperature (top right), and oxygen solubility (bottom right) values from 40-70 m layer in the Eastern Gulf of Finland in July-October of 1905-2021.

The long-term trends of DO and oxygen solubility indicate that oxygen has decreased in the surface layer mostly due to reduced solubility (Table 1). In the middle and deep layers, the change in solubility has a smaller influence on the DO decrease – oxygen saturation concentrations decreased slightly less than in the surface layer since the temperature increase in deeper layers was also smaller than in the surface layer. However, more importantly, the negative trend in DO in deeper layers was significantly larger than that near the sea surface. During the last 30 years, DO concentrations have been declining in the deep layer seven times faster than the 100-year average trend, while the trend in oxygen solubility was five times larger than the 100-year average trend (Table 1).

Table 1. Long-term linear trends of July-October dissolved oxygen (DO) concentration, salinity (SP), temperature (TEM) and oxygen solubility (OSOL) in three selected depth groups in the eastern Gulf of Finland. Bold numbers indicate p-value less than significance level (0.05).

Depth range (m)	1900-2021				1990-2021			
	DO mg L <sup>-1</sup> a <sup>-1</sup>	SP psu a <sup>-1</sup>	TEM °C a <sup>-1</sup>	OSOL mg L <sup>-1</sup> a <sup>-1</sup>	DO mg L <sup>-1</sup> a <sup>-1</sup>	SP psu a <sup>-1</sup>	TEM °C a <sup>-1</sup>	OSOL mg L <sup>-1</sup> a <sup>-1</sup>
0-20	-0.004	0.000	<b>0.025</b>	<b>-0.006</b>	0.008	0.006	0.018	-0.005
20-40	<b>-0.022</b>	0.002	0.011	-0.003	<b>-0.052</b>	-0.009	<b>0.098</b>	<b>-0.027</b>
40-70	<b>-0.022</b>	-0.002	<b>0.018</b>	<b>-0.006</b>	<b>-0.149</b>	<b>0.023</b>	<b>0.073</b>	<b>-0.026</b>

Table 2. Parameters of linear regression between salinity (SP) and dissolved oxygen (DO), and temperature (TEM) and dissolved oxygen (DO) in three selected depth groups in the eastern Gulf of Finland in July-October 1905-2021. All correlations are significant – p-values were below 0.001.

Depth range (m)	SP vs DO			TEM vs DO		
	R <sup>2</sup>	n	Slope estimate mg L <sup>-1</sup> psu <sup>-1</sup>	R <sup>2</sup>	n	Slope estimate mg L <sup>-1</sup> °C <sup>-1</sup>
0-20	0.13	71	0.49	0.19	71	-0.14
20-40	0.01	71	-0.17	0.02	71	-0.06
40-70	0.21	70	-1.42	0.31	70	-1.04

The strongest linear correlations between salinity/temperature and oxygen in the selected three layers was found in the 40-70 m layer (Table 2). The correlations were all significant (p-value less than 0.001). Based on the found significant correlation of oxygen with salinity in the 40-70 m layer, we suggested to use the linear relationship between oxygen and salinity to reduce the effect of changing hydrographic conditions when assessing the human-induced impact on oxygen conditions. The found slope of the regression line between oxygen and salinity was -1.42 mg L<sup>-1</sup> psu<sup>-1</sup> (Table 2), and the limits of its 95% confidence interval were -2.08 mg L<sup>-1</sup> psu<sup>-1</sup> and -0.76 mg L<sup>-1</sup> psu<sup>-1</sup> (Fig. 4).

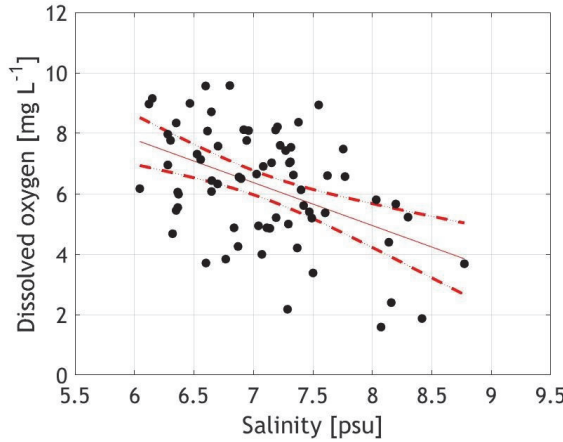


Figure 4. Scatter plot and linear regression line between salinity and oxygen in 40-70 m layer in the Eastern Gulf of Finland in July-October 1905-2021. Regression line is shown in a red solid line; red dashed lines indicate the ranges of the 95% confidence level.

### 3.2. Defining the extent of low-oxygen waters

To define the bottom area and volume of low-oxygen waters, we looked for the six-year average  $\text{DO} = 6 \text{ mg L}^{-1}$  isoline depth in July-October. To assess the status, we compared the estimated area and volume with the threshold values, indicating good environmental status (GES) derived based on the conditions in the reference period from 1926 to 1960, exemplifying a time with no/low human influence. The reference period  $\text{DO} = 6 \text{ mg L}^{-1}$  isoline depth was 63.2 meters, and the average area and volume estimates were  $1030 \text{ km}^2$  or 11.7% and  $7.9 \text{ km}^3$  or 2.1% of the total area and volume, respectively.

A threshold value, corresponding to good environmental status (GES), can be set by defining the allowable deviation from the reference state. Usually, the acceptable deviation from the reference value of 50% is used to define the threshold (HELCOM, 2013). We propose that the volume of water with oxygen concentrations below  $6 \text{ mg L}^{-1}$ , corresponding to GES, equals at least the two-fold reference volume since the initial volume was very small. The applied acceptable deviation of 100% yields the GES volume of waters with  $\text{DO} \leq 6 \text{ mg L}^{-1}$  of  $15.9 \text{ km}^3$  or 4.3% of the total EGOF volume. This GES volume is defined by the  $6 \text{ mg L}^{-1}$  isoline depth at 57.2 meters. Another option is to define the GES as a 50% increase in the area of low-oxygen waters compared to the reference period, which would set the  $6 \text{ mg L}^{-1}$  isoline depth at 58.3 meters ( $1550 \text{ km}^2$  or 17.5% of the total area and  $14.1 \text{ km}^3$  or 3.8% of the total volume). These different GES options, together with the hypsographic curve of the EGOF area, are presented in Fig. 5.

To reduce the hydrography effects on the status assessment, we adjusted measured oxygen values considering the 40-70 m layer differences between the average salinities in the assessment period and the reference period. This introduced method can be used since there was almost no long-term trend in salinity but a relatively high correlation between simultaneously measured oxygen content and salinity in the same depth range (see Table 2 and Fig. 4).

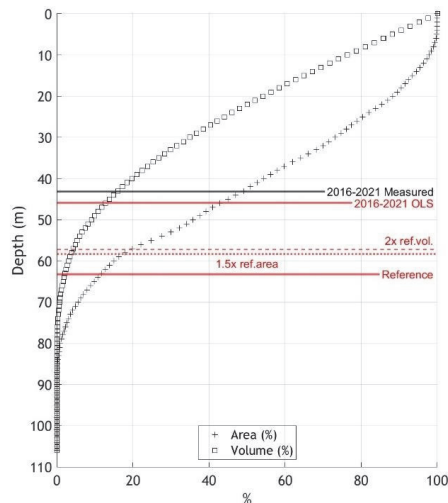


Figure 5. Hypsographic curves – area and volume – of the Eastern Gulf of Finland. Extent of low oxygen ( $\text{DO} \leq 6 \text{ mg L}^{-1}$ ) waters during the reference period, with possible GES options, based on reference period area and volume estimates and introduced maximum allowable deviations (either 50% or 100% of the reference value, respectively). The latest assessment period 2016-2021 estimates are shown based on monitoring data (black; 2016-2021 Measured) and monitoring data adjusted by the suggested method for reducing the impact of changing hydrographic conditions (red; 2016-2021 OLS).

Applying the suggested method of reducing the hydrography effects resulted in higher adjusted DO values than the observed concentrations during the periods when 40-70 m mean salinity was higher than during the reference period, e.g. in the 1970s and the early 1980s (Fig. 6, upper panel). During the period of low salinities and decreased stratification from the mid-1980s to the mid-1990s, the adjusted DO values were decreased by the applied method. Reducing the effect of the increasing salinity from the beginning of the 1990s to the present flattened the trend or even reversed it in the adjusted DO time series since 2010.

In accordance with the described adjustment of DO values, during the period with higher salinities, peaking in the 1970s, the  $6 \text{ mg L}^{-1}$  isoline depth of adjusted oxygen went deeper (Fig. 6, upper panel). The same effect of the adjustment applies for the most recent period with observed higher sub-surface salinities in the EGOF. As a result, from the mid-1990s to the present, when salinity has been increasing and DO simultaneously decreasing, the adjustment slowed down the rise of the  $\text{DO} = 6 \text{ mg L}^{-1}$  isoline and the tendency has reversed after 2010.

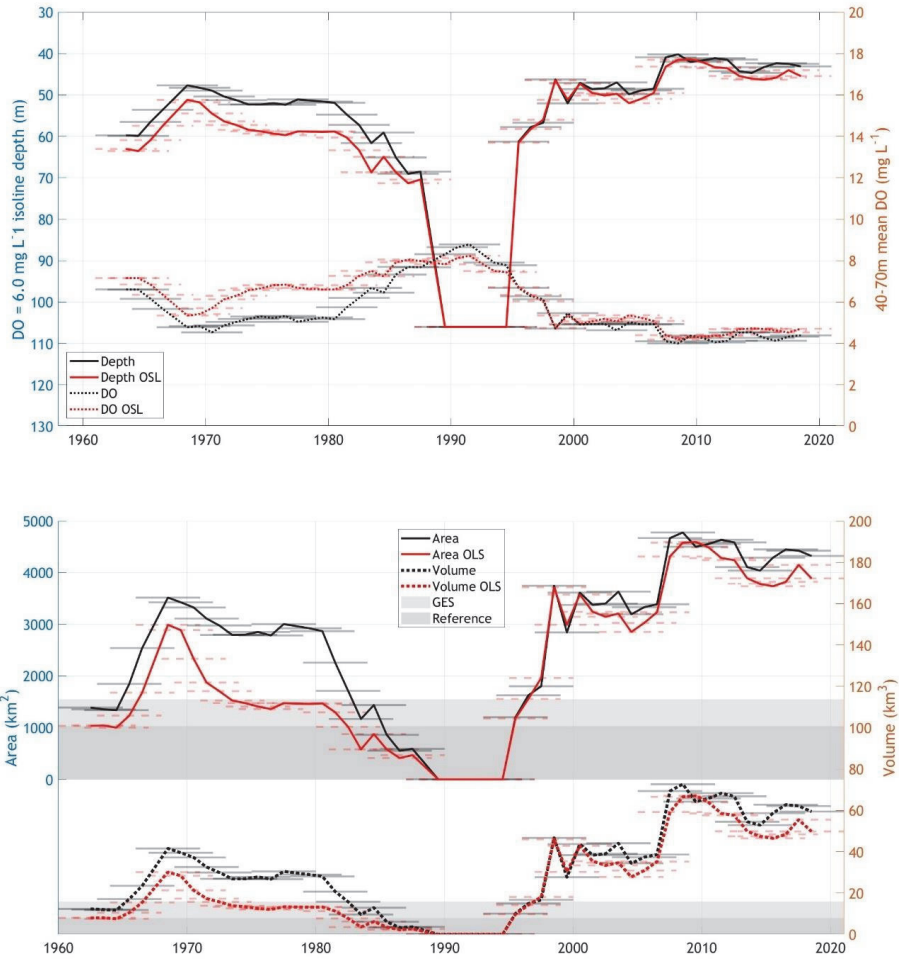


Figure 6. Upper panel: Six-year average DO concentrations in the 40-70 m layer (dotted lines) and DO = 6 mg L<sup>-1</sup> isoline depths (solid lines). Lower panel: Six-year average area of bottoms (solid lines) and volume of waters (dotted lines) with DO ≤ 6 mg L<sup>-1</sup> estimates. Darker gray denotes the area representing reference period conditions, derived from the reference period mean isoline depth. The entire gray area denotes good environmental status conditions, which are achieved with a 50% deviation from the reference period area and with a 100% deviation from the reference period volume estimates, respectively. Results based on measured data are shown in black and based on adjusted data in red.

Fig. 6 lower panel demonstrates how the introduced indicators, either based on water volume or bottom area with DO ≤ 6 mg L<sup>-1</sup>, have changed during the last 60 years. The temporal development of indicator values is similar and agrees with the changes in deep-layer oxygen concentrations and the changes in the isoline 6.0 mg L<sup>-1</sup> depth described above. It is interesting that the adjustment of oxygen values due to

changes in hydrographic conditions resulted in assessment results corresponding to GES in the 1970s but not during the last 20 years, although the adjustment moved the values towards the GES threshold. The assessed status corresponded to GES for the period of low deep-layer salinities and weak stratification in the late 1980s and early 1990s. This outcome and the noticed elevated values of the indicator a few years after every known Major Baltic Inflow (after 1993 and 2003, as well as after 2014, but the signal was less pronounced; see Fig. 6) will be discussed later in the paper.

The average volume of waters with  $\text{DO} < 6.0 \text{ mg L}^{-1}$  in 2016-2021 (matching the present HELCOM assessment period) without salinity adjustment was  $59.4 \text{ km}^3$  or 16.0 % of the EGOF total volume and bottom area  $4320 \text{ km}^2$  or 48.8 % of the EGOF total area – the  $6.0 \text{ mg L}^{-1}$  isoline depth was 43.1 m (Fig. 5). When adjusting DO values to salinity using the suggested method, the estimates decreased to  $49.8 \text{ km}^3$  or to 13.4 % of the volume and area to  $3890 \text{ km}^2$  or to 43.9 % of the bottom area (isoline depth was 45.5 m). These changes in the estimates are caused by the difference of 0.06 psu in average salinity in 2016-2021 and the reference period (1926-1960) in the 40-70 m layer, although the long-term trend in deep-layer salinity was almost absent (Fig. 2).

The increase in the extent of the low-oxygen waters in the EGOF compared to the period with no or low human impact before 1960 is well demonstrated in Fig. 7. The area and volume of waters with  $\text{DO} < 6 \text{ mg L}^{-1}$  has increased from  $1030 \text{ km}^2$  to  $4320 \text{ km}^2$  (from 11.7 % to 48.8 % of the total area) and from  $7.9 \text{ km}^3$  to  $59.4 \text{ km}^3$  (from 2.1 % to 16.0 % of the total volume). Adjusting oxygen to salinity decreases the estimated low-oxygen area, meaning that the hydrography effects were at least partly removed from the estimate. Thus, the differences left in the estimates for the reference and assessment periods could mostly be explained by the effects of climate change related temperature increase and eutrophication.

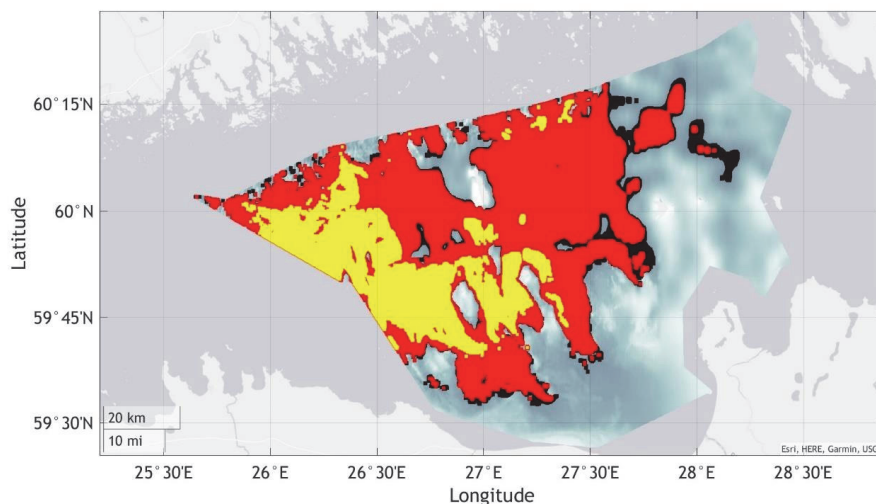


Figure 7. Extent of low oxygen ( $\text{DO} \leq 6 \text{ mg L}^{-1}$ ) water during the reference period (yellow) and the latest assessment period 2016-2021. The estimate based on monitoring data includes the black, red and yellow areas, monitoring data adjusted with the suggested method the red and yellow areas.

### 3.3. Impacts of different factors on long-term changes in oxygen conditions

The long-term trends in dissolved oxygen concentration and oxygen solubility were practically the same in the 0-20m layer of the EGOF in 1900-2021 (Table 1). It proves that the oxygen solubility change induced by the temperature increase dominated the DO decrease in the surface layer. In the deep layer (40-70 m), oxygen concentrations decreased four times faster than oxygen solubility. The respective trends were  $-0.022 \text{ mg L}^{-1} \text{ a}^{-1}$  and  $-0.006 \text{ mg L}^{-1} \text{ a}^{-1}$ , indicating that the decrease in saturation concentrations due to the temperature increase could have caused about 26% of the deep-layer DO decrease from 1900-2021.

DO solubility trend for the last 30 years was over four times ( $-0.026 \text{ mg L}^{-1} \text{ a}^{-1}$ ) of the long-term trend ( $-0.006 \text{ mg L}^{-1} \text{ a}^{-1}$ ), but the share of the DO solubility influence on the declining DO conditions has been smaller ( $\sim 17\%$  of the DO trend of  $-0.149 \text{ mg L}^{-1} \text{ a}^{-1}$  in 1990-2021). For this period with a clear salinity trend, the change in hydrographic conditions could have caused 22% (12-32 %) of the oxygen decline. This estimate ( $0.032 \text{ mg L}^{-1} \text{ a}^{-1}$ ) is obtained by multiplying the detected salinity trend ( $0.023 \text{ psu a}^{-1}$ ; see Table 1) with the respective linear regression slope estimate ( $-1.42 \text{ mg L}^{-1} \text{ psu}^{-1}$ ; see Table 2).

Among all the possible effects of the temperature increase on oxygen conditions, we accounted only for the decrease in oxygen solubility when the temperature rises. It has been suggested that the change in saturation concentration could cause only 25% of the deterioration in near-bottom oxygen conditions due to temperature increase (Bendtsen and Hansen, 2013), and other effects, e.g. increased respiration rates, are more important than the solubility decrease impact. Since the solubility change is steeper in low temperatures than in warmer waters (e.g., Tian et al., 2022), we used a conservative assumption that the other temperature-related effects are of similar value to the solubility decrease. The estimated proportions of solubility decrease were 26% for 1900-2021 and 17% for 1990-2021, and the effect of the salinity increase on DO conditions was  $\sim 0\%$  for 1900-2021 since the trend was practically absent, and 12-32% for 1990-2021. Applying our assumption leads to the estimates that about 48% of the oxygen decline in 1900-2021 ( $-0.022 \text{ mg L}^{-1} \text{ a}^{-1}$ ) and  $\sim 44\%$  (34-54%) in 1990-2021 ( $-0.149 \text{ mg L}^{-1} \text{ a}^{-1}$ ) occurred due to factors other than changes in hydrography and temperature. We can conclude that the relative scale of other factors (e.g. eutrophication) influencing oxygen conditions has remained roughly the same when comparing the long term and the recent 30 years.

Based on the HELCOM core indicator 'Input of nutrients', the input of nitrogen and phosphorus has decreased by 17% and 49%, respectively, in 2020 compared to the reference period of 1997-2003 (HELCOM, 2023c). This result could suggest a potential improvement in environmental conditions, including near-bottom oxygen concentrations (HELCOM, 2023c).



## 4. Discussion

Eutrophic conditions with the accompanying decline in oxygen concentrations have been observed and are under concern in many coastal systems around the world, including the Baltic Sea (e.g. Carstensen et al., 2014; Conley et al., 2009). Long-term monitoring data since the beginning of the 1900s revealed a statistically significant decreasing trend in deep-layer (40–70 m) oxygen values in the eastern Gulf of Finland ( $0.22 \text{ mg L}^{-1}$  per decade). This trend could be related to the anthropogenic impact either via the increase in nutrient loads (Carstensen et al., 2014) or climate change (Caballero-Alfonso et al., 2015). The hydrogen sulfide data was not used in the analysis, but we suggest that adding them would increase the detected long-term negative trend in this relatively shallow sea area only slightly.

The significant trend in deep layer temperature of  $0.18 \text{ }^{\circ}\text{C}$  per decade for July–October 1905–2021 and a steeper trend of  $0.73 \text{ }^{\circ}\text{C}$  per decade in the last 30 years agree with the earlier analyses of deep-water temperature changes in the Baltic Sea (e.g. Dutheil et al., 2022; Liblik and Lips, 2019). Dutheil et al. (2022) reported a temperature increase in 1850–2008 in the bottom and intermediate layer of the Baltic Sea of  $>0.04 \text{ }^{\circ}\text{C}$  per decade and  $<0.04 \text{ }^{\circ}\text{C}$  per decade, respectively, while Liblik and Lips (2019) estimated the trends in the ranges of  $0.35$ – $0.6 \text{ }^{\circ}\text{C}$  per decade in the central Gulf of Finland (layer below 50 m) in 1982–2016. In a more recent analysis, Kankaanpää et al. (2023) reported that the near-bottom temperature increased in the deeper areas of the EGOF by  $0.60 \text{ }^{\circ}\text{C}$  per decade in 1960–2021 and  $0.70 \text{ }^{\circ}\text{C}$  per decade in 1994–2021. Thus, the trend estimates depend on the period under investigation, but a steeper increase in water temperature in the last 30–35 years is a common conclusion. Similar fast warming of waters in recent decades has been observed in other estuarine regions, such as the Chesapeake Bay (Du et al., 2018).

Our results show that in the long term, the warming of the surface layer was larger than the deep layer. However, even if the magnitude of the temperature increase is the same, the effect on the density decrease would be much larger in the surface layer than in the deep layer because a temperature increase at low temperatures (close to the temperature of maximum density) causes a very modest density decrease. Thus, in the brackish sea areas with the seasonal thermocline, the observed water temperature increase has strengthened vertical stratification.

The near-bottom salinity revealed a very weak long-term trend, but an oscillatory nature of the changes is observed. Such decadal-scale fluctuations in hydrographic conditions (Meier et al., 2019; Schimanke and Meier, 2016) would play an important role in changes in oxygen conditions. In the Gulf of Finland, this variability could be interpreted as an influence of the lateral (longitudinal) movements of the deep layer, as described by, e.g., Alenius et al. (2016) and Lehtoranta et al. (2017). The decline in deep-layer salinities in the Baltic Sea from the 1960s/70s to the 1990s has been related to the positive trend in the NAO index in the same time period (Meier et al., 2022). The positive NAO trend means that the Baltic Sea region is influenced by stronger westerlies, which in the GOF/EGOF forces the saltier/low-oxygen deep layer to more westerly positions. From the mid-1990s to the early 2010s, the NAO index has shown a negative tendency (Meier et al., 2022), coinciding with the observed salinity increase during the last 30–35 years in the Baltic Sea deep basins (Liblik and Lips, 2019) and the EGOF deep layer shown in this study.

We developed a method to reduce the impact of changes in hydrography from the indicator assessment. The proposed adjustment of oxygen concentrations to changes in salinity decreases the interannual variability of the low-oxygen area/volume in the EGOF (as seen in Fig. 6). This result and previous studies (e.g. Liblik et al., 2013; Lips et al., 2017; Stoicescu et al., 2019) demonstrate that low oxygen conditions in

the GOF area are strongly influenced by lateral deep-water advection. However, deep-layer salinity also correlates strongly with stratification strength that controls vertical oxygen ventilation, thus contributing to the extent of oxygen deficiency (Lehtoranta et al., 2017; Liblik and Lips, 2019). Since the suggested method assumed a linear correlation between oxygen and salinity while the relationship could be non-linear, e.g., in the case of considerable weakening (or even collapsing) of vertical stratification, it does not remove the potential hydrographic effects completely. This incomplete adjustment is well seen in Fig. 6 for a weakly stratified period from the mid-1980s to the mid-1990s (Liblik and Lips, 2011).

For this period, the vertical gradient of oxygen in the sub-surface layer was very small, and extrapolation of it towards the seabed, even if the salinity adjustment was applied, did not reveal DO values below 6 mg L<sup>-1</sup>. We conclude that in the case of very weak stratification, the vertical mixing is intense enough to mask the eutrophication effects in the near-bottom layer – vertical oxygen fluxes prevail over near-bottom oxygen consumption even in the presence of relatively high consumption rates. Since the weakening of stratification also occurred in the western and central Gulf of Finland (Liblik and Lips, 2011), likely more intense vertical mixing resulted in more oxygen in the deep-layer water reaching the EGOF. These conditions occurred in the case of the long-term absence of Major Baltic Inflows and prevailing stronger westerlies (positive NAO index) that forced the stratified Gulf of Finland towards a partially stratified estuary (Lips et al., 2017).

A statistically significant increase in the surface-layer and deep-layer temperature in the last 100+ years affected the oxygen conditions in the deep layer, as the increasing water temperature decreases oxygen solubility (e.g. Carstensen et al., 2014). We estimated that the decrease in DO solubility explains 26% of the oxygen decline in long-term (100+ years) and 17% from 1990 to 2021. Besides the change in oxygen solubility, temperature increase also affects the consumption and degradation processes by increasing metabolism rates and enhancing respiration rates, which in turn reduce oxygen in water (Boesch et al., 2007; Rabalais et al., 2009). For the Bothnian Sea, it was estimated that the observed 0.78 °C increase in deep water temperature from 1992 to 2012 could have led to a 29 % increase in respiration rate (Ahlgren et al., 2017). Meier et al. (2018) have suggested that deep-water oxygen depletion has been aggravated in the Gulf of Finland in recent years due to an increase in zooplankton biomass, which enhances the oxygen respiration of zooplankton and higher trophic levels, decreasing the effectiveness of natural deep-water ventilation.

A modeling experiment by Bendtsen and Hansen (2013) suggested that in the case of an increase of deep-water temperature by 3 °C about 25 % of the predicted decrease in bottom water oxygen concentration in the North Sea-Baltic Sea transition zone could be assigned to the decreased solubility. Tian et al. (2022) simulated the near-bottom oxygen conditions in the Chesapeake Bay for 1995-2025 and reported that the change in DO solubility contributed 55% of the total climate warming effect, biological rates 33%, and strengthening of stratification 11%. Our very rough assumption that about 50% of the temperature increase effects could be assigned to the solubility decrease leads to the estimates that 48% of the oxygen decline in 1900-2021 and 44% in 1990-2021 occurred due to factors other than changes in hydrography and temperature. We can conclude that the relative scale of other factors (mostly eutrophication) influencing oxygen conditions has remained roughly the same. An explanation of this continuing expansion of low-oxygen conditions could be a very long time-lag between the reduction of loads and positive effects in the marine environment, as suggested, e.g. by Lønborg and Markager (2021).

For managing the human influence on marine ecosystems, in regards to eutrophication, an oxygen indicator, characterizing the indirect effects of excess nutrient inputs, has been missing in the relatively shallow open sea areas of the Baltic sea (HELCOM, 2018d). We have developed an indicator and, using data from the reference period (1926-1960), proposed a reference and GES value for the volume of low-oxygen waters in the EGOF. If applying a  $DO = 6.0 \text{ mg L}^{-1}$  isoline as the boundary of low-oxygen waters, the suggested reference and GES threshold values correspond to 2.1 % and 4.3 % of the total EGOF volume, respectively. The assumptions made involve some uncertainties due to the limited data availability from the reference period and subjective decisions regarding an allowable deviation from the reference state. We based our estimate of reference conditions on data from 1926-1960, as also for a developed shallow water oxygen indicator in the southern Baltic Sea, the desirable reference period before the 1960s was indicated (Piehl et al., 2022).

Applying the proposed indicator and threshold for the 2016-2021 assessment period shows that good environmental status has not been achieved regarding oxygen conditions in the eastern Gulf of Finland. This result agrees with the higher than maximum allowable inputs of nitrogen and phosphorus to the GOF (HELCOM, 2023c). However, the estimated expansion of the low-oxygen waters in the EGOF despite the observed significant decrease in nutrient loads in the recent 20-30 years (HELCOM, 2023c) has to be analyzed in more detail. The latter is also influenced by the internal loading of phosphorus, the so-called vicious cycle, which influences the decline in oxygen conditions, through providing additional nutrients to the productive zone (Vahtera et al., 2007). The retention of phosphorus in the sediments and import of phosphorus from the Baltic Proper vary with changes in winter wind forcing (Liblik et al., 2013; Lips et al., 2017), masking the notable reductions in phosphorus loading to the gulf (Lehtoranta et al., 2017). We conclude that even when the nutrient inputs would achieve the HELCOM Baltic Sea Action Plan targets (nutrient input ceilings; see HELCOM, 2021), no improvement in the water quality would be expected anytime soon due to the exceptionally long time scale of eutrophication in the stratified and enclosed Baltic Sea (Gustafsson et al., 2012). Although nutrient loads are at present significantly higher than they were at the beginning of the 20<sup>th</sup> century (Savchuk et al., 2008), which could be the main reason for nowadays near-bottom oxygen deficiency, the loads have decreased in the last 20-30 years (HELCOM, 2023c), but the oxygen conditions have not improved yet.

Considering the overall eutrophication status assessment, then this indicator targets the anthropogenic effects on oxygen conditions, and it is not directly related to the oxygen levels critical to the benthic communities. Therefore, the indicator will be applied along with an indicator of the status of the benthic macrofauna (HELCOM, 2018d), to take into account the ecological effects of the oxygen conditions. The prerequisite for this is that eutrophication is the main pressure affecting the benthic community in the area. The 2011-2016 assessment of the state of the soft-bottom macrofauna community indicator, which in the Gulf of Finland accounts only for the areas < 60 m deep, showed the achievement of GES (HELCOM, 2018d), whereas the nutrient related indicators revealed all a sub-GES status (HELCOM, 2018a, 2018b). For the HOLAS3 period (2016-2021), the macrofauna indicator displayed a non-GES status (HELCOM, 2023d) with the nutrient related indicators being also sub-GES (HELCOM, 2023a, 2023b). Ideally, at least the GES/sub-GES level assessment results would coincide, meaning that harmonization could be needed between the indicators.

## 5. Conclusions

The analysis of long-term monitoring data from the eastern Gulf of Finland revealed a statistically significant decline in near-bottom oxygen concentrations since the early 1900s. Also, the long-term near-bottom temperature increase and decadal-scale fluctuations of salinity have been detected. The changes in the deep-layer oxygen concentrations have been found to be significantly correlated with salinity, indicating a strong impact of the along-gulf movement of saltier near-bottom waters and changes in vertical stratification on oxygen conditions. The availability of long-term monitoring data enabled us to determine the reference conditions for the deep-layer oxygen in the eastern Gulf of Finland. For the period 1926-1960, assumed to be with no or low human-induced impact, the average area and volume with oxygen concentrations below  $6 \text{ mg L}^{-1}$  were  $1030 \text{ km}^2$  or 11.7 % of the total area and  $7.9 \text{ km}^3$  or 2.1 % of the total volume of the EGOF. The seabed and waters with low-oxygen have expanded since then to  $4320 \text{ km}^2$  or 48.8 % of the EGOF total area and  $59.4 \text{ km}^3$  or 16.0 % of the EGOF total volume. In the long term, since the early 1900s, the worsening of oxygen conditions can be mainly attributed to eutrophication, i.e. excess load of nutrients, and temperature increase. Increasing temperature affects the oxygen concentrations by reducing DO solubility, strengthening vertical stratification and intensifying biogeochemical processes, including respiration and oxygen consumption for the degradation of organic matter. The observed fast widening of low-oxygen areas in the EGOF since the 1990s can partly be related to the changes in hydrographic conditions and the increase in temperature – they make up about half of the factors influencing the oxygen decline. This means that the relative proportion of other influencing factors, including eutrophication, has remained relatively high in influencing the expansion of low-oxygen bottoms.

## Acknowledgements

We thank the agencies and institutes for funding and implementing the marine environmental monitoring programs in countries bordering the Gulf of Finland and databases collecting and handling environmental data. The work of Stella-Theresa Stoicescu and Urmas Lips has been supported by the Estonian Research Council grant (PRG602).

## References

- Ahlgren, J., Grimvall, A., Omstedt, A., Rolff, C., Wikner, J., 2017. Temperature, DOC level and basin interactions explain the declining oxygen concentrations in the Bothnian Sea, *J. Mar. Syst.*, 170, 22–30 [online] Available from: <http://dx.doi.org/10.1016/j.jmarsys.2016.12.010>.
- Alenius, P., Myrberg, K., Nekrasov, A., 1998. The physical oceanography of the Gulf of Finland: a review., *Boreal Environ. Res.*, 3, 97–125.
- Alenius, P., Myrberg, K., Roiha, P., Lips, U., Tuomi, L., Pettersson, H., Raateoja, M., 2016. Gulf of Finland physics, in *The Gulf of Finland assessment. Reports of the Finnish Environment Insitute 27:2016*, edited by M. Raateoja and O. Setälä.
- Bendtsen, J., Hansen, J. L. S., 2013. Effects of global warming on hypoxia in the Baltic Sea–North Sea transition zone, *Ecol. Model.*, 264, 17–26, doi:<https://doi.org/10.1016/j.ecolmodel.2012.06.018>.
- Bindoff, N. L., Cheung, W. W. L., Kairo, J. G., Arístegui, J., Guinder, V. A., Hallberg, R., Hilmi, N., Jiao, N., Karim, M. S., Levin, L., O'Donoghue, S., Cuicapusa, S. R. P., Rinkevich, B., Suga, T., Tagliabue, A., Williamson, P., 2019. Changing Ocean, Marine Ecosystems, and Dependent Communities., in *IPCC Special Report on the Ocean and Cryosphere in a Changing Climate*, edited by H.-O. Pörtner, D. C. Roberts, V. Masson-Delmotte, P. Zhai, M. Tignor, E. Poloczanska, K. Mintenbeck, A. Alegría, M. Nicolai, A. Okem, J. Petzold, B. Rama, and N. M. Weyer, In press.
- Boesch, D. F., Coles, V. J., Kimmel, D. G., Miller, W. D., 2007. Ramifications of climate change for Chesapeake Bay hypoxia, in *Regional Impacts of Climate Change: Four Case Studies in the United States*, edited by K. Ebi, G. Meehl, M. Blanchet, R. Twilley, and D. Boesch, pp. 57–70, Pew Center on Global Climate Change, Arlington, VA. [online] Available from: <https://www.c2es.org/site/assets/uploads/2007/12/regional-impacts-climate-change-four-case-studies-united-states.pdf>.
- Caballero-Alfonso, A. M., Carstensen, J., Conley, D. J., 2015. Biogeochemical and environmental drivers of coastal hypoxia, *J. Mar. Syst.*, 141, 190–199.
- Carroll, R. J., Ruppert, D., 1996. The Use and Misuse of Orthogonal Regression in Linear Errors-in-Variables Models, *Am. Stat.*, 50(1), 1–6, doi:10.2307/2685035.
- Carstensen, J., Andersen, J. H., Gustafsson, B. G., Conley, D. J., 2014. Deoxygenation of the Baltic Sea during the last century, *P. Natl. Acad. Sci. USA*, 111(15), 5628–33 [online] Available from: <http://www.pubmedcentral.nih.gov/articlerender.fcgi?artid=3992700&tool=pmcentrez&rendertype=abstract>.
- Codiga, D. L., Stoffel, H. E., Oviatt, C. A., Schmidt, C. E., 2022. Managed Nitrogen Load Decrease Reduces Chlorophyll and Hypoxia in Warming Temperate Urban Estuary, *Front. Mar. Sci.*, 9, doi:10.3389/fmars.2022.930347.
- Conley, D. J., Björck, S., Bonsdorff, E., Carstensen, J., Destouni, G., Gustafsson, B. G., Hietanen, S., Kortekaas, M., Kuosa, H., Meier, H. E. M., Müller-Karulis, B., Nordberg, K., Norkko, A., Nürnberg, G., Pitkänen, H., Rabalais, N. N., Rosenberg, R., Savchuk, O. P., Slomp, C. P., Voss, M., Wulff, F., Zillén, L.,

2009. Hypoxia-Related Processes in the Baltic Sea, *Environ. Sci. Technol.*, 43(10), 3412–3420 [online]  
Available from: <http://pubs.acs.org/doi/abs/10.1021/es802762a>.

Dutheil, C., Meier, H. E. M., Gröger, M., Börgel, F., 2022. Warming of Baltic Sea water masses since 1850, *Clim. Dynam.*, doi:10.1007/s00382-022-06628-z.

European Parliament and Council, 2000. Directive 2000/60/EC of the European Parliament and of the Council of 23 October 2000 establishing a framework for Community action in the field of water policy. [online] Available from: <http://data.europa.eu/eli/dir/2000/60/2014-11-20>.

European Parliament and Council, 2008. Directive 2008/56/EC of the European Parliament and of the Council of 17 June 2008 establishing a framework for community action in the field of marine environmental policy (Marine Strategy Framework Directive). *Off. J. Eur. Union* L164, 19–40. [online] Available from: <http://data.europa.eu/eli/dir/2008/56/2017-06-07>.

Geyer, W. R., MacCready, P., 2014. The Estuarine Circulation, *Annu. Rev. Fluid Mech.*, 46(1), 175–197, doi:10.1146/annurev-fluid-010313-141302.

Gustafsson, B. G., Schenk, F., Blenckner, T., Eilola, K., Meier, H. E. M., Müller-Karulis, B., Neumann, T., Ruoho-Airola, T., Savchuk, O. P., Zorita, E., 2012. Reconstructing the Development of Baltic Sea Eutrophication 1850–2006, *Ambio*, 41, 534–548.

HELCOM, 2013. Approaches and methods for eutrophication target setting in the Baltic Sea region, *Balt. Sea Environ. Proc.* No. 133.

HELCOM, 2014. Eutrophication status of the Baltic Sea 2007-2011. A concise thematic assessment, *Balt. Sea Environ. Proc.* No. 143.

HELCOM, 2018a. Dissolved inorganic nitrogen (DIN). HELCOM core indicator report. Online., [online] Available from: <https://helcom.fi/wp-content/uploads/2019/08/Dissolved-inorganic-nitrogen-DIN-HELCOM-core-indicator-2018.pdf>.

HELCOM, 2018b. Dissolved inorganic phosphorus (DIP). HELCOM core indicator report. Online., [online] Available from: <https://helcom.fi/wp-content/uploads/2019/08/Dissolved-inorganic-phosphorus-DIP-HELCOM-core-indicator-2018.pdf>.

HELCOM, 2018c. Guidelines for sampling and determination of dissolved oxygen in seawater. Online. Available from: <https://helcom.fi/wp-content/uploads/2019/08/Guidelines-for-sampling-and-determination-of-dissolved-oxygen.pdf>.

HELCOM, 2018d. HELCOM thematic assessment of eutrophication 2011-2016., *Balt. Sea Environ. Proc.* No.156.

HELCOM, 2021. Baltic Sea Action Plan. 2021 update. [online] Available from: <https://helcom.fi/wp-content/uploads/2021/10/Baltic-Sea-Action-Plan-2021-update.pdf>.

HELCOM, 2023a. Dissolved inorganic nitrogen (DIN). HELCOM core indicator report. Online., Available from: <https://indicators.helcom.fi/indicator/dissolved-inorganic-nitrogen/>

HELCOM, 2023b. Dissolved inorganic phosphorus (DIP). HELCOM core indicator report. Online., Available from: <https://indicators.helcom.fi/indicator/dissolved-inorganic-phosphorus/>

HELCOM, 2023c. Inputs of nutrients to the sub-basins (2020). HELCOM core indicator report. Online., ISSN 2343-2543. Available from: <https://indicators.helcom.fi/indicator/inputs-of-nutrients/>

HELCOM, 2023d. State of the soft-bottom macrofauna community. HELCOM core indicator report. Online., ISSN 2343-2543. Available from: [Kabel, K., Moros, M., Porsche, C., Neumann, T., Adolphi, F., Andersen, T. J., Siegel, H., Gerth, M., Leipe, T., Jansen, E., Damsté, J. S. S., 2012. Impact of climate change on the Baltic Sea ecosystem over the past 1,000 years, \*Nat. Clim. Change\*, 2, 871–874.](https://indicators.helcom.fi/indicator/soft-bottom-macrofauna/IOC, SCOR, IAPSO, 2010. The international thermodynamic equation of seawater - 2010: Calculation and use of thermodynamic properties. [online] Available from: http://www.teos-10.org.</a></p></div><div data-bbox=)

Kankaanpää, H. T., Alenius, P., Kotilainen, P., Roiha, P., 2023. Decreased surface and bottom salinity and elevated bottom temperature in the Northern Baltic Sea over the past six decades, *Sci. Total Environ.*, 859, 160241, doi:<https://doi.org/10.1016/j.scitotenv.2022.160241>.

Lehtoranta, J., Dahlbo, K., Raateoja, M., Kauppila, P., Savchuk, O., Kuosa, H., Räike, A., Pitkänen, H., 2016. Processes controlling P storages., in *The Gulf of Finland assessment. Reports of the Finnish environment institute 27/2016*, edited by M. Raateoja and O. Setälä.

Lehtoranta, J., Savchuk, O. P., Elken, J., Kim, D., Kuosa, H., Raateoja, M., Kauppila, P., Räike, A., Pitkänen, H., 2017. Atmospheric forcing controlling inter-annual nutrient dynamics in the open Gulf of Finland, *J. Mar. Syst.*, 171, 4–20, 2017.

Liblik, T., Lips, U., 2011. Characteristics and variability of the vertical thermohaline structure in the Gulf of Finland in summer, *Boreal Environ. Res.*, 16A, 73–83.

Liblik, T., Lips, U., 2019. Stratification Has Strengthened in the Baltic Sea – An Analysis of 35 Years of Observational Data, *Front. Earth Sci.*, 7:174, doi:10.3389/feart.2019.00174, 2019.

Liblik, T., Laanemets, J., Raudsepp, U., Elken, J., Suhhova, I., 2013. Estuarine circulation reversals and related rapid changes in winter near-bottom oxygen conditions in the Gulf of Finland, *Baltic Sea, Ocean Sci.*, 9, 917–930.

Liblik, T., Wu, Y., Fan, D., Shang, D., 2020. Wind-driven stratification patterns and dissolved oxygen depletion off the Changjiang (Yangtze) Estuary, *Biogeosciences*, 17, 2875–2895, doi:<https://doi.org/10.5194/bg-17-2875-2020>.

Lips, U., Laanemets, J., Lips, I., Liblik, T., Suhhova, I., Suursaar, Ü., 2017. Wind-driven residual circulation and related oxygen and nutrient dynamics in the Gulf of Finland (Baltic Sea) in winter, *Estuar. Coast. Shelf S.*, 195, 4–15, doi:10.1016/j.ecss.2016.10.006.

Lønborg, C., Markager, S., 2021. Nitrogen in the Baltic Sea: Long-term trends, a budget and decadal time lags in responses to declining inputs. *Estuar. Coast Shelf S.*, 261, <https://doi.org/10.1016/j.ecss.2021.107529>

Meier, H. E. M., Väli, G., Naumann, M., Eilola, K., Frauen, C., 2018. Recently Accelerated Oxygen Consumption Rates Amplify Deoxygenation in the Baltic Sea, *J. Geophys. Res.-Oceans*, 123(5), 3227–3240, doi:<https://doi.org/10.1029/2017JC013686>.

- Meier, H. E. M., Eilola, K., Almroth-Rosell, E., Schimanke, S., Kniebusch, M., Höglund, A., Pemberton, P., Liu, Y., Väli, G., Saraiva, S., 2019. Disentangling the impact of nutrient load and climate changes on Baltic Sea hypoxia and eutrophication since 1850, *Clim. Dynam.*, 53(1), 1145–1166, doi:10.1007/s00382-018-4296-y.
- Meier, H. E. M., Kniebusch, M., Dieterich, C., Gröger, M., Zorita, E., Elmgren, R., Myrberg, K., Ahola, M. P., Bartosova, A., Bonsdorff, E., Börgel, F., Capell, R., Carlén, I., Carlund, T., Carstensen, J., Christensen, O. B., Dierschke, V., Frauen, C., Frederiksen, M., Gaget, E., Galatius, A., Haapala, J. J., Halkka, A., Hugelius, G., Hünicke, B., Jaagus, J., Jüssi, M., Käyhkö, J., Kirchner, N., Kjellström, E., Kulinski, K., Lehmann, A., Lindström, G., May, W., Miller, P. A., Mohrholz, V., Müller-Karulis, B., Pavón-Jordán, D., Quante, M., Reckermann, M., Rutgersson, A., Savchuk, O. P., Stendel, M., Tuomi, L., Viitasalo, M., Weisse, R., Zhang, W., 2022. Climate change in the Baltic Sea region: a summary, *Earth Syst. Dynam.*, 13(1), 457–593, doi:10.5194/esd-13-457-2022.
- Norkko, J., Gammal, J., Hewitt, J. E., Josefson, A. B., Carstensen, J., Norkko, A., 2015. Seafloor Ecosystem Function Relationships: In Situ Patterns of Change Across Gradients of Increasing Hypoxic Stress, *Ecosystems*, 18(8), 1424–1439.
- Oschlies, A., Brandt, P., Stramma, L. and Schmidtko, S., 2018. Drivers and mechanisms of ocean deoxygenation, *Nat. Geosci.*, 11(7), 467–473, doi:10.1038/s41561-018-0152-2.
- Piehl, S., Friedland, R., Heyden, B., Leujak, W., Neumann, T., Schernewski, G., 2022. Modeling of Water Quality Indicators in the Western Baltic Sea: Seasonal Oxygen Deficiency, *Environ. Model. Assess.*, doi:10.1007/s10666-022-09866-x.
- Rabalais, N. N., Turner, R. E., Diaz, R. J., Justić, D., 2009. Global change and eutrophication of coastal waters, *ICES J. Mar. Sci.*, 66(7).
- Reusch, T. B. H., Dierking, J., Andersson, H. C., Bonsdorff, E., Carstensen, J., Casini, M., Czajkowski, M., Hasler, B., Hinsby, K., Hyytiäinen, K., Johannesson, K., Jomaa, S., Jormalainen, V., Kuosa, H., Kurland, S., Laikre, L., MacKenzie, B. R., Margonski, P., Melzner, F., Oesterwind, D., Ojaveer, H., Refsgaard, J. C., Sandström, A., Schwarz, G., Tonderski, K., Winder, M., Zandersen, M., 2018. The Baltic Sea as a time machine for the future coastal ocean, *Sci. Adv.*, 4(5), eaar8195, doi:10.1126/sciadv.aar8195.
- Savchuk, O. P., Wulff, F., Hille, S., Humborg, C., Pollehne, F., 2008. The Baltic Sea a century ago — a reconstruction from model simulations, verified by observations, *J. Mar. Syst.*, 74(1), 485–494, doi:https://doi.org/10.1016/j.jmarsys.2008.03.008.
- Schimanke, S., Meier, H. E. M., 2016. Decadal to centennial variability of salinity in the Baltic Sea, *J. Climate.*, 29(20), 7173–7188, doi:http://dx.doi.org/10.1175/JCLI-D-15-0443.1.
- Stoicescu, S.-T., Lips, U., Liblik, T., 2019. Assessment of Eutrophication Status Based on Sub-Surface Oxygen Conditions in the Gulf of Finland (Baltic Sea), *Front. Mar. Sci.*, 6, 54, doi:10.3389/fmars.2019.00054.
- Stoicescu, S.-T., Laanemets, J., Liblik, T., Skudra, M., Samlas, O., Lips, I., Lips, U., 2022. Causes of the extensive hypoxia in the Gulf of Riga in 2018, *Biogeosciences*, 19(11), 2903–2920, doi:10.5194/bg-19-2903-2022.



Tian, R., Cerco, C.F., Bhatt, G., Linker, L.C., Shenk, G.W., 2022. Mechanisms Controlling Climate Warming Impact on the Occurrence of Hypoxia in Chesapeake Bay. *J. Am. Water. Resour. As.* 58 ( 6): 855– 875. <https://doi.org/10.1111/1752-1688.12907>.

Vahtera, E., Conley, D. J., Gustafsson, B. G., Kuosa, H., Pitkänen, H., Savchuk, O. P., Tamminen, T., Viitasalo, M., Voss, M., Wasmund, N., Wulff, F., 2007. Internal Ecosystem Feedbacks Enhance Nitrogen-fixing Cyanobacteria Blooms and Complicate Management in the Baltic Sea, *Ambio*, 36, 186–194 [online] Available from: [http://www.mare.su.se/dokument/evaluation/ecology/vahtera et al \(2007 in press\).pdf](http://www.mare.su.se/dokument/evaluation/ecology/vahtera%20et%20al%20(2007%20in%20press).pdf).

Vaquer-Sunyer, R., Duarte, C. M., 2008. Thresholds of hypoxia for marine biodiversity, *P. Natl. Acad. Sci. USA*, 105(40), 15452–15457, doi:10.1073/pnas.0803833105.

Wehr, R., Saleska, S. R., 2017. The long-solved problem of the best-fit straight line: application to isotopic mixing lines, *Biogeosciences*, 14(1), 17–29, doi:10.5194/bg-14-17-2017, 2017.

#### **Paper IV**

Liblik, T., Stoicescu, S-T., Buschmann, F., Lilover, M-J., and Lips, U., 2023. High-resolution characterization of the development and decay of seasonal hypoxia in the Gulf of Riga, Baltic Sea. *Front. Mar. Sci.* 10:1119515. <https://doi.org/10.3389/fmars.2023.1119515>





## OPEN ACCESS

EDITED BY  
Kui Wang,  
Zhejiang University, China

REVIEWED BY  
Rene Friedland,  
Leibniz Institute for Baltic Sea Research  
(LG), Germany  
Gwénaëlle Chaillou,  
Université du Québec à Rimouski, Canada  
Markus Meier,  
Leibniz Institute for Baltic Sea Research  
(LG), Germany

\*CORRESPONDENCE  
Taavi Liblik  
✉ taavi.liblik@taltech.ee

SPECIALTY SECTION  
This article was submitted to  
Ocean Observation,  
a section of the journal  
Frontiers in Marine Science

RECEIVED 08 December 2022  
ACCEPTED 27 February 2023  
PUBLISHED 10 March 2023

CITATION  
Liblik T, Stoicescu S-T, Buschmann F,  
Lilover M-J and Lips U (2023) High-  
resolution characterization of the  
development and decay of seasonal  
hypoxia in the Gulf of Riga, Baltic Sea.  
*Front. Mar. Sci.* 10:1119515.  
doi: 10.3389/fmars.2023.1119515

COPYRIGHT  
© 2023 Liblik, Stoicescu, Buschmann, Lilover  
and Lips. This is an open-access article  
distributed under the terms of the [Creative  
Commons Attribution License \(CC BY\)](#). The  
use, distribution or reproduction in other  
forums is permitted, provided the original  
author(s) and the copyright owner(s) are  
credited and that the original publication in  
this journal is cited, in accordance with  
accepted academic practice. No use,  
distribution or reproduction is permitted  
which does not comply with these terms.

# High-resolution characterization of the development and decay of seasonal hypoxia in the Gulf of Riga, Baltic Sea

Taavi Liblik\*, Stella-Theresa Stoicescu, Fred Buschmann,  
Madis-Jaak Lilover and Urmas Lips

Department of Marine Systems, Tallinn University of Technology, Tallinn, Estonia

The Gulf of Riga is a shallow basin in the eastern Baltic Sea connected to the Central Baltic Sea via shallow straits. Seasonal oxygen depletion occurs in the deep layer of the gulf. We conducted hourly measurements of dissolved oxygen, temperature, and salinity in the deep layer (50 m) of the gulf and observed the full cycle of development and relaxation of hypoxia in 2021. Hypoxia ( $<2.9 \text{ mg l}^{-1}$ ) first occurred on 27 June and was observed for 71 days until its complete decay on 22 October. Average oxygen decline of  $0.10 \text{ mg l}^{-1} \text{ d}^{-1}$  from saturation in mid-April until mid-July and  $0.04 \text{ mg l}^{-1} \text{ d}^{-1}$  onwards until the end of August were observed. This seasonal pattern was superimposed by short-term variability in time scales from hours to days and was probably caused by inertial oscillations, (sub)mesoscale processes, deep layer currents, and pycnocline movements. Ventilation events with a relatively low impact and duration of up to ten days occurred in the deep layer due to the inflows of the saltier water from the Central Baltic. The inflowed water originated from the upper layer in winter and the thermocline in summer and was almost saturated in oxygen. Mostly mixing with existing oxygen-depleted water in the Gulf of Riga, but also local consumption declined the oxygen levels in the inflow water before it arrived at the observing station. Monthly standard deviations in oxygen varied from  $0.3$  to  $2.8 \text{ mg l}^{-1}$  and illustrated the added value of Eulerian measurements to complement the conventional monitoring.

## KEYWORDS

seasonal hypoxia, mooring measurement, eutrophication, estuarine, deoxygenation

## 1 Introduction

Oxygen depletion in the coastal ocean has expanded globally (Diaz and Rosenberg, 2008) and in the Baltic Sea (Schmidt et al., 2021; Krapf et al., 2022) since the 1960s. In many coastal areas, oxygen declines have been caused by increased loadings of nutrients (Breitburg et al., 2018), and the semienclosed Gulf of Riga in the Baltic Sea is a showcase of such changes.

Unlike the Central Baltic (CB) Sea, where hypoxia/anoxia below the permanent halocline can last for years and can only be interrupted by Major Baltic Inflows (Mohrholz et al., 2015; Liblik et al., 2018), oxygen depletion in the Gulf of Riga (GoR) is a seasonal phenomenon (Berzinsh, 1995; Stoicescu et al., 2022), which is characteristic of coastal marine systems under the anthropogenic impact (e.g. Dietze and Löptien, 2021; Lee et al., 2021; Sun et al., 2022).

The GoR is located in the Eastern Baltic Sea and is connected to the saltier CB *via* Irbe Strait in the west and Suur Strait (Figure 1). The Irbe Strait is the major contributor to the saltier water input to the GoR. The sill depths in the straits (25 m and 5 m, respectively) are clearly shallower than the halocline, which separates oxic and oxygen-depleted water in the CB (Meyer et al., 2018; Almroth-Rosell et al., 2021). Thus, hypoxic/anoxic water from the CB cannot enter the GoR, and oxygen depletion in the GoR is a result of local processes. The present extent of deoxygenation in the Baltic Sea is caused by eutrophication (Conley et al., 2009).

Convection and wind stirring ventilate the whole water column in the GoR in winter. The onset of stratification in spring is created by buoyancy forcing resulting from riverine freshwater flux (Stipa et al., 1999), which is concentrated in the southern part of the gulf (Stipa et al., 1999; Skudra and Lips, 2017). Stratification in summer is mostly maintained by the vertical temperature gradient, while haline stratification is a minor contributor (Liblik et al., 2017). Oxygen consumption exceeds the oxygen import to the sub-surface layer by physical processes, and as a result, oxygen concentration declines in the deep layer during summer (Berzinsh, 1995; Liblik et al., 2017; Stoicescu et al., 2022).

Southwesterly winds cause downwelling in the western (CB) side of the Irbe Strait. Part of the downwelling water enters the GoR and mixes with ambient fresher GoR water and forms buoyant saline and warm (sub)mesoscale features, which do not ventilate the

deep layer in the GoR (Liblik et al., 2017). Northeasterly winds cause upwelling on the western side of the Irbe Strait. Part of the upwelling water likely enters the gulf and could be dense enough for deepwater renewal.

The variability in meteorological conditions could cause inter-annual variability in the deep layer oxygen conditions, and as a result, hypoxia does not occur every year (Stoicescu et al., 2022). However, the current evaluations of deep water oxygen conditions rely solely on sparse shipborne conventional monitoring, which is done by research vessels 5–6 times a year (Liblik et al., 2017; Stoicescu et al., 2022). The high-frequency temperature and salinity profiling (Liblik et al., 2017) and near-bottom temperature observations (Raudsepp and Kõuts, 2001) have hinted that the infrequent shipborne sampling might miss a large extent of variability and events. Variability in oxygen conditions alters nutrient fluxes at the sediment boundary (Eglite et al., 2014; Stoicescu et al., 2022), benthic communities (e.g. Rousi et al., 2013), and pelagic fish (e.g. Limburg and Casini, 2018). In conclusion, the ecological consequences of the variability in oxygen depletion could be significant, but the deep-layer oxygen conditions are currently studied only by sparse shipborne measurements in the GoR.

In the present work, we report the results from the first continuous measurements of dissolved oxygen, salinity, and temperature in the deep layer of the GoR. The main aim of the work was to analyze and describe the time series of deep layer observations from the saturated state in spring to the formation of oxygen depletion (hypoxia) in summer/autumn until the decay of depletion.

Particularly, the following objectives were set in this study: Estimate the characteristic oxygen decline rate in the near-bottom layer of the GoR; Describe the governing processes causing shorter-term variability in oxygen, their time scales and the magnitude of caused changes; Estimate the impact of inflowing CB water on the oxygen conditions in the GoR deep layer; Assess the added value of near-bottom moorings on the existing observing program in the GoR.

## 2 Data and methods

SBE 37-SMP-ODO MicroCAT (Sea-Bird Scientific) recorder was deployed to measure temperature, conductivity (to calculate Absolute Salinity), and dissolved oxygen at 50.5 m depth at the RD station on 28 January 2021. The sea bottom depth in the mooring location was 54 m. We present the time series until 23 October 2021, when turnover and ventilation of the water column occurred (Figure 2). The monthly standard deviations of oxygen were calculated until the end of the year.

The recorder was calibrated by the manufacturer, and it was checked against RV Salme measurements before and after deployment, as described in the best practices of ocean observatories (Venkatesan et al., 2018). The recorder was attached to the CTD Rosette, and parallel measurements at selected depths were carried out (Karstensen, 2005). The profiles onboard RV Salme were recorded using an Ocean Seven 320plus CTD probe

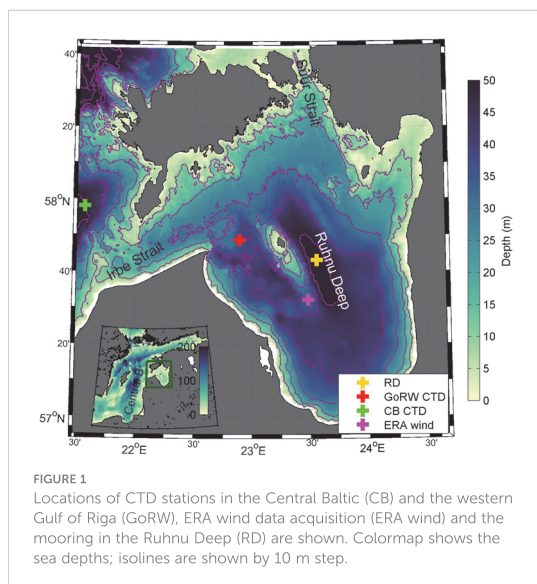


FIGURE 1  
Locations of CTD stations in the Central Baltic (CB) and the western Gulf of Riga (GoRW), ERA wind data acquisition (ERA wind) and the mooring in the Ruhn Deep (RD) are shown. Colormap shows the sea depths; isolines are shown by 10 m step.

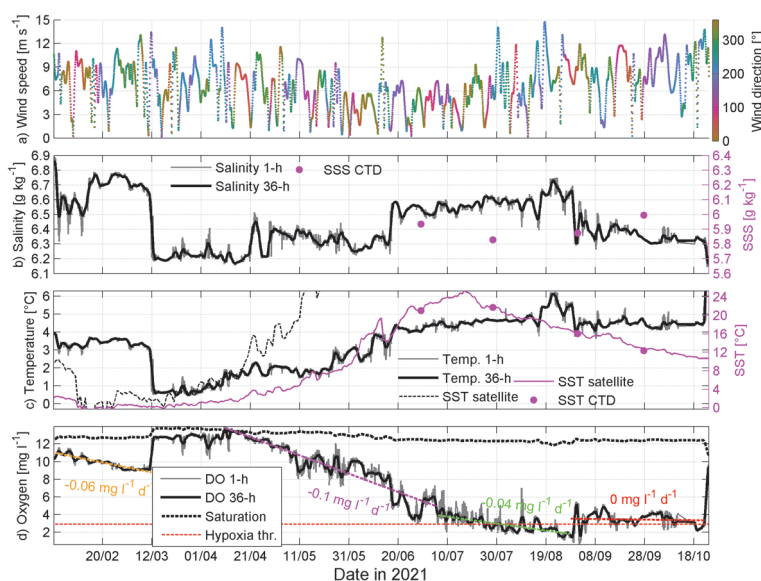


FIGURE 2

Wind speed and direction (ERA wind in Figure 1), salinity, temperature, and dissolved oxygen at 50 m depth in RD station from 28 January to 23 October 2021. Bold lines correspond to 36-h smoothed values. Sea surface temperature (from remote sensing as the purple line and CTD profiles as the purple dots) and salinity (dots) are shown in the middle panels (the scale of the right axis is different from the left axis).

(Idronaut S.r.l.). The oxygen sensor (Idronaut S.r.l.) attached to the probe was calibrated before each cruise and oxygen profiles were quality-checked against bottle samples that were analyzed using the MU 6100 L multi-parameter meter (VWR International, LLC). The salinity data of the RV probe was checked against the water sample analyses using a salinometer 8410A Portasal (Guildline). No correction of MicroCAT recorder measurements was needed. Hourly, 10 m level wind velocities of ERA5 reanalysis data (Hersbach et al., 2020) were used (see Figure 1 for location).

The MATLAB function 'pwelch' was used to estimate the power spectral density (PSD). To increase the accuracy of the PSD estimates, the time series were divided into eight equal-length segments. The calculated spectra having 16 degrees of freedom were presented with 95%-confidence bounds.

The MATLAB function 'findchangepts' (Killick et al., 2011) was used to estimate the shift in linear trend in mid-summer.

### 3 Results and discussion

#### 3.1 Time-series of water properties in the Ruhnu Deep

The oxygen depletion cycle started in mid-April when water was saturated and lasted until 23 October, when the turnover of the water column occurred (Figure 2D).

Water was well ventilated, although not saturated in oxygen until mid-March. Salinity was high and water was rather warm compared to previous observations (Raudsepp, 2001; Stoicescu

et al., 2022), indicating that an inflow of the CB water had occurred (Figures 2B–D). Oxygen decline trend of  $-0.06 \text{ mg l}^{-1} \text{ d}^{-1}$  was observed from the end of January to 11 March. Only the eastern part of the gulf was covered by ice in winter (not shown). A strong mixing event occurred as a result of strong winds in the first half of March (Figure 2A), and consequently, temperature and salinity decreased and oxygen concentration rose. Water was fully saturated in oxygen in mid-April, and as stratification formed, oxygen concentration started to decrease. A relatively stable decreasing trend of  $-0.10 \text{ mg l}^{-1} \text{ d}^{-1}$ , although superimposed by shorter-term variability, was observed until 5 July (Figure 2C). According to the breakpoint analysis, the trend eased off around 5 July, and a decline in oxygen concentration of  $-0.04 \text{ mg l}^{-1} \text{ d}^{-1}$ , on average, lasted until the strong SW wind event, which caused an instantaneous oxygen increase on 29 August. The AOU (apparent oxygen utilization) trends during the same periods before and after 5 July were 0.09 and  $0.03 \text{ mg l}^{-1} \text{ d}^{-1}$ , respectively. Thus, the trend in oxygen solubility due to temperature and salinity changes had a minor effect on the seasonal oxygen decrease. The faster oxygen decline in spring and early summer was probably related to the higher primary production (spring bloom), related sedimentation of organic matter, and consequent oxygen consumption (Olli and Heiskanen, 1999; Aigars et al., 2015; Purina et al., 2018). The connection between primary production in the upper layer and oxygen depletion in the near-bottom layer has been found in many estuarine environments, e.g., in the Changjiang (Yangtze) Estuary (e.g. Wei et al., 2021; Wei et al., 2022). The second reason for the faster oxygen decrease in spring and early summer was likely the strengthening of the stratification.

Various oxygen metrics have been established to describe oxygen deficiency (e.g. Piehl et al., 2022). In the present work, we describe the deficiency by the temporal presence of hypoxia ( $< 2.9 \text{ mg l}^{-1}$ ). The first oxygen value below the hypoxic level was registered already on 27 June and occasional hypoxia was observed until mid-July, after which hypoxic conditions prevailed until the end of August (Figure 2D). After the mixing event on 29 August, hypoxia occurred occasionally, and oxygen concentration did not show any significant trend until turnover of the water column on 23 October. The last day hypoxia occurred was 22 October. In total, hypoxic water was present for 1050 hours, i.e., 44 days. There were 71 days when hypoxia was at least once observed and the longest continuous period of such days was 23 days in the beginning of August.

Water gradually got saltier and warmer until the second half of August. Despite high short-term variability, several gradual shifts can be distinguished in salinity. From mid-March to mid-April, salinity was mostly around  $6.2\text{--}6.3 \text{ g kg}^{-1}$ , until mid-June  $6.3\text{--}6.4 \text{ g kg}^{-1}$ , until mid-August  $6.5\text{--}6.6 \text{ g kg}^{-1}$ , and peaked at  $6.75 \text{ g kg}^{-1}$  on 23 August. After the latter, salinity dropped to  $6.3\text{--}6.5 \text{ g kg}^{-1}$  and again on 23 October to  $6.1\text{--}6.2 \text{ g kg}^{-1}$ . The temperature did not exactly follow the temporal course of salinity. Shifts in salinity in mid-April and mid-June were preceded by smoother temperature increases during about 3–4 weeks. Compared to previous observations (Raudsepp, 2001; Skudra and Lips, 2017; Stoicescu et al., 2022), the near-bottom water was warmer and saltier in the summer of 2021, indicating higher salty water inflow activity than usual. The details and spatial features behind detected gradual shifts can be effectively analyzed in further studies where high-resolution vertical

profiling with a moored profiler and underwater glider is included in an observing system.

### 3.2 Variability of deep water characteristics

On top of the seasonal trends in oxygen, shorter-term variability was observed. Spectra of oxygen, temperature, and salinity variance revealed elevated energy at 14.2 h, which is associated with the inertial oscillations also observed earlier in the GoR (Raudsepp and Kõuts, 2001). Internal waves probably impact the time series in shorter time scales, while irregular variability in the time scale from day to week reflects synoptic-scale changes in forcing.

The oxygen and water temperature spectral slopes between the temporal scales of 25 h and 7 d were about  $-1.8$  to  $-2$  (in logarithmic scale). Wavenumber spectra slope around  $-2$  suggests a significant role of sub-mesoscale processes in vertical exchanges (Lips et al., 2016; Väli et al., 2017). The profiling data collected over 4 months revealed the existence of submesoscale features within the seasonal thermocline of the GoR (Liblik et al., 2017). High-resolution measurements in space are required to understand better the role of submesoscale processes in the Gulf of Riga deep layer.

Next, we analyze and discuss the synoptic scale variability of water column properties. In Figures 3A–C, we present the daily changes in salinity (a), temperature (b), and oxygen (c). In panel d, changes in detrended 3-day mean oxygen are shown.

Throughout the time series, the increase in salinity corresponded mostly to the decrease in oxygen (red and pink

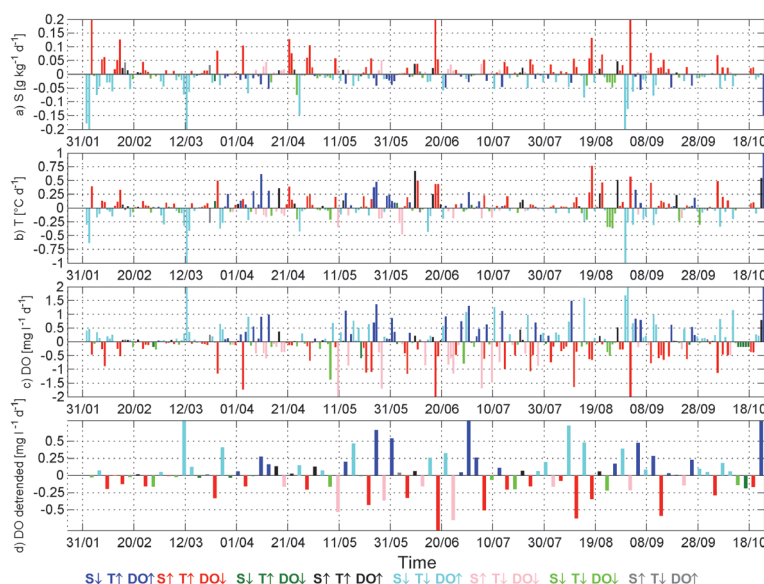


FIGURE 3

Daily changes in salinity, temperature, and oxygen (A–C) from 28 January to 23 October 2021. Detrended (according to the linear trends shown in Figure 2C) 3-day mean changes of oxygen (D). Colors show the positive or negative changes of variables, as shown at the bottom of the figure.



color in Figures 3A, C) and vice-versa (blue and cyan color in Figures 3A, C) (red and pink color in Figures 3A, C). These events were probably related to the upward and downward movement of clines caused by the wind-driven current in the upper layer and return flow in the deep layer (Raudsepp and Kõuts, 2001).

Until March, an increase in oxygen and decrease in salinity were associated with a temperature decrease (cyan color in Figure 3A) and lower oxygen was associated with higher salinity and higher temperature (red color in Figure 3A). This can be explained by cooling of the upper layer water and reversed thermal stratification (i.e. colder water at the sea surface, warmer in the near-bottom layer). When vertical mixing occurred (e.g. the main event on 8–13 March, see Figures 3A–C) or pycnocline moved downwards, oxygen increased and temperature/salinity decreased. Saltier and warmer water re-appearance caused a decrease in oxygen.

High salinity-low oxygen and vice-versa relation kept prevailing the variability after March, but the temperature and salinity relationship were not that obvious until autumn, i.e. sometimes high salinity-low oxygen associated with higher temperature (red color on Figures 3A–C), sometimes with lower temperature (pink color on Figures 3A–C). It is probably related to the cold intermediate layer, which is not well pronounced in the GoR (Stipa et al., 1999; Liblik et al., 2017; Skudra and Lips, 2017; Stoicescu et al., 2022).

The arrival of oxygenated water from the CB is revealed by a simultaneous increase in salinity, temperature, and oxygen (black color in Figures 3A–C). These events are rather rare compared to the upward and downward movements of pycnoclines. Several small positive oxygen fluxes as a result of transport from the CB occurred in mid-

April, mid-June, on 20–21 July, and on 20 and 27 August. Sometimes, oxygen decrease occurred simultaneously with the decrease in salinity and temperature (green color, Figures 3A–C). These cases likely indicate the events of reappearance of older low-oxygen GoR water after the mixing event or the CB inflow event, e.g. after the event on 20 August.

Most of the oxygen increase events were followed by oxygen decrease and salinity increase events due to the cline variability. We removed seasonal linear trends (Figure 2D) and calculated changes in the 3-day mean oxygen content to present the multi-day changes of oxygen (Figure 3D). The ventilation events caused by the CB water arrival can be recognized in the time series, but compared to the magnitude of internal variability of the GoR they are rather small (Figure 3D). Moreover, the amount of oxygen the inflows brought to the Ruhnu Deep was so small that this new oxygen disappeared after few days if considering the seasonal trends (Figure 2C).

### 3.3 Ventilation events: Origin and fate of inflowing waters

Several small ventilation events were detected in the time series and can be seen in OS diagrams (Figures 4B, D). Transport through the Irbe Strait plays an important role in the deep water renewal in the GoR (Raudsepp and Kõuts, 2001; Stoicescu et al., 2022). This is confirmed by the TS- and OS-diagrams – the origin of the arrived water with higher oxygen content was saltier and warmer (Figures 4A–D). Both northerly or southerly wind-generated flow events in the Irbe Strait and simultaneous upwelling and

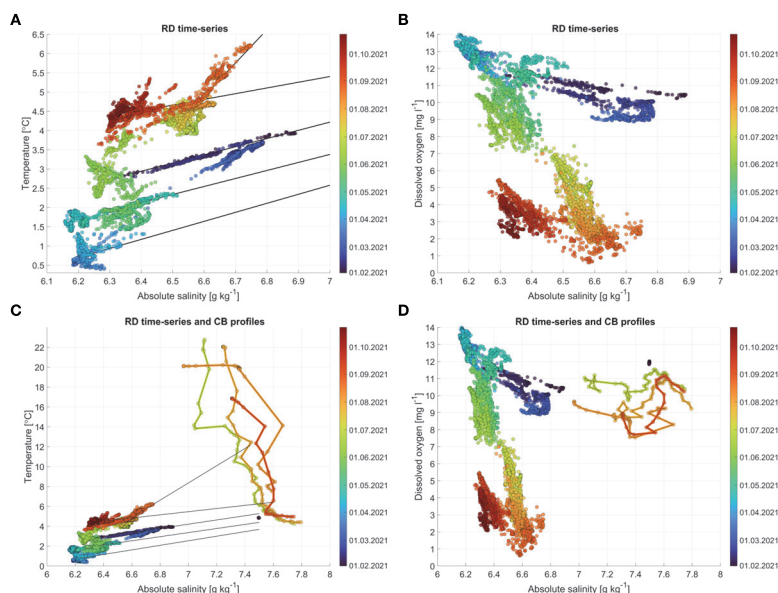


FIGURE 4

Ruhnu Deep time-series (A–D) with CB profiles (C, D) in temperature-salinity (A, C) and salinity-oxygen diagrams (B, D). CB profile data points are connected with lines.



downwelling, respectively, at the western side of the strait, could potentially bring water to the deep layers of the GoR.

The water column was well mixed in the CB (Figure 4C) and the arrivals of more saline water in mid-February and at the end of April were likely caused by the barotropic flow in the Irbe Strait and downwelling at the CB side of the strait, which occur in response to southerly winds (Otsmann et al., 2001; Liblik et al., 2022). A comparison of temperature-salinity characteristics in the Ruhnu Deep time series and the profile in the CB at the end of January confirms the origin (Figure 4C).

Further saltier water arrivals rather originated from the thermocline of the CB; see the regression lines for an indication of the potential origin of the saltier water mass in the CB (Figure 4C). Northerly wind directions cause upwelling at the eastern coast of the CB, onshore flow within or below the thermocline (Liblik et al., 2022) and likely inflow of colder waters to the GoR via Irbe Strait (Lilover et al., 1998). This water can be dense enough to penetrate the deep layers of the GoR (Stoicescu et al., 2022). Inflow events also occur in the case of southerly wind events and downwellings along the CB coast in summer, but in these cases, water is too warm (light) and forms buoyant salinity maxima in the GoR and does not ventilate deep layers (Liblik et al., 2017). It has been suggested that the period when inflows generated by the southerly wind do not interrupt the deep layer lasts from May/June to September (Liblik et al., 2017).

The actual wind events that caused the arrival of the CB waters to the Ruhnu Deep cannot be distinguished from existing data. The rapid increase in salinity observed in mid-June was preceded by several northerly wind events in April and May, and the same wind prevailed in the first half of June (Figure 2A). Another weaker northerly wind impulse occurred during a week from the end of June – early July. Likewise, northerly winds prevailed during the next small ventilation event on 20–21 July. Latter wind impulse probably also contributed to the higher salinity water arrival to the Ruhnu Deep on 20 August. Thus, on the one hand, the assumption of one month arrival time from Irbe Strait to Ruhnu Deep, suggested by Stoicescu et al. (2022), might be valid. However, the CTD profiles measured in the western GoR (GoRW in Figure 1) show the highest near bottom salinity ( $6.84 \text{ g kg}^{-1}$ ) already on 29 June, lower on 28 July ( $6.67 \text{ g kg}^{-1}$ ), and even lower on 31 August ( $6.52 \text{ g kg}^{-1}$ ). The highest salinity ( $6.74 \text{ g kg}^{-1}$ ) was observed in the Ruhnu Deep on 20–23 August. The TS characteristics of the water in the Irbe Strait on 29 June hint that the water arrival, which we observed on 20–23 August, might have crossed the Irbe Strait already in June. It could be that several wind impulses are required for the salty water transport over the sill and to the deeper areas of the GoR. Continuous simultaneous measurements in the Irbe Strait and Ruhnu Deep would help to understand the connectivity of the water characteristics in the strait and deep layers of the GoR.

On the way from Irbe Strait to the deeper part of the GoR, water mixes with ambient oxygen-depleted GoR water, and oxygen is consumed due to biogeochemical processes. We estimated the share of the CB water and ambient GoR water in the arrived water. Taking into account the mean salinity before the arrival of new water, the salinity of new water, and the salinity of the CB water ( $7.4 \text{ g kg}^{-1}$ ), the estimated share of the CB water in the water mass was about 15% in the water that arrived in the second half of April, 19% in the second half of June and 16% in the arrival of 20 August. Thus, the

inflowing water is the subject of an active mixing process before arrival to the deep layers of the GoR.

To illustrate the impact of mixing on oxygen content, we describe the 20 August saltier water arrival event. Taking the oxygen concentration of the CB water ( $9 \text{ mg l}^{-1}$ , Figure 4D) and one-month average concentration (the assumed travel time of inflowed water) before the event in the near-bottom layer of the GoR ( $2.8 \text{ mg l}^{-1}$ ) and the shares of waters (84% - old GoR water and 16% - CB water), we get that without local oxygen consumption, the oxygen concentration in the arrived water mass would be  $3.8 \text{ mg l}^{-1}$  solely due to mixing with the GoR water. Thus, the oxygen import by advection ( $\text{DO}_{\text{adv}}$ ) would be  $1 \text{ mg l}^{-1} \text{ month}^{-1}$ , i.e.  $0.03 \text{ mg l}^{-1} \text{ d}^{-1}$ . If we apply the mean seasonal trend of oxygen decrease during one month ( $0.04 \text{ mg l}^{-1} \text{ d}^{-1}$ , Figure 2D), the concentration would be  $2.6 \text{ mg l}^{-1}$ , which is very close to the observed 3-day mean oxygen concentration after the appearance of new water ( $2.5 \text{ mg l}^{-1}$ ). Despite losses of oxygen on the way, it still slightly ventilated the deep layer as the 3-day mean concentration before the event was  $2.1 \text{ mg l}^{-1}$ . Thus, it took about 10 days for oxygen concentration to decline to the level measured before the arrival of inflow water. We can conclude that inflow events have some potential for ventilation of deep water of the GoR. Stronger ventilation events did not occur because of oxygen loss due to mixing on the way to the Ruhnu Deep (approximately 80%) and local seasonal oxygen depletion (20%).

It has been suggested that the arrival of CB water strengthens the deep layer stratification, which leads to faster oxygen consumption due to the thinner near-bottom layer (Stoicescu et al., 2022). Thus, although the inflows bring oxygen to the deep layers, the net impact of inflows might be negative for deep-layer oxygen conditions. Targeted observations, including Eulerian measurements in the deep layer presented in the current study, high-resolution spatial measurements along the pathway from the CB to the Ruhnu Deep, and dedicated numerical simulations are required to confirm our estimates and improve understanding of the deep-layer oxygen budgets in the GoR.

### 3.4 The added value of Eulerian observations for the monitoring system

Next, we discuss the variability of near-bottom oxygen observations in the context of the potential of Eulerian observations to complement the existing conventional monitoring in the GoR. Conventional monitoring is usually conducted once in January, April, May, July, August, and October (Stoicescu et al., 2022).

The standard deviation of oxygen was lower in February ( $0.60 \text{ mg l}^{-1}$ ), April ( $0.67 \text{ mg l}^{-1}$ ), August ( $0.93 \text{ mg l}^{-1}$ ), September ( $0.80 \text{ mg l}^{-1}$ ), and November–December ( $<0.38 \text{ mg l}^{-1}$ ), i.e. in months when oxygen depletion did not occur or when it was already well established. Standard deviation was higher in May–July ( $>1.16 \text{ mg l}^{-1}$ ), particularly in June ( $2.22 \text{ mg l}^{-1}$ ), i.e. when oxygen depletion developed. Standard deviations were lower if linear trends in summer months presented in Figure 3 were removed ( $>0.74 \text{ mg l}^{-1}$  in May and July,  $0.91 \text{ mg l}^{-1}$  in August,  $1.45 \text{ mg l}^{-1}$  in June). The high standard deviations in March ( $1.76 \text{ mg l}^{-1}$ ) and October ( $2.82 \text{ mg l}^{-1}$ ) were a result of the turnover of the water column. Variability was

quite low before and after the mixing events. Although hypoxia prevailed from the second half of July, the maximum concentrations were as high as  $7.3 \text{ mg l}^{-1}$ ,  $7.0 \text{ mg l}^{-1}$ , and  $5.2 \text{ mg l}^{-1}$  in July, August, and September, respectively. The probability of hypoxia was highest in August (81.9%) and lower in July (23.5%), September (16.3%), and October (20.3%). Only one hourly observation of hypoxia was captured at the end of June.

Major signals, such as the decrease in near-bottom oxygen concentration and strong inter-annual differences, can be detected by conventional monitoring (Stoicescu et al., 2022), but our statistics suggest that uncertainties of these estimates are high. Moreover, the variability, including the duration of hypoxic conditions, is not captured by conventional monitoring. Conditions were extremely different before and after the turnover event in October. Thus, depending on the exact visit time of a monitoring cruise, the observations of near-bottom oxygen conditions can be radically different in autumn. This could impact seasonal hypoxic area estimates (e.g. Krapf et al., 2022) and long-term trend estimates (e.g. Lainela et al., 2020). The continuous Eulerian measurements considerably contribute to the understanding of the processes, complement spatial mappings (Meyer et al., 2018; Mohrholz, 2018) and improve the confidence of the assessments of eutrophication status (Stoicescu et al., 2019).

Assuming that changes in oxygen concentration in the near-bottom layer ( $\text{DO}_{\text{change}}$ ) are defined by oxygen consumption ( $\text{DO}_{\text{cons}}$ ), oxygen fluxes due to advection ( $\text{DO}_{\text{adv}}$ ) and vertical mixing ( $\text{DO}_{\text{vertmix}}$ ), and short-term variability caused by internal waves and mesoscale/submesoscale processes ( $\text{DO}_{\text{changeHF}}$ ), we can express it as

$$\text{DO}_{\text{change}} = \text{DO}_{\text{adv}} + \text{DO}_{\text{vertmix}} - \text{DO}_{\text{cons}} + \text{DO}_{\text{changeHF}} \quad (1)$$

While Stoicescu et al. (2022) used the same equation to estimate oxygen consumption in the near-bottom layer of the GoR but without considering short-term variability, the current dataset allows us to evaluate what would be the error estimate of such calculations based on measurements with a monthly timestep.

The impact of advection estimated in relation to the inflow, which arrived in the RD on 20 August 2021, was  $1.0 \text{ mg l}^{-1} \text{ month}^{-1}$  or  $0.03 \text{ mg l}^{-1} \text{ d}^{-1}$  (see section 3.3). Assuming a similar to Stoicescu et al. (2022) impact of vertical mixing of  $0.02\text{--}0.03 \text{ mg l}^{-1} \text{ d}^{-1}$ , and considering the two estimates of long-term trends based on the present dataset of  $-0.10 \text{ mg l}^{-1} \text{ d}^{-1}$  and  $-0.04 \text{ mg l}^{-1} \text{ d}^{-1}$ , we can estimate the oxygen consumption rate in spring-summer 2021. It would be between  $0.09 \text{ mg l}^{-1} \text{ d}^{-1}$  and  $0.16 \text{ mg l}^{-1} \text{ d}^{-1}$ . Stoicescu et al. (2022) obtained similar consumption rate estimates for 2018, ranging from  $0.10$  to  $0.16 \text{ mg l}^{-1} \text{ d}^{-1}$ .

Considering the found monthly standard deviations of oxygen concentration in different months 2021 from spring to autumn in a range from  $0.67$  to  $2.82 \text{ mg l}^{-1}$  as an estimate of short-term changes (e.g.,  $\text{DO}_{\text{changeHF}} = 0.67 \text{ mg l}^{-1}$  per month or another selected period) and trends between  $1.20$  and  $3.33 \text{ mg l}^{-1} \text{ month}^{-1}$ , the error of consumption rate estimates based on monthly measurements could be  $>50\%$ . We suggest that sustainable continuous measurements of near-bottom water characteristics would enhance the knowledge and lower the uncertainties of estimates of oxygen conditions in the Gulf of Riga.

## 5 Conclusion

Continuous deep layer measurements in the Ruhnu Deep revealed characteristics of seasonal oxygen depletion in the Gulf of Riga. On top of the seasonal oxygen decline, short-term variability, likely caused by inertial oscillations, (sub)mesoscale processes, deep layer currents, and pycnocline movements, was observed. The inflow events from the Central Baltic slightly ventilated the hypoxic deep layer. Although the inflowed water was nearly saturated in oxygen, once it arrived to the Ruhnu Deep, it has lost its high oxygen content due to mixing with existing oxygen-depleted water in the Gulf of Riga and local consumption on the way.

The revealed short-term variability points to uncertainties of conventional monitoring and demonstrates the added value of permanent continuous measurements to the observing system. Targeted high-resolution spatial measurements along the pathway from the Central Baltic to the Ruhnu Deep, combined with Eulerian measurements, conventional monitoring, and dedicated numerical simulations, are required to improve our understanding of the deep layer dynamics in the Gulf of Riga.

## Data availability statement

The raw data supporting the conclusions of this article will be made available by the authors, without undue reservation.

## Author contributions

TL designed the experiment and led the analyses of the data and writing of the paper. FB contributed with in-situ data gathering, calibration and data processing. ST-S, UL and M-JL contributed to the writing of the manuscript.

## Funding

This research has been supported by the Estonian Research Council (grant no. PRG602).

## Acknowledgments

We thank our colleagues who help to conduct the measurements and the ship crew of the RV Salme. We thank Germa Väli for his help with breakpoint analysis.

## Conflict of interest

The authors declare that the research was conducted in the absence of any commercial or financial relationships that could be construed as a potential conflict of interest.

## Publisher's note

All claims expressed in this article are solely those of the authors and do not necessarily represent those of their affiliated

organizations, or those of the publisher, the editors and the reviewers. Any product that may be evaluated in this article, or claim that may be made by its manufacturer, is not guaranteed or endorsed by the publisher.

## References

- Aigars, J., Poikane, R., Dalsgaard, T., Eglite, E., and Jansons, M. (2015). Biogeochemistry of n, p and SI in the gulf of Riga surface sediments: Implications of seasonally changing factors, cont. *Shelf Res.* 105, 112–120. doi: 10.1016/j.csr.2015.06.008
- Almroth-Rosell, E., Wählström, I., Hansson, M., Väli, G., Eilola, K., Andersson, P., et al. (2021). A regime shift toward a more anoxic environment in a eutrophic Sea in northern Europe. *Front. Mar. Sci.* 8. doi: 10.3389/FMARS.2021.799936/BIBTEX
- Berzins, V. (1995). *Hydrology, in ecosystem of the gulf of Riga between 1920 and 1990*. Ed. E. Ojaveer (Tallinn: Estonian Acad. Publ.), 7–31.
- Breitburg, D., Levin, L. A., Oschlies, A., Grégoire, M., Chavez, F. P., Conley, D. J., et al. (2018). Declining oxygen in the global ocean and coastal waters. *Science* 359, eam7240. doi: 10.1126/science.1156401
- Conley, D. J., Björck, S., Bonsdorff, E., Carstensen, J., Destouni, G., Gustafsson, B. G., et al. (2009). Hypoxia-related processes in the Baltic Sea, environ. *Sci. Technol.* 43 (10), 3412–3420. doi: 10.1021/es802762a
- Diaz, R. J., and Rosenberg, R. (2008). Spreading dead zones and consequences for marine ecosystems. *Science* 321 (5891), 926–929. doi: 10.1126/science.1156401
- Dietze, H., and Löptien, U. (2021). Retracing hypoxia in eckernförde bight (Baltic Sea). *Biogeosciences* 18 (14), 4243–4264. doi: 10.5194/bg-18-4243-2021
- Eglite, E., Lavrinovičs, A., Müller-Karulis, B., Aigars, J., and Poikane, R. (2014). Nutrient turnover at the hypoxic boundary: flux measurements and model representation for the bottom water environment of the gulf of Riga. *Baltic Sea Oceanol.* 56 (4), 711–735. doi: 10.5697/OC.56-4.711
- Hersbach, H., Bell, B., Berrisford, P., Hirahara, S., Horányi, A., Muñoz-Sabater, J., et al. (2020). The ERA5 global reanalysis, q. *J. Meteorol. Soc.* 146 (730), 1999–2049. doi: 10.1002/qj.3803
- Karstensen, J. (2005). "Calibration of physical data," in *A cookbook for MicroCat (ADCP and RCM data)*. doi: 10.25607/OBP-1509
- Killick, R., Fearnhead, P., and Eckley, I. A. (2011). Optimal detection of changepoints with a linear computational cost. *J. Am. Stat. Assoc.* 107 (500), 1590–1598. doi: 10.1080/01621459.2012.737745
- Krapf, K., Naumann, M., Duthell, C., and Meier, H. E. M. (2022). Investigating hypoxic and eutrophic area changes based on various datasets from the Baltic Sea. *Front. Mar. Sci.* 9. doi: 10.3389/FMARS.2022.823476/BIBTEX
- Lainela, S., Herkül, K., Leito, I., Jaanus, A., and Suursaar, Ü. (2020). Contemporary trends in hydrophysical and hydrochemical parameters in the NE Baltic Sea. *Est. J. Earth Sci.* 69 (2), 91–108. doi: 10.3176/earth.2020.06
- Lee, Y. W., Park, M. O., Kim, S. G., Kim, S. S., Khang, B., Choi, J., et al. (2021). Major controlling factors affecting spatiotemporal variation in the dissolved oxygen concentration in the eutrophic masan bay of Korea. *Reg. Stud. Mar. Sci.* 46, 101908. doi: 10.1016/j.rsmas.2021.101908
- Liblik, T., Naumann, M., Alenius, P., Hansson, M., Lips, U., Nausch, G., et al. (2018). Propagation of impact of the recent major Baltic inflows from the Eastern gotland basin to the gulf of Finland. *Front. Mar. Sci.* 5. doi: 10.3389/fmars.2018.00222
- Liblik, T., Skudra, M., and Lips, U. (2017). On the buoyant sub-surface salinity maxima in the gulf of Riga. *Oceanologia* 59 (2), 113–128. doi: 10.1016/J.OCEANO.2016.10.001
- Liblik, T., Väli, G., Salm, K., Laanemets, J., Lilover, M. J., and Lips, U. (2022). Quasi-steady circulation regimes in the Baltic Sea. *Ocean Sci.* 18 (3), 857–879. doi: 10.5194/OS-18-857-2022
- Lilover, M.-J., Lips, U., Laanejaru, J., and Liljebladh, B. (1998). Flow regime in the irbe strait. *Aquat. Sci.* 60 (3), 253. doi: 10.1007/s000270050040
- Limburg, K. E., and Casini, M. (2018). Effect of marine hypoxia on Baltic Sea cod gadus morhua: Evidence from otolith chemical proxies. *Front. Mar. Sci.* 5 (DEC). doi: 10.3389/FMARS.2018.00482/BIBTEX
- Lips, U., Kikas, V., Liblik, T., and Lips, I. (2016). Multi-sensor in situ observations to resolve the sub-mesoscale features in the stratified gulf of Finland. *Baltic Sea Ocean Sci.* 12 (3), 715–732. doi: 10.5194/os-12-715-2016
- Meyer, D., Lips, U., Prien, R. D., Naumann, M., Liblik, T., Schuffenhauer, I., et al. (2018). Quantification of dissolved oxygen dynamics in a semi-enclosed sea – a comparison of observational platforms. *Cont. Shelf Res.* 169, 34–45. doi: 10.1016/j.csr.2018.09.011
- Mohrholz, V. (2018). Major Baltic inflow statistics – revised. *Front. Mar. Sci.* 5. doi: 10.3389/fmars.2018.00384
- Mohrholz, V., Naumann, M., Nausch, G., Krüger, S., and Gräwe, U. (2015). Fresh oxygen for the Baltic Sea – an exceptional saline inflow after a decade of stagnation. *J. Mar. Syst.* 148, 152–166. doi: 10.1016/j.jmarsys.2015.03.005
- Olli, K., and Heiskanen, A. S. (1999). Seasonal stages of phytoplankton community structure and sinking loss in the gulf of Riga. *J. Mar. Syst.* 23 (1–3), 165–184. doi: 10.1016/S0924-7963(99)00056-1
- Otsmann, M., Suursaar, Ü., and Kullas, T. (2001). The oscillatory nature of the flows in the system of straits and small semienclosed basins of the Baltic Sea. *Cont. Shelf Res.* 21 (15), 1577–1603. doi: 10.1016/S0278-4343(01)00002-4
- Piehl, S., Friedland, R., Heyden, B., Leujak, W., Neumann, T., and Schernewski, G. (2022). Modeling of water quality indicators in the Western Baltic Sea: Seasonal oxygen deficiency. *Environ. Model. Assess.* 1, 1–18. doi: 10.1007/S10666-022-09866-X/FIGURES/10
- Purina, I., Labucis, A., Barda, I., Jurgensone, I., and Aigars, J. (2018). Primary productivity in the gulf of Riga (Baltic Sea) in relation to phytoplankton species and nutrient variability. *Oceanologia* 60 (4), 544–552. doi: 10.1016/J.OCEANO.2018.04.005
- Raudsepp, U. (2001). Interannual and seasonal temperature and salinity variations in the gulf of Riga and corresponding saline water inflow from the Baltic proper, nord. *Hydrol Res* 32 (2), 135–160. doi: 10.2166/nh.2001.0009
- Raudsepp, U., and Kõuts, T. (2001). Observations of near-bottom currents in the gulf of Riga. *Baltic Sea Aquat. Sci.* 63, 385–405. doi: 10.1007/s00027-001-8040-y
- Rousi, H., Laine, A. O., Peltonen, H., Kangas, P., Andersin, A. B., Rissanen, J., et al. (2013). Long-term changes in coastal zoobenthos in the northern Baltic Sea: the role of abiotic environmental factors. *ICES J. Mar. Sci.* 70 (2), 440–451. doi: 10.1093/ICESJMS/FSS197
- Schmidt, B., Wodzinowski, T., and Bulczak, A. I. (2021). Long-term variability of near-bottom oxygen, temperature, and salinity in the southern Baltic. *J. Mar. Syst.* 213, 103462. doi: 10.1016/J.JMARSYS.2020.103462
- Skudra, M., and Lips, U. (2017). Characteristics and inter-annual changes in temperature, salinity and density distribution in the gulf of Riga. *Oceanologia* 59 (1), 37–48. doi: 10.1016/J.OCEANO.2016.07.001
- Stipa, T., Tamminen, T., and Seppälä, J. (1999). On the creation and maintenance of stratification in the gulf of Riga. *J. Mar. Syst.* 23 (1–3), 27–49. doi: 10.1016/S0924-7963(99)00049-4
- Stoicescu, S. T., Laanemets, J., Liblik, T., Skudra, M., Samlas, O., Lips, I., et al. (2022). Causes of the extensive hypoxia in the gulf of Riga in 2018. *Biogeosciences* 19 (11), 2903–2920. doi: 10.5194/bg-19-2903-2022
- Stoicescu, S.-T., Lips, U., and Liblik, T. (2019). Assessment of eutrophication status based on Sub-surface oxygen conditions in the gulf of Finland (Baltic Sea). *Front. Mar. Sci.* 6. doi: 10.3389/fmars.2019.00054
- Sun, X., Li, Z., Ding, X., Ji, G., Wang, L., Gao, X., et al. (2022). Effects of algal blooms on phytoplankton composition and hypoxia in coastal waters of the northern yellow Sea. *China Front. Mar. Sci.* 9. doi: 10.3389/FMARS.2022.897418/BIBTEX
- Väli, G., Zhurbas, V., Lips, U., and Laanemets, J. (2017). Submesoscale structures related to upwelling events in the gulf of Finland, Baltic Sea (numerical experiments). *J. Mar. Syst.* 171, 31–42. doi: 10.1016/J.JMARSYS.2016.06.010
- Venkatesan, R., Ramesh, K., Kishor, A., Vedachalam, N., and Atmanand, M. A. (2018). Best practices for the ocean moored observatories. *Front. Mar. Sci.* 5 (DEC). doi: 10.3389/FMARS.2018.00469/BIBTEX
- Wei, Q., Yao, P., Xu, B., Zhao, B., Ran, X., Zhao, Y., et al. (2021). Coastal upwelling combined with the river plume regulates hypoxia in the changjiang (Yangtze river) and adjacent inner East China Sea shelf. *J. Geophys. Res. Ocean.* 126 (11), e2021JC017740. doi: 10.1029/2021JC017740
- Wei, Q., Yuan, Y., Song, S., Zhao, Y., Sun, J., Li, C., et al. (2022). Spatial variability of hypoxia and coupled physical-biogeochemical controls off the changjiang (Yangtze river) estuary in summer. *Front. Mar. Sci.* 9. doi: 10.3389/FMARS.2022.987368/BIBTEX

## Curriculum vitae

### Personal data

Name:	Stella-Theresa Stoicescu
Date of birth:	15.06.1988
Place of birth:	Estonia
Citizenship:	Estonian

### Contact data

E-mail:	stella.stoicescu@taltech.ee
---------	-----------------------------

### Education

2015–2023	Tallinn University of Technology, PhD
2012–2014	Tallinn University of Technology, Earth Sciences, MSC
2009–2012	Estonian University of Life Sciences, Natural Resources Management, BSC
2005–2007	Tallinn Secondary School No 32

### Language competence

Estonian	Native
English	Fluent
Russian	Basic skills

### Professional employment

01.07.2022–present	Tallinn University of Technology, School of Science, Department of Marine Systems, Engineer (1.00)
01.05.2021–30.06.2022	Tallinn University of Technology, School of Science, Department of Marine Systems, Junior Researcher (1.00)
17.08.2020–30.04.2021	Tallinn University of Technology, School of Science, Department of Marine Systems, Junior Researcher (0.50)
01.01.2017–16.08.2020	Tallinn University of Technology, School of Science, Department of Marine Systems, Junior Researcher (1.00)
04.01.2016–31.12.2016	Tallinn University of Technology, Institute of Marine Systems at TUT, Department of Marine Physics, Junior Researcher (1.00).
16.06.2014–03.01.2016	Tallinn University of Technology, Institute of Marine Systems at TUT, Department of Marine Physics, Technical staff (1.00)

### Academic degrees

Stella-Theresa Stoicescu, Master's Degree, 2014, (sup) Urmas Lips, Soome lahe keskkonnaseisundi hindamine: erinevate meetodite võrdlus (eutrofeerumise valdkonnas) (Assessment of the eutrophication status of the Gulf of Finland: a comparison of available tools), Tallinn University of Technology Institute of Marine Systems at TUT

Stella-Theresa Stoicescu, Bachelor's Degree, 2012, (sup) Diana Laarmann, Aidu karjääri taasmetsastatud aladel alustaimestiku analüüs (Analysis of understory on reforested areas in Aidu quarry), Estonian University of Life Sciences

### Scientific work

Publications according to ETIS:

- 1.1. Liblik, T.; Stoicescu, S.-T.; Buschmann, F.; Lilover, M.-J.; Lips, U. (2023). High-resolution characterization of the development and decay of seasonal hypoxia in the Gulf of Riga, Baltic Sea. *Frontiers in Marine Science*, 10, 1–8. DOI: 10.3389/fmars.2023.1119515.  
  
Stoicescu, S.-T.; Laanemets, J.; Liblik, T.; Skudra, M.; Samlas, O.; Lips, I.; Lips, U. (2022). Causes of the extensive hypoxia in the Gulf of Riga in 2018. *Biogeosciences*, 19, 2903–2920. DOI: 10.5194/bg-19-2903-2022.  
  
Stoicescu, S.-T.; Lips, U.; Liblik, T. (2019). Assessment of Eutrophication Status Based on Sub-Surface Oxygen Conditions in the Gulf of Finland (Baltic Sea). *Frontiers in Marine Science*, 6, UNSP 54. DOI: 10.3389/fmars.2019.00054.  
  
Stoicescu, S.-T.; Lips, U.; Lips, I. (2018). Assessing the eutrophication status of Estonian marine waters. *Фундаментальная и прикладная гидрофизика*, 11 (2), 62–74. DOI: 10.7868/S2073667318020053.
- 2.3. Stoicescu, S.-T. (2014). Soome lahe keskkonnaseisundi hindamine: erinevate meetodite võrdlus (eutrofeerumise valdkonnas) [Assessment of the eutrophication status of the Gulf of Finland: the comparison of available tools]. Magistritöö, Tallinna Tehnikaülikool.
- 2.5. Stoicescu, S.-T.; Lips, U. (2021). Compatibility of targets under different marine policies - Sufficiency of the EU WFD targets for individual rivers basins to achieve the BSAP goals. *Baltic Marine Environment Protection Commission – Helsinki Commission*.

## Elulookirjeldus

### Isikuandmed

Nimi:	Stella-Theresa Stoicescu
Sünniaeg:	15.06.1988
Sünnikoht:	Eesti
Kodakondsus:	Eesti

### Kontaktandmed

E-post:	stella.stoicescu@taltech.ee
---------	-----------------------------

### Hariduskäik

2015–2023	Tallinna Tehnikaülikool, PhD
2012–2014	Tallinna Tehnikaülikool, Maateadused, MSC
2009–2012	Eesti Maaülikool, Loodusvarade kasutamine ja kaitse, BSC
2005–2007	Tallinna 32. Keskkool

### Keelteoskus

Eesti keel	Emakeel
Inglise keel	Kõrgtase
Vene keel	Algtase

### Teenistuskäik

01.07.2022–tänaeni	Tallinna Tehnikaülikool, Loodusteaduskond, Meresüsteemide instituut, Insener (1.00)
01.05.2021–30.06.2022	Tallinna Tehnikaülikool, Loodusteaduskond, Meresüsteemide instituut, Nooremteadur (1.00)
17.08.2020–30.04.2021	Tallinna Tehnikaülikool, Loodusteaduskond, Meresüsteemide instituut, Nooremteadur (0.50)
01.01.2017–16.08.2020	Tallinna Tehnikaülikool, Loodusteaduskond, Meresüsteemide instituut, Nooremteadur (1.00)
04.01.2016–31.12.2016	Tallinna Tehnikaülikool, TTÜ Meresüsteemide Instituut, Merefüüsika osakond, Nooremteadur (1.00).
16.06.2014–03.01.2016	Tallinna Tehnikaülikool, TTÜ Meresüsteemide Instituut, Merefüüsika osakond, Insener (1.00)

### Teaduskraadid

Stella-Theresa Stoicescu, magistrikraad, 2014, (juh) Urmas Lips, Soome lahe keskkonnaseisundi hindamine: erinevate meetodite võrdlus (eutrofeerumise valdkonnas) (Assessment of the eutrophication status of the Gulf of Finland: a comparison of available tools), Tallinn University of Technology Institute of Marine Systems at TUT

Stella-Theresa Stoicescu, bakalaureusekraad, 2012, (juh) Diana Laarmann, Aidu karjääri taasmetsastatud aladel alustaimestiku analüüs (Analysis of understory on reforested areas in Aidu quarry), Estonian University of Life Sciences

## **Teadustegevus**

Publikatsioonid Eesti Teadusinfosüsteemi klassifikaatori järgi

- 1.1. Liblik, T.; Stoicescu, S.-T.; Buschmann, F.; Lilover, M.-J.; Lips, U. (2023). High-resolution characterization of the development and decay of seasonal hypoxia in the Gulf of Riga, Baltic Sea. *Frontiers in Marine Science*, 10, 1–8. DOI: 10.3389/fmars.2023.1119515.  
  
Stoicescu, S.-T.; Laanemets, J.; Liblik, T.; Skudra, M.; Samlas, O.; Lips, I.; Lips, U. (2022). Causes of the extensive hypoxia in the Gulf of Riga in 2018. *Biogeosciences*, 19, 2903–2920. DOI: 10.5194/bg-19-2903-2022.  
  
Stoicescu, S.-T.; Lips, U.; Liblik, T. (2019). Assessment of Eutrophication Status Based on Sub-Surface Oxygen Conditions in the Gulf of Finland (Baltic Sea). *Frontiers in Marine Science*, 6, UNSP 54. DOI: 10.3389/fmars.2019.00054.  
  
Stoicescu, S.-T.; Lips, U.; Lips, I. (2018). Assessing the eutrophication status of Estonian marine waters. *Фундаментальная и прикладная гидрофизика*, 11 (2), 62–74. DOI: 10.7868/S2073667318020053.
- 2.3. Stoicescu, S.-T. (2014). Soome lahe keskkonnaseisundi hindamine: erinevate meetodite võrdlus (eutrofeerumise valdkonnas) [Assessment of the eutrophication status of the Gulf of Finland: the comparison of available tools]. Magistritöö, Tallinna Tehnikaülikool.
- 2.5. Stoicescu, S.-T.; Lips, U. (2021). Compatibility of targets under different marine policies - Sufficiency of the EU WFD targets for individual rivers basins to achieve the BSAP goals. *Baltic Marine Environment Protection Commission – Helsinki Commission*.

ISSN 2585-6901 (PDF)  
ISBN 978-9916-80-048-5 (PDF)